การกำจัดสาร2,4-ไดคลอโรฟีนอลและไตรโคลซานด้วยกระบวนการเฟนตันและอิเลคโตรเฟนตัน

นายธนากร เมธาธรรม

วิทยานิพนธ์นี้เป็นส่วนหนึ่งของการศึกษาตามหลักสูตรปริญญาวิศวกรรมศาสตรดุษฎีบัณฑิต
สาขาวิชาวิศวกรรมสิ่งแวดล้อม ภาควิชาวิศวกรรมสิ่งแวดล้อม
คณะวิศวกรรมศาสตร์ จุฬาลงกรณ์มหาวิทยาลัย
ปีการศึกษา 2554

REMOVAL OF 2,4-DICHLOROPHENOL AND TRICLOSAN BY FENTON AND ELECTRO-FENTON PROCESSES

Mr. Thanakorn Methatham

A Dissertation Submitted in Partial Fulfillment of the Requirements

for the Degree of Doctor of Philosophy Program in Environmental Engineering

Department of Environmental Engineering

Faculty of Engineering

Chulalongkorn University

Academic Year 2011

Thesis Title	REMOVAL OF 2,4-DICHLOROPHENOL AND TRICLOSAN BY FENTON AND ELECTRO-FENTON PROCESSES
By	Mr. Thanakorn Methatham
Field of Study	Environmental Engineering
Thesis Advisor	Associate Professor Chavalit Ratanatamskul, Ph.D.
Thesis Co-advisor	Professor Ming-Chun Lu, Ph.D.

Accepted by Faculty of Engineering, Chulalongkorn University in Partial Fulfillment of the Requirements for the Doctoral Degree

.... Dean of Faculty of Engineering
(Associate Professor Boonsom Lerdhirunwong, Dr. Ing.)

THESIS COMMITTEE

.... Chairman
(Associate Professor Sutha Khaodhiar, Ph.D.)

.... Thesis Advisor
(Associate Professor Chavalit Ratanatamskul, Ph.D.)

.... Thesis Co-advisor
(Professor Ming-Chun Lu, Ph.D.)

.... Examiner
(Assistant Professor Khemarath Osathaphan, Ph.D.)

.... Examiner
(Assistant Professor Pisut Painmanakul, Ph.D.)

.... External Examiner
(Associate Professor Jin Anotai, Ph.D.)

ธนากร เมธาธรรม : การกำจัดสาร 2,4-ไดคลอโรฟีนอลและไตรโคลซานด้วยกระบวนการเฟนตันและอิเลคโตรเฟนตัน. (REMOVAL OF 2,4-DICHLOROPHENOL AND TRICLOSAN BY FENTON AND ELECTRO-FENTON PROCESSES) อ. ที่ปรึกษาวิทยานิพนธ์หลัก : รศ. ดร. ชวลิต รัตนธรรมสกุล, อ. ที่ปรึกษาวิทยานิพนธ์ร่วม: Prof. Ming-Chun Lu, Ph.D., 274 หน้า.

งานวิจัยนี้ศึกษาการกำจัดสาร 2,4-ไดคลอโรฟีนอล (2,4-DCP) และไตรโคลซานด้วยกระบวนการออกซิเดชั่นขั้นสูง โดยมุ่งศึกษากระบวนการประเภทเฟนตัน และอิเลคโตรเฟนตันในแง่ของสภาวะที่เหมาะสมสำหรับการดำเนินระบบให้เกิดประสิทธิภาพสูงสุด และศึกษากลไกทางจลน์ศาสตร์ของกระบวนการภายในระบบ รวมถึงผลิตภัณฑ์ที่เกิดจากปฏิกิริยาของกระบวนการในระบบเป็นหลัก ตัวแปรในการศึกษาครั้งนี้ได้แก่ พีเอช, ค่ากระแสไฟฟ้าต่อหน่วยพื้นที่, ปริมาณความเข้มข้นของ H_2O_2 และ Fe^{2+}, อัตราส่วนของปริมาณ H_2O_2 ต่อ Fe^{2+} และสภาวะในการจ่ายสาร H_2O_2 ต่อระบบ ผลการทดลองพบว่า กระบวนการเฟนตัน และอิเลคโตรเฟนตันมีประสิทธิภาพในการกำจัดสาร 2,4-DCP และไตรโคลซานในช่วง 70-100% ขึ้นกับสภาวะที่ใช้ดำเนินระบบ ประสิทธิภาพของระบบอิเลคโตรเฟนตันถูกควบคุม และขึ้นกับประเภทของการจ่ายสาร H_2O_2 เป็นสำคัญ โดยจากการทดลองพบว่า การจ่ายสาร H_2O_2 ให้กับระบบในรูปแบบของการกระจายสารจ่ายเป็นช่วงทุกๆ 2 นาทีหรือ step feed ให้ผลลัพธ์ในแง่การย่อยสลายได้สมบูรณ์แบบมากกว่าการจ่ายสารแบบครั้งเดียวในช่วงเริ่มต้นปฏิกิริยา งานวิจัยนี้ได้นำเสนอนวัตกรรมแบบจำลองทางจลน์ศาสตร์ของกระบวนการอิเลคโตรเฟนตัน ซึ่งพัฒนาเพื่อใช้ประโยชน์ในการทำนายค่าคงที่ทางจลน์ศาสตร์ที่แท้จริงของปฏิกิริยาออกซิเดชั่นระหว่าง·OH กับสารอินทรีย์ที่มีคลอรีนเป็นองค์ประกอบ ซึ่งมีความสำคัญต่อการออกแบบ และดำเนินระบบในด้านวิศวกรรม โดยจากการทดลองพบว่า ค่าคงที่ทางจลน์ศาสตร์ของปฏิกิริยาระหว่าง ·OH กับ 2,4-DCP มีค่าเฉลี่ยอยู่ที่ $1.437\times10^{9}\ M^{-1}s^{-1}$ ขณะที่ค่าคงที่ทางจลน์ศาสตร์ของปฏิกิริยาระหว่าง ·OH กับ ไตรโคลซาน มีค่าเฉลี่ยอยู่ที่ $5.434\times10^{9}\ M^{-1}s^{-1}$ โดยผลการทดลองพบว่า แบบจำลองที่นำเสนอดังกล่าวมีความเหมาะสม ความถูกต้องแม่นยำ และความชัดเจนในด้านการอธิบายกลไกทางจลน์ศาสตร์ของปฏิกิริยาได้ดี และเหมาะสมมากกว่าการใช้แบบจำลองชนิด pseudo 1st-model อย่างมีนัยสำคัญ สำหรับผลิตภัณฑ์ที่พบจากปฏิกิริยาการย่อยสลาย 2,4-DCP จากการทดลอง ได้แก่ 2-คลอโรฟีนอล, ฟีนอล, ไฮโดรควิโนน, พีเบนโซควิโนน, กรดมาเลอิค, กรดอะซิติค, กรดออกซาลิค และกรดฟอร์มิค ขณะที่ผลิตภัณฑ์จากปฏิกิริยาการย่อยสลายไตรโคลซาน ที่พบจากการทดลอง ได้แก่ 2,4-DCP, 4-คลอโรคะตาคอล, ฟีนอล, ไฮโดรควิโนน, พีเบนโซควิโนน, กรดมาเลอิค, กรดอะซิติค, กรดออกซาลิค และกรดฟอร์มิค โดยประเภทของผลิตภัณฑ์ที่เกิดขึ้นในแต่ละปฏิกิริยาของแต่ละกระบวนการนั้นจะขึ้นกับตัวแปรที่ใช้ดำเนินระบบ และลักษณะรูปแบบของการจ่ายสาร H_2O_2 ให้กับระบบเป็นสำคัญ

ภาควิชา วิศวกรรมสิ่งแวดล้อม ลายมือชื่อนิสิต
สาขาวิชา วิศวกรรมสิ่งแวดล้อม ลายมือชื่อ อ.ที่ปรึกษาวิทยานิพนธ์หลัก
ปีการศึกษา 2554 ลายมือชื่อ อ.ที่ปรึกษาวิทยานิพนธ์ร่วม

4971884021 : MAJOR ENVIRONMENTAL ENGINEERING

KEYWORDS : 2,4-DICHLOROPHENOL (2,4-DCP) / TRICLOSAN / ENDOCRINE DISRUPTER / ADVANCED OXIDATION PROCESSES (AOPs) / FENTON PROCESS / ELECTRO-FENTON PROCESS / HYDROXYL RADICALS/ NOVEL KINETIC MODEL

THANAKORN METHATHAM: REMOVAL OF 2,4-DICHLOROPHENOL AND TRICLOSAN BY FENTON AND ELECTRO-FENTON PROCESSES. ADVISOR: ASSOC. PROF. CHAVALIT RATANATAMSKUL, Ph.D., CO-ADVISOR: PROF. MING-CHUN LU, Ph.D., 274 pp.

2,4-Dichlorophenol (2,4-DCP) and triclosan are defined as endocrine disruption organic compounds and toxic pollutants as listed by the U.S. EPA. The advanced oxidation processes in the type of Fenton and electro-Fenton processes were investigated in order to ascertain the process optimization, kinetics of process and the feasibility of intermediate occurring during the process for enhancement of 2,4-DCP and triclosan degradation. The effect of operating parameters such as pH, current density, Fe^{2+} and H_2O_2 concentration, H_2O_2 to Fe^{2+} (H/F) molar ratio and H_2O_2 feeding mode of operation were investigated to determine the evolution of 2,4-DCP and triclosan which were used to indicate the optimum operating conditions. Additionally, the initial degradation rate was also used as a process optimization indicator. 2,4-DCP and triclosan can be oxidized up to 70-100% under various conditions depends on the effect of operating parameters. The performance of the process when using the H_2O_2 step feed condition was found to be better than that of the conventional initial feed as shown by a better mineralization. The novel kinetic model of the electro-Fenton process was proposed to be employed with 2,4-DCP and triclosan as a chlorinated organic reference to determine the kinetic rate constant of process. The operating parameters; pH, current densities and H_2O_2 concentrations were varied to validate this novel model and intrinsic kinetic rate constant determination. The kinetic rate constant of $\cdot OH$ with 2,4-DCP and triclosan obtained by the novel model from this experiment was $1.437 \times 10^9\ M^{-1}s^{-1}$ for 2,4-DCP and $5.434 \times 10^9\ M^{-1}s^{-1}$ for triclosan. As a result, the correlation coefficients demonstrated that the novel model can well describe the kinetics of chlorinated organic compound degradation more suitably and better than pseudo 1^{st}-order model. In the electro-Fenton process, 2-chlorophenol, phenol, hydroquinone, p-benzoquinone, maleic, acetic, oxalic and formic acids were the main oxidation intermediates of 2,4-DCP degradation whereas 2,4-DCP, 4-chlorocatechol, phenol, hydroquinone, p-benzoquinone, maleic, acetic, oxalic and formic acids were the main oxidation intermediates of triclosan degradation. The occurrence of intermediates depended on the H_2O_2 feeding mode of process majority. The degradation pathway for 2,4-DCP and triclosan degradation by electro-Fenton process were proposed on the basis of the intermediate compounds that were detected.

Department : Environmental Engineering	Student's Signature
Field of study : Environmental Engineering	Advisor's Signature
Academic Year : 2011	Co-advisor's Signature

ACKNOWLEDGEMENTS

I would like to express my gratitude to, Associate Professor Dr. Chavalit Ratanatamskul my advisor and Professor Ming-Chun Lu my co-advisors for their valuable suggestion, encouragement, and supports throughout my study.

My gratitude is also extended to Associate Professor Dr. Sutha Khaodhair, Assistant Professor Dr. Khemarath Osathaphan, Assistant Professor Dr. Pisut Painmanakul and Associate Professor Dr. Jin Anotai, for serving as thesis committee, for their recommendations and also useful suggestions.

Thanks to THE 90th ANNIVERSARY OF CHULALONGKORN UNIVERSITY FUND (Ratchadaphiseksomphot Endowment Fund) and The Ministry of Education (Grant: P9605), The 380 National Science Council, Taiwan (Grant: NSC 96-2628-E-041-002-MY3) for the full scholarship and partially funding for the thesis work and all useful supporting facilities.

I would like to thanks to Miss Nalinrat Masomboon and Mr. Piyawat Tanvanit for some technical suggestions and facilitating information. In addition, I would like to thank all my friends for their friendly help and suggestions.

Finally, a very special thank you belongs to my beloved family for their unconditional love, a whole understanding, great patience and consistent support throughout my entire study.

CONTENTS

Page

Page

Page

LIST OF TABLES

Table Page

Table Page

LIST OF FIGURES

Figure Page

Figure Page

Figure Page

Figure Page

Figure Page

LIST OF ABBREVIATIONS

•OH	Hydroxyl radical
°C	Degree celsius
λ	Relative ratio of ferric and ferrous
$\propto$	Relative ratio of hydrogen peroxide at time t and initial concentration
2-CP	2-chlorophenol
2,4-DCP	2,4-dichlorophenol
AOPs	Advanced oxidation processes
C	Organic pollutant concentration
C_0	Initial organic pollutant concentration
cm	Centimeter
CO_2	Carbon dioxide
COD	Chemical oxygen demand
E^0	Oxidation –reduction potential
EDCs	Endocrine-disrupting compounds
EF-FeOx	Electro-Fenton in type of ferrous generation at anode
EF-H_2O_2	Electro-Fenton in type of hydrogen peroxide generation at cathode
Fe^{2+}	Ferrous ion
Fe^{2+}_0	Initial ferrous ion

Fe^{3+}	Ferric ion
FSR	Fenton sludge recycling
GC-MS	Gas chromatography and mass spectophotometer
H/F	Hydrogen peroxide per ferrous ratio
$HClO_4$	Hypo-chloric acid
$HO_2^{\bullet}$	Hydroperoxyl radical
H_2O	Water
H_2O_2	Hydrogen peroxide
HPLC	High performance liquid chromatography
I	Current
IC	Ion chromatography
INF	Hydrogen peroxide initial feed condition
k	Kinetic constant
ln	Natural logarithm
M	Molar
mg L^{-1}	Milligram per liter
min	Minute
mM	Milli molar
mA	Milli ampere

ng L^{-1}	Nanogram per liter
$O_2^{-\bullet}$	Superoxide ion
O_3	Ozone
PPCPs	Pharmaceuticals and personal care products
ROP	Relative oxidation performance ratio
rpm	Round per minute
s	Second
S	Organic pollutant concentration
S_0	Organic pollutant initial concentration
STF	Hydrogen peroxide step feed condition
TCS	Triclosan
Ti/ RuO_2/IrO_2	Titanium coated with rubidium dioxide and iridium dioxide
TiO_2	Titanium dioxide
TOC	Total organic carbon
US EPA	United States environmental protection agency
UV	Ultra violet
WWTP	Wastewater treatment plant

CHAPTER I
INTRODUCTION

1.1. Rationale

Over recent years, wastewater not only contains organic matter, suspended solids or nutrients, but also contains synthetic traces of organic contaminants. These include chemicals that are used for household cleaning, endocrine-disrupting compounds (EDCs), persistent hazardous compounds, pharmaceuticals and personal care products (PPCPs). The variety and frequency of usage of these substances have increased rapidly over recent years. These chemicals ended up in surface water supplies through the pathways of wastewater treatment plants. After the household products are used, they are discharged down the drain into septic, municipal sewer systems and afterwards are treated in wastewater treatment plants (WWTP). The biodegradation of EDCs, persistent hazardous compounds and PPCPs in conventional wastewater treatment plants has been studied by numerous papers and in general, most of them were found to have been effectively eliminated by conventional wastewater treatment. However, despite the high elimination rates due to high influent concentrations (typically in mg L^{-1} level), they comprise a significant portion of trace organics detected in WWTP effluents and are considered as one of the most relevant organic contaminants of anthropogenic origin characterized by a very high potential to enter the environment. Additionally, all EDCs and PPCPs classes have been found to undergo primary biodegradation under aerobic conditions; however, not all compounds are amenable to ultimate biodegradation and the formation of persistent biodegradation products can represent a serious problem. The EDCs of most concerned, in terms of persistency and impact on environment, is triclosan (TCS) which can generate 2,4-dichlorophenol (2,4-DCP) as a by-product from many processes.

2,4-DCP is a non-ionic surfactant widely used globally in a number of commercial and household formulations, including detergents, cosmetic products, water-based paints, inks and textiles. Its many common usages include in the production of dyes, herbicides, pesticides, fungicides, chemicals, wood preservatives, and pharmaceutical manufacturing. The substance is released into the environment mainly by the chlorination of municipal water, the degradation of some chemicals and the manufacturing of various products such as pesticides, pharmaceuticals and dyes. However, this chemical is toxic to humans. It is readily absorbed into the body by inhalation of aerosols, through the skin and by ingestion which can causes irritation symptoms of nose, eyes, respiratory tract, and skin contact. It is also a suspected mutagen and carcinogen to humans. Moreover, the accumulation of chlorinated aromatic compounds in the environment has become a serious problem. Upon entering the environment, 2,4-dichlorophenols are toxic and persistent organic pollutants which cause considerable damage to the aquatic ecosystem as well as human health. Therefore, in this type of environment and under these conditions, measurement of chemical oxidation is needed and important for effective wastewater treatment (Bell et al., 2003).

Triclosan is a broad-spectrum antimicrobial agent that is widely used in personal-care products such as soaps, toothpastes, cosmetics, skin creams and deodorants, as well as in textiles such as sportswear, shoes and carpets. Triclosan is reported to be highly toxic to certain aquatic organisms, particularly to green algae (Tatarazako et al, 2004). Besides, triclosan has been shown to indirectly affect aquatic organisms by blocking enzyme carrying proteins, leading to concerns of the possible build-up of bacterial resistance in these organisms. Another concern of the presence of triclosan in surface water is the formation of more toxic by-products such as dioxin and endocrine disruptor chemicals (Ingerslev et al., 2003). The hydrophobic nature of triclosan (log K_{OW} ~ 4.86) allows for its easy removal in wastewater treatment plants (94% removal by biodegradation and sorption), but residual concentrations of 40–200 and 140 ng L^{-1} still have been found in secondary wastewater effluents and surface water, respectively (Singer et al., 2002).

Advanced oxidation processes (AOPs) are technologically available as an alternative process option for removing persistent complex pollutants from liquid, solid and gaseous streams. AOPs are regarded as promising in achieving the further removal of persistent and complex micro-pollutants in comparison to conventional wastewater treatment plant. In recent years, AOPs have been described as efficient procedures for obtaining high oxidation yields from several kinds of organic compounds. These methods allow their rapid mineralization, i.e. their conversion into CO_2, H_2O and inorganic ions, through the action of hydroxyl radical (•OH), which acts as a nonselective, strong oxidant of organics yielding dehydrogenated or hydroxylated derivatives. Hydroxyl radical can be produced by different techniques in AOPs such as H_2O_2/Fe^{2+} (Fenton's reagent) and H_2O_2/O_3 as chemical procedures, $H_2O_2/Fe^{3+}/UV$ as a photochemical treatment, and TiO_2/UV, $TiO_2/UV/O_3$ and $Fe^{2+}/UV/O_3$ as photocatalytic methods. For the many kinds of AOPs and among the catalysts used, both the Fenton and electro-Fenton processes are considered to be very efficient method of AOPs. Recently, mainly because of its amenability to automation, high efficiency and environmental compatibility, there has been a growing interest in the use of effective direct or indirect electrochemical degradation of organic pollutants in water. Advantages include operating at ambient temperature and pressure, and the ability to exploit either oxidative or reductive chemistries, using electrons as the only added "reagents". In fact, the main reagent is the electron, which is a "clean reagent". Electrons are cheaper than any chemical reagent on a molar basis; hence, even moderate values of current efficiency allow electrolytic remediation to be economically viable. Although the Fenton and electro-Fenton processes are high performance for persistent complex micro-pollutant removal, their mechanisms are not clear and the real removal efficiency of this system is still largely unknown.

The objective of this research is to assess the viability of advanced oxidation processes, specifically Fenton and electro-Fenton processes, in the removal of 2,4-dichlorophenol and triclosan. This research aims to find out the removal mechanism, by-products of the oxidation process and the optimum conditions for 2,4-dichlorophenol and triclosan. Moreover, the kinetics of the processes and the possibility of application to conventional treatment systems were also determined.

1.2. Objectives of the study

1. To investigate the optimum conditions of two advanced oxidation processes: Fenton and electro-Fenton processes for removal of 2,4-dichlorophenol and triclosan from synthetic wastewater.
2. To investigate the 2,4-dichlorophenol and triclosan removal efficiencies in terms of COD and TOC removal by both the Fenton and electro-Fenton processes.
3. To investigate the kinetics of 2,4-dichlorophenol and triclosan which were removed from synthetic wastewater by the electro-Fenton process.
4. To propose novel kinetic model for organic removal by electro-Fenton process.
5. To investigate the removal mechanisms of 2,4-dichlorophenol and triclosan from synthetic wastewater by the electro-Fenton process.
6. To investigate the by-products and propose the pathways of 2,4-dichlorophenol and triclosan that are removed by the electro-Fenton process.

1.3 Hypotheses

1. 2,4-dichlorophenol and triclosan can be removed by the Fenton and electro-Fenton processes.
2. The efficiency of Fenton and electro-Fenton processes on 2,4-dichlorophenol and triclosan oxidation depend on initial pH value, electrical current density, H_2O_2 to Fe^{2+} ratio and H_2O_2 operational feeding.

1.4. Scope of the study

1. This research was performed on a laboratory scale at Chia Nan University of Pharmacy and Science, Taiwan and Chulalongkorn University, Thailand.
2. The main targets of this study focused on the experiment on 2,4-dichlorophenol and triclosan from synthetic wastewater.
3. This research was carried out using batch Fenton and electro-Fenton reactors with 5-liter volume.
4. This research was performed at a room temperature and at a controlled temperature for kinetic experiment.

1.5. Expected results

1. To gain knowledge about the optimum conditions and operating systems criteria of two advanced oxidation processes: Fenton and electro-Fenton processes for removal of 2,4-dichlorophenol and triclosan.
2. To gain knowledge about the removal efficiencies in term of COD and TOC removal by the Fenton and electro-Fenton processes
3. To gain knowledge about the kinetics of 2,4-dichlorophenol and triclosan which were removed from synthetic wastewater by the electro-Fenton process.
4. To gain the novel kinetic model for organic removal by electro-Fenton process.
5. To gain knowledge about the removal mechanisms of 2,4-dichlorophenol and triclosan by the electro-Fenton process.
6. To gain knowledge about the by-products and pathways of the 2,4-dichlorophenol and triclosan which degraded by the electro-Fenton process.

CHAPTER II
LITERATURE REVIEWS

2.1. Endocrine Disruptors

Over recent years, there has been increasing concern over the effect of synthetic organic chemicals and how they disrupt the endocrine systems in living organisms. This has especially been the case following the general acceptance that the environment has actually been contaminated by numerous “endocrine disrupting compounds” (EDCs) that exert hormonal activity (Metzler and Pfeiffer, 2001). An endocrine disruptor is defined as being an exogenous agent that interferes with the synthesis, secretion, transport, binding, action and elimination of the natural hormones in the body responsible for the maintenance of homeostasis, reproduction, development and behavior (US Environmental Protection Agency [US EPA], 2001). An endocrine system has as its main role the transformation of various exogenous stimuli into chemical messengers and hormones. Consequently, these messengers and hormones bring about the appropriate gene expressions while synthesizing proteins and/or activating already existing tissue-specific enzyme systems (Jintelmann et al., 2003).The major endocrine disruption endpoints belong to either of three types: estrogenic (compounds that mimic or block natural estrogens), androgenic (compounds that mimic or block natural testosterone), and thyroidal (compounds with direct and/or indirect impacts on the thyroid) (Synder et al., 2003). As regards their effects, EDCs have been found to be detrimental to the health of the environment and species in many and various forms, including reproductive system disorders, reduction in reproductive fitness as well as hormone-dependent cancers (Fry et al., 1987; Synder et al., 2003; Alum et al., 2004). Taking on a broad diversity of chemical structures, most endocrine disruptors are synthetic, but may also be natural (Metzler and Pfeiffer, 2001). Chemicals that contain EDCs, most notably, include natural estrogens, plasticizers (diethylphthalate, BPA), phytoestrogens, organohalogens (PCBs and dioxin), pesticides (methoxychlor),), and surfactants (nonylphenol) (US EPA, 2001).

Due to imperfect manufacturing processes as well as leaching from final end products, most EDCs can be found throughout all aspects of the environment (water, air, soil and sediments). As a consequence of both industrial and household usage and discharge, EDCs can contaminate surface water through sewage effluents (Gomes and Lester, 2003). Male and female hormones as well as ingested synthetic steroids constitute the majority of EDCs found in domestic sewage. These are discharged into municipal systems on a daily basis through urine, becoming active estrogens in surface waters after being only partly removed through biochemical oxidation (Deborde et al., 2005; D'Ascenzo et al., 2003; Panter et al., 1999; Ternes et al., 1999). Despite varying in concentration, ranges of ng L^{-1} have been previously reported in some sites for natural synthetic hormones (Ying et al., 2002a; Belfroid et al., 1999) and mg L^{-1} for alkylphenols (AP) and bisphenols (Blackburn and Waldock, 1995; Ahel et al., 1994) and these levels have been proved to affect aquatic life. Indeed, one report found that feminization was in fact induced in male fish and intersex induction (Gray and Metcalfe, 1997). Despite some findings establishing falling human sperm production and rising estrogen-dependent cancers over recent years (Herbst et al., 1989; Mocarelli et al., 1996), EDC exposure has as yet to be conclusively correlated to reproductive disorders in humans. However, reproductive abnormalities in animals and links to exposure to EDCs have been reported (Guillette et al., 1994; Andersson et al., 1988; Morrison et al., 1985). As concerns groundwater, contamination can result from percolation from agricultural areas in addition to rainwater infiltrating through landfills (Gomes and Lester, 2003). Although their concentrations are low in the aquatic environment, trace amounts do have the capacity to trigger estrogenic activity and, subsequently, the EU has categorized hormone-like chemicals as "hazardous".

2.2 2,4-Dichlorophenol

2.2.1 Properties of 2,4-Dichlorophenol

2.2.1.1 General Information

Chlorophenols are organic halogen compounds of cyclic aromatics formed by replacing hydrogen atoms in phenol by 1-5 atoms of chlorine. There are five basic types of chlorophenols: monochlorophenols, dichlorophenols, trichlorophenols, tetrachlorophenols and pentachlorophenols. There are 19 compounds of chlorophenols of three mono-, six isomeric substances each of di-, tri-, as well as three isomeric substances tetra-, and fully chlorinated pentachlorophenol. Chlorinated phenol compounds are solids at room temperature, except 2-Monochlorophenol which melts at 8 ^{o}C. Main uses of chlorinated phenols include as antiseptics, disinfectants, wood preservatives herbicides, and pesticides. Under the US EPA Clean Water Act, they are considered priority toxic pollutants and have proven difficult to remove from water bodies (Zhou et al., 2008). One such compound is 2,4-dichlorophenol, which is also referred to as 2,4-DCP , 2,4-dichlorohydroxyl-benzene, 4,6-dichlorophenol, 1-hydroxy-2,4-dichlorobenzene and 4-hydoxy-1,3-dichlorobenzene. As shown below in Figure 2.1., the molecular formula is $C_6H_4Cl_2O$ It is mainly used as an intermediate in the preparation of the herbicide 2,4-dichlorophenoxy acetic acid (2,4-D) and 2-(2,4-dichlorophenoxy) propionic acid (2,4-DP). Industrially, 2,4-dichlorophenol can be obtained by chlorinating phenol, *p*-chlorophenol, *o*-chlorophenol, or a mixture of these compounds in cast-iron reactors.

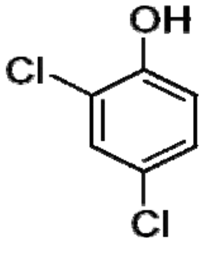

Figure 2.1 Structure of 2,4-dichlorophenol (2,4-DCP)

Microbial activities in natural water or in nearby soil or solar photolysis cause, 2,4-D to reverse to 2,4-DCP . Not only is this chemical harmful to the aquatic environment, but in substantial amounts it is also potentially lethal for humans if in any way inhaled, ingested or absorbed through the skin. Aside from this, it is also thought to be a mutagen and carcinogen. The compound itself has been discovered in the flue gas of municipal waste incineration, pulp and paper wastewater as well as the effluence of disinfected water following chlorination, (Li et al., 2007).

2.2.1.2 Physical and Chemical Properties

2,4-dichlorophenol is an organic halogen hydrocarbon mainly used as an ingredient in antiseptics and a material starter for chlorophenols production in addition to being an intermediate for the production of 2,4-dichlorophenoxy acetic acid and other related herbicides. At ambient temperature 2,4-dichlorophenol is solid (colorless crystals). Despite being highly soluble in alcohols, the compound is only slightly soluble in water. The chemical is also characterized by its strong odor The physical and chemical properties of 2,4-dichlorophenol are provided below in Table 2.1.

2.2.1.3 Toxicology

Symptoms experienced during the production of chlorophenol include irritation to the nose, eyes, respiratory tract, and the skin with the onset of chloracne. However, the long-term effects of chlorophenols remain inconclusive with conflicting results among epidemiology studies.

The compound can be absorbed into the body through the skin as well as by inhalation of aerosols and by ingestion (see Table 2.2). There exists no recommendation for the threshold limit value (TLV) level as it still has not been established. For rats, the lethal dose (LD50) has been found to be 580 mg kg^{-1}(oral) and 1730 $mg.kg^{-1}$ (percutaneous). However, it is stressed that care be taken when dealing with the substance due to the lack of sufficient data on the compound’s effects on human health.. Currently, under the testing program for high-production-volume chemicals by the U.S. Environmental Protection Agency, focus has centered on the risks of 2,4-dichlorophenol arising from skin adsorption. It is also the recommendation of this federal agency that no more than 0.03 mg L^{-1} of this chemical be present in drinking water.

2.1.3.1 Acute Toxicity

Routes of exposure: 2,4-dichlorophenol can be absorbed into the body through the skin, by ingestion and by the inhalation of aerosols, .

Affected organs: Skin, eyes, central nervous system (CNS)

Table 2.1 Physical and chemical properties of 2,4-dichlorophenol.

Properties	Value
Molecular formula	$C_6H_4Cl_2O$
Molecular weight	163.00 g/mol
CAS NO.	120-83-2
Appearance	Colorless crystals; white or pale yellow solid
Odor	Strong medicinal
Melting point	45 °C
Boiling point	210 °C
Specific gravity	1.383
Solubility in water	0.45 g/l at 20 °C
Solubility in organic solvent	Soluble in carbon tetrachloride, ethyl ether; Soluble in aqueous alkali
Vapor density	5.62
Vapor pressure	133 kPa @ 53 °C
Density	1.388 g/ml @ 50 °C
Specific heat	190 $J.mol^{-1}.K^{-1}$ @ 20 °C
Viscosity	2.65 mPa.s @ 50 °C
Flash point	113 °C
Stability	Stable under ordinary conditions

Table 2.2 Symptoms, Prevention and First Aid of 2,4-dichlorophenol (International Chemical Safety Cards,1993)

Route of Exposure	Symptoms	Prevention	First aid
Inhalation	Burning sensation. Coughing. Shortness of breath. Sore throat.	Local exhaust or breathing protection.	Fresh air, rest. Artificial respiration if indicated. Refer for medical attention.
Skin	Redness. Pain. Blisters.	Protective gloves. Protective clothing.	Remove contaminated clothes. Rinse and then wash skin with water and soap.
Eyes	Redness. Pain. Severe deep burns.	Face shield, or eye protection in combination with breathing protection.	First rinse with plenty of water for several minutes (remove contact lenses if easily possible), then take to a doctor.
Ingestion	Burning sensation. Abdominal pain. Tremor. Weakness. Labored breathing. Shock or collapse.	Do not eat, drink, or smoke during work.	Rinse mouth. Do not induce vomiting. Refer for medical attention.

2.1.3.2 Chronic Toxicity

- Carcinogenicity

- Human carcinogenicity data

. Several related studies have investigated mortality as well as cancer incidence among chemical manufacturers. These have mostly been carried out within a multicentre international collaborative study as well as a case–control study. Of note, there have been another two studies on locations where chlorophenols were used; the first on sawmills in Canada and the second on leather tanneries in Sweden. Further to this, chlorophenols and their relationships to thyroid cancer, nasal and nasopharyngeal cancer, colon cancer, liver cancer, soft-tissue sarcoma and non-Hodgkin lymphoma have also been investigated through case–control studies with significant associations being revealed. (ATSDR,1999). However, of these studies, it is the findings of the latter two – soft-tissue sarcoma and non-Hodgkin lymphoma – that have been the most consistent. It is possible that the odds ratios in some case–control studies had been inflated by recall bias; however, this does not adequately explain all of these findings. Chance is also very unlikely to have played a part. Despite this, a confounding effect of polychlorinated dibenzo-*para*-dioxins which occur as contaminants in chlorophenols cannot be ruled out (IARC,1999).

- Animal carcinogenicity data

Animals have experienced adverse or negative health effects after being exposed to food or drinking water containing large amounts of chlorophenols, with the liver and the immune system suffering the greatest damage. Of further note, it was found that the weight of animals consuming chlorophenols did not increase as much as those that consumed food or water without chlorophenols being present (IARC,1999).

Table 2.3 Results of carcinogenicity studies of 2,4-dichlorophenol (National Toxicology Program, 1989)

Animal species	Administration method	Administration period	Dose	Results	References
Mouse (B6C3F, male and female) 50 mice/group	Feeding	2 years	0, 5,000, 10,000 ppm (Male: Corresponding to 0, 800 and 1300 mg/kg/day, Females: Corresponding to 0, 430 and 820 mg/kg/day	Suppression of body weight gain in females in the 10,000 ppm group. Appearance of multinuclear hepatocytes in males in all treated group (control group: 11/50, 5,000 ppm group: 33/49, 10,000 ppm group 42/48). No evidence of carcinogenicity.	NTP, 1989
Rats (F344, male and female) 50 rats/group	Feeding	2 years	Male: 0, 5,000, 10,000 ppm (Corresponding to 0.210 and 440 mg/kg) Females: 0, 2,500, 5,000 ppm (Corresponding to 0, 120 and 250 mg/kg)	Suppression of body weight gain in both sexes in the highest dose group. Decrease in incidence of mononuclear cell leukemia (control group: 62%, treated group: 34%, background data: 36.3%). No evidence of carcinogenicity.	NTP, 1989

As can be seen from the above table, although no incidences of cancers or tumors were discovered among rats and mice fed high doses of 2,4-dichlorophenol for substantial periods of time, it was different for high doses of 2,4,6-trichlorophenol within the same time periods. The rats and mice were administered the substance orally with the former species developing leukemia and the latter liver cancer. One study on mice and rat in a screening test for lung tumours, there was increased the incidences of benign and malignant tumours of the liver of mice and mononuclear cell leukaemia in rats, but all of them was no lung adenomas in mice. Another separate study involved screening test for lung tumours and again involved the same two species, with the mice benign and malignant tumours in the liver did increase; however, there were no lung adenomas. For the rats, there was a reported increase in mononuclear cell leukaemia. According to the findings of the study, it was indicated that 2,4,6-trichlorophenol could be carcinogenic (ATSDR and EPA, 1999).

As concerns humans and the carcinogenicity of combined exposures to polychlorophenols, the evidence remains insufficient and inconclusive. Regarding tests on animals, the evidence has so far pointed to 2,4-dichlorophenol lacking carcinogenicity. With the carcinogenicity of 2,4,6-trichlorophenol the evidence is also limited; however, the evidence has proven sufficient as regards the carcinogenicity of pentachlorophenol. Considering the above-mentioned evidence, it can be surmised that combined exposures of polychlorophenols are possibly carcinogenic to humans (Group 2B). Both the Department of Health and Human Services and the Environmental Protection Agency (EPA) have come to the similar conclusion that 2,4,6-trichlorophenol can reasonably be anticipated to be a carcinogen. As a group, chlorophenols have been determined by the International Agency for Research on Cancer (IARC, 1999) to be possibly carcinogenic to humans (Group 2B).

2.2.1.4 Exposure

Chlorophenols are usually released into the environment during their use as pesticides or in their production, mainly by penetrating water and to a much lesser extent by being released into the air. Due to their high volatility, those compounds most likely to be released into the air are mono- and dichlorophenols where they are destroyed partly through sunlight and washed out from the air by rain. As for soil and sediment in water bodies, microorganisms break down the small quantities of chlorophenols that stick there over a duration of a few days or weeks at the maximum (ATSDR, 1999).

Humans come into contact with very low levels of chlorophenols in drinking water disinfected with chlorine. In this chlorinated drinking water chlorophenols are measured in parts per trillion concentrations. In lakes, rivers, and streams, chlorophenols were found in less than 1 percent of the water that was tested. Chlorophenols have been measured in city air at concentrations of less than a part per trillion. In urban areas, chlorophenol concentrations constitute less than a part per trillion in the air while for lakes, rivers, and streams, the amount came to less than 1 percent of the water tested. Although there are no estimates for the exposure by people at work to most chlorophenols, there is data for 4-chlorophenol, 2,4,5-trichlorophenol, or 2,4,6-trichlorophenol. From 1981-1983, the National Occupational Exposure Survey (NOES) concluded that about 5,000 people in the United States are exposed to these three particular substances. Unsurprisingly, those specifically involved in the use or production of chlorophenols or in their use as pesticides are most likely to have high exposure to these chemicals. One such example is that of sawmills where the wood preservatives used are mixtures of tetrachlorophenols which and are more likely to come into contact with the skin. Another probable means of exposure is through the inhalation of mono- and dichlorophenols in the air (ATSDR, 1999).

2.2.1.5 Environmental levels

Residues of all chlorophenol isomers have been detected in measurable concentrations in aquatic systems. In general, they are present in discharges from a variety of sources like, for instance, wood-treatment facilities, manufacturing plants, municipal waste discharges, and in the receiving water adjacent to these sources.

One study was conducted into the chlorophenols in sewage, stream water and tap water in the vicinity of Seoul in South Korea from January to September 1979. Chlorinated phenols can be produced by the chlorination of phenol with hyperchlorite in water. The chlorophenols identified in the tap water in the Korean study were as follows: *o*-chlorophenol 0.042 ppb; 2,6-dichlorophenol 0.033 ppb; 2,4-dichlorophenol 0.003 ppb.

Regarding drinking water, federal studies of finished drinking water have found 2,4-dichlorophenol to be present in 17.2% of ground water supplies. In one study of 40 potable water treatment facilities in Canada between October, 1984 and July 1985, from a total of 480 samples 2,4-dichlorophenol was detected in 8 raw water samples and 26 treated water samples. The maximum concentrations came to 17 and 72 ng L^{-1} in raw and treated water, respectively.

As concerns research into surface water, the USEPA STORET database found that of 876 effluent reporting stations 2,4-dichlorophenol was positively detected in 0.4% of them at a median level of below 10 ppb. In August 1978, water samples were taken from the Weser estuary in Germany and 2,4-dichlorophenol (plus 2,5-dichlorophenol) levels of 1.8 ug kg^{-1} were detected, while in the same year a 2,4-dichlorophenol level of 0.45 ppb was found in the Rhine River. In the Rhine at Lobith, Netherlands in 1976 and 1977, maximum levels reached 0.59 and 0.35 ppb for each year.

Over the period between October 1981 and March 1983, groundwater was taken from two wells nearby an unused creosote facility in Texas; 6 of the 10 samples contained 2,4-dichlorophenol (concentration of 3.2-79.7 ppb)). In addition, research into the groundwater in one Australian quarry revealed 2,4-dichlorophenol to be resent. This was linked to the fact that the site had been used for organic waste dumping.

As concerns seawater, samples were taken from the Gulf of Bothnia in Sweden on September 13, 1982 and November 3, 1983 with 2,4-dichlorophenol levels found to be present at 2-400 ng L^{-1} Effluent discharges from a sulfate pulp mill were believed to be behind the discovery of chlorophenols in the seawater .

As for rain and snow, between February and April 1984 monitoring was carried out into the rainwater in Portland, Oregon, revealing an average 2,4-dichlorophenol concentration of 1.3 ng L^{-1} (range of 0.56-2.5 ng L^{-1}). In February and April 1982, levels of 0.55-20 ng L^{-1} were also recorded for rainwater collected in suburban Beaverton in Oregon

Regarding effluent a major component of pulp mill effluents is the 2,4-dichlorophenol formed during the multi-step bleaching of cellulose for the removal of colored lignin constituents. The US EPA STORET database shows that among 1319 effluent reporting stations 2,4-dichlorophenol was positively detected in 3.0% of them at a median level less than 10 ppb. Samples from waste liquors from Finnish pulp mills taken in 1983 revealed levels of 2,4-dichlorophenol at 2-11 ng L^{-1}, while samples from two municipal refuge incinerators gave levels of 234 and 570 ng L^{-1} in the combusted ash. In coal-fired power plants a 2,4-dichlorophenol concentration of 0.1 ng g^{-1} was detected in particle effluents. Finally, 2,4-dichlorophenol has also been detected in combustion effluents from the combustion of municipal solid waste, peat, and wood wastes. .

2.2.1.6 Environmental considerations of chlorophenols

Making up a group of organic substances chlorophenols are released into the environment as a consequence of man-made activities. Examples include the unregulated use of wood preservatives and waste incineration as well as pesticides, fungicides and herbicides. Chlorophenols are also released as by-products from the processes of pulp being bleached with chlorine and in the disinfection of drinking water by chlorination (Ahlborg and Victori, 1987).

The bactericidal activities present in all chlorophenols increase with the degree of chlorination. Most plants are very sensitive to the phytotoxicity of chlorophenols and, in fact,chlorophenols are highly toxic to algae. As for aquatic life, these animals are normally exposed to chlorophenols through their gills, skin or gastrointestinal tracts. It is the recommendation of the EPA that 2,4-dichlorophenol concentration in surface waters reach no more than a maximum average of 2.02 mg.L^{-1}.

In the aquatic environment, chlorophenols may be found in a variety of forms; adsorbed on suspended inert solid or benthic sediments, dissolved in a free or complex form, or even present in biological tissues. Volatilization transfers the chlorophenol from water to air but does not otherwise affect it. Biodegradation is the principal means by which chlorophenols are removed. It must be induced because the antimicrobial activities of these products require that the bacteria to adapt. Chlorophenols are mainly removed through biodegradation, a process which needs to be induced as the antimicrobial activities of these products require bacteria to adapt. Although chlorophenol is transferred from the water to the air through volatilization, it does not have any other effect upon it.

2.3. Triclosan

Triclosan (2,4,4'-trichloro-2'-hydroxydiphenyl ether, TCS) is a chlorinated phenoxyphenol. Demand for hygienic products among the public has increased and consequently this chemical has many everyday uses and applications these include household cleaners in addition to textiles and plastics applications, like sportswear, shoes, carpets, and pizza-cutters (Okumura and Nishikawa, 1996; Schweizer, 2001; McAvoy et al., 2002; Singer et al., 2002). The substance has also been employed as an antimicrobial or antibacterial agent in a diverse range of personal hygiene and beauty products, including cosmetics, shampoos, soaps, creams and mouthwashes. Triclosan has a low water solubility of approximately 2000–4600 μg L^{-1} at 25 ^{0}C. It has a molecular weight of 289.6 and a high octanol/water partitioning coefficient (log10 K_{OW}) of 4.8 at neutral pH, indicating a significant potential for particle sorption. Its trichlorinated binuclear aromatic structure is similar in several ways to dioxins (Latch et al., 2003), which suggests potentially problematic properties such as persistence and bioaccumulation. Figure 2.2 provides the chemical structure of triclosan. The extended environmental half-life of triclosan is in the range of 540 d upon deposition in aquatic sediment according to quantitative structure activity relationship (QSAR) models.

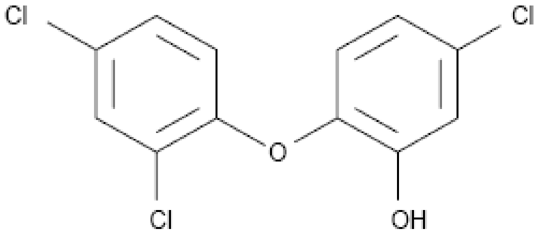

Figure 2.2 Chemical structure of triclosan. (Latch et al., 2003)

In Europe, the current use of triclosan as an antimicrobial substance in several products amounts to around a total of 350 tons (Singer et al., 2002). Triclosan exhibits a broad spectrum of bacteriostatic activity against gram-negative and gram-positive bacteria, molds, and yeasts even at levels of 0.1–0.3% (w/w) (McAvoy et al., 2002). Furthermore, it has more recently been found that by specifically inhibiting the enoyl-acyl carrier protein reductase, lipid biosynthesis is blocked by triclosan (Heath et al., 1999; Levy et al., 1999; Tixier et al., 2002). The pathway is an attractive target for development as antibacterial substances due to the important role of fatty acid biosynthesis in cell growth and function. Following extensive testing, the concentrations in consumer products have found to be safe for human contact with the substance proven to not be acutely toxic or irritating to the eyes and skin.. Due to its decades-long usage in personal care products together with the extensive data collected on its safety, triclosan as an antimicrobial or antibacterial agent has been considered safe for human use and contact. However, because of the common usage of triclosan in a variety of everyday products, the substance has been discharged into surface waters via wastewater treatment plants.

Triclosan has been found as a contaminant of rivers and lakes (Latch et al., 2003). The substance has been discovered to occur in the environment and has even been detected in coastal water (Hua, Bennett, and Letcher, 2005). As previously mentioned, every year about 350 tonnes of triclosan are produced in Europe for commercial applications (Singer et al., 2002). As a compound, triclosan is relatively stable and lipophilic. Most triclosan is released into sewer systems and then transported to wastewater sewage treatment plants due to its being a common constituent of consumer products. Of interest is the spike in the usage of household cleaning agents containing triclosan in Hong Kong following the widely publicized SARS (severe respiratory syndrome) outbreak in 2003 (Yu et al., 2006). Triclosan has been detected in sewage sludge, discharge effluent, receiving surface waters and sediments (Okumura, and Nishikawa, 1996; Hua, Bennett, and Letcher, 2005). This compound has also been found in rivers, lakes and the open sea at ng L^{-1} levels (Kolpin et al., 2004; Thomas, and Foster, 2004; Kolpin et al., 2002). Triclosan and its toxicity with regard to humans has long been a focus of research with mild itching and allergic redness on sensitive skin being listed among the adverse effects. Being such relatively mild reactions, triclosan is generally considered a low toxicity chemical (Lindström et al., 2002; Tixier et al., 2002).

More recently, because of the similarity in their chemical structure to highly toxic contaminants such as dioxins, triclosan and its degradation products have come under the greater scrutiny. It has been suggested by recent research that through cyclization triclosan can form 2,8-dichlorodibenzo-*p*-dioxin (2,8-DCDD) in an aqueous solution under UV irradiation (Latch et al., 2003). Furthermore, chlorinated derivatives converted to chlorinated dioxins upon heating and UV irradiations are produced by triclosan being easily chlorinated by sodium hypochlorite solution. In addition, 2,4-dichlorophenol and 2,4,6-trichlorophenol have been detected as the degradation products of triclosan in water with the presence of low concentrations of free chlorine or in chloraminated waters. Consequently, to support investigations into triclosan and its environmental outcome, it is important that sensitive and selective analytical methods be developed.

Triclosan removal using trickling-filter treatment ranges from 58% to 86% compared to the roughly 96% using activated- sludge treatment (McAvoy et al., 2002). Subsequently, triclosan has often been detectable in the aquatic environment, for example in wastewater (0.07–14000 μg L^{-1}), in seawater (50–150 ng L^{-1}), and in sediments (1–35 μg kg^{-1}) (Lopez- Avila and Hites, 1980; Okumura and Nishikawa, 1996; Lindstrom et al., 2002; McAvoy et al., 2002; Singer et al., 2002). Arising from the extensive application and high levels of triclosan in wastewater, the degradation of the substance into toxic compounds is becoming increasingly problematic. As textile products are treated with sodium hypochlorite (a domestic bleaching agent), or as chlorine is used in wastewater treatment plants, any triclosan at that moment present could become chlorinated at the ortho- and para-positions relative to the –OH to produce 3-chlorotriclosan, 5-chlorotriclosan and 3,5-dichlorotriclosan (Okumura and Nishikawa, 1996). It has been shown that triclosan and the chlorinated triclosans have undergone both thermal and photochemical ring closure to form a variety of toxic compounds like, for example, polychlorinated dibenzo- p-dioxins (PCDDs) (Okumura and Nishikawa, 1996; Latch et al., 2003; Aguera et al. 2004; Mezcua et al., 2004; Morrall et al., 2004). Due to the potential of triclosan, given certain conditions, to transform into dioxins, the development of practical removal means is essential. This is despite the fact that triclosan itself is considered to be low in toxicity.

Viewed as a “down the drain” contaminant, research has shown that triclosan passes through domestic sewage to municipal wastewater treatment plants (WWTPs), and from there this bactericide is finally discharged in wastewater effluents into the aquatic environment (Hua, Bennett, and Letcher, 2005; Singer et al., 2002; Lindstrom et al., 2002). In a survey conducted on US streams, triclosan was among the most frequently detected organic pollutants. In a recent finding, Halden and Paul (Halden, and Paul, 2005) observed triclocarban to be a co-contaminant with triclosan both surface water and wastewater. As it appears that triclocarban is more persistent than triclosan in WWTPs the former substance could have the greater potential for contamination of surface water, (Heidler et al., 2006; Thrall, 2006). Triclosan has been shown to be acutely toxic to aquatic organisms, especially to algal species (Orvos et al., 2002), while was also having been recently shown to modulate thyroid function in amphibians at concentrations as low as 0.15 μg L^{-1}. In addition, triclosan has been shown to phototransform into chlorinated dibenzodioxins (Mezcua et al., 2004). The effects upon the environment from the release of these two bactericidal compounds from wastewater treatment plants is the subject of much concern. At the heart of this is the fact that the potential toxicity of triclocarban has been largely unascertained with few evaluations having been carried out. Triclosan and triclocarban are both relatively hydrophobic, with estimated log octanol-water partition coefficients (i.e., log K_{ow}) at neutral pH of 4.8 for triclosan and 4.9 for triclocarban (Halden, and Paull, 2005). These compounds are expected to adsorb to particulate material due to their high hydrophobicity (Halden, and Paull, 2005; Orvos et al., 2002).A significant proportion of triclosan is partitioned into sewage sludge during wastewater treatment (Singer et al., 2002; Heidler et al., 2006; Lishman et al., 2006). This compound has been shown to be relatively persistent in municipal sewage sludge despite being susceptible to microbial degradation under aerobic conditions, (McAvoy et al., 2002). Halden and Paull (Halden, and Paull, 2005) investigated the persistence of triclocarban in the environment and found it to have a half-life of 120 days in soil and 540 days in sediment. Biosolids (i.e., treated sewage sludge) are commonly applied to agricultural land for soil amendment and it is the application of contaminants in the biosolids to soils that could potentially be a worry. Triclosan has also been shown to be transported in runoff from agricultural fields amended with biosolids, which may persist for up to 266 days post-application. For these reasons, there exists the need for the evaluation of the concentrations of triclosan and triclocarban both in municipal biosolids and in agricultural soils. As concerns their molecular structure, triclosan and triclocarban are not closely related. Triclocarban is a weak base with a pK_a of 12.77 while triclosan is a phenolic compound with a pK_a of 4.5 (http: //webbook.nist.gov/chemistry). Subsequently, both compounds are commonly analyzed in environmental matrices using separate methods; however, this can involve a great deal of time.

According to the European Economic Community (EEC) Directive 76/768 (Annex VI and subsequent amendments) (European Economic Community Council Directive 76/768 EEC (Appendix VI 81976)), the use of triclocarban is permitted at a maximum concentration of 0.3% (w/w). In order to subsequently ensure that finished products adhere to the ECC legislation, analytical methods are needed to selectively and sensitively determine triclosan in complex formulations. Under isocratic and gradient conditions, triclosan in cosmetics has reportedly been determined using methods based on reversed phase liquid chromatography (HPLC).Due to cosmetics being complex in their compositions, a careful preliminary sample preparation needs to involve the careful removal of any components that potentially interfere with the analytes determination. As a rule, those methods that have been developed for screening purposes, involve solvent extraction procedures with high levels of organic solvent. The drawback of such solvent systems has been that they suffer from poor selectivity. They are also potentially responsible for the injection on column of significant amounts of lipophilic components, which are then deleterious for the analytical column performance and lifetime. However, based on supercritical fluid extraction (SFE) using carbon dioxide, an approach considered to be more selective and which allows the automation of the extraction process , has been introduced. However, this approach does involve the use of expensive SFE apparatus, which are usually not available in common quality control laboratories.

Triclosan in water has been analysed with LC–UV (Tixier et al., 2002), LC–MS (Hua et al., 2005) and GC–MS using the selected ion monitoring technique (Okumura and Nishikawa, 1996; van Stee et al., 1999; Adolfsson-Erici et al., 2002; Lindstrom et al., 2002; Singer et al., 2002). Ion trap mass spectrometry has been carried out inmass spectrometry (MS/MS) mode and utilised in the detection and quantitation of chlorinated environmental pollutants (Plomley et al., 2000; Cai et al., 2003; Ma et al., 2003). Operating in the MS/MS mode, the ion trap can monitor the product ions of the analytes with high specificity. To the best of the author's knowledge, analysis of triclosan in water by using GC–ion trap MS has not been reported.

2.4. Advanced Oxidation Processes (AOPs)

Advanced oxidation processes (AOPs) have been viewed with great interest as a promising means for the removal of organic contaminants from water. Table 2.4 shows the potential of chemical reagents for water and wastewater treatment. Common processes involved in AOPs are Fenton's reagent, ozone, ozone/H_2O_2, and UV/H_2O_2 of which the primary intermediate is the hydroxyl radicals (·OH). Advanced oxidation processes are chemical oxidation techniques able to produce in situ reactive free radicals by means of different reacting systems. The most commonly produced is the hydroxyl radical, one of the most reactive free radicals, which is short-lived, highly reactive, and one of the strongest oxidants. The kinetics of reaction is generally first order as concerns the concentration of hydroxyl radicals and the concentration of the species to be oxidized. The concentration of hydroxyl radicals falls between 10^{-10} and 10^{-12} M while rate constants lie usually within the range of 10^{8} - 10^{11} $M^{-1}.s^{-1}$. Subsequently, a pseudo-first-order constant 20 between 1 and 10^{-4} s^{-1} is obtained (Glaze et al., 1987).

There are a variety of ways AOPs are applied in treating contaminated groundwater, purifying and disinfecting drinking water and processing water, as well as destroying refractory organics in industrial water. The highly reactive hydroxyl radical species can be generated through a multitude of processes able to generate. These include heterogeneous photocatalytic, photo and non-photocatalytic homogeneous processes. In heterogeneous photolysis, in the presence of UV-A, ·OH is generated at the surface of a semiconductor (usually TiO_2). Other common photocatalytic combinations which can also generate ·OH include O_3/UV, O_3/H_2O_2/UV and H_2O_2/UV (Rodger and Bunce, 2001). However, of most interest in this study is Fenton's reagent (Fe^{2+}/H_2O_2).

2.5. Fenton Process

Of the various AOPs, the Fenton process (H_2O_2/Fe^{2+}) effectively treats various organic contaminants. “Fenton’s reagent” refers to the combination of hydrogen peroxide and a ferrous ion and the system and its reactivity was first observed by H.J.H. Fenton in 1894. However, it was not until the 1960s that its utility was recognized following the identification of its mechanisms. The process is highly advantageous in that contaminants are completely broken down into harmless compounds, e.g. CO_2, water and inorganic salts. The result of the Fenton reaction is the dissociation of the oxidant and the formation of highly reactive hydroxyl radicals which, under atmospheric pressure and room temperature, then attack and destroy the organic pollutants (Neyens and Baeyens, 2003),. Despite all this, this homogeneous process does have drawbacks by way of its limited range of pH (3-5), in which the reaction takes place as well as the recovery of iron species.

2.5.1. Hydrogen Peroxide

2.5.1.1. General Information

Hydrogen peroxide, a ubiquitous compound present in natural water, was discovered by L.J. Therald in 1818. Although in its pure state it is fairly stable, it decomposes into water and oxygen when heated to around $60^{o}C$ and above. An advantage of the decomposition of hydrogen peroxide is that aerobic biological activity can be stimulated by the released oxygen. Hydrogen peroxide also decomposes in the presence of numerous catalysts, such as most metals, acids, bases, salts of metals, reducing agents, oxidizable organic materials, or flammable substances. The commercial preparation of hydrogen peroxide is carried out through the oxidation of alkylhydro-anthraquinones or by electrolysis of ammonium bisulfate, as well as by the reaction of barium peroxide with sulfuric acid or (with acetone) by oxidation of isopropanol.

An aqueous solution of hydrogen peroxide is primarily employed in oxidation reactions, including the blenching process, chemical syntheses, and for water and wastewater treatment, hydrogen peroxide is used to pre-oxidize organic constituents and to eliminate iron and manganese ions in the purifying of drinking water.

2.5.1.2. Physical and Chemical Properties

Hydrogen peroxide as an aqueous solution is clear, colorless and water-like in appearance and nonflammable. It is miscible with cold water and is soluble in alcohol and ether. At high concentrations, the substance has a slightly pungent or acidic odor. The chemical formula for hydrogen peroxide is H_2O_2 and its molecular weight is 34.015 g mole^{-1}.

2.5.1.3. Toxicology Information

According to US regulations, no concentration of H_2O_2 is listed as a regulated substance (i.e., a persistent environmental hazard) in the Comprehensive Environmental Response Compensation and Liability Act (CERCLA). This is also the case for the standard industrial strength of hydrogen peroxide (that < 52% wt.) covered under Federal Risk Management guidelines. However, local response agencies may require a Hazardous Materials Inventory Statement (HMIS), in other words a hazardous material permit, , depending on factors such as the concentration, volume, and location of the stored hydrogen peroxide. If hydrogen peroxide enters the environment, it decomposes into oxygen and water with concurrent heat generation.

Table 2.4 Oxidation-Reduction Potentials of Chemical Reagents for Water and Wastewater Treatment

Reaction	Potential in Volts (E^0) at 25 °C
$F_2 + 2e^- = 2F^-$	2.87
$\bullet OH + H^+ + e^- = H_2O$	2.33
$FeO_4^{2-} + 8H^+ + 3e^- = Fe^{3+} + 4H_2O$	2.20
$O_3 + 2H^+ + 2e^- = O_2 + H_2O$	2.07
$H_2O_2 + 2H^+ + 2e^- = 2H_2O_2$ (acid)	1.76
$MnO_4^- + 4H^+ + 3e^- = MnO^2 + 2H_2O$	1.68
$HClO_2 + 3H^+ + 4e^- = Cl^- + 2H_2O$	1.57
$MnO_4^- + 8H^+ + 5e^- = Mn^{2+} + 4H_2O$	1.49
$HOCl + H^+ + 2e^- = Cl^- + H_2O$	1.49
$Cl_2 + 2e^- = 2Cl^-$	1.36
$HOBr + H^+ + 2e^- = Cl^- + H_2O$	1.33
$O_3 + H_2O + 2e^- = O_2 + 2OH^-$	1.24
ClO_2 (gas) $+ e^- = ClO_2^-$	1.15
$Br_2 + 2e^- = 2Br^-$	1.07
$HOI + H^+ + 2e^- = I^- + H_2O$	0.99
$ClO_2(aq) + e^- = ClO_2^-$	0.95
$ClO^- + 2H_2O + 2e^- = Cl^- + 2OH^-$	0.90
$H_2O_2 + 2H_3O + 2e^- = 4H_2O$ (basic)	0.87
$ClO_2 + 2H_2O + 4e^- = Cl^- + 4OH^-$	0.78

Source: Lide, D.R. et al., CRC Handbook of Chemistry and Physics, 73rd ed., CRC Press, Boca Raton, FK, 1992.

2.5.2. Fenton Reaction

In the Fenton process, H_2O_2 is decomposed by Fe^{2+} to produce highly reactive hydroxyl radical as expressed by equation (2.1)

$$Fe^{2+} + H_2O_2 \longrightarrow Fe^{3+} + \bullet OH + OH^- \qquad (2.1)$$

In addition to being capable of degrading many solvents, haloalkanes, esters, aromatics and pesticides, the hydroxyl radical can non-selectively attack the C-H bonds of organic molecules (Haag and Yao, 1992). According to Huang et al. (1993), the major benefits of using Fenton's process over other oxidation processes in the treatment of hazardous wastes are:

1) No chlorinated organic compounds are formed throughout the oxidation process as in chlorination.
2) Both iron and hydrogen peroxide are inexpensive and non-toxic.
3) Since the reaction is homogeneous, there are no mass transfer limitations.
4) The design is far simpler than ultraviolet light systems as no light is required as a catalyst.
5) Hydrogen peroxide can be electrochemically generated in situ, potentially increasing the economic feasibility and effectiveness of the process in the treatment of contaminated sites.

The hydroxyl radical generated under acidic conditions and with an excess of ferrous ion can further react with ferrous ion and thereby produce ferric ion:

$$Fe^{2+} + \bullet OH \longrightarrow Fe^{3+} + OH^- \qquad (2.2)$$

Through the appropriate control of the experimental conditions, ferric ion can be regenerated back to ferrous ion in a subsequent reaction with another molecule of hydrogen peroxide:

$$Fe^{3+} + H_2O_2 \longrightarrow Fe\text{-}OOH^{2+} + H^+ \qquad (2.3)$$

$$Fe\text{-}OOH^{2+} + H^+ \longrightarrow Fe^{2+} + HO_2\bullet + H^+ \qquad (2.4)$$

The $HO_2\bullet$ radical produced has been shown to also participate in the oxidation of some organic compounds, although they are much less reactive than hydroxyl radical. The reaction of hydrogen peroxide with ferric ion is referred to as a Fenton-like reaction (equation (2.3) and (2.4)) (Walling and Goosen, 1973; DeLaat and Gallard, 1999).

$$\bullet OH + H_2O_2 \longrightarrow H_2O + HO_2\bullet \qquad (2.5)$$

$$Fe^{2+} + HO_2\bullet \longrightarrow Fe^{3+} + HO_2^- \qquad (2.6)$$

$$Fe^{3+} + HO_2\bullet \longrightarrow Fe^{2+} + O_2 + H^+ \qquad (2.7)$$

As seen in equation (2.5), H_2O_2 can act as an $\bullet OH$ scavenger as well as an initiator (equation (2.1)) and it will produce $HO_2\bullet$ that can react with ferrous to reduce the removal efficiency.

Organics (RH) can be oxidized by hydroxyl radicals through the abstraction of protons producing organic radicals (R•). These radicals are highly reactive which can then be further oxidized (Walling and Kato, 1971; Venkatadri and Peters, 1993; Lin and Lo, 1997).

$$RH + \bullet OH \longrightarrow H_2O + R\bullet \longrightarrow \text{further oxidation} \qquad (2.8)$$

The organics can be completely detoxified by a full conversion to CO_2i water if there is no limit to the concentrations of the reactants are not limited, Also, in the case of substituted organics, inorganic salts if the treatment is continued.

By taking dissociation water into account, Walling (1975) simplified the overall Fenton chemistry (reaction (2.1))

$$2Fe^{2+} + H_2O_2 + 2H^- \longrightarrow 2Fe^{3+} + 2H_2O \qquad (2.9)$$

This equation suggests that the presence of H^+ is required in the decomposition of H_2O_2. Therefore, this indicates that in order to produce the maximum amount of hydroxyl radicals, there is the need for an acidic environment. From previous Fenton studies, it has been established that for Fenton oxidations an acidic pH near 3 is usually the optimum level (Hickey et al., 1995). Hydroxyl radicals In the presence of organic substrates (RH), excess ferrous ion, and at low pH can also add to the aromatic or heterocyclic rings in addition to the unsaturated bonds of alkenes or alkynes. .A hydrogen atom can also be abstracted, thereby initiating a radical chain oxidation (Walling, 1975; Lipczynska-Kochany et al., 1995)

$$RH + \bullet OH \longrightarrow H_2O + R\bullet \qquad (2.10)$$

$$R\bullet + H_2O_2 \longrightarrow ROH + \bullet OH \qquad (2.11)$$

$$R\bullet + O_2 \longrightarrow ROO\bullet \qquad (2.12)$$

The organic free radicals produced in equation (2.10) can then be reduced by Fe^{2+}, oxidized by Fe^{3+}, or dimerised according to the following reactions (Tang and Tassos, 1997):

$$R\bullet + Fe^{3+}\text{-oxidation} \longrightarrow R^{+} + Fe^{2+} \qquad (2.13)$$

$$R\bullet + Fe^{2+}\text{-reduction} \longrightarrow R^{-} + Fe^{3+} \qquad (2.14)$$

$$2R\bullet\text{-dimerisation} \longrightarrow R - R \qquad (2\text{-}15)$$

The sequence of equations (2.1), (2.2), (2.10) and (2.13) comprise the present accepted scheme for Fenton’s reagent chain.

Depending on the $H_2O_2/FeSO_4$ ratio, Fenton’s reagent has differing treatment functions. When the amount of Fe^{2+} used is more than that of H_2O_2, the treatment has a tendency to have a chemical coagulation effect, while when there is a reversal on the two amounts, the treatment tends to have a chemical oxidation effect.

2.6. Electro-Fenton Process

Research has been conducted into another wastewater treatment method more recently; one which employs electrochemically generated hydroxyl radicals. Among the differing techniques employed for wastewater treatment, electrochemical methods have established themselves as relevant. The mineralization of toxic and biorefractory organic pollutants to carbon dioxide, water, and inorganic ions can be produced by anodic oxidation or indirect electro-oxidation. As regards electro-oxidation, the water oxidation produces hydroxyl radicals which are then adsorbed on the anode (Pt, PbO_2, doped SnO_2, bboron-doped dimond, etc.) (Casado et al, 2005). One advantage of electrochemical techniques is that they are more environmentally friendly than the typical chemical methods used in polluted water treatment. One of these techniques is the electro-Fenton process. This process is based on the use of an undivided electrolytic cell which contains an anode and a cathode where H_2O_2 is electro generated via two-electron reduction of O_2 at the cathode. Following the addition of Fe^{2+} to the solution, pollutants can be mostly destroyed by the •OH, produced via the Fenton reaction. Fe^{3+} can be continuously transformed to Fe^{2+} via one-electron reduction at the cathode. The reduction of Fe^{3+} to Fe^{2+} is more efficient and rapid when electricity is employed in the process, with the reaction rate subsequently increasing.

Varying in accordance with the objective of current supply, the electro-Fenton process can be typically divided into three groups

The first of these (EF-H_2O_2 method) uses both Fe^{2+} and electro-generated H_2O_2 that can be produced from the two-electron reduction of sparked oxygen on graphite, reticulated vitreous carbon, or carbon-PTFE cathodes, when O_2 is reduced to H_2O_2 on cathode, while simultaneously resulting in the reduction of some reducible substances. This direct cathode reduction may represent one possible pathway for the degradation of the substances, particularly when reducible compounds such as nitrophenols are present. This direct cathode reduction is just one possible pathway for the degradation of the substances. This is especially the case when there is the presence of reducible compounds like nitrophenols. Despite this, there has been little written or researched about how cathode reduction contributes to the degradation of pollutants in the electro-Fenton process. It is known, however, that one of its drawbacks is its low current efficiency in acidic conditions (Sudoh et al., 1986; Tzedakis et al., 1989; Hsiao and Nobe, 1993; Brillas et al., 1996).

On Cathode Side:

$$O_2 + 2H^+ + 2e^- \longrightarrow H_2O_2 \qquad (2.16)$$

On Anode Side:

$1/2O_2 + H_2O \longrightarrow 2{\bullet}OH$ (2.17)

The second group (EF-FeOx method) utilizes the H_2O_2 and electro-generated Fe^{2+} produced via the oxidation of a sacrificial iron anode which is used as Fe^{2+} source. Furthermore, depending on the setup of the electrolytic cell, Fe^{2+} can continuously be regenerated at cathode. The applications of this process include the detoxification of herbicide, pesticide and insecticide containing wastewater. Like Fenton's reagent, however, this method also encounters the same limitations. In Brillas et al's use of this process to treat aniline and 4-chlorophenol containing wastewater, most of the TOC was surprisingly removed by $Fe(OH)_3(s)$ precipitate and not organic mineralization as was expected. The oversupply of current density resulted in the production of a large amount of iron sludge (Pratap and Lemley, 1994; Brillas et al., 1998; Huang et al., 1997).

The final group is referred to as the Fenton sludge recycling (FSR) system. In order to reduce the ferric hydroxide sludge to ferrous ion, the FSR system employs a Fenton reactor and electrolytic cell (Gnann, 1993). In this system, through the use of an electron supplied from electrical current, Fe^{3+} can be directly reduced to Fe^{2+} more effectively and at a faster rate, as shown in equation (2.18). It is followed the promotion of the hydroxyl radical generation rate and then the organic decomposition rate in that order (Anotai et al., 2006).

On Cathode Side:

$Fe^{3+} + e^- \longrightarrow Fe^{2+}$ (2.18)

$H_2O + e^- \longrightarrow 1/2H_2 + OH^-$ (2.19)

On Anode Side:

$Fe^{2+} \longrightarrow Fe^{3+} + e^-$ (2.20)

$H_2O \longrightarrow 2H^+ + 1/2O_2 + 2e^-$ (2.21)

In the following equations, the radicals $\bullet OH$, $OH_2\bullet$, and $OH_2\bullet^-$ are consumed and regenerated in the reaction system, which is influenced by H_2O_2, Fe^{2+}, and Fe^{3+} as shown in Figure 2.3 and equations (2.22) to (2.27). Following the introduction of electricity in the process, the reduction of Fe^{3+} to Fe^{2+} becomes more efficient and rapid, thereby increasing the reaction rate. Researchers make further use of low pH and anaerobic conditions in the prevention of the oxidation of ferrous ion. However, the solution pH needs to be maintained at an optimum pH values, otherwise a very low pH will result in a decreasing reaction rate and therefore affect the efficiency of the hydrogen peroxide decomposition to hydroxyl radicals.

$$Fe^{2+} + H_2O_2 \longrightarrow Fe^{3+} + OH^- + \bullet OH \qquad (2.22)$$

$$\bullet OH + \text{Organic} \longrightarrow \text{Products} \qquad (2.23)$$

$$Fe^{3+} + H_2O_2 \longrightarrow FeOOH^{2+} + H^+ \qquad (2.24)$$

$$FeOOH^{2+} \longrightarrow Fe^{2+} + OH_2\bullet \qquad (2.25)$$

$$Fe^{2+} + OH_2\bullet \longrightarrow Fe^{3+} + OH_2\bullet^- \qquad (2.26)$$

$$Fe^{3+} + OH_2\bullet^- \longrightarrow Fe^{2+} + O_2 + H^+ \qquad (2.27)$$

Iron salt acts as a catalyst for hydrogen peroxide decomposition with further reactions (2.24) and (2.25) regenerating Fe^{2+}. In addition to free radical scavengers, the process is inhibited by (iron) chelants such as phosphates, EDTA, formaldehyde, and citric/oxalic acids. As Fenton’s reagent is sensitive to different wastewaters, before they proceed to plant scale reactions should always be characterized through laboratory treat-ability tests.

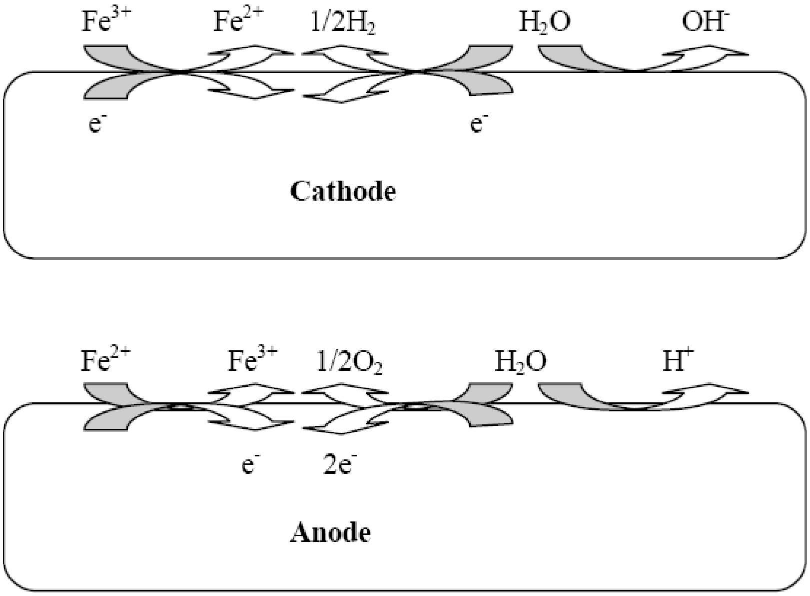

Figure 2.3 Electro-Fenton reactions (Ferrous Regeneration System)

The electro-Fenton process has proven capable through its more than 90% COD removal of solutions containing phenol, aniline, acetic acid, formaldehyde, three azo dyes, and other organics. The current efficiencies are greater than 50% while the energy consumptions are also at acceptable levels.

2.7. Literature Reviews

2.7.1 Degradation of 2,4-dichlorophenol.

Doocey et al. (2004) studied of the zeolite-mediated using model of chlorinated phenolic aqueous waste of advanced oxidation. They investigated the adsorption of 2,4-dichlorophenol (2,4-DCP) in aqueous solution onto zeolites Beta and Y at 20°C. The same team also looked into the Fenton oxidation of 2,4-DCP without zeolite at a pH level of 3.5. Further research was also conducted intothe effect of model inorganic and organic “scavengers” on the adsorption process using 0.1 M sodium sulphate and 1% and 10% acetone as the “scavengers”. The study found Fenton’s reagent to be an effective advanced oxidation process for treatment of 2,4-DCP in an aqueous water stream. In addition, through the effective elimination of the “scavenger” effects, the advanced oxidation process was made more efficient through the use of Zeolites Beta and Y as effective selective adsorbents. Despite having a lower adsorption capacity than Y, Beta exhibited the preferred adsorption behavior in addition to being a successful adsorbent in an adsorption column for 2,4-DCP in an aqueous waste stream. This zeolite was also successfully regenerated through the use of Fenton's reagents.

Momani et al. (2004) focused on AOPs and the degradation of 2,4-dichlorophenol by UV, UV/H_2O_2, Fenton and photo-Fenton processes, specifically assessing the factors of different reactant concentrations, pH, temperatures and irradiation times Their results indicated that among the AOPs, UV photolysis was less efficient as concerned total DCP degradation, while the photo-Fenton and Fenton reactions were both successfully used . Many factors - initial iron concentration, initial hydrogen peroxide concentration, initial DCP concentration, temperature and pH - influenced degradation rate . As for the photo-Fenton reaction, this proved to be the most effective in eliminating DCP, in releasing chlorine ions as well as in changing oxidation state. A 100% removal rate of DCP was achieved after 60 minutes of treatment using 75 mg L^{-1} H_2O_2 and 10 mg L^{-1} Fe(II) initial concentrations. It was also under these conditions that a first-order degradation constant for DCP of 0.057 min^{-1} was obtained.

Li et al. (2007) focused on the use of a hybrid oxidation process in the degradation of 2,4-dichlorophenol in aqueous solution. The process comprised the following three functional electrodes: a TiO_2/Ti sheet as the anode, a steel (Fe) sheet as another anode in parallel and a piece of graphite felt (GF) as the cathode. The electro-Fenton and photoelectrocatalytic (PEC) reactions are involved at the same time as the application of an electrical current between the Fe anode and the GF cathode and the irradiation of the UV light on the surface of the TiO_2/Ti anode. After 60 minutes, this hybrid oxidation process achieved a successful degradation of the 2,4-DCP in the aqueous solution by 93% in addition to a mineralization by 78%. Furthermore, the application of a current intensity of 3.2 mA on the GF cathode resulted in a current efficiency for H_2O_2 generation of 61%. Additionally, the two combined reactions would on a practical level be preferable for water and wastewater treatment. This is due to the process becoming less pH sensitive with potential application under more neutralized pH conditions as a result of the combination of the reactions.

Zhao at el. (2007) treated 2,4-dichlorophenol using a novel TiO_2/Ti-Fe-graphite felt photo-electrocatalytic (PEC) oxidation process. . The application of current and O_2, saw the production of H_2O_2 close to the cathode and the continuous generation of Fe^{2+} from Fe anode in solution. The process resulted in H_2O_2 conducting H_2O_2-assisted TiO_2 PEC and ferrous conducting electro-Fenton reaction. Adscititious voltage, applied current, initial 2,4-DCP concentration, pH, and flow speed of O_2 were all investigated as to the degree of their effect upon the degradation rate as well as their optimization. This integrative process worked most efficiently in a wide pH range from pH 3 to pH 9 and the degradation ratio of 2,4-DCP reached 93%. This compared to the 46% achieved by the H_2O_2- assisted TiO_2 PEC process and the 31% achieved by the electro-Fenton process. A further high point was that the whole integrative reaction abided by first-order kinetics. In sum, by combining electro-Fenton and H_2O_2- assisted TiO_2 PEC oxidation the degradation of 2,4-DCP was enhanced.

Zhou et al. (2008) carried out further research into the degradation of 2,4-dichlorophenol using ultrasound (US) enhancement in a new Fenton-like system

(Fe/EDTA). The use of US resulted in a clear synergistic effect in the system. With the same operating conditions of pH, US input power, iron and EDTA dosage, the decomposition of DCP followed the sequences of US/Fe/EDTA > Fe/EDTA > US/Fe > US alone. The degradation of DCP in US/Fe/EDTA, Fe/EDTA and US system followed pseudo-first-order kinetics with the k_{obs} being 0.0725 in US/Fe/EDTA, 0.0094 in Fe/EDTA and 0.0022 min^{-1} in the US system. DCP was completely removed after 60 minutes into the reaction while the rates for TOC and EDTA were 81% and 89% respectively. It was found that low molecular weight organic acids contributed to the solution self-buffer at about pH 6.5 together with the reaction. Furthermore, Zhou's study looked into the effect of the initial condition (DCP concentration, iron addition, US input power and EDTA dosage) as well as reaction temperature. Reaction activation energy (Ea) was also calculated.

2.7.2. Degradation of triclosan

Bester, K. (2003) do experiment in comparisons of the triclosan concentrations measured in sludge (1200 ng g^{-1}) of sewage treatment plant carrying out the daily treatment of 200,000 m^3 of wastewater in Germany. 2,4,4'- trichloro, 2'-hydroxy-phenylether (triclosan) concentrations in the in-flowing water came to ~1000 ng L^{-1} while the out-flowing water measured ~50 ng L^{-1}. The concentration of triclosan in the mass flow of water and sludge in the plant were assessed. Only small amounts were sorbed as bound residues in the sludge, thirty percent of the triclosan was sorbed with weak bonds onto the sludge with about 5% dissolved in the out-flowing water. Therefore it was concluded that most of the in-flowing material was not recovered as the parent compound. However, it was probably transformed into other metabolites or unrecovered bound residues. These findings were found to be generally larger than those for the sewage sludge from 20 other plants in the same region, the concentrations of which varied from 1000–8000 ng g^{-1}.

Chu, S and Metcalfe, C.D. (2007) simultaneously determined triclosan and triclocarban in sludge and treated biosolids from municipal wastewater treatment plants (WWTPs). Their sensitive yet accurate method involved pressurized liquid extraction

(PLE). A sample clean-up on a Oasis HLB solid phase extraction (SPE) cartridge then followed with liquid chromatography with electrospray ionization and tandem mass spectrometry (LC–ESI-MS/MS) being employed for analysis. Through the use of stable isotopes of triclosan and triclocarban as the internal standards, quantification was accurately obtained by isotope dilution. A standard addition method was employed to assess the matrix effects (ME) in spiked biosolid samples (n = 5) . For triclosan and triclocarban the mean ME values came to 79.7±6.7% and 100.5±8.4%, respectively which showed the sample clean-up method to have been effective in its removal of the interferences. Regarding triclosan, the mean recovery from the spiked biosolid sample was 97.7±6.2% with the limit of detection (LOD) at 1.5 ng g^{-1} (d.w.), while as concerned triclocarban, the mean recovery was 98.3±5% and, the LOD 0.2 ng g^{-1} (d.w.). The same method was used in three WWTPs in Ontario, Canada. The preliminary results from samples of activated sludge and treated biosolids showed triclosan and triclocarban to co-occur in municipal sludge and treat biosolids at concentrations ranging from 0.62 to 11.55 µg g^{-1} dry weights for triclosan, and from 2.17 to 5.97 µg g^{-1} dry weights for triclocarban.

Suarez et al. (2007) investigated the oxidation of the triclosan by aqueous ozone (O_3). They tried to ascertain the associated reaction kinetics, reaction site(s), and consequent changes in the antibacterial activity of triclosan. Specific second-order rate constants, k_{O3}, were examined for the reaction of O_3 with each of triclosan's acid-base species. The values of k_{O3} in anionic triclosan and neutral triclosan came to 5.1(±0.1) $\times 10^{8}$ M^{-1} s^{-1} and 1.3 (±0.1) $\times 10^{3}$ M^{-1} s^{-1}, respectively. As a result, triclosan reacted rapidly with O_3 at circumneutral pH (the pH-dependent, apparent second-order rate constant, $k_{app,O3}$, was 3.8 $\times 10^{3}$ M^{-1} s^{-1} at pH 7). The pH-dependence of $k_{app,O3}$ together with the triclosan reactivity toward O_3 compared to other phenolic compounds indicated that O_3 reacts initially with triclosan at the latter's phenol moiety. The k_{O3} values for neutral and anionic triclosan were successfully related to phenol ring substituent effects via Brown–Okamoto correlation with other substituted phenols. This was found to be consistent with the electrophilic attack of the triclosan phenol ring. In addition, the biological assay of

O_3-treated triclosan solutions indicated that the reaction with O_3 subsequently eliminated the triclosan's antibacterial activity efficiently. However, such observations needed to be assessed in terms of how they could actually apply to actual wastewater. Therefore, triclosan oxidation during the ozonation of effluent samples from two conventional wastewater treatment plants was also researched. For a 4 mg L^{-1} (8.3×10^{-5} mol L^{-1}) O_3 dose applied to a wastewater sample containing 7.5 mg L^{-1} of DOC close to 100% triclosan depletion was achieved while for a dosage of 6mg L^{-1} (1.3×10^{-4} mol L^{-1})O_3 to a wastewater sample containing 12.4mg L^{-1} of DOC triclosan depletion reached 58% . Hydroxyl radical reactions made up less than 35% of observed triclosan losses in the wastewater samples with O_3 doses greater than 1mg L^{-1} (2.1×10^{-5} mol L^{-1}). This indicated that the direct triclosan–O_3 reaction was mainly responsible for the triclosan oxidation. In conclusion, ozonation has been indicated to be an effective means of eliminating the antibacterial activity of triclosan during wastewater treatment.

The overall conclusions concerning 2,4-dichlorophenol and triclosan removal are provided in the table below:

Table 2.5 2,4-dichlorophenol and triclosan removal by various processes

Process	2,4-dichlorophenol and triclosan removal efficiency
Aerobic	>98% (but transfer to sludge)
Anaerobic	39% (in sludge) Patureau, D. et al. (2008)
AOPs	>99% (complete degrade) Inumaru, K. et al. (2004)

2.7.3. The removal of organic compound by the Fenton, and electro-Fenton Processes

Brillas et al. (1998) investigated various AOPs which are anodic oxidation, photocatalysis, electro-Fenton, and photoelectron-Fenton processes for aniline mineralization. Brillas's team researched the degradation of aniline at pH 3 under photocatalytic and electrochemical conditions. The electrochemical experiments were performed in the presence of both species (electro-Fenton conditions) resulting in the rapid mineralization of aniline which was further increased by UV-A irradiation (photoelectron-Fenton process). A general pathway for aniline mineralization was subsequently proposed in which products are formed via hydroxyl radical degradation.

Chou et al. (1999) studied the treatment of high strength hexamine contaminating wastewater by the electro-Fenton method. The performance of Fe^{2+} generation in the electrolytic system was evaluated, including the factor of cathode material, initial pH, initial ferric concentration and current density. When the pH value exceeded 2.5, the current efficiency decreased due to the formation of $Fe(OH)_3$. Between 3,000-10,000 mg L^{-1} of Fe^{2+}, the initial current efficiency of Fe^{2+} generation was almost constant (85-87%), but dropped sharply to 39% at 1,000 mg L^{-1}. The COD removal efficiency attained more than 94% after 5 hrs of reaction. The changes in hexamine and its oxidation intermediates (methanol, formaldehyde, formate, ammonium and nitrate) during the reaction were also investigated.

Oturan et al. (2001) used the electro-Fenton process for degradation of p-Nitrophenol in aqueous medium. The electro-Fenton is based on the electrocatalytical generation of Fenton's reagent to produce hydroxyl radical. The intermediates of the degradation products were hydroquinone, benzoquinone, 1,2,4- trihydroxybenzene, 3,4,5-trihydroxynitrobenzene and 4-nitrocatechol. The mineralization of the initial pollutant and the intermediates formed during electro-Fenton treatment was studied using TOC analysis. The mineralization rate was higher at the beginning of the electrolysis, but diminished with the decrease in compound concentration in the reaction mixture and with changes in their structure, such as from aromatics to aliphatics which are more resistant to mineralization by ring disrupting reactions. Under the optimum conditions, the mineralization process reached 95% removal efficiency.

Brillas et al. (2001) research through electro-Fenton and peroxicoagulation processes using a flow reactor for wastewater treatment specified in aniline degradation. An insoluble violet polymer was produced from the electro-Fenton process with 1 mM Fe^{2+} and Ti/Pt or DSA anode. At the same time, the soluble TOC reached 61% degradation after 2 hrs at 20 Amperes, indicating a gradual removal. In this experiment, Fe^{2+} reacted with H_2O_2 resulting in the formation of hydroxyl radicals formed in the solution which then oxidized the aniline. The higher degradation power of the peroxicoagulation process with a Fe anode resulted in more than 95% of the pollutants being removed at 20 Amperes.

Ventura et al. (2002) addressed the electrochemical generation of Fenton's reagent using atrazine as a model. The model was chosen due to its reaction with hydroxyl radical have been the subject of much previous study. Both the electro-Fenton and conventional Fenton processes were utilized in the degradation of atrazine, with the former proving to be the more efficient of the two. It was the first 15 minutes of degradation that were faster than at any other time in the Fenton process, which indicated that the Fenton's reagent can be electrochemically produced in aqueous solution and therefore bring about hydroxyl radical production both efficiently and continuously, with limited competitive reaction. This simple system produced ferrous iron *in situ* through ferric iron being reduced at the same time oxygen was reduced into hydrogen peroxide.

Brillas et al. (2003) employed the peroxi-coagualtion method for determined the electrochemical degradation of chlorophenoxy and chlorobenzoic herbicide in acidic aqueous medium. In an acidic aqueous medium of pH 3.0, this electrochemical method proved highly effective in degradation all compounds. The result was the substantial oxidization of target compounds by the corresponding Fe anode and O_2-diffusion cathode. Their products were then able to be removed through mineralization or both degradation paths were conducted at low currents with the decay of all herbicides following a pseudo-first-order reaction.

Anotai et al. (2006) use of the Fenton and electro-Fenton processes for investigated the degradation of aniline at pH 2. The results of the latter process proved to be better than those of the conventional Fenton process. The current impacts ranged from 1.2 to 3.1 for removal efficiency and 1.2 to 5.8 for degradation rate in relation to the initial Fe^{2+} concentration. Also, for the complete removal of 0.01 M aniline, the delay in the initial current supply could result in a total energy saving of to one-third compared to that used in the conventional Fenton process. These findings suggest that operating costs and energy consumption can be significantly reduced as obtained by the current-delay operating mode.

Yuan et al. (2006) conducted into a study of the degradation of various nitrophenols by eletro-Fenton and cathode reduction. These included: phenol (Poh), 2-nitrophenol (2-NP), 3-nitrophenol (3-NP), 4-nitrophenol (4-NP) and 2,4-dinitrophenol (2,4-DNP), cyclic voltammetry was employed to analyze the electrochemical behavior on graphite cathode and Pt anode with 4-NP as the model nitrophenol . The degradation of 4-NP was much faster in the cathode cell than in the anodic cell. The treatment of a high concentration of 4-NP in the undivided cell revealed the removal rate to be more than 98% removal of 4-NP and about 13% of the TOC obtained for both processes. Gas chromatography/mass spectrum was used to detect intermediates such as hydroquinone and benzoquinone. The degradation pathway of the 4-NP in electro-Fenton process was proposed as the reduction by the cathode was then followed by hydroxyl oxidation.

Zhang et al. (2006) studied landfill leachate removal by electro-Fenton process with a batch electrolytic reactor. The duration of the total process lasted 75 minutes, reacting very quickly in the first 30 minutes and then slowing down. As the current was increased so did the COD removal efficiency when hydrogen peroxide was applied by itself to the electrolytic reactor the COD removal was only at 65%, while the presence of ferrous ion greatly improved COD removal. As the ferrous ion dosage increased at a fixed hydrogen peroxide dosage, COD removal efficiency increased, reaching its highest level of 0.038 mol L^{-1} ferrous ion concentration.

Liu et al. (2007) developed a new kinetic model relating to the generally accepted mechanism of the electro-Fenton reaction in aqueous solution.. The model specifically accounts for the rates of hydrogen peroxide (H_2O_2) generation and consumption in the reaction solution while also embracing three key operating factors – current density, dissolved oxygen concentration and initial ferrous ion concentration – that influence the organic degradation in the E-Fenton reaction. This analytical model was then validated by experiments of phenol degradation in aqueous solution which demonstrated that the H_2O_2 gradually increased the longer the duration until it finally reached its maximum value in the reaction solution. In addition, the experiments showed that phenol was degraded at a slow rate early on in the reaction, then faster midway, before returning to a slow rate once more towards the end. All experiments showed the curves of phenol degradation (concentration vs. time) to take on an inverted "S" shape. The data from the experiments proved a good fit using both the normal first-order model and his model, respectively. The goodness of fit demonstrated that the new model better fit the experimental data than the first-order model. So, from a mathematical and chemical perspective this analytical model better describe the kinetics of the E-Fenton reaction.

Sires et al. (2007) studied the degradation of antimicrobials triclosan (2,4,4'-trichloro-2'-hydroxydiphenyl ether) and triclocarban (*N*-(4-chlorophenyl)-*N*'-(3,4-dichlorophenyl)urea) by four electro-Fenton systems using undivided electrolytic cells with a Pt or boron-doped diamond (BDD) anode as well as a carbon felt or O_2 diffusion cathode. The main oxidant was hydroxyl radical (•OH) which was produced both on the anode surface from water oxidation and in the medium by Fenton's reaction, taking place between electro-generated H_2O_2 and Fe^{2+} coming from the cathodic reduction of O_2 and Fe^{3+}, respectively. In a saturated aqueous solution of pH 3.0 the complete removal of triclosan occurred in all cells, with the decay rate decreasing in the following order: Pt/carbon felt > BDD/carbon felt > Pt/O_2 diffusion > BDD/O_2 diffusion, in agreement with their •OH generation ability from Fenton's reaction. Glyoxylic, maleic and oxalic acids were identified as aliphatic intermediates. Despite Fe^{2+}–oxalato complexes being mineralized by •OH in the medium and Fe^{3+}–oxalato complexes being destroyed by •OH on BDD, complexes between oxalic acid and iron ions largely persisted in solution. Analogous treatments of more concentrated triclosan solutions were conducted with a 20:80 (v/v) acetonitrile/water mixture as solvent. This further proved the role of hydroxyl radicals in the degradation. In this hydroorganic medium hydroxylated derivatives like 2,4-dichlorophenol, 4-chlorocatechol, chlorohydroquinone and chloro-*p*-benzoquinone, and carboxylic acids like maleic, oxalic, formic and acetic acids were identified as products. The complete destruction of iron–oxalato complexes and released Cl^- ion involved some oxidizing species coming from parallel acetonitrile oxidation. The same electro-Fenton systems also resulted in the overall removal of triclocarban in acetonitrile/water mixtures, further resulting in the primary intermediates of urea, hydroquinone, chlorohydroquinone, 1-chloro-4-nitrobenzene and 1,2-dichloro-4-nitrobenzene.

Sun (2007) established a detailed kinetic model for the degradation of *p*-nitroaniline (PNA) by Fenton oxidation. Batch experiments were conducted to research the role of hydrogen peroxide, pH and Fe^{2+} levels, PNA concentration and temperature on PNA oxidation. The kinetic rate constants, k_{ap}, for PNA degradation at different reaction conditions were also ascertained. According to the findings, the decomposition of PNA proceeded rapidly only at the pH value of 3.0. By increasing the dosage of H_2O_2 and Fe^{2+} the k_{ap} of PNA degradation was further enhanced, but higher levels of H_2O_2 did also inhibit the reaction kinetics. As the initial PNA concentration increased, the k_{ap} of PNA degradation decreased; however, it increased with a rise in temperature. Based on the rate constants observed at different temperatures, the empirical Arrhenius expression of PNA degradation was derived. The derived activation energy for PNA degradation by Fenton oxidation was 53.96 kJ mol^{-1}.

Pimentel et al. (2008) investigated the oxidation of phenol in aqueous media by the electro-Fenton process type of using cathode as a carbon felt. The salts of iron, cobalt, manganese, and copper were used to provide the metal cations as a catalyst in the Fenton reaction to produce hydroxyl radicals. The 10^{-4} M of soluble iron (II) sulfate salt supplied the optimum catalytic condition. This resulted in the 100% removal of TOC of aqueous phenol solutions. The main reaction intermediates formed during the electro-Fenton treatment were hydroquinone, p-benzoquinone, and catechol. Carboxylic acids were predominantly identified, like maleic, fumaric, succinic, glyoxylic, oxalic, and formic, as the end products before mineralization was completed. The absolute rate constant of phenol degradation by hydroxyl radicals was observed in acid medium ($2.5 < pH < 3.0$), equaling $(2.62 \pm 0.23) \times 10^{9}$ M^{-1} s^{-1}. Experiments with the electro-Fenton oxidation of each aromatic intermediate allowed the possibility of a complete mineralization pathway.

Ting et al. (2008) oversaw the development of a new means for promoting ferric reduction efficiency through a different electrochemical cell and the photo electro-Fenton process. Employing UVA light and electric current as electron donors they could initiate the Fenton reaction efficiently. The target compound was benzene sulfonic acid (BSA) in this study. To assess the reactor design the parameters that were investigated included the electrode working area, electrode distance, and energy consumption. In addition, the study also included the intermediates and the mineralization efficiency of electrolysis, the Fenton, electro-Fenton and photo electro-Fenton processes. Oxalic acid, the major intermediate of aromatic compound degradation, can complex with ferric ions. At the same time, the current efficiency can be increased by 7% through a double cathode reactor. This results in a higher degradation rate and greater ferrous production. Even though the results showed that the electronic expense using an electrode gap of 5.5 cm after 2 hours of electrolysis was far higher than 3.0 cm, the current efficiency of an electrode distance 5.5 cm device was 19% higher than 3.0 cm, The final TOC removal efficiency reached 46, 64 and 72% using the Fenton, electro-Fenton and photo electro-Fenton processes in that order.

CHAPTER III

METHODOLOGY

3.1 The scope of experiment

This experiment studied the removal of 2,4-dichlorophenol and triclosan as endocrine disruptors by two advanced oxidation processes: Fenton and electro-Fenton processes. The experiment can be divided into two parts - the first experiment with the Fenton process and the second with the electro-Fenton process. The triclosan experiment was carried out at Chulalongkorn University in Thailand and the 2,4-dichlorophenol experiment was carried out at Chia Nan University of Pharmacy and Science in Taiwan. Synthetic wastewater was used in all experiments.

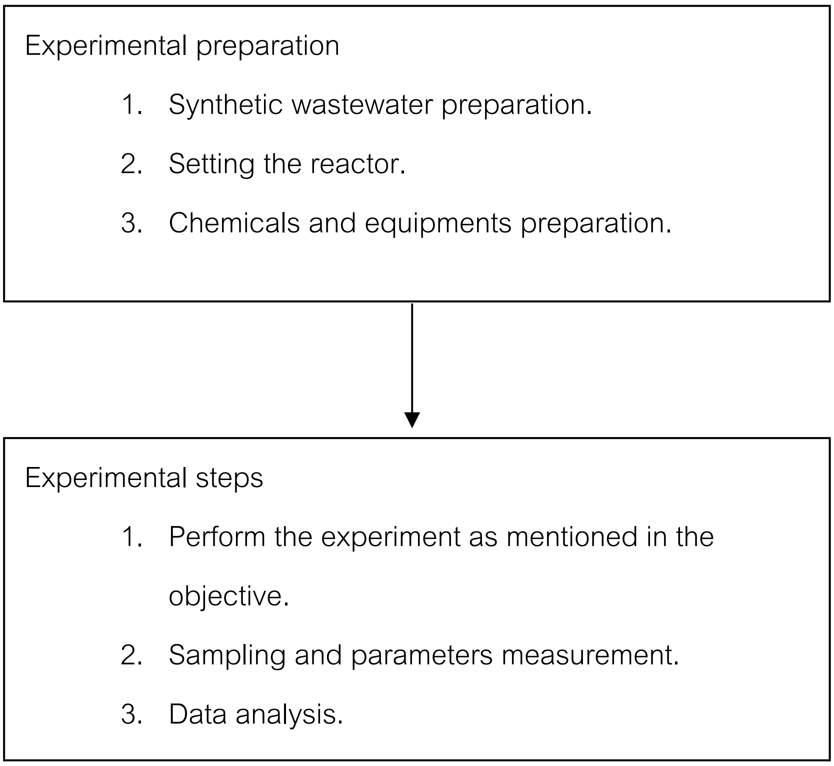

Experimental preparation

1. Synthetic wastewater preparation.
2. Setting the reactor.
3. Chemicals and equipments preparation.

Experimental steps

1. Perform the experiment as mentioned in the objective.
2. Sampling and parameters measurement.
3. Data analysis.

Figure 3.1 Experimental scope diagram

3.2. Experimental chemicals and equipments

3.2.1 Chemicals

All chemicals used in this study were reagent grade and obtained from Merck Co., Ltd., except triclosan which was purchased from SIGMA ALDRICH Co., Ltd. All of the solutions were prepared by de-ionized water from a Millipore system with a resistivity of 18.2 MΩ cm^{-1}.

1. Target organic compounds
   - 2,4-dicholorophenol (98%) $C_6H_4Cl_2O$, MERCK Co., Ltd.
   - Triclosan (98%) $C_{12}H_7Cl_3O_2$, SIGMA ALDRICH Co., Ltd.
2. Fenton's reagent
   - Ferrous sulfate hepta- hydrated $FeSO_4.7H_2O$, MERCK Co., Ltd.
   - Hydrogen peroxide (35%) H_2O_2, MERCK Co., Ltd.
3. Chemical for stopping the reaction
   - Sodium hydroxide (0.1 Normality of NaOH) NaOH, MERCK Co., Ltd.
4. Chemical for pH adjustment
   - Sodium hydroxide (1 Normality of NaOH) NaOH, MERCK Co., Ltd.
   - Perchloric acid (70-72%) ($HClO_4$), MERCK Co., Ltd.
5. Ferrous ion measurement
   - Hydrochloric acid (0.64%) HCl, MERCK Co., Ltd.
   - Ammonium acetate $NH_4C_2H_3O_2$, MERCK Co., Ltd.
   - 1,10- phenanthroline $C_{12}H_8N_2.H_2O$, MERCK Co., Ltd.
6. Hydrogen peroxide measurement
   - Potassium titatium (IV) oxalate K_2TiO, MERCK Co., Ltd.

7. HPLC measurement

- Acetonitrile CH_3CN, MERCK Co., Ltd.

8. COD measurement

- Silver sulfate $AgSO_4$, MERCK Co., Ltd.
- Mercury sulfate $HgSO_4$, MERCK Co., Ltd.
- Sulfuric acid H_2SO_4, MERCK Co., Ltd.
- Ammonium iron(III) sulfate hexahydrate $FeH_8N_2O_8S_2.6\ H_2O$, MERCK Co., Ltd.
- Potassium dichromate $Cr_2K_2O_7$, MERCK Co., Ltd.
- Ferroin indicator solution, MERCK Co., Ltd.

3.2.2. Experimental equipments

1. pH meter: SUNTEX TS-1 Digital pH/MV meter
2. UV-VIS Spectrophotometer: Thermo Spectronic™ GENESYS™ 20
3. Thermometer 0-100 °C
4. Auto Pipette 1 and 10 ml, 1 and 10 µl: Nichiro-Nichipet EX
5. Weighing Machine (4-Digits Balance): METTLER TOLEDO (AB 204-5)
6. Magnetic Stirrer: Fargo (MS-90)
7. Thermal controller
8. 5-liters Fenton and electro-Fenton reactors with recycle pump
9. 3 Stanslead steel electrodes and 2 $Ti/RuO_2/IrO_2$ electrodes
10. Clock Timer
11. Membrane Filter 0.2 and 0.45 µm
12. DC power supply (Topward 3301D)
13. HPLC (Thermo SCIENTIFIC Model)
14. IC, (Dionex DX-120)
15. GC-MS

14\. TOC analyzer (SHIMADZU TOC-V_{CPH})

3.2.3. Fenton and electro-Fenton reactors

The 5-liter volume of Fenton and electro-Fenton reactor was made of acrylic (15cm x 21cm x 20cm). The electro-Fenton anode was a special net made from Ti/RuO_2/IrO_2 and the cathode was made from stainless steel. The anodes and cathodes were connected with a DC power supply. Mixers or stirrers were installed in the reactor to provide agitation.

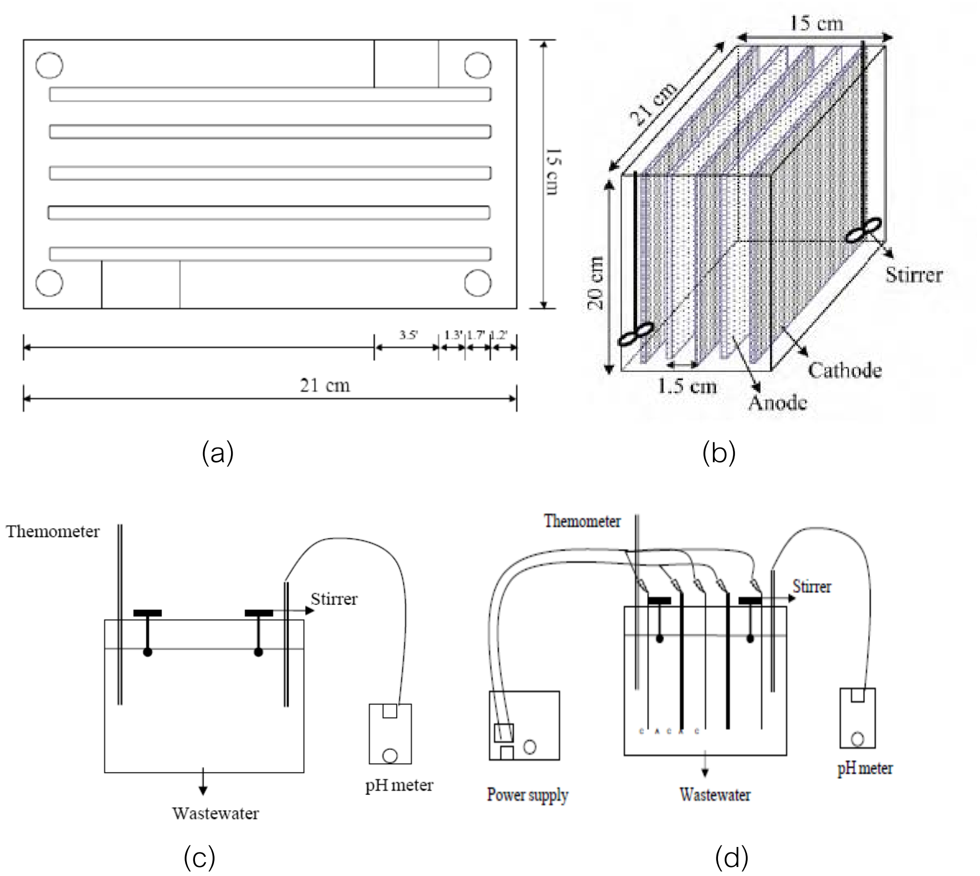

Figure 3.2 Fenton and electro-Fenton reactor compartments and set-up ((a) Top view; (b) reactor compartment; (c) Fenton reactor set-up; (d) electro-Fenton reactor set-up) (Anotai et al., 2010; Masomboon et al., 2009)

3.2.4. Synthetic wastewater

The synthetic wastewater was prepared by dissolving 2,4-dicholorophenol chemical (98%) in de-ionized water from a Millipore system with a resistivity 18.2 MΩ cm^{-1} for generated 2,4-DCP synthetic wastewater. The 2,4-DCP synthetic wastewater had the initial COD 200-230 mg L^{-1} and Initial TOC 50-55 mg L^{-1} depended on the experimental runs. For triclosan synthetic wastewater, it was prepared by dissolving Triclosan (98%) chemical with de-ionized water (Millipore system with a resistivity of 18.2 MΩ cm^{-1}) which adjusted to pH around 10 by 0.1 mM NaOH for dissolve triclosan and return it to desire pH by 0.1 mM $HClO_4$. The triclosan synthetic wastewater had the initial COD 390-400 mg L^{-1} and Initial TOC 135-145 mg L^{-1} depended on the experimental runs.

3.3. Experimental variables

Experimental variables are classified as Fix variables, Independent variables, and Dependent variables. Variables for all experiments are summarized as follow:

3.3.1. Fix variables were the constant parameters in the experiments, which were

- Volume of reactor
- Anode and Cathode electrodes type and distance
- Temperature was fixed for kinetic model validation experiments
- Mixing speed

3.3.2. Independent variables were parameters that can be changed to identify their effects on system performance, which were

- pH
- Concentration of H_2O_2
- Concentration of Fe^{2+}
- H_2O_2 per Fe^{2+} ratio
- Electrical current density
- H_2O_2 feeding mode

3.3.3. Dependent variables were parameters that are changed resulting from changes in independent variables, which were

- Concentration of 2,4-dichlorophenol at time t

- Concentration of triclosan at time t
- Concentration of Fe^{2+} at time t
- Concentration of H_2O_2 at time t
- COD at time t
- TOC at time t
- Type and amount of intermediates and by-products of any reactions

3.4. Fenton and electro-Fenton experimental procedures

3.4.1. Effect of operating conditions on the decomposition of 2,4-dichlorophenol and triclosan by the Fenton process

The study on operating conditions includes:

- Effect of initial pH
- Effect of initial ferrous ion concentration
- Effect of hydrogen peroxide concentration

The experiment began with a concentration of 2,4-dichlorophenol at 1 mM and triclosan at 1mM. For dissolving triclosan 1 mM, the pH adjustment technique as mentioned in synthetic wastewater part was applied for this experiment.

3.4.1.1. The effect of initial pH values on 2,4-dichlorophenol and triclosan removal

The initial pH values were varied to 1.5, 2, 2.5, 3 and 3.5, while 1 mM of 2,4-dichlorophenol and triclosan was used as the initial concentration in evaluating the effect of the initial pH value.

3.4.1.2. The effect of ferrous ion dosage on 2,4-dichlorophenol and triclosan removal

To investigate the effect of ferrous ion on pollutant removal, the amounts of ferrous ion were varied to 0.1, 0.2, 0.3, 0.4, and 0.5 mM for 1 mM initial concentration of 2,4-dichlorophenol and triclosan.

3.4.1.3. The effect of hydrogen peroxide dosage on 2,4-dichlorophenol and triclosan removal

To study the effect of hydrogen peroxide dosage on the degradation of 2,4-dichlorophenol and triclosan, H_2O_2 concentrations were varied to 10, 20, 30, 40, and 50 mM for 1 mM initial concentration of 2,4-dichlorophenol and triclosan.

From these studies, the optimum conditions for treating 2,4-dichlorophenol and triclosan were obtained.

3.4.2 Electrolysis experiment

An electrolysis experiment was performed as a control experiment in comparison with the Fenton and electro-Fenton process experiments. The 2,4-dichlorophenol and triclosan solutions were adjusted to pH 3.0 by the addition of $HClO_4$. After that, various amounts of electrical current were supplied to the cathode and anode and the solution was thoroughly agitated by two mechanical mixers. A sample of 5 ml was taken at a selected times by immediate injection into tubes (volume 25 ml) containing 5 ml of 0.1 mM NaOH - the same as in the Fenton and electro-Fenton experiments. The solutions were filtered by a 0.45 μm syringe micro-filters before analysis. The samples were taken at 0, 1, 2, 5, 10, 20, 30, 60 and 90 minutes and were analyzed for 2,4-dichlorophenol and triclosan concentrations and its removal efficiency at 90 minutes.

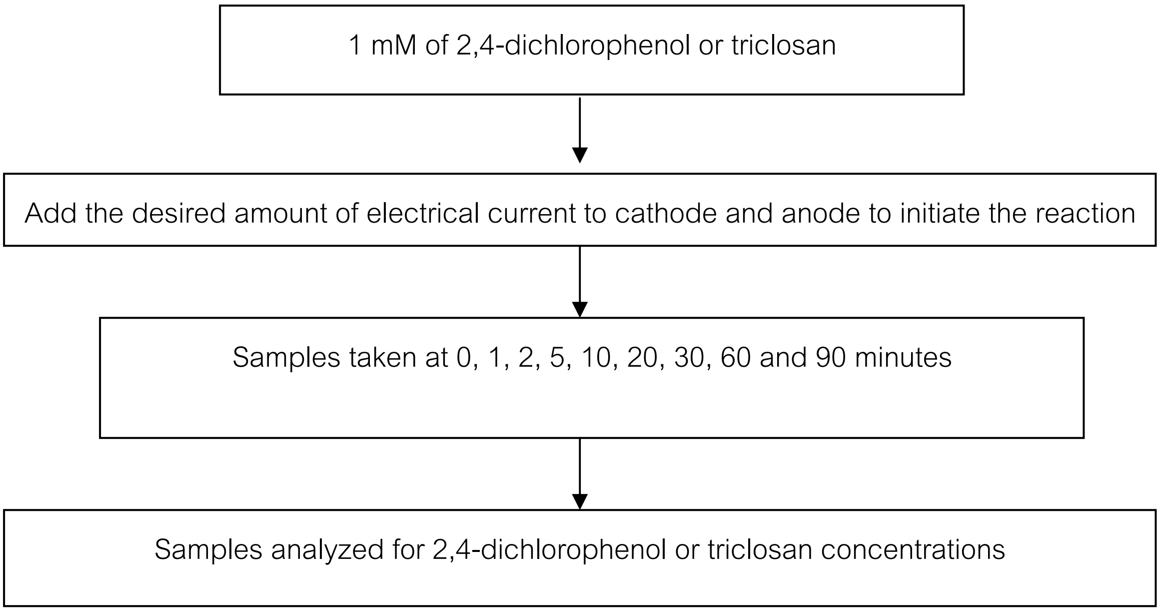

Figure 3.3 Flow chart of the electrolysis experiment

3.4.3. Fenton experiment

The 2,4-dichlorophenol and triclosan solution were adjusted to pH 3.0 by the addition of $HClO_4$. After that, a predetermined amount of catalytic ferrous sulfate was added and the solution was thoroughly agitated by two mechanical mixers until the solid particles completely dissolved. The solution pH was rechecked again prior to the addition of H_2O_2 solution and the reaction was simultaneously started. The desired H_2O_2 was supplied to the solution in function of initial feed or step feed which fed every 2 minutes interval. The samples were taken at the selected times of 0, 1, 2, 5, 10, 20, 30, 60 and 90 minutes. The samples of 5 ml were taken at the selected times by immediately injection into a tube (volume 25 ml) containing 5 ml of 0.1 mM NaOH for stopping the reaction. After the reaction was halted, the solutions were filtered through 0.45 µm syringe micro-filters before analysis. Samples were analyzed for Fe^{2+}, H_2O_2, 2,4-dichlorophenol, triclosan, TOC, COD, by-products and removal efficiency at 90 minutes.

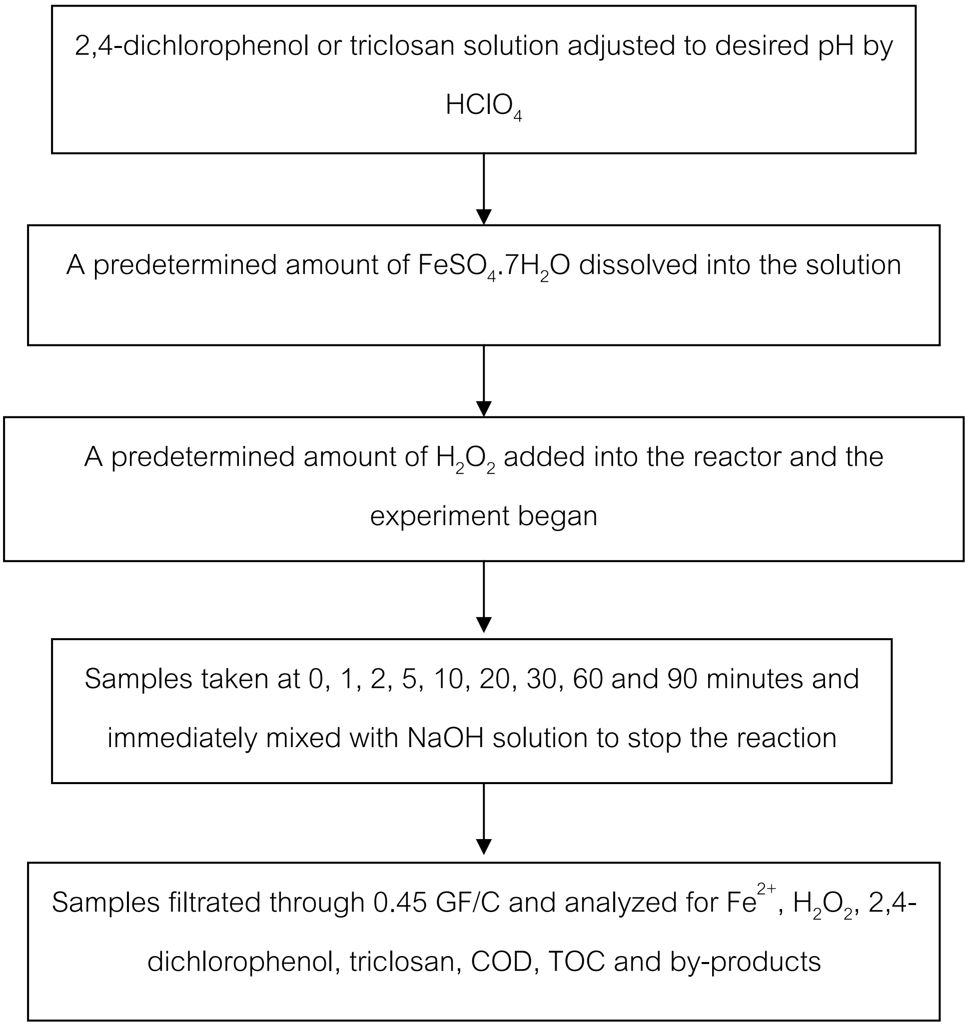

2,4-dichlorophenol or triclosan solution adjusted to desired pH by $HClO_4$

A predetermined amount of $FeSO_4.7H_2O$ dissolved into the solution

A predetermined amount of H_2O_2 added into the reactor and the experiment began

Samples taken at 0, 1, 2, 5, 10, 20, 30, 60 and 90 minutes and immediately mixed with NaOH solution to stop the reaction

Samples filtrated through 0.45 GF/C and analyzed for Fe^{2+}, H_2O_2, 2,4-dichlorophenol, triclosan, COD, TOC and by-products

Figure 3.4 Flow chart of the Fenton experiment

3.4.4. Electro-Fenton experiment

In this experiment, an electrical supply unit which consisted of 3-stainless steel cathode electrodes, 2-Ti/ RuO_2/IrO_2 anode electrodes, and a regulator DC power supply were additionally installed in the reactor. Most procedures were similar to those of a typical Fenton reaction, however, in this scenario, the electrical current was delivered by the electrode throughout the whole experimental periods.

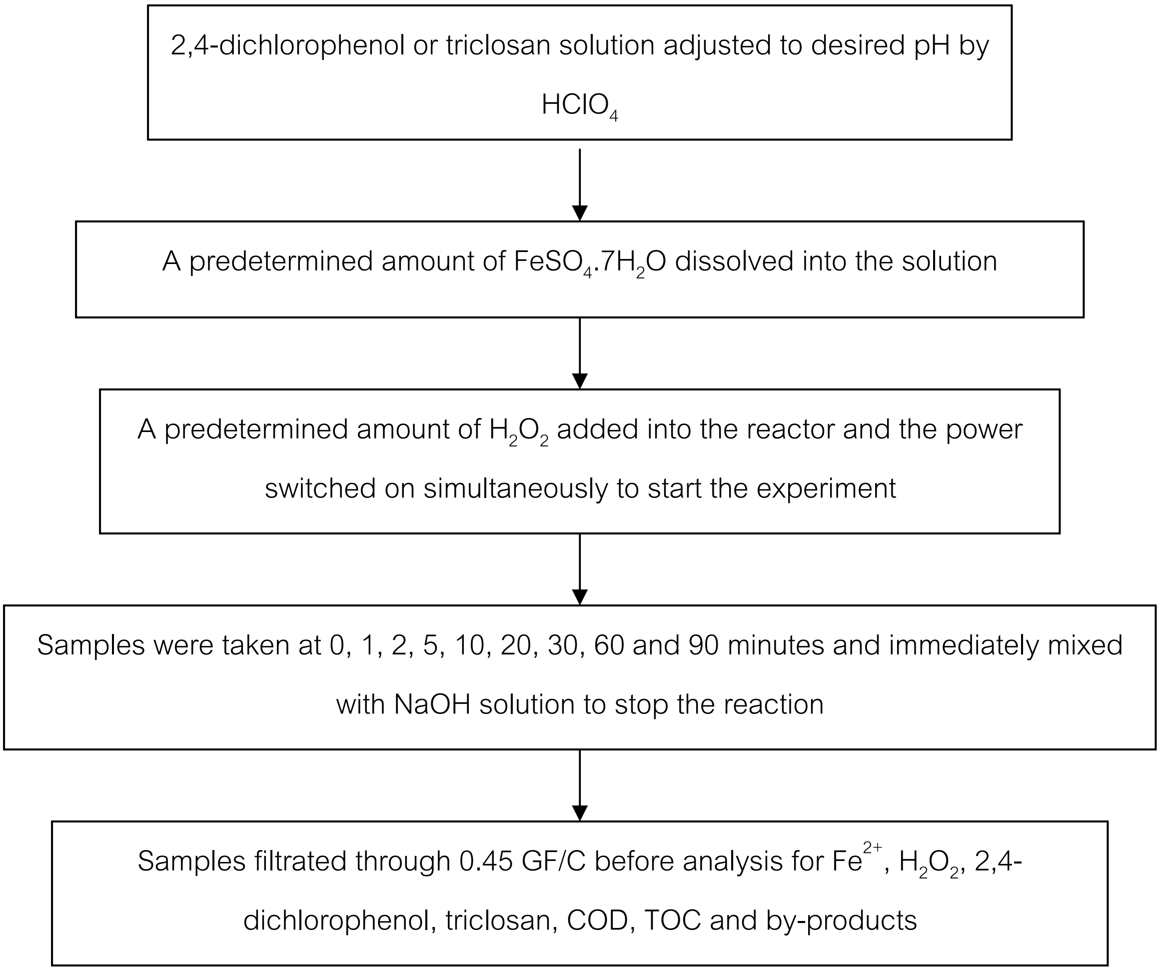

Figure 3.5 Flow chart of the electro-Fenton experiment

3.5. Experimental scenarios

3.5.1. Fenton experimental scenarios

Scenario A

Parameters which affected the degradation of 2,4-dichlorophenol and triclosan by the Fenton process as shown in Table 3.1.

Table 3.1 Details of Scenario A

2,4-dichlorophenol, triclosan (mM)	Operating parameters
1	pH
	Fe^{2+} concentration
	H_2O_2 concentration
	H_2O_2 feeding mode

Scenario B

Determination of the effect of pH on the degradation of 2,4-dichlorophenol and triclosan by the Fenton process with the conditions as shown in Table 3.2.

Table 3.2 Details of Scenario B

2,4-dichlorophenol, triclosan (mM)	H_2O_2 (mM)	Fe^{2+} (mM)	pH
1	1	0.1	2.0
			3.0
			3.5

Scenario C

Determination of effect of Fe^{2+} concentration on the degradation of 2,4-dichlorophenol and triclosan by the Fenton process with the conditions as shown in Table 3.3.

Table 3.3 Details of Scenario C

2,4-dichlorophenol, triclosan (mM)	pH	H_2O_2(mM)	Fe^{2+} (mM)
1	From Scenario B	1	0.1
			0.2
			0.3
			0.4
			0.5

Scenario D

Determination of effect of H_2O_2 concentration on the degradation of 2,4-dichlorophenol and triclosan by the Fenton process with the conditions as shown in Table 3.4.

Table 3.4 Details of Scenario D

2,4-dichlorophenol, triclosan (mM)	pH	Fe^{2+} (mM)	H_2O_2 (mM)
1	From Scenario B	From Scenario C	1
			2
			3
			4
			5

Scenario E

Determination of effect of H_2O_2 feeding mode on the degradation of 2,4-dichlorophenol and triclosan by the Fenton process with the conditions as shown in Table 3.5.

Table 3.5 Details of Scenario E

2,4-dichlorophenol, triclosan (mM)	pH	Fe^{2+} (mM)	H_2O_2 (mM)	H_2O_2 Feeding Mode
1	From Scenario B	From Scenario C	From Scenario D	Initial Feeding Mode
				Step Feeding Mode

From Scenarios A-E, the optimum condition for the Fenton process of 2,4-dichlorophenol and triclosan at concentration 1 mM will be obtained.

3.5.2. Electro-Fenton experimental scenarios

Scenario F

Parameters which affected the degradation of 2,4-dichlorophenol and triclosan by the electro-Fenton process as shown in Table 3.6.

Table 3.6 Details of Scenario F

2,4-dichlorophenol, triclosan (mM)	Operating parameters
1	pH
	Fe^{2+}
	H_2O_2
	Electrical current
	H_2O_2 feeding mode

Scenario G

Determination of effect of pH on the degradation of 2,4-dichlorophenol and triclosan by the electro-Fenton process with the conditions as shown in Table 3.7.

Table 3.7 Details of Scenario G

2,4-dichlorophenol, triclosan (mM)	H_2O_2 (mM)	Fe^{2+} (mM)	Current Density (mA cm^{-2})	pH
1	1	0.1	0.05	1.5
				2.0
				2.5
				3.0
				3.5

Scenario H

Determination of effect of current density on the degradation of 2,4-dichlorophenol and triclosan by the electro-Fenton process with the conditions as shown in Table 3.8 for 2,4-dichlorophenol and Table3.9 for triclosan

Table 3.8 Details of Scenario H (2,4-dichlorophenol)

2,4-dichlorophenol (mM)	pH	Fe^{2+} (mM)	H_2O_2 (mM)	Current Density (mA cm^{-2})
1	From Scenario B	0.1	1	0.01
				0.05
				0.12
				0.25
				0.50

Table 3.9 Details of Scenario H (Triclosan)

Triclosan (mM)	pH	Fe^{2+} (mM)	H_2O_2 (mM)	Current Density (mA cm^{-2})
1	From Scenario B	0.1	1	0.01
				0.15
				0.24
				0.35
				0.50

Scenario I

Determination of effect of H_2O_2 per Fe^{2+} ratio on the degradation of 2,4-dichlorophenol and triclosan by the electro-Fenton process with the conditions as shown in Table 3.10

Table 3.10 Details of Scenario I

2,4-dichlorophenol, triclosan (mM)	pH	Current Density (mA cm^{-2})	Fe^{2+} (mM)	H_2O_2 per Fe^{2+} ratio (H/F Ratio) (mM/mM)
1	From Scenario B	From Scenario C	From optimum condition of Fenton experiment	10
				20
				30
				40
				50

Scenario J

Determination of effect of H_2O_2 feeding mode on the degradation of 2,4-dichlorophenol and triclosan by the electro-Fenton process with the conditions as shown in Table 3.11

Table 3.11 Details of Scenario J

2,4-dichlorophenol, triclosan (mM)	pH	Current Density (mA cm^{-2})	Fe^{2+} (mM)	H_2O_2 per Fe^{2+} ratio (H/F Ratio) (mM/mM)	H_2O_2 Feeding Mode
1	From Scenario B	From Scenario C	From optimum condition of Fenton experiment	From Scenario D	Initial Feeding Mode
					Step Feeding Mode

From Scenarios F-J, the optimum condition for the electro-Fenton process of 2,4-dichlorophenol and triclosan at concentration 1 mM were obtained.

3.5.3. Kinetics of the electro-Fenton experiments scenarios

The validation in this experiment was performed in three sets of experiments which used 2,4-DCP and triclosan as the chlorinated organic representatives. For each chlorinated organic representative, three sets of experiments were conducted to study the effect of operating pH, current density, and hydrogen peroxide concentration for kinetic model validation. In this experiment the hydrogen peroxide was fed in continuous feed by chemical pump at flow rate 0.5 ml min^{-1}. All of the experiments were compared with both the pseudo-first order kinetic model and our novel model. The validated conditions in the kinetics of 2,4-DCP and triclosan removal by the electro-Fenton are shown in Tables 3.12 and 3.13, respectively.

Table 3.12 Experimental conditions for validating the novel kinetic model of an electro-Fenton process on 2,4-DCP removal

Experimental Conditions	Operating pH	Electrical current density (mA cm^{-2})	Fe^{2+} (mM)	H_2O_2 (mM)	Temperature	H_2O_2 feeding mode
1	2, 3, 3.5	0.05	0.1	1	25±0.2	Continuous Feed 0.5 ml min^{-1}
2	3	0.01, 0.05, 0.10, 0.25, 0.50	0.1	1	25±0.2	
3		0.05	0.1	1, 3, 5	25±0.2	
4		0.10				

Table 3.13 Experimental conditions for validating the novel kinetic model of an electro-Fenton process on triclosan removal

Experimental Conditions	Operating pH	Electrical current density (mA cm^{-2})	Fe^{2+} (mM)	H_2O_2 (mM)	Temperature	H_2O_2 feeding mode
1	2, 3, 3.5	0.15	0.1	1	25±0.2	Continuous Feed 0.5 ml min^{-1}
2	3	0.01, 0.15, 0.24, 0.35, 0.50	0.1	1	25±0.2	
3		0.15	0.1	1, 3, 5	25±0.2	
4		0.24				

3.5.4. Oxidation mechanisms and intermediate investigation of the electro-Fenton experiments scenarios

For this experiment, high performance liquid chromatography (HPLC) and ion chromatography (IC) were applied to investigate and classify the amount and types of various intermediates which were confirmed by GC-MS analysis. The carboxylic acid group was examined by an ion chromatograph (Dionex DX-120). The samples at 0, 1, 2, 5, 10, 20, 30, 60 and 90 minutes of selected condition were used for intermediate investigation. The conditions of this experiment are shown in Table 3.14.

Table 3.14 Experimental conditions for investigate the oxidation mechanisms of an electro-Fenton process on 2,4-dichlorophenol and triclosan degradation

Experimental Conditions	Operating pH	Electrical current density (mA cm^{-2})	Fe^{2+} (mM)	H_2O_2 (mM)	H_2O_2 feeding mode
2,4-DCP 112 mg L^{-1}	3.0	0.05	0.1	3	Initial and Step Feeding
		0.12	1	20	
Triclosan 284 mg L^{-1}		0.15	0.1	4	
		0.24	1	50	

3.6. Analytical methods

1. The concentrations of 2,4-dichlorophenol, triclosan, and by-products from the reaction were measured by high performance liquid chromatography (HPLC) and/or ion chromatography (IC).
2. The concentration of total organic carbon was analyzed by TOC analyzer.

3. The concentration of ferrous concentration was measured by phenanthroline method.
4. The concentration of H_2O_2 was measured by standard iodometric method.
5. COD was measured by closed reflux titrimetric method.
6. The solution pH was measured by pH meter.

3.6.1. Analysis of 2,4-dichlorophenol, triclosan, and by-products of reaction

3.6.1.1. 2,4-dichlorophenol (2,4-DCP)

The samples were filtered with 0.20 µm micro-filters to separate the iron from the solution before analyzing the 2,4-DCP concentration. 2,4-DCP concentration was determined by high performance liquid chromatograph (HPLC) (Thermo SCIENTIFIC Model) equipped with a UV detector (FINNIGAN SPECTRA SYSTEM UV1000). The UV wavelength for detection was 285 nm. The retention time for 2,4-DCP was 10 minutes and injected volume was 20 µL. The separation column was a reverse-phase column (Shodex Asahipak, ODP-506D 6 mm × 150 mm × 5 µm) equipped with a Spectra SYSTEM SN4000 model pump at the operating flow rate of 1ml min^{-1}. The column was operated at temperatures between 18 and 22 ^{o}C. The mobile phase consisted of acetonitrile : water : acetic acid (69 : 30 : 1).

3.6.1.2. Triclosan

The sample was filtered with 0.20 µm micro-filters to separate the iron from the solution before analyzing the triclosan concentration. Triclosan concentration was determined by high performance liquid chromatograph (HPLC Thermo SCIENTIFIC Model) equipped with a UV detector (FINNIGAN SPECTRA SYSTEM UV1000). The UV wavelength for detection was 220 nm. The retention time for triclosan was 5 minutes. A sample injection volume of 50 µL was used. The separation column was a reverse-phase column (Zorbax XDB-C18 4.6 mm × 250 mm, 5 µm) and the flow rate was set at 1 mL min^{-1}. The column temperature was maintained at 25 ˚C. The mobile phase was consists of acetonitrile : water (70 : 30). (Piccoli et al. 2002; Behera et al., 2010)

3.6.1.3. By-products of 2,4-dichlorophenol and triclosan

To identify the by-products of 2,4-dichlorophenol and triclosan, high performance liquid chromatography (HPLC) was applied to detect aromatic intermediate compounds and ion chromatography (IC) was applied to detect all of carboxylic acids. All of intermediates were classified the amount and types of various intermediates by the technique of the same retention peak with the intermediate standard solution, and then reconfirmed by GC-MS analysis. From the review of the many past work in the literature, the by-products of 2,4-dichlorophenol might be in hydroquinone, groups of phenols, chloride ions and group of carboxylic acids. The by-products of triclosan might be in groups of 2,4-dichlorophenol, hydroquinone, groups of carboxylic acids and chloride ions. (Sires et al. 2007)

Ion chromatograph (IC) (Dionex DX-120) equipped with RFC-30 EGCII (KOH), IonPac® AG 11 guard column (4 mm × 50 mm), IonPac® AS11 analytical column (4 mm × 250 mm), ASRS®-ULTRA II (4mm) suppressor and conductivity detector were applied to identify the intermediates in the group of carboxylic acids.

3.6.2. Analysis of Chemical Oxygen Demand (COD)

The sample was stay over night to remove the residual H_2O_2 that might remain in the sample before measure COD by a closed reflux titrimetric method based on the standard methods, APHA, 1992 as mentioned in the Appendix A.

3.6.3. Analysis of Total Organic Carbon (TOC)

The SHIMADZU TOC-V_{CPH} is used for analyzing the total organic carbon. Before the analysis, all supernatants were diluted 10 times by NaOH, and then the solutions were filtered with 0.20 μm micro-filters to separate iron sludge from the solutions.

3.6.4. Analysis of ferrous ion (Fe^{2+}) concentration

The samples were analyzed by phenanthroline method as provided in the Appendix. The RO water was added to make the volume up to 50 ml. The DI water mixed with the sample but no phenanthroline was used as a blank for every sample.

3.6.5. Analysis of hydrogen peroxide (H_2O_2) concentration

The concentration of hydrogen peroxide was determined by a spectrophotometric method using potassium titanium (IV) oxalate as described in the Appendix. The absorbance of samples was measured by the Spectronic™ GENESYS™ 20 spectrophotometer.

3.6.6. Other measurements

The pH measurement was carried out by a SUNTEX TS-1 Digital pH/MV meter.

CHAPTER IV

RESULTS AND DISCUSSIONS

4.1 Removal of 2,4-dichlorophenol (2,4-DCP) ($C_6H_4OCl_2$) by advanced oxidation processes (AOPs)

4.1.1 Control experiments in 2,4-DCP removal

4.1.1.1 Volatizing of 2,4-DCP control experiment

Since 2,4-DCP is a volatile organic compound, in the study of its degradation using an advanced oxidation process, its removal by volatizing must be considered. The volatizing removal efficiencies of 2,4-DCP under different pH conditions with a stirring rate of 400 rpm in 2 hours are presented in Figure 4.1. As can be seen, the volatizing removal efficiencies were very low and remained almost unchanged at pH 7, but with a decreasing solution pH the efficiency increased significantly. In the aqueous medium of pH< pKa (pKa = 7.85, the dissociated constant of 2,4-DCP), 2,4-DCP mainly exists in the form of molecules, while in the aqueous medium of pH> pKa, it mainly exists in the form of ions. This is the reason why the lower pH tends to cause more 2,4-DCP volatizing. However, the volatizing of 2,4-DCP in this experiment had small effects its process performance and could be ignored within the experimental period.

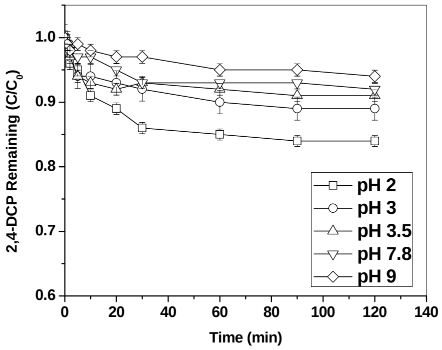

Figure 4.1 2,4-DCP removal by volatizing ([2,4-DCP] = 1 mM, at 400 rpm, pH = 2, 3, 3.5, 7.8 and 9).

4.1.1.2 Electrolysis process of 2,4-DCP removal control experiment

The control experiments were carried out to investigate the effects of electrical current density on 2,4-DCP degradation. From the results shown in Figure 4.2, it was found that an electrolysis system with electrical current densities at 0.01 to 0.50 mA cm^{-2} could remove 2,4-DCP at a low percentage range of about 5-8 %, which was less than the 2,4-DCP removal by volatizing. The results indicate that electrical current in the absence of Fenton's reagent could clearly remove 2,4-DCP at a lower level of efficiency than the Fenton and electro-Fenton processes which were compared as shown in Figure 4.3.

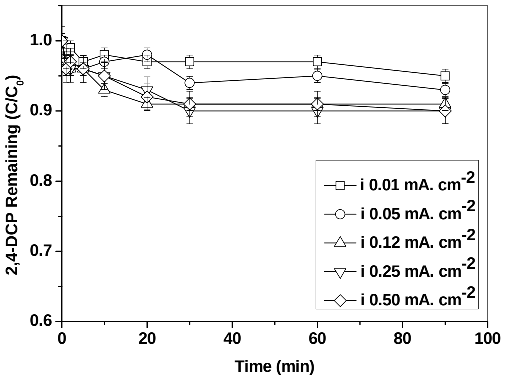

Figure 4.2 2,4-DCP removal efficiency (at 90 min.) by the electrolysis process at various current densities (I). ([2,4-DCP] = 1 mM, [Fe^{2+}] = 0.1 mM, [H_2O_2] = 1 mM, pH = 3).

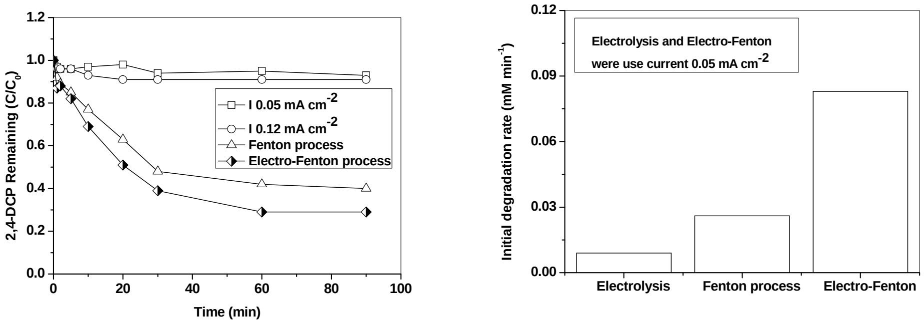

(a) (b)

Figure 4.3 2,4-DCP removal efficiency by various processes (a) and initial degradation of various processes (b). ([2,4-DCP] = 1 mM, [Fe^{2+}] = 0.1 mM, [H_2O_2] = 1 mM, pH = 3, current density at 0.05 and 0.12 mA. cm^{-2} (The electrolysis process used current densities of 0.05 mA. cm^{-2} and the electro-Fenton process used a current density of 0.05 mA. cm^{-2})

4.1.2 Fenton process in 2,4-DCP removal

In the Fenton process experiment, the operating parameters of pH, ferrous ion concentration (Fe^{2+}) and hydrogen peroxide concentration (H_2O_2), were investigated to process optimization. The detail of each parameter effect is given below.

4.1.2.1 Effect of pH on 2,4-DCP removal in the Fenton process

The pH level is an important parameter of the treatment efficiency in Fenton's reaction. Normally, the Fenton reaction has the highest efficiency when the pH is around 2-4. In the 2,4-DCP degradation by the Fenton process, the pH dropped a few levels of 0.2 as time progressed (90 minutes). The result on the effect of pH on the 2,4-DCP degradation, the remaining ferrous ion and hydrogen peroxide concentration is shown in Figures 4.4 and 4.5. The result shows that pH affected 2,4-DCP removal efficiency in the Fenton process. The efficiency at 90 minutes in 2,4-DCP removal increased from 50% to 60% when the pH increased from 2 to 3, and decreased from 60% to 40% when the pH increased from 3 to 3.5. This is the same as the initial degradation rate which increased from 0.022 to 0.034 mM min^{-1} when the pH increased from 2 to 3 and decreased from 0.034 to 0.012 mM min^{-1} when the pH increased from 3 to 3.5. The methodology for the initial degradation rate investigation was described in the part of Appendix A. The experimental data indicated and confirmed that pH 3 is the optimum pH in this experiment. The decrease in the performance of 2,4-DCP degradation at pH less than 3 might likely be due to the formation of $Fe(OH)^+$which has been affected by the variation of pH in the process.

At pH less than 3, the inhibition of prior complex of Fe^{3+} by H_2O_2 was occurred as can be seen in equation (4.1). The formation of $FeOOH^{2+}$ is the key step in the regeneration of Fe^{3+} to Fe^{2+}, so that H_2O_2 can be converted to hydroxyl radicals by Fe^{2+}. At high $[H^+]$ concentration at the lower pH, the generation of $FeOOH^{2+}$ is inhibited and the reaction tended to go to the left side of equation (4.1). This induced the process to reduce the degradation efficiency. In addition, the scavenging effect of hydroxyl radicals by hydrogen ions becomes significant at a very low pH and also the reaction of Fe^{3+} with hydrogen peroxide is inhibited (Pignatello, 1992, Wang, 2008). On the contrary, ferrous ions are unstable at a pH > 3.0 and they easily form ferric ions, which have a tendency to produce ferric hydroxo complexes or ferric oxyhydroxides (Wang, 2008). At a higher pH (pH more than 3), the oxidation efficiency of Fenton's reagent may decrease because ferric ions could form $Fe(OH)_3$, which has a low activity and will not react with hydrogen peroxide. The ferric ions in the solution that can react with hydrogen peroxide are so reduced via equation (4.1) with the rate constant 0.001-0.01 $M^{-1}s^{-1}$ (Neyen et al., 2003).

$$Fe^{3+} + H_2O_2 \leftrightarrow Fe\text{-}OOH^{2+} + H^+ \qquad (4.1)$$

Hence, from the experimental results in this section, it can be concluded that the optimum initial pH for this Fenton process should be pH 3.

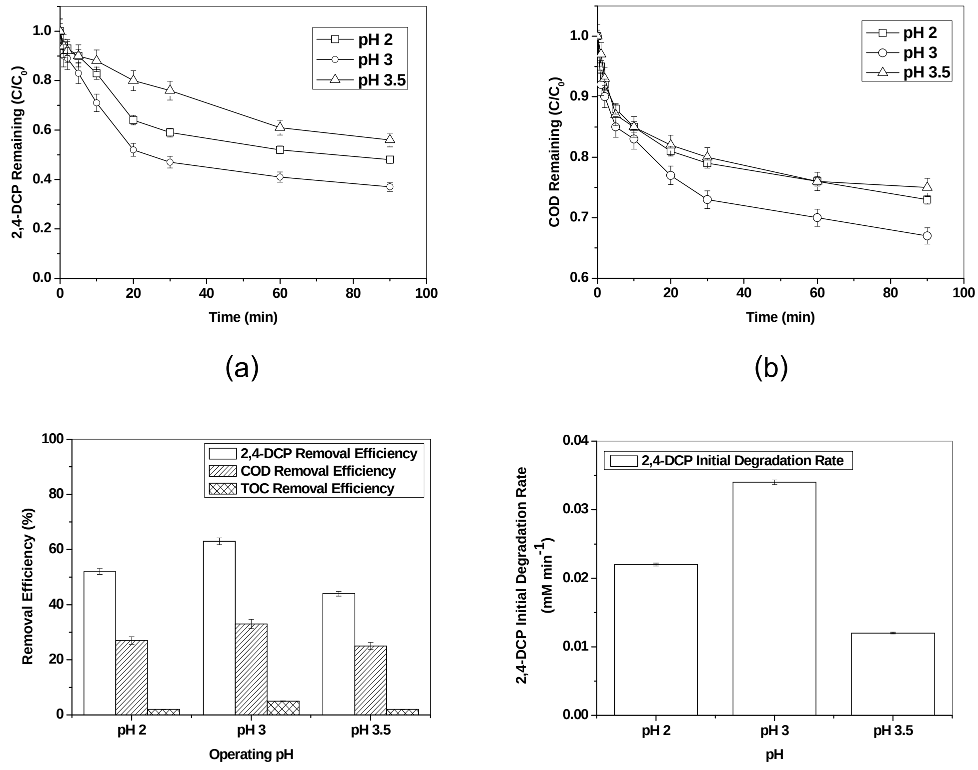

(a) (b)

(c) (d)

Figure 4.4 Effect of operating pH on 2,4-DCP (a), COD (b), TOC (c) removal and 2,4-DCP initial degradation rate (d) by Fenton process ([2,4-DCP] = 1 mM, [Fe^{2+}] = 0.1 mM, [H_2O_2] = 1 mM)

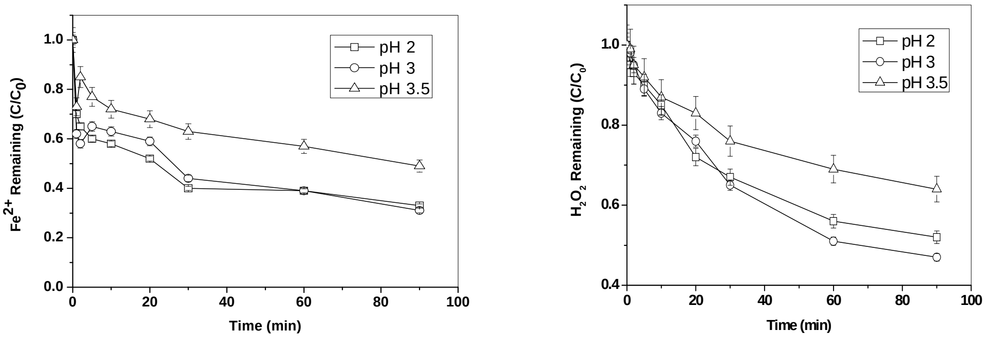

(a) (b)

Figure 4.5 Effect of operating pH on Fe^{2+} (a) and H_2O_2 (b) remaining in the Fenton process ([2,4-DCP] = 1 mM, [Fe^{2+}] = 0.1 mM, [H_2O_2] = 1 mM)

4.1.2.2 Effect of ferrous ion concentration on 2,4-DCP removal in the Fenton process

The ferrous ion concentration (Fe^{2+}) is one major parameter in the Fenton process. Ferrous ion acts as a catalyst in the Fenton process. Catalyst concentration increases the oxidation rate because iron activates the hydrogen peroxide to form hydroxyl radicals (Mijangos et al., 2006). However, ferrous ion can also be scavengers of hydroxyl radicals (Pignatello, 1992). When there are excess amounts of ferrous ion, a reaction can occur with the hydroxyl radical. Then, the hydroxyl radical in the system will decrease and the organic degradation will also reduce. To evaluate the effect of ferrous ion, the experiments were conducted on various amounts of ferrous ion as shown in Figures 4.6 and 4.7. It can be seen from Figure 4.7 that increasing the Fe^{2+} concentration from 0.1 to 0.5 mM enhanced the 2,4-DCP and COD removal efficiencies. The removal of 2,4-DCP showed in percentage values, which were 63%, 65%, 61%, 55% and 53% when ferrous ions were applied in concentrations of 0.10, 0.20, 0,30, 0.40 and to 0.50 mM, respectively. The highest removal efficiency of 2,4-DCP was achieved when the Fe^{2+} concentration was 0.20 mM. However, In terms of removal efficiency which was less difference and being more economic in terms of chemical cost, a ferrous concentration of 0.10 mM was applied for the optimized process in this Fenton experiment.

Figure 4.6 also shows the effect of the initial ferrous ion on the 2,4-DCP removal but in terms of the COD and TOC removal efficiencies. The COD removal efficiencies also did not differ with the different ferrous ion concentrations of 0.10, 0.20, 0.30, 0.40 and 0.50 mM. The COD removals of 33%, 26%, 31%, 32% and 29% were noted in the experiments respectively. The highest COD removal of 33% was observed with the initial Fe^{2+} concentration of 0.10 mM. The COD removal efficiency did not increase proportionally with the increase of ferrous ion concentration possibly due to the ratio in the process of ferrous and hydrogen peroxide not being appropriate. Moreover, the results showed an initial degradation rate in the range of 0.033-0.038 mM min^{-1} were received when ferrous ion concentration was 0.10 to 0.50 mM with the highest being

0.38 with a ferrous concentration of 0.3 mM. Although the highest 2,4-DCP removal and COD removal were received in the difference of ferrous concentrations 0.2 and 0.1 mM, respectively, it was not a really represent for indicated the efficiency of process compared with the initial degradation rate which received the highest when the ferrous concentration of 0.3 mM was applied. Therefore, it can be concluded that the optimum ferrous concentration for this experiment was 0.3 mM based on the highest initial degradation rate. Moreover the result also indicates that ferrous ions are consumed faster than they are produced. So, when ferrous ions reach optimum concentration, the higher removal efficiency becomes, and tended to decreases beyond the optimum point.

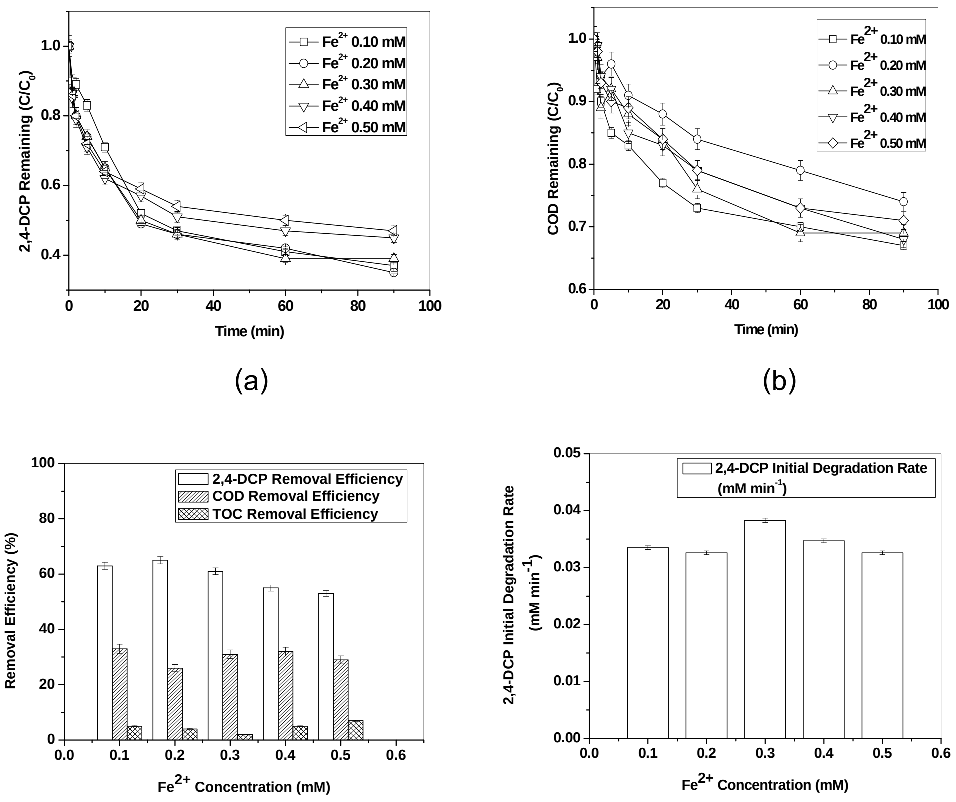

(a) (b)

(c) (d)

Figure 4.6 Effect of ferrous ion (Fe^{2+}) concentration on 2,4-DCP (a), COD (b) and TOC (c) removal and 2,4-DCP initial degradation rate (d) by the Fenton process ([2,4-DCP] = 1 mM, pH = 3, [H_2O_2] = 1 mM)

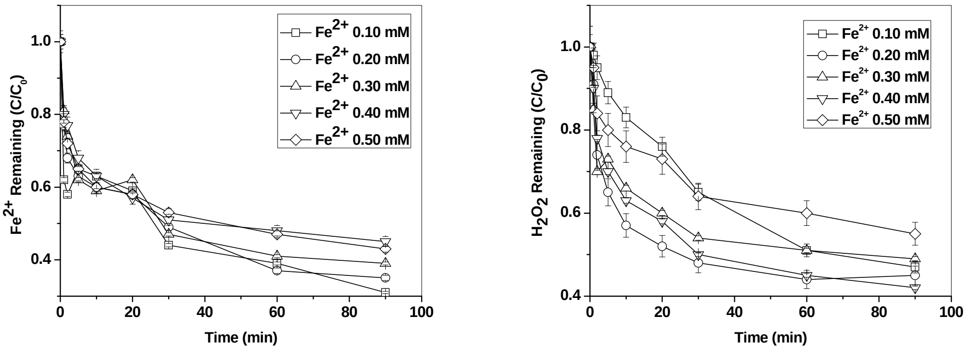

(a) (b)

Figure 4.7 Effect of ferrous ion concentration (Fe^{2+}) on Fe^{2+} (a) and H_2O_2 (b) remaining in the Fenton process ([2,4-DCP] = 1 mM, pH = 3, [H_2O_2] = 1 mM)

4.1.2.3 Effect of hydrogen peroxide concentration on 2,4-DCP removal in the Fenton process

Hydrogen peroxide (H_2O_2) plays the role of an oxidizing agent in the Fenton reaction. The review of former literature reported that only the addition of ferrous ions did not result in high performance in organic removal (Masomboon et al., 2009). This experiment was performed in order to study the effect of H_2O_2 concentrations varying in the range of 1 mM to 5 mM on the performance of the Fenton process for 2,4-DCP removal, as shown in Figure 4.8 and 4.9. The results showed that increasing the initial concentration of H_2O_2 from 1 to 5 mM can have the effect of increasing 2,4-DCP removal efficiency to 63%, 65%, 69%, 75%, 79%, respectively. The COD and TOC removal efficiency results also increased the same as the initial degradation rate of 2,4-DCP removal increased with increased concentrations of H_2O_2. The increase in the initial concentration of H_2O_2 affecting the 2,4-DCP rate removal might be due to the increasing amount of H_2O_2 reacting with Fe^{2+} in the solution. Moreover, the result of the remaining ferrous and hydrogen peroxide concentration possibly confirms that the increasing H_2O_2 concentration affected the amount of ferrous and hydrogen peroxide concentrations in the process which affected to 2,4-DCP removal efficiency as can be seen in Figure 4.9. It can be concluded that the hydrogen peroxide concentration 5 mM should be the optimum condition for this experiment based on the highest efficiency and initial degradation rate.

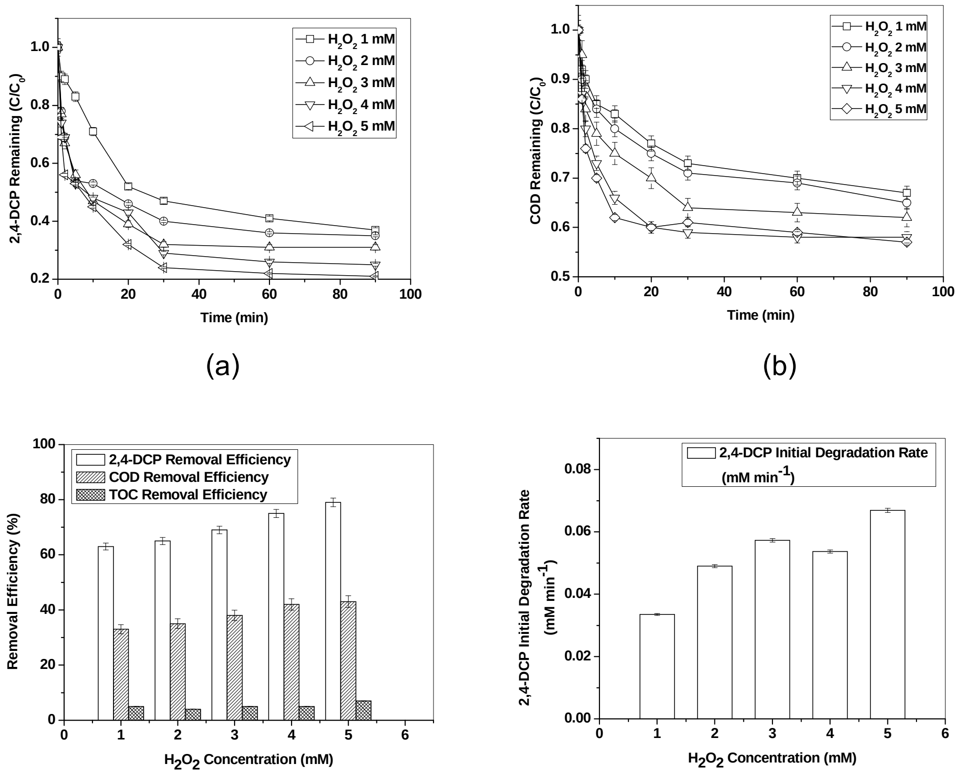

(a) (b)

(c) (d)

Figure 4.8 Effect of hydrogen peroxide (H_2O_2) concentration on 2,4-DCP (a), COD (b) and TOC (c) removal and 2,4-DCP initial degradation rate (d) by the Fenton process ([2,4-DCP] = 1 mM, [Fe^{2+}] = 0.3 mM, pH = 3)

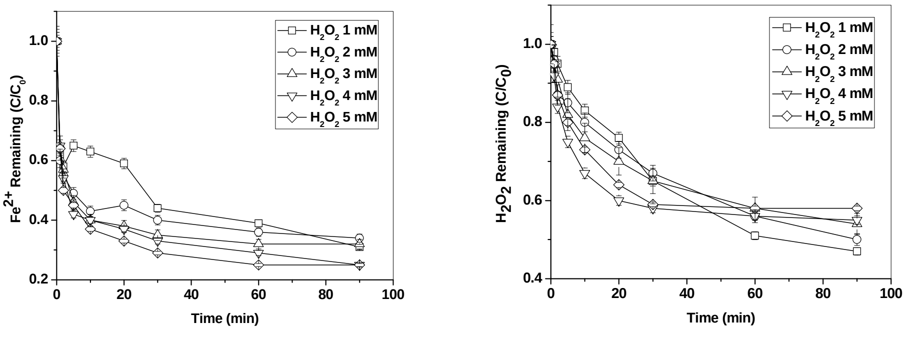

(a) (b)

Figure 4.9 Effect of hydrogen peroxide (H_2O_2) concentration on Fe^{2+} (a) and H_2O_2 (b) remaining in the Fenton process ([2,4-DCP] = 1 mM, [Fe^{2+}] = 0.3 mM, pH = 3)

4.1.2.4 Effect of hydrogen peroxide (H_2O_2) feeding mode on 2,4-DCP removal in the Fenton process

The effect of the H_2O_2 operation feeding mode on 2,4-DCP removal by the Fenton process was studied in this section. The H_2O_2 feeding condition in this operation was compared in terms of 2,4-DCP degradation efficiency between step feeding mode which fed H_2O_2 at 2 minute-intervals and initial feeding mode as shown in Figure 4.10. The results showed that the good performance of initial feeding was the same as step feeding in all durations in the experiment. The cause of this result might be the low regeneration of Fenton's reagents in term of Fe^{2+} concentration for generating hydroxyl radicals among the process. It can be seen in the reaction between Fe^{3+} and H_2O_2 by equation (4.1) during the operation of the initial feeding condition which has the low rate of Fe^{2+} regeneration. The same as step feeding condition that might be low of Fenton's reagents due to the Fe^{2+} was decreasing during the process whereas the H_2O_2 increased at high operation time.

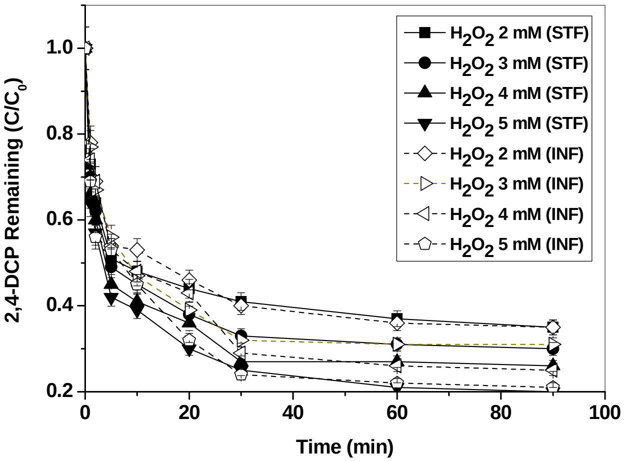

Figure 4.10 Effect of hydrogen peroxide (H_2O_2) feeding mode (Initial Feeding, INF and Step Feeding, STF) on 2,4-DCP removal by the Fenton process ([2,4-DCP] = 1 mM, [Fe^{2+}] = 0.3 mM, pH = 3)

4.1.3 Electro-Fenton process in 2,4-DCP removal

4.1.3.1 Effect of pH on 2,4-DCP removal in the electro-Fenton process

Operating pH is commonly considered to be a significant parameter that can affect the efficiency of the Fenton and also the electro-Fenton processes. The effective pH was around 2-4 in the conventional Fenton process, depending on the kind of pollutants to be removed. Here, the effect of operating pH for 2,4-DCP removal by the electro-Fenton process was investigated. The results obtained from this experiment are shown in Figure 4.11. From the results obtained here, pH 3 was the best condition for 2,4-DCP removal by the electro-Fenton process as a result of the higher initial degradation rate than those of other pH. The cause of this might be at the pH below 3, the inhibition of prior complex of Fe^{3+} by H_2O_2 was occurred as can be seen in equation (4.1). The formation of $FeOOH^{2+}$ is the key step in the regeneration of Fe^{3+} to Fe^{2+}, so that H_2O_2 can be converted to hydroxyl radicals by Fe^{2+}. At high $[H^+]$ concentration at the lower pH, the generation of $FeOOH^{2+}$ is inhibited and the reaction tended ti go to the left side of equation (4.1). In addition, the scavenging effect of hydroxyl radicals by hydrogen ions could become significant at a very low pH that might also inhibit the process efficiency. In contrast, at a pH of above 3.5, the process performance was significantly decreased, mainly due to a decrease in the dissolved fraction of iron species (Duesterberg et al., 2008; Pera-Titus et al., 2004) Consequently, a lower amount of dissolved Fe(II) species could react toward the H_2O_2. Then the process performance was affected because a smaller steady-state concentration of hydroxyl radicals was attained. The Fe^{2+} and H_2O_2 remaining in the process also confirmed that pH 3 is the best and optimum operating pH because it was highest in H_2O_2 consumption and Fe^{2+} regeneration for this experiment as shown in Figure 4.12.

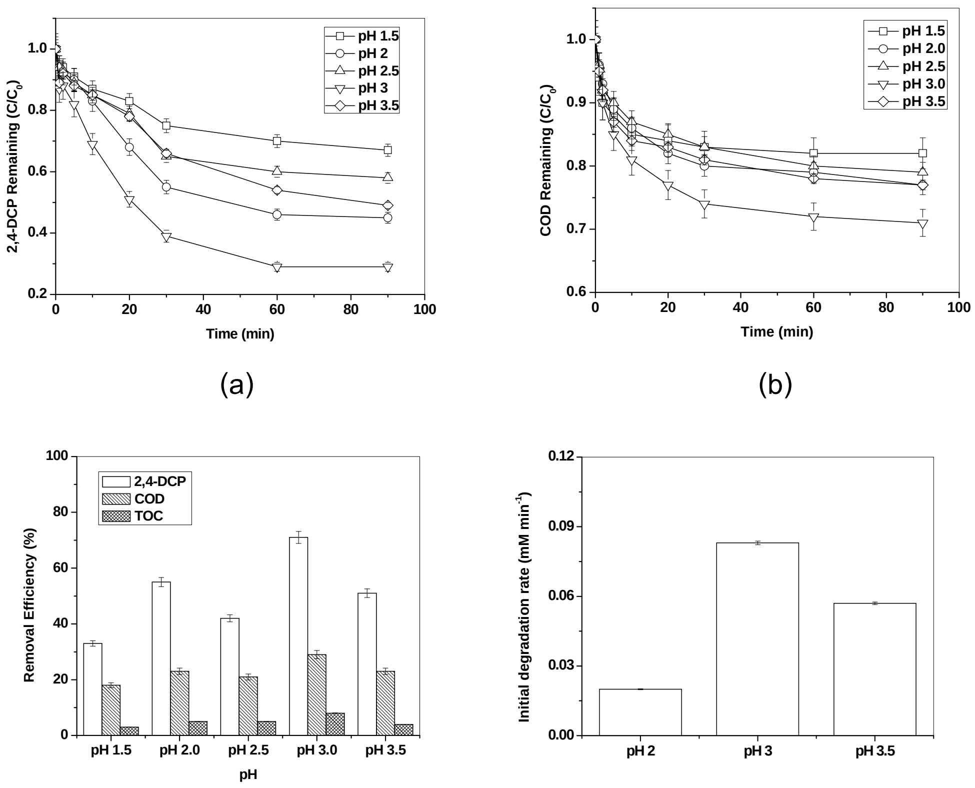

(a) (b)

(c) (d)

Figure 4.11 Effect of operating pH on 2,4-DCP (a), COD (b) and TOC (c) removal and 2,4-DCP initial degradation rate (d) by the electro-Fenton process ([2,4-DCP] = 1 mM, [Fe^{2+}] = 0.1 mM, [H_2O_2] = 1 mM, electrical current of 0.05 mA cm^{-2})

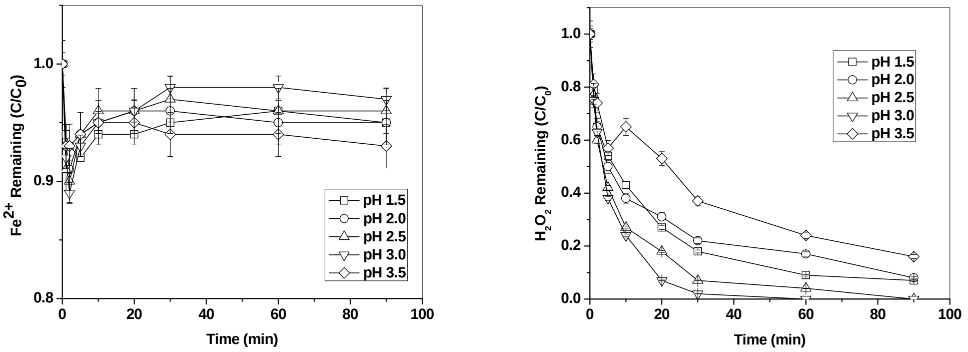

(a) (b)

Figure 4.12 Effect of operating pH on Fe^{2+} (a) and H_2O_2 (b) remaining in the electro-Fenton process ([2,4-DCP] = 1 mM, [Fe^{2+}] = 0.1 mM, [H_2O_2] = 1 mM, electrical current of 0.05 mA cm^{-2})

4.1.3.2 Effect of current density on 2,4-DCP removal in the electro-Fenton process

The effect of current density on the performance of the electro-Fenton process is investigated in this study with the results shown in Figures 4.13 and 4.14. The results demonstrated that the current density affected 2,4-DCP, COD and TOC removal efficiency. The most effective 2,4-DCP removal efficiency with a greater energy saving was obtained when the current density of 0.05 mA cm^{-2} was applied in this experiment. The experimental results indicate that the optimum current density could help increase process efficiency with a high initial degradation rate. The lowering initial degradation rate and removal efficiency might be caused from a lower or higher current density. The decrease in removal efficiency was probably due to a lower amount of electrons for Fe^{2+} regeneration at a low current condition and also the scavenging effect from much more Fe^{2+} regeneration at a higher current condition. A higher current condition continuously promoted the regeneration of [Fe^{3+}] to [Fe^{2+}] in the process which was confirmed by the results of the remaining ferrous and hydrogen peroxide concentrations as shown in Figure 4.14. The results also indicate that when the current density was increased up to 0.12 mA cm^{-2} or more, the removal efficiency was almost the same. Therefore, the current density of 0.05 mA cm^{-2} was found to be most efficient in this application.

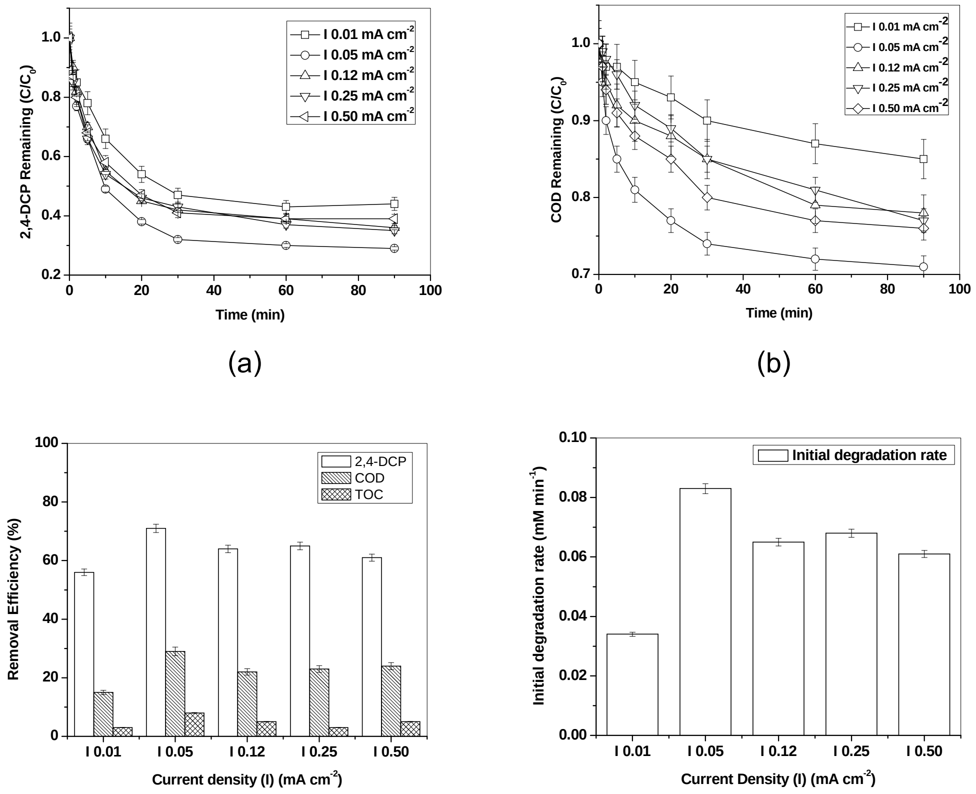

(a) (b)

(c) (d)

Figure 4.13 Effect of current density on 2,4-DCP (a), COD (b) and TOC (c) removal and 2,4-DCP initial degradation rate (d) by the electro-Fenton process ([2,4-DCP] = 1 mM, [Fe^{2+}] = 0.1 mM, [H_2O_2] = 1 mM, pH = 3)

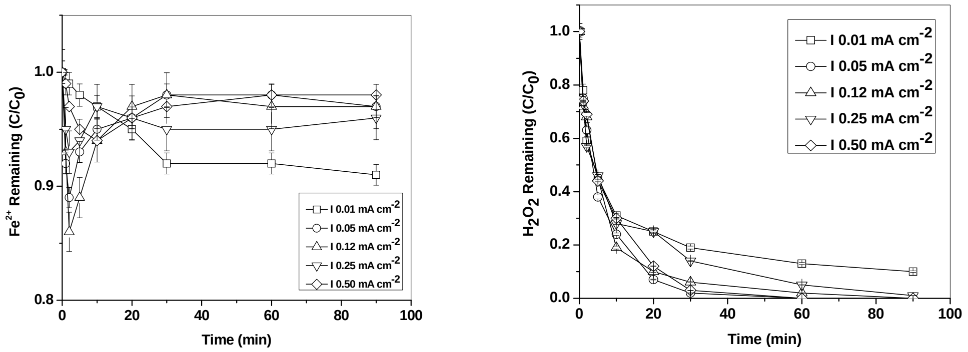

(a) (b)

Figure 4.14 Effect of current density on Fe^{2+} (a) and H_2O_2 (b) remaining in the electro-Fenton process ([2,4-DCP] = 1 mM, [Fe^{2+}] = 0.1 mM, [H_2O_2] = 1 mM, pH 3)

4.1.3.3 Effect of H_2O_2 to Fe^{2+} ratio (H/F ratio) on 2,4-DCP removal in the electro-Fenton process

The effect of the H_2O_2 to Fe^{2+} ratio (H/F ratio) (mM/mM), a major parameter in the efficiency of 2,4-DCP degradation by electro-Fenton process, is shown in Figures 4.15 and 4.16. The experimental result indicates that increasing the H/F ratio could induce the removal efficiency to accelerate and reach the maximum level. Moreover, the H/F ratio value at 30 was found to be the most effective H/F ratio as 100 percent 2,4-DCP removal efficiency from 2,4-DCP initial concentration of 1 mM could be achieved by the electro-Fenton process. Increasing the H/F ratios by more than 30 was not effective in the increasing of removal efficiencies. The constant of 2,4-DCP removal efficiency when using the H/F ratios at more than 30 indicates that the chemicals might be in excess of the requirements by this process for 1 mM 2,4-DCP removal and/or might be from the scavenging with the other compounds in this process.

$$relative\ oxidation\ performance\ ratio = \frac{\%\,pollutant\ removal}{\%\,H_2O_2\ consumed} \qquad (4.2)$$

The relative oxidation performance ratio was developed as described by equation (4.2). It is used for indicating the oxidation efficiency relating to H_2O_2 consumption as reported in Figure 4.17. From Figure 4.17, the decrease in the effective performance of H_2O_2 at the H/F ratios of above 30 might be due to an excessive amount of H_2O_2 molecules in the process. This condition makes activity in the H_2O_2 react with hydroxyl radicals to scavenge with other pollutant removal in the process that produces $HO_2^{\cdot}$ via a reaction. The generating of $HO_2^{\cdot}$ can participate in propagating radical chain reactions by reducing ferric to ferrous ion. This can induce ferrous scavenging to increase too. The result of relative oxidation performance ratio indicated that, the oxidation power of 2,4-DCP removal increased when the H/F ratios were less than 30 and decreased when more than 30. The data of 2,4-DCP removal per unit consumption of H_2O_2 and relative oxidation performance ratio can confirm that, H_2O_2 concentration and/or H/F ratio were a major critical parameter and the optimum H/F ratio for this process is 30 which highest of the relative oxidation performance.

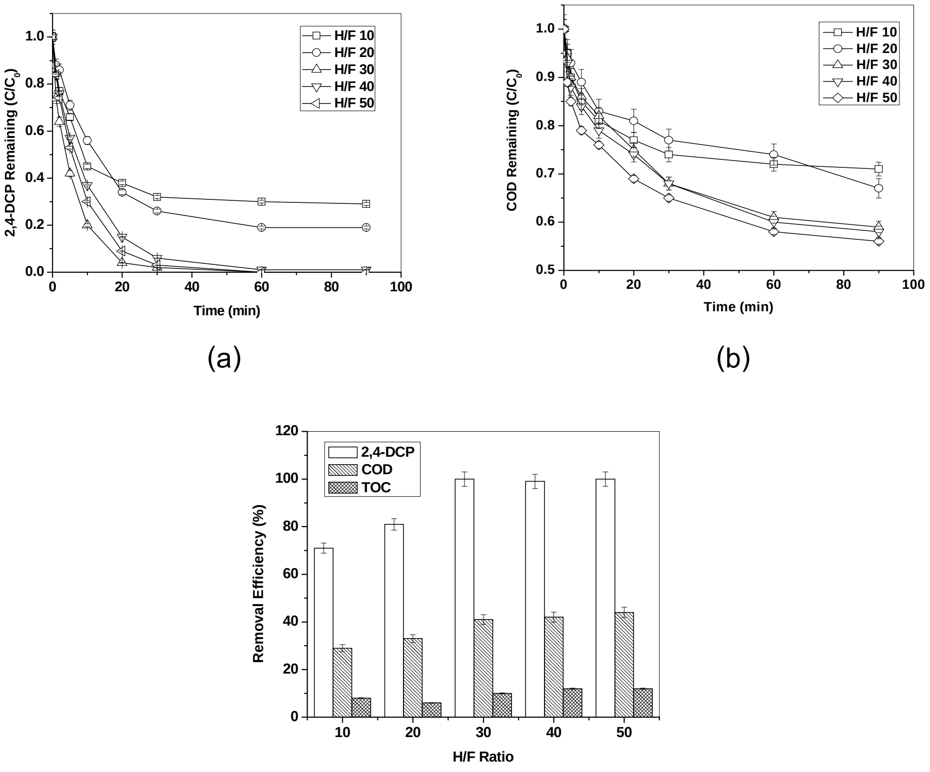

(a) (b)

(c)

Figure 4.15 Effect of H_2O_2 to Fe^{2+} ratios (H/F) on 2,4-DCP (a), COD (b) and TOC (c) removal by the electro-Fenton process ([2,4-DCP] = 1 mM, [Fe^{2+}] = 0.1 mM, electrical current of 0.05 mA cm^{-2}, pH = 3)

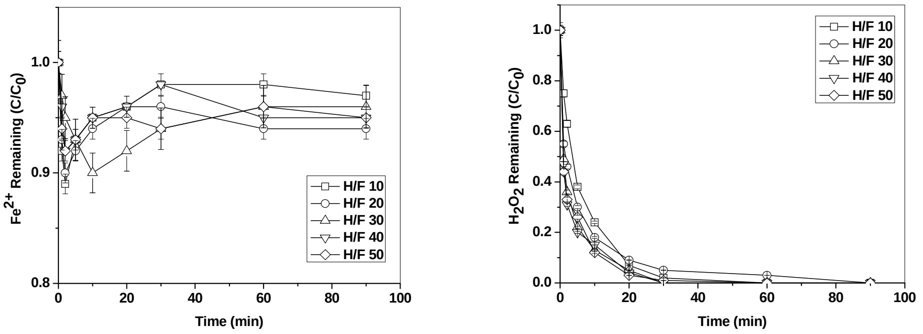

(a) (b)

Figure 4.16 Effect of H_2O_2 to Fe^{2+} ratios (H/F) on Fe^{2+} (a) and H_2O_2 (b) remaining in the electro-Fenton process ([2,4-DCP] = 1 mM, [Fe^{2+}] = 0.1 mM, electrical current of 0.05 mA cm^{-2}, pH 3)

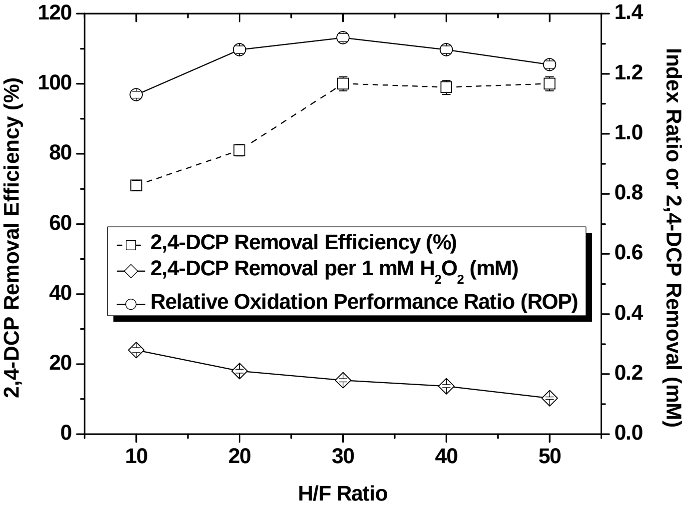

Figure 4.17 Effect of H_2O_2 to Fe^{2+} ratios (H/F) on removal efficiency and Relative Oxidation Performance (ROP) ratio ([2,4-DCP] = 1 mM, [Fe^{2+}] = 0.1 mM, pH = 3, electrical current of 0.05 mA cm^{-2})

4.1.3.4 Effect of H_2O_2 operation feeding mode on 2,4-DCP removal in the electro-Fenton process

2,4-DCP degradation was investigated with two different H_2O_2 feeding modes of operation, the original one-time initial feeding mode and the step feeding mode at 2 minute-intervals, as shown in Figure 4.18. The results show that the feeding mode dominated when applied at a higher current density (at 0.12 mA cm^{-2}). The reason might be that the higher current density had greater electron supply for Fe^{2+} regeneration. The best degradation efficiency was obtained by using the step feeding operation because it could generate ·OH continuously and homogeneously. The step feeding operation mode could also help avoid the presence of excessive ·OH concentrations during the earlier oxidation stages and provide a better ability of this species throughout the whole oxidation process. The sufficient level of H_2O_2 concentration in the step feeding operation as well as the optimum ratio of substrate per H_2O_2 consumption reduced the extension of scavenging reactions involving H_2O_2 and ·OH, thus minimizing the H_2O_2 that was inefficient consumption. On the other hand, the Fe^{2+} generation per H_2O_2 ratio was also higher, thus favoring the decomposition of H_2O_2 almost into ·OH instead of O_2. At the lower current density (at 0.05 mA cm^{-2}), the effect of operation feeding modes for both the step feeding mode and the original one-time initial feeding mode did not indicate any significant differences in degradation efficiencies. On the other hand, the total organic carbon (TOC) removal also confirmed that the step feeding operation mode was better than the original initial feeding mode in mineralization as shown in Figure 4.19.

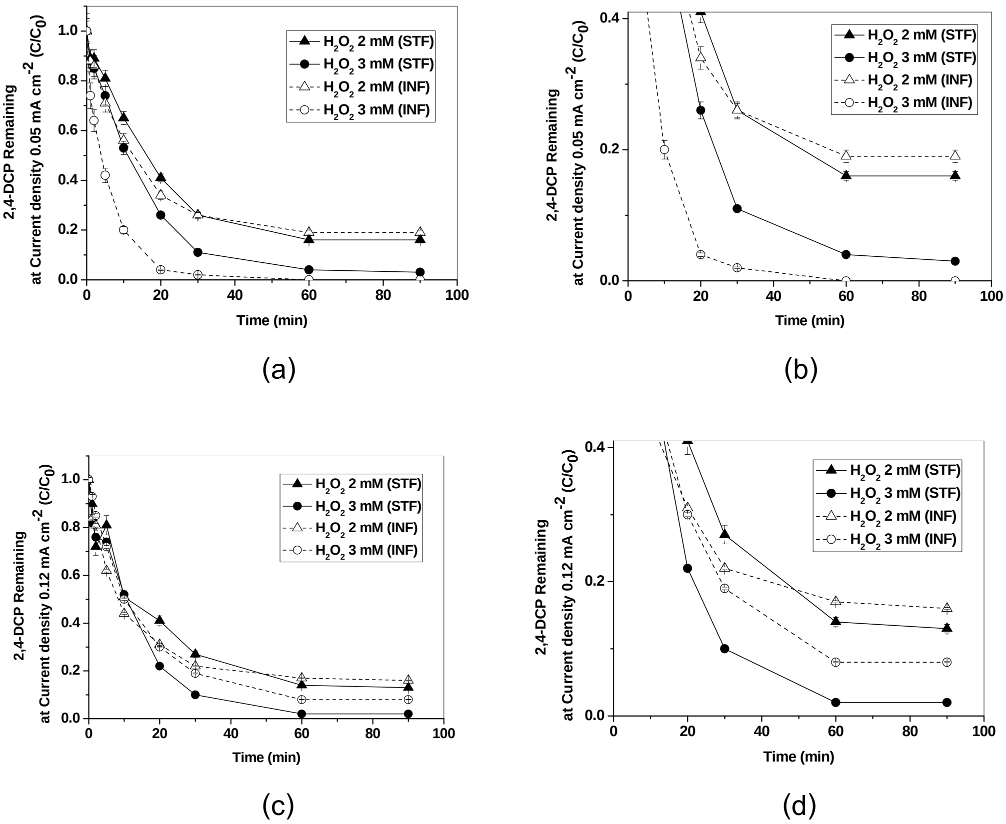
(a) (b)

(c) (d)

Figure 4.18 Effect of H_2O_2 operational feeding mode (step feeding mode; STF, original one time initial feeding mode; INF) on 2,4-DCP removal by the electro-Fenton process ([2,4-DCP] = 1 mM, [Fe^{2+}] = 0.1 mM, [H_2O_2] = 2 and 3 mM, electrical current of 0.05 mA cm^{-2} (a and b) and 0.12 mA cm^{-2}(c and d), pH = 3)

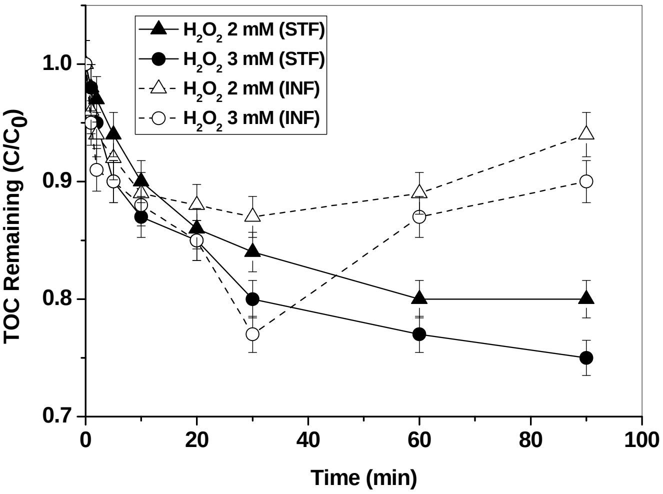

Figure 4.19 Effect of H_2O_2 operational feeding mode (step feeding mode; STF, original one time initial feeding mode; INF) on TOC removal by the electro-Fenton process ([2,4-DCP] = 1 mM, [Fe^{2+}] = 0.1 mM, [H_2O_2] = 2 and 3 mM, electrical current of 0.12 mA cm^{-2}, pH = 3)

4.1.3.5 Effect of various conditions on 2,4-DCP in term of COD and TOC removal in the electro-Fenton process

The efficiencies in COD and TOC removal at various operating conditions were investigated and reported in Table 4.1. The data from the experiment showed that under the conditions of a current density of 0.05 mA cm^{-2} with initial Fe^{2+} and H_2O_2 of 0.1 and 3 mM, respectively at pH 3 could give 1 mM of 2,4-DCP removal reaching up to 70%. However, the data shown in Table 4.1 also indicates that 80% of COD and 50% of TOC removal could be obtained when increasing the current density to 0.12 mA cm^{-2} and Fe^{2+}, H_2O_2 up to 1 and 20 mM, respectively. It can be concluded from this section that the various operating parameters especially current density had effects on the degrees of 2,4-DCP, COD and TOC removal performances.

Table 4.1 Percentages of COD and TOC removal in 2,4-DCP removal by the electro-Fenton process ([2,4-DCP] = 1 mM, pH = 3)

Current Density (mA cm^{-2})	Fe^{2+} (mM)	H_2O_2 (mM)	COD Removal (%)	TOC Removal (%)
0.05	0.1	3	40±5	17±0.5
0.05	1	20	60±3	38±1.0
0.12	1	20	80±2	50±0.3

4.2 Removal of triclosan (2,4,4'-trichloro-2'-hydroxydiphenyl ether, $C_{12}H_7O_2Cl_3$) by advanced oxidation processes (AOPs)

4.2.1 Electrolysis process in triclosan removal

Control experiments were carried out to investigate the effect of electrical current density on triclosan removal. From the results shown in Figure 4.20, it was found that the electrolysis system alone, with electrical current densities at 0.15 and 0.24 mA cm^{-2}, could remove triclosan at a low percentage range of about 3-4 %. On the other hand, the Fenton process alone and application of Fenton's reagents combined with the electrochemical system or the electro-Fenton process could remove triclosan as high as 55% and 61%, respectively. The results indicated that the electrical current, in the absence of Fenton's reagents, obviously could remove triclosan at a low level of efficiency but the removal performance could be enhanced with the electro-Fenton process as a result of continuous hydroxyl radical generation as confirmed by the increase in the initial degradation rate (0.038 mM min^{-1}), compared to the Fenton process without an electrical current (0.032 mM min^{-1}) as shown in Table 4.2.

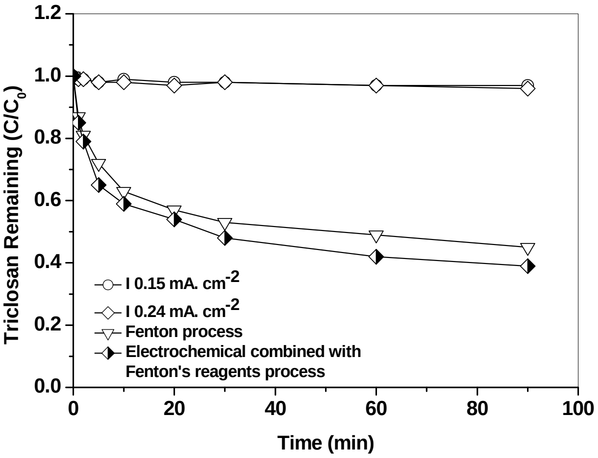

Figure 4.20 Triclosan remaining in application of various processes. ([Triclosan] = 1 mM, $[Fe^{2+}]$ = 0.1 mM, $[H_2O_2]$ = 1 mM, pH = 3, current density at 0.15 and 0.24 mA. cm^{-2} (electro-Fenton process used current density 0.15 mA. cm^{-2})

Table 4.2 Initial degradation rate of triclosan removal by various process ([Triclosan] = 1 mM, $[Fe^{2+}]$ = 0.1 mM, $[H_2O_2]$ = 1 mM, pH = 3, electrical current 0.15 mA cm^{-2})

Type of process	Removal efficiency (%)	Initial degradation rate (mM. min^{-1})*
Electrolysis (Current 0.15 mA cm^{-2})	3	0.001
Fenton process (No current)	55	0.032
Electro-Fenton process (Current 0.15 mA cm^{-2})	61	0.038

* The kinetic constant for initial degradation rate investigation was calculated at initial 20 minutes of reaction time.

4.2.2 Fenton process in triclosan removal

According to the previously mentioned Fenton theory in 2,4-DCP experiment section, it can be reported that the methodology of the triclosan experiment was the same as the 2,4-DCP experiment. Details of which are described in this section:

4.2.2.1 Effect of pH on triclosan removal in the Fenton process

As is commonly known, the Fenton reaction has the highest efficiency when the pH is around 2-4. In the triclosan degradation by the Fenton process experiment, the result of the effect of pH on triclosan degradation is shown in Figures 4.21 and 4.22. The result showed that pH has a major effect on triclosan removal efficiency in the Fenton process. The efficiency in triclosan removal increased slightly from 56% to 58% when the pH increased from 2 to 3, and decreased to 45% when the pH increased from 3 to 3.5. The experimental data showed that the result of the triclosan degradation is similar at pH 2 and 3 but different at pH 3.5. This indicates that pH 3 is the optimum pH in this experiment based on highest performance and costs of the chemicals for pH adjustment. The decrease in triclosan degradation at a low pH is probably due to the inhibition of prior complex of Fe^{3+} by H_2O_2 was occurred as can be seen in equation (4.1). The formation of $FeOOH^{2+}$ is the key step in the regeneration of Fe^{3+} to Fe^{2+}, so that H_2O_2 can be converted to hydroxyl radicals by Fe^{2+}. At high $[H^+]$ concentration at the lower pH, the generation of $FeOOH^{2+}$ is inhibited and the reaction tended to go to the left side of equation (4.1). In addition, the scavenging effect of hydroxyl radicals by hydrogen ions becomes significant at a very low pH and also the reaction of Fe^{3+} with hydrogen peroxide is also inhibited. However, ferrous ions are unstable at a pH > 3.0 and easily form ferric ions, which have a tendency to produce ferric hydroxo complexes or ferric oxyhydroxides. At a higher pH, the oxidation efficiency of Fenton's reagent may decrease because ferric ions could form $Fe(OH)_3$, which has low activity and will not react with hydrogen peroxide. The ferric ions in the solution that can react with hydrogen peroxide are so reduced with the rate constant 0.001-0.01 $M^{-1}S^{-1}$ (Neyen et al., 2003).

Hydrogen peroxide is also unstable in basic solution and may decompose to give oxygen and water and lose its oxidation ability. Thus, hydrogen peroxide and ferrous ions have difficulty in establishing an effective redox system and their degradation is also less effective (Kuo, 1992). Hence, the optimum initial pH for this Fenton process should be pH 3.

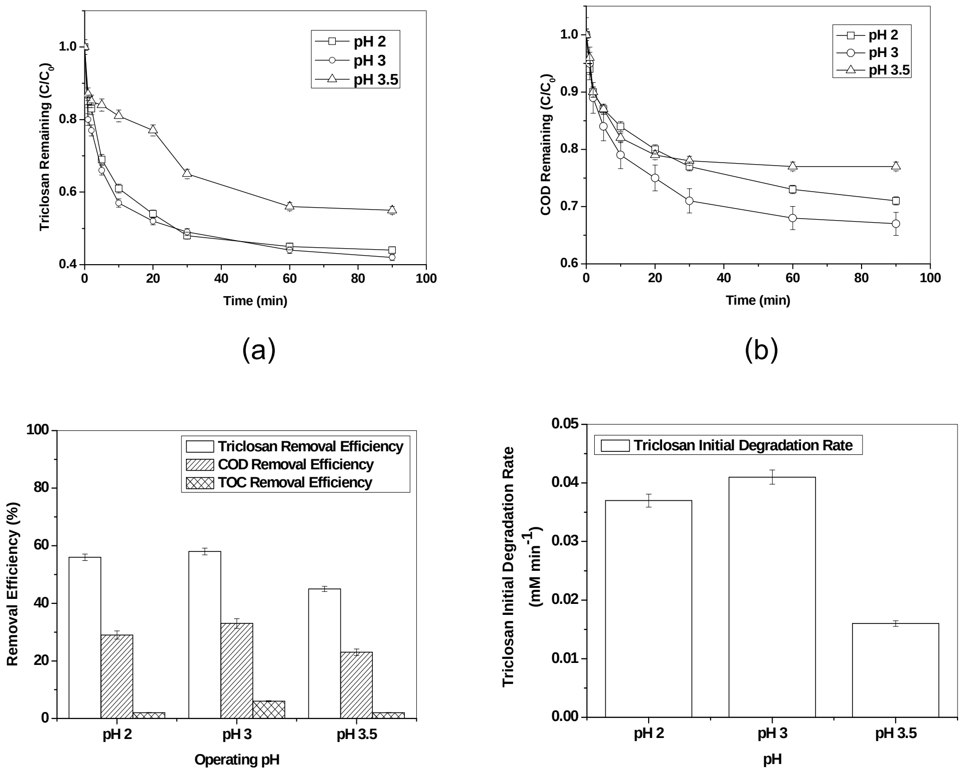

(a) (b)

(c) (d)

Figure 4.21 Effect of operating pH on triclosan (a), COD (b) and TOC (c) removal and triclosan initial degradation rate (d) by the Fenton process ([Triclosan] = 1 mM, $[Fe^{2+}]$ = 0.1 mM, $[H_2O_2]$ = 1 mM)

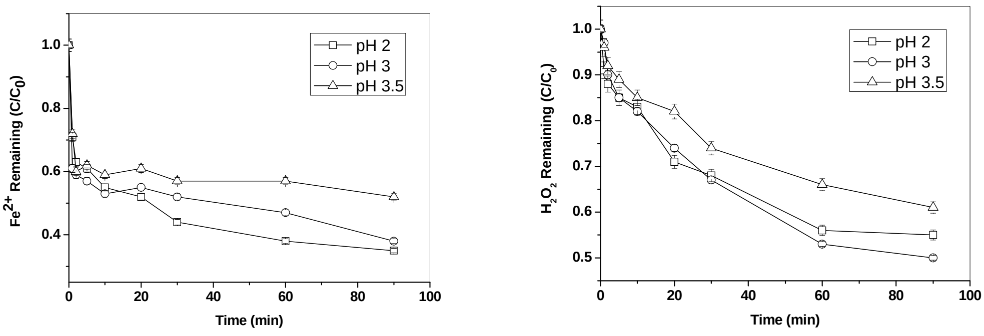

(a) (b)

Figure 4.22 Effect of operating pH on Fe^{2+} (a) and H_2O_2 (b) remaining in the Fenton process ([Triclosan] = 1 mM, $[Fe^{2+}]$ = 0.1 mM, $[H_2O_2]$ = 1 mM)

4.2.2.2 Effect of ferrous ion concentration on triclosan removal in the Fenton process

To evaluate the effect of ferrous ion, the experiments were conducted on various amounts of ferrous ion as shown in Figures 4.23 and 4.24. It can be seen from Figure 4.24 that increasing the Fe^{2+} concentration from 0.1 to 0.5 mM enhanced the triclosan and COD removal efficiencies. The triclosan removal was 58%, 59%, 57%, 55%, 52% when ferrous ions were applied at 0.10, 0.20, 0.30, 0.40, 0.50 mM, respectively. The highest removal efficiency of triclosan was achieved with a Fe^{2+} concentration of 0.10 and 0.20 mM which were both similar in process performance.

Figure 4.23 also shows the effect of initial ferrous ion concentration on the COD removal efficiency of triclosan. The COD removal was also depended on the ferrous ion concentration increased from 0.10 mM to 0.50 mM. The COD removal was received from 26% to 33% which were not different results. The highest COD removal of 33% was observed when the initial Fe^{2+} concentration of 0.10 mM was added to the reactor. However, the COD removal efficiency tended to exhibit a similar performance for each Fe^{2+} concentration. The results showed that the initial degradation rate tended to decrease from 40×10^{-3} to 30×10^{-3} mM min^{-1} when the ferrous ion concentration increased from 0.10 to 0.50 mM. This indicates that ferrous ions might inhibit the process. So when increasing the ferrous ions, a lower removal efficiency can be obtained than the optimum point. It can conclude that the concentration of ferrous ions 0.10 mM should be the optimum ferrous ions condition for this process.

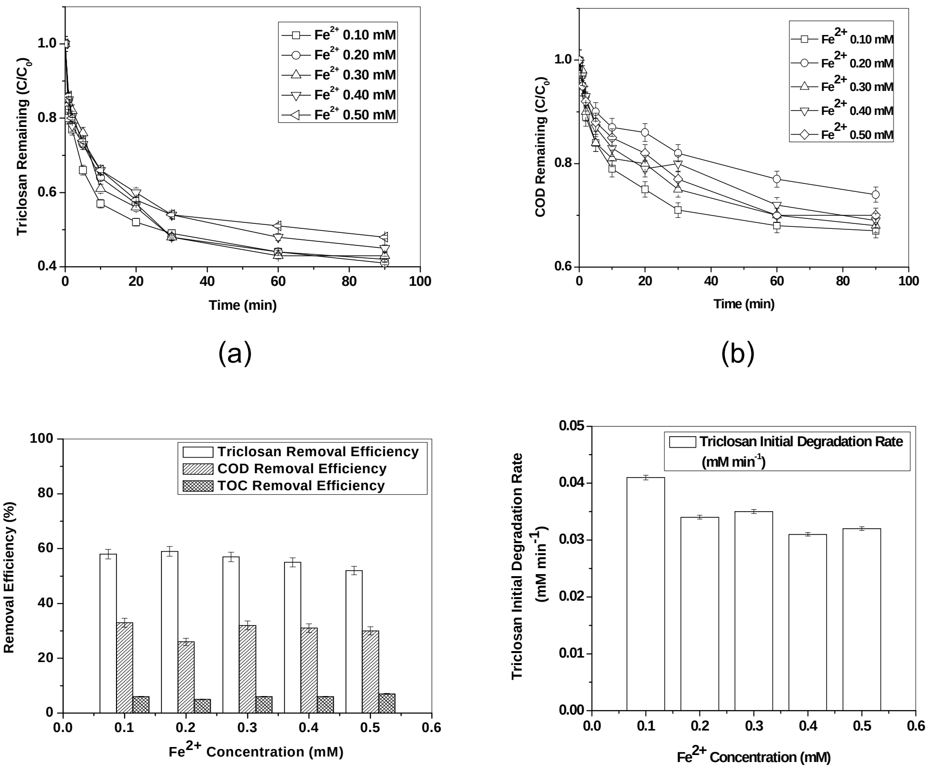

(a) (b)

(c) (d)

Figure 4.23 Effect of ferrous ion (Fe^{2+}) concentration on triclosan (a), COD (b) and TOC (c) removal and triclosan initial degradation rate (d) by the Fenton process ([Triclosan] = 1 mM, pH = 3, [H_2O_2] = 1 mM)

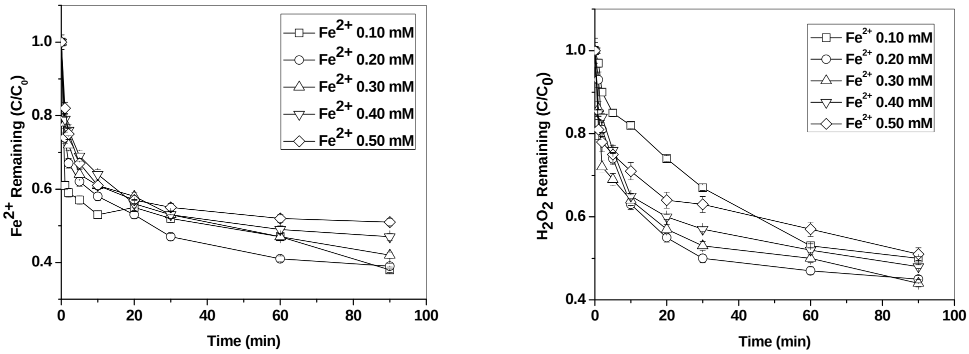

(a) (b)

Figure 4.24 Effect of ferrous ion (Fe^{2+}) concentration on Fe^{2+} (a) and H_2O_2 (b) remaining in the Fenton process ([Triclosan] = 1 mM, pH = 3, [H_2O_2] = 1 mM)

4.2.2.3 Effect of hydrogen peroxide concentration on triclosan removal in the Fenton process

Hydrogen peroxide (H_2O_2) plays the role of an oxidizing agent in the Fenton reaction for triclosan degradation, in the same manner as in the 2,4-DCP experiment. In this experiment, H_2O_2 varied in the range of 1 mM to 5 mM and the results are shown in Figure 4.25. The results indicate that increasing the initial concentration of H_2O_2 from 1 to 5 mM can increase the triclosan removal efficiency. This is the same with the initial degradation rate of triclosan removal which increases with the increase in H_2O_2 as also shown in Figure 4.25. As can be seen in Figure 4.25, at the initial time (0-20 min) the initial degradation rate increased with the increase in H_2O_2 concentration. Therefore, it can be inferred that the increase in the initial concentration of H_2O_2 affects the rate of triclosan removal, which might be the cause of the increase in the amount of H_2O_2 reacting with Fe^{2+} in the solution. For this experiment the H_2O_2 concentration 5 mM is selected for optimum condition base on the highest of the initial degradation and the removal efficiencies.

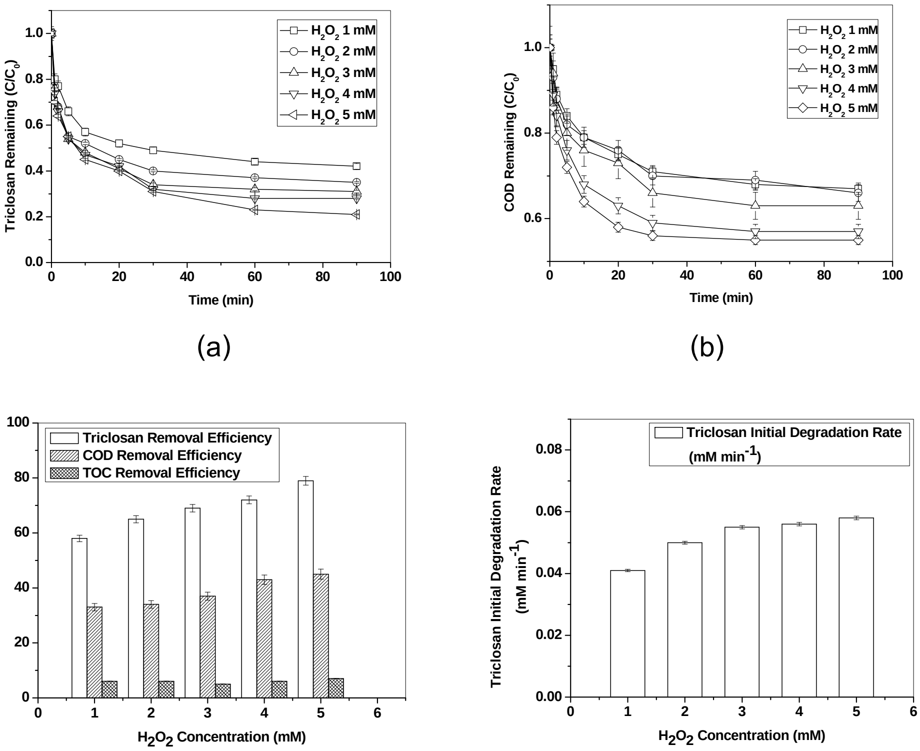

(a) (b)

(c) (d)

Figure 4.25 Effect of hydrogen peroxide (H_2O_2) concentration on triclosan (a), COD (b) and TOC (c) removal and triclosan initial degradation rate (d) by Fenton process ([Triclosan] = 1 mM, [Fe^{2+}] = 0.1 mM, pH = 3)

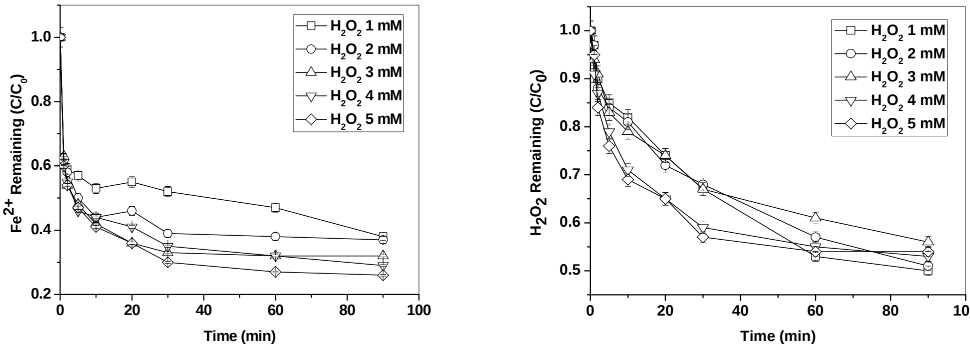

(a) (b)

Figure 4.26 Effect of hydrogen peroxide (H_2O_2) concentration on Fe^{2+} (a) and H_2O_2 (b) remaining in the Fenton process ([Triclosan] = 1 mM, [Fe^{2+}] = 0.1 mM, pH = 3)

4.2.2.4 Effect of hydrogen peroxide (H_2O_2) feeding mode on triclosan removal in the Fenton process

The effect of the H_2O_2 operation feeding mode on triclosan removal is studied in this section. As regards the H_2O_2 feeding condition in this operation, comparison was made between the initial feeding condition and step feeding condition as it was in the 2,4-DCP experiment, but with the study on the triclosan degradation efficiency. The results of the original one-time initial feeding mode and the step feeding mode at 2 minute-intervals are shown in Figure 4.27. The results show that the initial feeding condition performed well in the initial 20 minutes, in the same manner as the step feeding condition. The cause of this result might be the low regeneration of Fenton's reagents in term of Fe^{2+} concentration for generating hydroxyl radicals among the process. It can be seen in the reaction between Fe^{3+} and H_2O_2 by equation (4.1) during the operation of the initial feeding condition which has the low rate of Fe^{2+} regeneration. The same as step feeding condition that might be low of Fenton's reagents due to the Fe^{2+} was decreasing during the process whereas the H_2O_2 increased at high operation time.

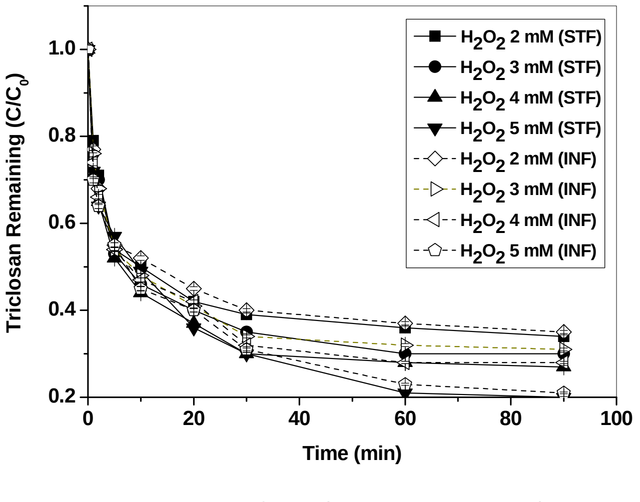

Figure 4.27 Effect of hydrogen peroxide (H_2O_2) feeding mode (Initial Feeding, INF and Step Feeding, STF) on triclosan removal in the Fenton process ([Triclosan] = 1 mM, [Fe^{2+}] = 0.1 mM, pH = 3)

4.2.3 Electro-Fenton process in triclosan removal

4.2.3.1 Effect of pH on triclosan removal in the electro-Fenton process

To clarify the effect of pH on triclosan removal by the electro-Fenton process, triclosan solutions with various pH values were investigated. The results obtained from this experiment are shown in Figures 4.28 and 4.29. As the results indicate, the best conditions for triclosan removal by the electro-Fenton process were at pH 2, 2.5 and 3 with the result of a higher initial degradation rate than those of other pH levels the same as Fenton process. The cause of this result might be that the inhibition of prior complex of Fe^{3+} by H_2O_2 was occurred as can be seen in equation (4.1). The formation of $FeOOH^{2+}$ is the key step in the regeneration of Fe^{3+} to Fe^{2+}, so that H_2O_2 can be converted to hydroxyl radicals by Fe^{2+}. At high $[H^+]$ concentration at the lower pH, the generation of $FeOOH^{2+}$ is inhibited and the reaction tended to go to the left side of equation (4.1). In addition, the scavenging effect of hydroxyl radicals by hydrogen ions could become significant at a very low pH (pH < 2), which might also inhibit the process efficiency. In contrast, at a pH of above 3 or 3.5, the performance of the process significantly decreased, mainly due to a decrease in the dissolved fraction of iron species. Consequently, the lower amounts of dissolved Fe(II) species could have reacted toward the H_2O_2. Then the process performance would have been affected because a smaller steady-state concentration of hydroxyl radicals was attained.

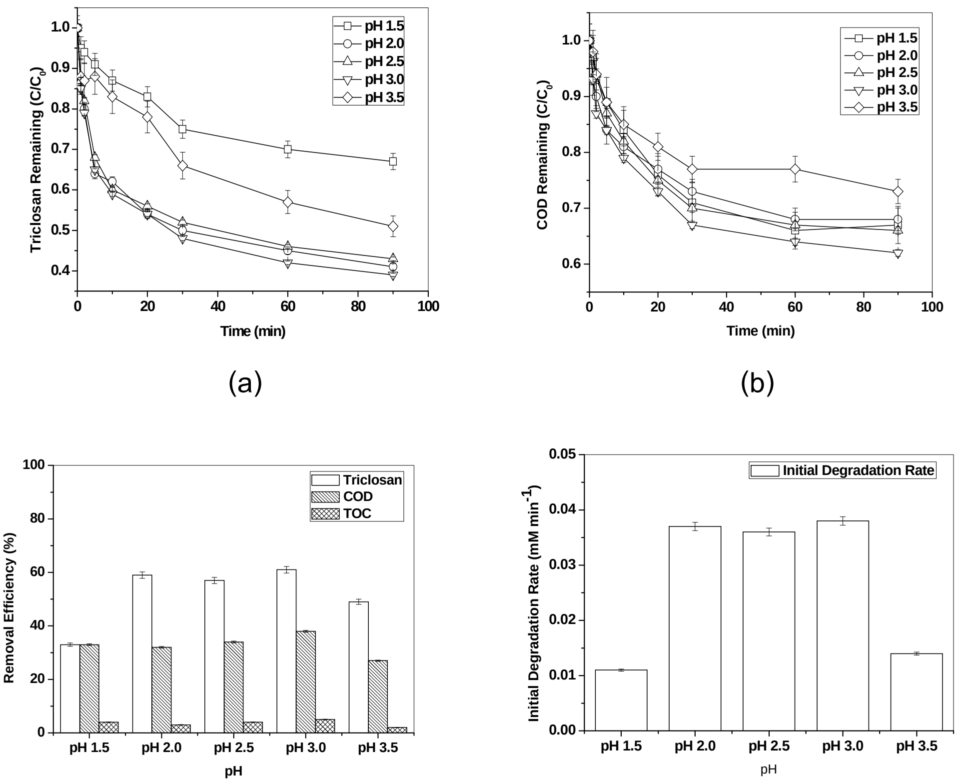

(a) (b)

(c) (d)

Figure 4.28 Effect of operating pH on triclosan (a), COD (b) and TOC (c) removal and triclosan initial degradation rate (d) by the electro-Fenton process ([Triclosan] = 1 mM, [Fe^{2+}] = 0.1 mM, [H_2O_2] = 1 mM, electrical current density of 0.15 mA cm^{-2})

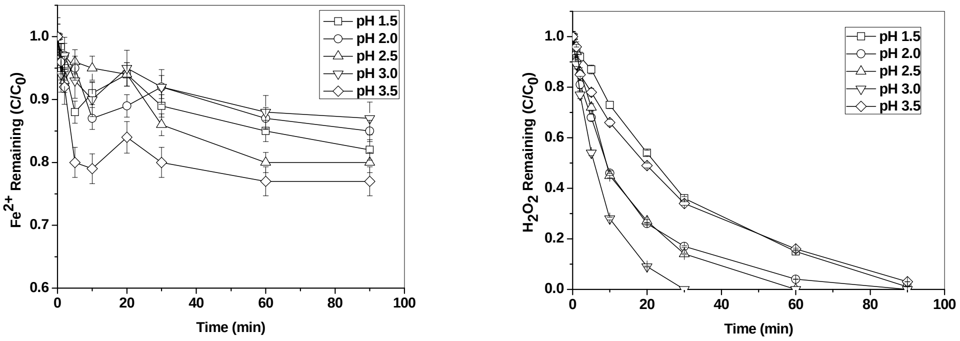

(a) (b)

Figure 4.29 Effect of operating pH on Fe^{2+} (a) and H_2O_2 (b) remaining in the electro-Fenton process ([Triclosan] = 1 mM, [Fe^{2+}] = 0.1 mM, [H_2O_2] = 1 mM, electrical current density of 0.15 mA cm^{-2})

4.2.3.2 Effect of current density on triclosan removal in the electro-Fenton process

The effect of the current density on the performance of the electro-Fenton process is investigated in this study with the results shown in Figures 4.30 and 4.31. The results demonstrated that the current density affected the triclosan removal efficiency. The most effective triclosan removal efficiency with the greatest energy saving was obtained when the current density of 0.15 mA cm^{-2} was applied in this experiment. The experiments results indicate that the optimum current density could help increase process efficiency with a high initial degradation rate. The lower initial degradation rate and removal efficiency might be caused by lower or higher current densities. The decrease in removal efficiency was probably due to the lower amount of electrons for Fe^{2+} regeneration at a low current condition and also the scavenging effect from much more Fe^{2+} regeneration at a higher current condition which continuously promoted the regeneration of [Fe^{3+}] to [Fe^{2+}] in the process. As can be seen from the results, when the current density increased up to 0.15 mA cm^{-2} or more, the removal efficiency was almost the same. Therefore, the current density of 0.15 mA cm^{-2} was found to be sufficient in this application.

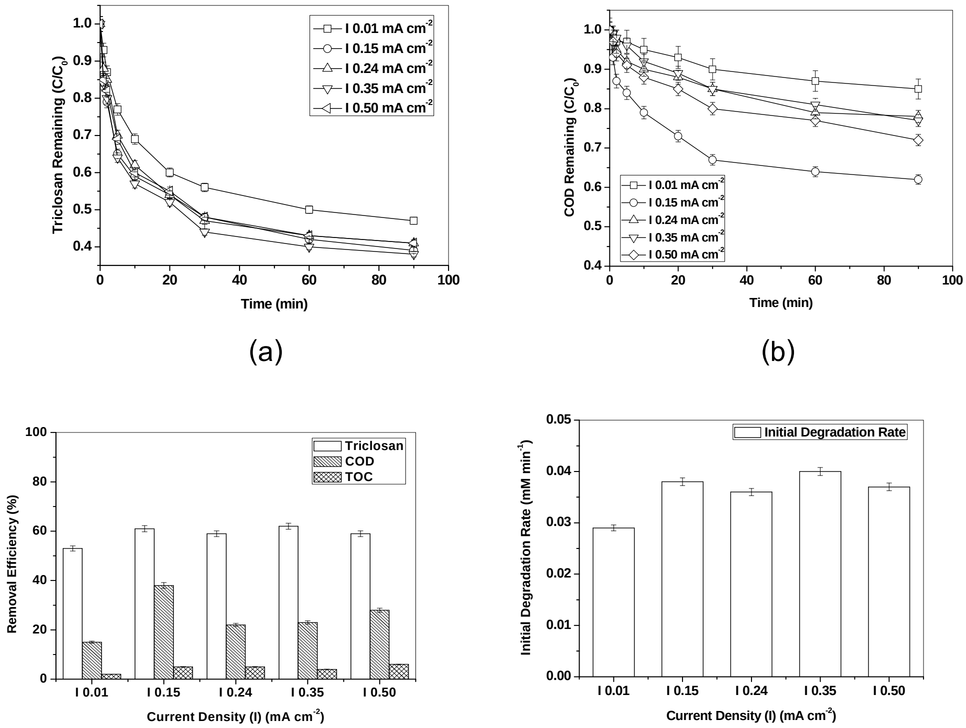

(a) (b)

(c) (d)

Figure 4.30 Effect of current density on triclosan (a), COD (b) and TOC (c) removal and triclosan initial degradation rate (d) by the electro-Fenton process ([Triclosan] = 1 mM, [Fe^{2+}] = 0.1 mM, [H_2O_2] = 1 mM, pH = 3)

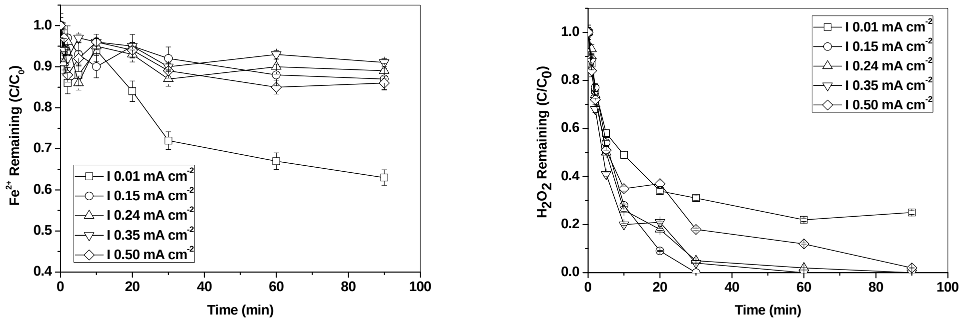

(a) (b)

Figure 4.31 Effect of current density on Fe^{2+} (a) and H_2O_2 (b) remaining in the electro-Fenton process ([Triclosan] = 1 mM, [Fe^{2+}] = 0.1 mM, [H_2O_2] = 1 mM, pH = 3)

4.2.3.3 Effect of H_2O_2 to Fe^{2+} ratio (H/F ratio)

This study addressed the effect of the H_2O_2 to Fe^{2+} ratio (H/F ratio) (mM/mM), a critical parameter in the Fenton process and also in the electro-Fenton process, in determining the optimum ratio for the best triclosan degradation efficiency as shown in Figures 4.32 and 4.33. The experimental results indicate that increasing the H/F ratio could induce the removal efficiency to accelerate and reach the maximum level by increasing the production of hydroxyl radical under reaction (4.3). However, the efficiency of the process also depending on reaction (4.4) but it was not significant which can be confirmed by the control experimentation (only 2% removal) outside this experiment. From this experiment, the most effective H/F ratio value was found to be at 40 as 100 percent of the 1 mM triclosan removal efficiency could be achieved by the electro-Fenton process. Increasing the H/F ratios above 40 was not effective in increasing the removal efficiencies. The less difference of efficiency when using the H/F ratios above 40 indicates that the chemicals might be in excess of the requirements of this process for 1 mM triclosan removal and/or might be from the scavenging with other pollutants in this process. It is reasonable to expect that an increase in H_2O_2 will result in more hydroxyl radicals. However, such an input-response correlation may not be linear, because other side reactions that occur simultaneously may also favor a high concentration of H_2O_2. For example, reaction (4.5) shows that H_2O_2 may react with hydroxyl radical to form peroxyl radical ($HO_2^{\cdot}$), which is a much weaker oxidant than hydroxyl radical (Chan and Chu, 2005).

$$ROP\ ratio\ =\ \frac{\%\, pollutant\ \ removal}{\%\, H_2O_2\, consumed} \tag{4.2}$$

$$Fe^{2+} + H_2O_2 \longrightarrow Fe^{3+} + \bullet OH + OH^- \tag{4.3}$$

$$H_2O_2 + organic \rightarrow\ products \tag{4.4}$$

$$\bullet OH + H_2O_2 \rightarrow HO_2^{\bullet} + H_2O \qquad (4.5)$$

Moreover, in this section, the relative oxidation performance (ROP) ratio was also developed as described by equation (4.2) like in the 2,4-DCP section. It was used to indicate the oxidation efficiency related to H_2O_2 consumption as reported in Figure 4.34.

It can be inferred from Figure 4.34 that even though consumption of H_2O_2 increased with the H/F ratios increasing, the real performance in degradation was not the same when the H/F ratios were above 40. This might be due to excessive H_2O_2 molecules in the process. This condition makes activity in H_2O_2 react with hydroxyl radicals to scavenge with other pollutants removal in the process that produces $HO_2^{\cdot}$ via a reaction (reaction (c)). Therefore, generating $HO_2^{\cdot}$ can participate in propagating radical chain reactions by reducing ferric to ferrous ion, which can also induce an increase in ferrous scavenging too. The relative oxidation performance ratio indicated that the oxidation power of triclosan removal increased when the H/F ratios were less than 40 and decreased when more than 40. The data on triclosan removal efficiency and ROP ratio confirms that, the H_2O_2 concentration was a major critical parameter and the H/F ratios at 40 should be the optimum ratio for this process.

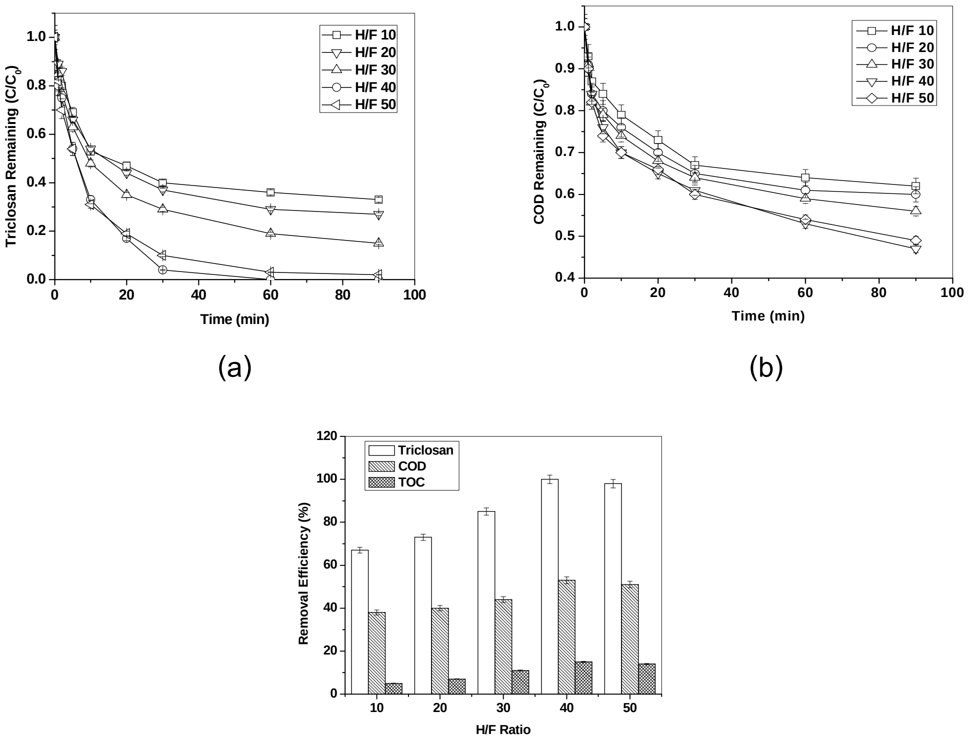

(a) (b)

(c)

Figure 4.32 Effect of H_2O_2 to Fe^{2+} ratio (H/F) on triclosan (a), COD (b) and TOC (c) removal by the electro-Fenton process ([Triclosan] = 1 mM, [Fe^{2+}] = 0.1 mM, electrical current density of 0.15 mA cm^{-2})

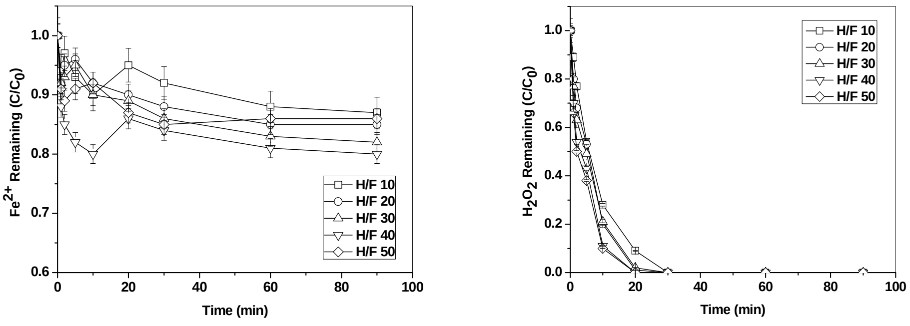

(a) (b)

Figure 4.33 Effect of H_2O_2 to Fe^{2+} ratio (H/F) on Fe^{2+} (a) and H_2O_2 (b) remaining in the electro-Fenton process ([Triclosan] = 1 mM, [Fe^{2+}] = 0.1 mM, [H_2O_2] = 1 mM, electrical current density of 0.15 mA cm^{-2})

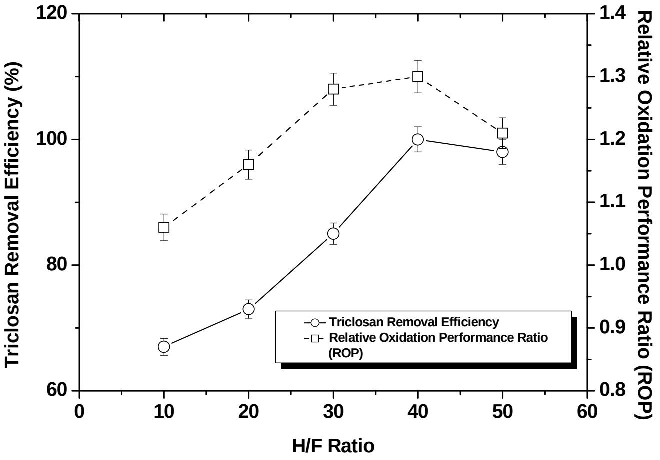

Figure 4.34 Effect of H_2O_2 to Fe^{2+} ratios (H/F) on removal efficiency and Relative Oxidation Performance (ROP) ratio ([Triclosan] = 1 mM, [Fe^{2+}] = 0.1 mM, pH = 3, electrical current density of 0.15 mA cm^{-2})

4.2.3.4 Effect of H_2O_2 feeding mode of operation

Two different H_2O_2 feeding modes of operation - the one-time initial feeding mode and the step feeding mode at 2 minute-intervals - were performed to investigate the effect on triclosan degradation as shown in Figure 4.35. The result, which is significant to this research experiment, shows that the feeding mode had a dominant effect when increasing the current density (0.15 to 0.24 mA cm^{-2}). The reason might be that the higher current density had more electrons for Fe^{2+} regeneration which induced faster regeneration than a lower current or the original Fenton process. In this experiment, the best degradation efficiency was obtained by using the step feeding operation because the step feeding operation could generate ·OH continuously and homogeneously. The step feeding operation mode could also help avoid the presence of excessive ·OH concentrations during the earlier oxidation stages and provide the better ability of this species throughout the whole oxidation process. The level of a sufficient amount of H_2O_2 concentration in the step feeding operation, as well as the optimum ratio of substrate per H_2O_2 consumption reduced the extension of scavenging reactions involving H_2O_2 and ·OH, thus minimizing the H_2O_2 that was inefficient consumption. On the other hand, the Fe^{2+} generation per H_2O_2 ratio was also higher, thus favoring the decomposition of H_2O_2 almost into ·OH instead of O_2. In the lower current density (at 0.15 mA cm^{-2}), no significant difference was observed in the effects of operation feeding modes for both the step feeding mode and the one-time initial feeding mode on degradation efficiencies. On the other hand, the total organic carbon (TOC) removal also confirmed that the step feeding operation mode was better than the initial feeding mode in mineralization as shown in Figure 4.36.

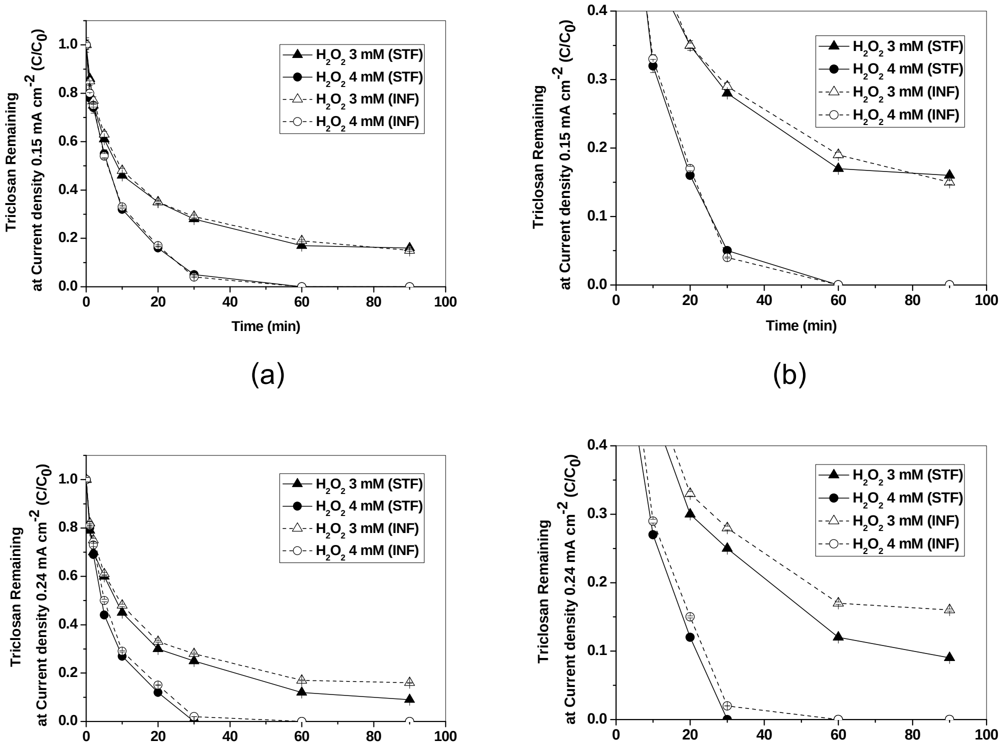

(a) (b)

(c) (d)

Figure 4.35 Effect of H_2O_2 operational feeding mode (step feeding mode; STF, original one time initial feeding mode; INF) on triclosan removal by the electro-Fenton process ([Triclosan] = 1 mM, [Fe^{2+}] = 0.1 mM, [H_2O_2] = 3 and 4 mM, electrical current of 0.15 mA cm^{-2} (a and b) and 0.24 mA cm^{-2}(c and d), pH = 3)

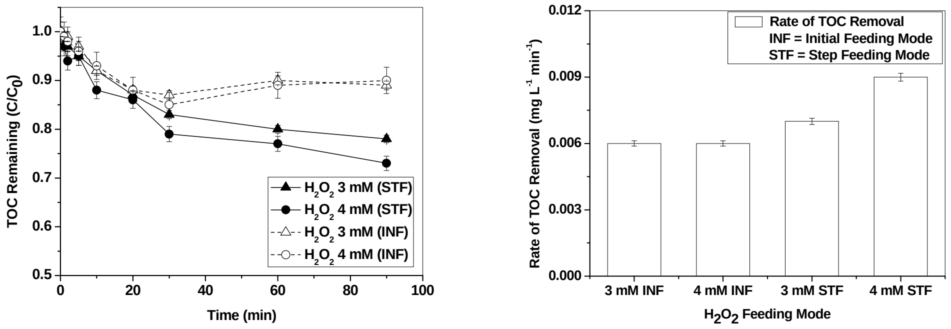

(a) (b)

Figure 4.36 Effect of H_2O_2 operational feeding mode (step feeding mode; STF, original one time initial feeding mode; INF) on TOC removal (a) and rate of TOC removal at initial 20 minutes (b) by the electro-Fenton process ([Triclosan] = 1 mM, [Fe^{2+}] = 0.1 mM, [H_2O_2] = 3 and 4 mM, electrical current of 0.24 mA cm^{-2}, pH = 3)

4.2.3.5 Effect of various conditions on COD and TOC removal

The triclosan removal efficiencies in terms of COD and TOC removal were investigated at various operating conditions as reported in Table 4.3. The data from the experiment showed that under the conditions of the current density of 0.15 mA cm^{-2} with initial Fe^{2+} and H_2O_2 0.1 and 4 mM respectively, at pH 3 could give 1 mM of triclosan removal in terms of COD removal of up to 59%. However, the data shown in Table 5 also shows that 70% of COD and 47% of TOC removal could be obtained when increasing the current density to 0.24 mA cm^{-2} and Fe^{2+}, H_2O_2 up to 1 and 50 mM, respectively. It can be concluded from this section that the various operating parameters especially current density had affected the degrees of triclosan, COD and TOC removal performances.

TABLE 4.3 Percentages of COD and TOC removal in triclosan removal by the electro-Fenton process ([Triclosan] = 1 mM, pH = 3)

Current Density ($mA\ cm^{-2}$)	Fe^{2+} (mM)	H_2O_2 (mM)	COD Removal (%)	TOC Removal (%)
0.15	0.1	4	53±3	15±1.0
0.15	1	50	59±4	33±0.5
0.24	1	50	70±5	47±0.2

4.3 Kinetic of 2,4-dichlorophenol and triclosan removal by the electro-Fenton process

4.3.1. Proposed the novel kinetic modeling of the electro-Fenton process in type of ferrous regeneration

Although the first-order and pseudo-first order model is commonly used to describe kinetics, there are some inaccuracies and limitations in precisely describing the reaction and the phenomena of the electrochemical in cooperation with Fenton's reagents process in ferrous regeneration and continuous H_2O_2 supply (Gözmen et al., 2003). A second-order kinetic model is also used to describe the kinetics of electrochemical combination with Fenton's reagents, where the degradation of 2,4-dichlorophenoxyacetic acid in an aqueous solution was used in the study of Wang and Lemley (Wang and Lemley, 2001). However, it had only described for the kinetics of the anodic Fenton process. Another method is the competitive technique, which is also known to be more accurate than the first-order model method. It has a limitation of determination in using the original substances which the kinetic data is already known and corrects (Boonrattanakij et al., 2009). Though the competition kinetics have given much kinetic data for hydroxyl radicals through various applications, such as the Fenton reaction, photolysis of H_2O_2, photo-Fenton reaction and ozone reactions, neither hydroxyl radicals nor the reaction products could be measured directly (Kwon et al., 2009). In addition to the above-mentioned methods, a study by Anotai et al, 2006 on kinetic determination compared the kinetics of aniline degradation using Fenton and electro-Fenton reactions in terms of overall rate equation for aniline degradation. However, the outcome from this method would be in a reaction order of 1.1 through the Fenton's reaction (almost a first-order reaction) and a reaction order of 0.46 through the electro-Fenton's reaction (about a half-order reaction). In the other studies, the first-order model was applied to describe the kinetics in terms of the total organic carbon (Brillas et al., 1998, 2000) of the reaction in the process of electrochemical combination with Fenton's reagents as well as representing the kinetic constants in each phase of the overall reaction period when divided into two or three phases (Chu et al., 2005). In order to discover a good kinetic model that could describe the reaction of electrochemical combination with Fenton's reagents or electro-Fenton process, some key factors are not to be overlooked, such as the concentration of hydrogen peroxide and the ferrous ion, and the current density. Although there have been studies on the oxidation of organic compounds and hydroxyl radical, none of the reports have been able to attest to the intrinsic kinetic rate constant of its reaction by an electro-Fenton process of the type ferrous regeneration. The intrinsic kinetic rate constant of such a reaction is essential to the number of scientific studies in the engineering field. This research attempts to verify the validation of the kinetic model using the novel analytical kinetic model to find the kinetic constant of the organics oxidation by hydroxyl radicals in an electro-Fenton process of the type ferrous regeneration. For this research 2,4-DCP and triclosan were used as the organic representative.

The basic reaction of electro-Fenton process of the type Fe^{2+} regeneration should involve three key reactions: the regeneration of Fe^{2+} from Fe^{3+} on the surface of the cathode (Reaction 4.6), the generation of hydroxyl radicals (·OH) between Fe^{2+} and H_2O_2 (Reaction 4.7), and the degradation of an organic substance by the ·OH (Reaction 4.10). Some reverse reactions and side reactions (Reactions 4.8, 4.9, 4.11 and 4.12) coexist simultaneously with the key reactions as summarized below (Walling, 1975; Ting et al., 2009; Neyens and Baeyens, 2003):

$$Fe^{3+} + e^{-} \xrightarrow{k_1} Fe^{2+} \qquad (4.6)$$

$$Fe^{2+} + H_2O_2 \xrightarrow{k_2} Fe^{3+} + \bullet OH + OH^{-} \qquad (4.7)$$

$$Fe^{2+} + \bullet\, OH \xrightarrow{k_3} Fe^{3+} + OH^{-} \qquad (4.8)$$

$$Fe^{3+} + H_2O_2 \xrightarrow{k_4} Fe^{2+} + HO_2^{\bullet} + H^{+} \qquad (4.9)$$

$$\bullet\, OH + organic \xrightarrow{k_5} products \qquad (4.10)$$

$$H_2O_2 + organic \xrightarrow{k_6} products \qquad (4.11)$$

$$\bullet\, OH + H_2O_2 \xrightarrow{k_7} HO_2^{\bullet} + H_2O \qquad (4.12)$$

The novel kinetic model for describing the electro-Fenton process of the type Fe^{2+} regeneration can be determined by assuming that the organic substance (S) is primarily degraded by ·OH and its reaction rate (d[S]/dt) can be supposed by equation (4.13)

$$-\left[\frac{d[S]}{dt}\right] = k_5[\bullet OH][S] \qquad (4.13)$$

From the reactions 4.7, 4.8, 4.10, and 4.12, the adjustment of ·OH concentration (d[·OH]/dt) in relation to its generation rate from H_2O_2 and Fe^{2+}, and its consumption rate reacting with Fe^{2+}, organic substance and H_2O_2 are shown below:

$$\frac{d[\bullet OH]}{dt} = k_2[Fe^{2+}][H_2O_2] - k_3[Fe^{2+}][\bullet OH] - k_5[\bullet OH][S] - k_7[\bullet OH][H_2O_2] \qquad (4.14)$$

Moreover, the result of many studies support the theory that ·OH is a highly reactive free radical with an extremely short lifetime of nanoseconds (Liu et al., 1999). Its concentration is usually considered to be constant but only at a low level and the d[·OH]/dt approaches zero according to a steady state approximation. Then equation

(4.13) can be rearranged in terms of organic degradation rate, becoming a function of $[H_2O_2]$ and [S] mainly, as shown in equation (4.16)

$$[\bullet OH] = \left(\frac{k_2[Fe^{2+}][H_2O_2]}{k_3[Fe^{2+}] + k_7[H_2O_2] + k_5[S]} \right) \tag{4.15}$$

$$-\left[\frac{d[S]}{dt} \right] = k_5[S]\left(\frac{k_2[Fe^{2+}][H_2O_2]}{k_3[Fe^{2+}] + k_7[H_2O_2] + k_5[S]} \right) \tag{4.16}$$

The concentration of Fe^{2+} in the system is dependent on its regeneration rate by an electron supplying from the electrical current at the cathode (Reaction 4.6) and the decomposition rate (Reaction 4.7 and 4.8). It can be inferred that there is a relationship between the rate of Fe^{2+} concentration and the current applied (I) on the cathode, as can be expressed by equation (4.18).

$$[e^-] = It \tag{4.17}$$

$$\frac{d[Fe^{2+}]}{dt} = k_1It[Fe^{3+}] - k_2[Fe^{2+}][H_2O_2] - k_3[Fe^{2+}][\bullet OH] + k_4[Fe^{3+}][H_2O_2] \tag{4.18}$$

Assuming that the $[H_2O_2]$ during the reaction is dependent on its initial concentration $[H_2O_2]_0$ with a fixed ratio of α and according to the same reactor and electrode type which done experiment by Masomboon et al., 2009, the ferrous mechanism of electro-Fenton process could be described as $[Fe^{3+}]$ is completely regenerated to $[Fe^{2+}]$ with the relationship as shown in equation (4.19)-(4.20).

$$[H_2O_2] = \alpha[H_2O_2]_0 \tag{4.19}$$

$$\begin{aligned} [Fe^{3+}] &= \frac{1}{kt}[Fe^{2+}] \\ &= \frac{\lambda}{t}[Fe^{2+}] \end{aligned} \tag{4.20}$$

For the initial condition at t=0, [Fe^{2+}] = [Fe^{2+}]$_0$, [Fe^{2+}], it can be shown and expressed as equations (4.21) and (4.24).

$$\frac{d[Fe^{2+}]}{dt} = \left(k_1 I\lambda - k_2\alpha[H_2O_2]_0\right)[Fe^{2+}] \tag{4.21}$$

$$\int_{[Fe^{2+}]_0}^{[Fe^{2+}]_t} \frac{1}{[Fe^{2+}]} d[Fe^{2+}] = \int_0^t (k_1 I\lambda - k_2 \propto [H_2O_2]_0)dt \tag{4.22}$$

$$\ln\left(\frac{[Fe^{2+}]}{[Fe^{2+}]_0}\right) = (k_1 I\lambda - k_2 \propto [H_2O_2]_0)t + C \tag{4.23}$$

At t = 0 , [Fe^{2+}] = [Fe^{2+}]$_0$, C = 0

$$[Fe^{2+}] = [Fe^{2+}]_0 e^{(k_1 I\lambda - k_2\alpha[H_2O_2]_0)t} \tag{4.24}$$

The above equation indicates that [Fe^{2+}] is a function of experimental time. It was demonstrated that [Fe^{2+}] in this system depends on its initial concentration and the factors of I, [H$_2$O$_2$]$_0$ and time. Once we replace equation (4.24) with equation (4.16), the rate of organic degradation can be further expressed in equation (4.25)-(4.30) as follows:

$$-\frac{d[S]}{dt} = k_5[S]\left(\frac{k_2[Fe^{2+}]}{k_3\frac{[Fe^{2+}]}{[H_2O_2]} + k_7 + k_5\frac{[S]}{[H_2O_2]}}\right) \tag{4.25}$$

$$-\frac{1}{[s]}(k_3\frac{[Fe^{2+}]}{[H_2O_2]} + k_5\frac{[S]}{[H_2O_2]} + k_7)d[S] = k_5 k_2[Fe^{2+}]dt \tag{4.26}$$

$$(-k_3\frac{[Fe^{2+}]}{[H_2O_2]}\frac{1}{[S]}-\frac{k_5}{[H_2O_2]}+k_7\frac{1}{[S]})d[S]=k_5k_2[Fe^{2+}]dt \qquad (4.27)$$

$$\int_{S_0}^{S}([-k_3\frac{[Fe^{2+}]}{[H_2O_2]}+k_7]\frac{1}{[S]}-\frac{k_5}{[H_2O_2]})d[S]=\int_0^t(k_5k_2[Fe^{2+}]_0e^{(k_1I\lambda-k_2\propto[H_2O_2]_0)t})dt \qquad (4.28)$$

$$(k_3\frac{[Fe^{2+}]}{[H_2O_2]}+k_7)\ln\frac{[S_0]}{[S]}+\frac{k_5}{[H_2O_2]}([S_0]-[S])=k_5k_2[Fe^{2+}]_0\frac{1}{(k_1\lambda I-k_2\propto[H_2O_2]_0)}e^{(k_1\lambda I-k_2\propto[H_2O_2]_0)t}+C \qquad (4.29)$$

Divide all by $(k_3\frac{[Fe^{2+}]}{[H_2O_2]}+k_7)$

$$\begin{aligned}&\ln\frac{[S_0]}{[S]}+\frac{k_5}{[H_2O_2](k_3\frac{[Fe^{2+}]}{[H_2O_2]}+k_7)}([S_0]-[S])\\&=\frac{k_5k_2[Fe^{2+}]_0}{(k_3\frac{[Fe^{2+}]}{[H_2O_2]}+k_7)(k_1\lambda I-k_2\propto[H_2O_2]_0)}e^{(k_1\lambda I-k_2\propto[H_2O_2]_0)t}+C\end{aligned} \qquad (4.30)$$

At t = 0, [S] = [S_0] , C = $-\frac{k_5k_2[Fe^{2+}]_0}{(k_3\frac{[Fe^{2+}]}{[H_2O_2]}+k_7)(k_1\lambda I-k_2\propto[H_2O_2]_0)}$

After integration, the organic concentration [S] becomes a function of experimental time, decreasing from its initial concentration [S_0] at the beginning of the reaction (t=0) gradually as described by equation (4.31).

$$\begin{aligned}&\ln\frac{[S_0]}{[S]}+\frac{k_5}{(k_3[Fe^{2+}]+k_7[H_2O_2]\ )}\left([S_0]-[S]\right)\\&=\frac{k_5k_2[Fe^{2+}]_0}{(k_3\left(\frac{[Fe^{2+}]}{[H_2O_2]}\right)+k_7)(k_1\lambda I-k_2\alpha[H_2O_2]_0)}(e^{(k_1\lambda I-k_2\alpha[H_2O_2]_0)t}-1)\end{aligned} \qquad (4.31)$$

To simplify Equation (4.31), let

$$A = \frac{k_5}{(k_3[Fe^{2+}] \ + k_7[H_2O_2] \ )}$$

$$B = \frac{k_5 k_2 [Fe^{2+}]_0}{(k_3(\frac{[Fe^{2+}]}{[H_2O_2]}) + k_7)(k_1 \lambda I - k_2 \propto [H_2O_2]_0)}$$

$$C = k_1 \lambda I - k_2 \propto [H_2O_2]_0$$

The above equation can be re-arranged into a simplified form as shown below in equation (4.32):

$$\ln\frac{[S_0]}{[S]} + A([S_0] - [S]) = B(e^{Ct} - 1) \qquad (4.32)$$

From the rate equation (equation (4.16)), term A in equation (4.32) can be derived by using the modification of the inverse of the initial graphical method (Liou and Lu, 2007), and obtained from the intercept per slope of the graphical plot as shown below:

$$r = -\frac{d[S]}{dt} = k_5[S]\left(\frac{k_2[Fe^{2+}][H_2O_2]}{k_3[Fe^{2+}] + k_7[H_2O_2] + k_5[S]}\right) \qquad (4.33)$$

$$\frac{1}{r} = \frac{1}{initial\ rate} = \frac{t}{1 - \frac{[S]}{[S_0]}} = \left(\frac{k_3[Fe^{2+}] + k_7[H_2O_2]}{k_5 k_2 [Fe^{2+}][H_2O_2]}\right)\frac{1}{[S]} + \frac{1}{k_2[Fe^{2+}][H_2O_2]} \qquad (4.34)$$

The ferrous mechanism equation (equation (4.24)) can be adapted to a natural logarithm as shown in equation (4.35) for finding term C from the slope of the graphical plot which is shown below:

$$\ln\frac{[Fe^{2+}]}{[Fe^{2+}]_0} = (k_1 \lambda I - k_2 \alpha [H_2O_2]_0)t \qquad (4.35)$$

In conclusion, the novel proven kinetic equation (equations (4.32), (4.33), (4.34), and (4.35)) has been established as the main kinetic model for an electro-Fenton process of the type ferrous regeneration to describe Fe^{2+} regeneration and the organic degradation in an aqueous solution against reaction time.

4.3.2 Validation of the novel kinetic model of an electro-Fenton process by experimentation

Model set-up

To validate and establish the novel kinetic model, the assumptions were as follows:

1. The solution in the batch reactor was mixed completely and continuously in H_2O_2 feeding by using chemical feeding pump (0.5 ml min^{-1}) for hydroxyl radical steady state condition.
2. The temperature was constant at 25 °C.
3. The value of pH was 3, Fe^{2+} was the dominant form of Fe(II) species at pH 2.6-3.0 (Kang et al., 2002). The change of pH was omitted as the maximum variation of 0.20 was allowed throughout the process controlled by pH controller.
4. The hydroxyl radical was the main radical to attack all organic substances in the solution. H_2O_2, $HO_2^{\cdot}$ and $O_2^{-\cdot}$ were unable to degrade the contaminant.
5. The resistance at anode and cathode electrodes was so minimal that it can be disregarded.
6. The value of $k_2 = 55\ M^{-1}s^{-1}$, $k_3 = 3.2 \times 10^8\ M^{-1}s^{-1}$ and $k_7 = 3.3 \times 10^7\ M^{-1}s^{-1}$ are the rate constants which were received by the value from the experiment of Buxton et al, 1988.

Validation was done in three sets of experiments which used 2,4-DCP and triclosan as the organic representative. Three sets of experiments were conducted to study the effects of operating pH, current density, and hydrogen peroxide concentration. All of the experiments were compared with both the pseudo-first order kinetic model and our novel model.

4.3.3 Kinetics of 2,4-dichlorophenol (2,4-DCP) removal by the electro-Fenton process

4.3.3.1 Effect of different operating pH on kinetics of 2,4-DCP removal by the electro-Fenton process

In the Fenton and electro-Fenton processes, the productivity of hydroxyl radicals and the concentration of ferrous ions were controlled by the pH solution (Ting et al., 2009). Hence, pH is also an important parameter for the electro-Fenton process of the type ferrous regeneration. Currently, it is well known that the reaction of both the Fenton and electro-Fenton process have the highest efficiency when the pH is around 2-4 (Duesterberg et al., 2008). In this experiment, constant pH 2, 3, 3.5 were used for investigating the effect of pH on the kinetic of electro-Fenton process of the type ferrous regeneration. The experiment was conducted for kinetic constant determination, using both the pseudo-first order kinetic model and the novel model as shown in Figure 4.37. The result of both models indicated that pH 3 was the best condition in 2,4-DCP removal by the electro-Fenton process of the type ferrous regeneration with confirmation by a higher initial degradation rate than other pH that was reported in Table 4.4. From Table 4.4, the results of both models indicate that the rate constant depended on the pH of the solution. At a pH of over 3.0, the decreasing oxidation potential of ·OH affected the reduction of the decomposition rate, and also the increase of pH induced a decrease in the fraction of dissolved iron species. While at pH under 3.0, the electro-generated hydrogen peroxide solvates a proton to form an oxonium ion ($H_3O_2^+$) which enhances its stability and reduces the reactivity with ferrous ions and consequently less hydroxyl radicals are produced by reaction (4.7) (Kwon et al., 1999).

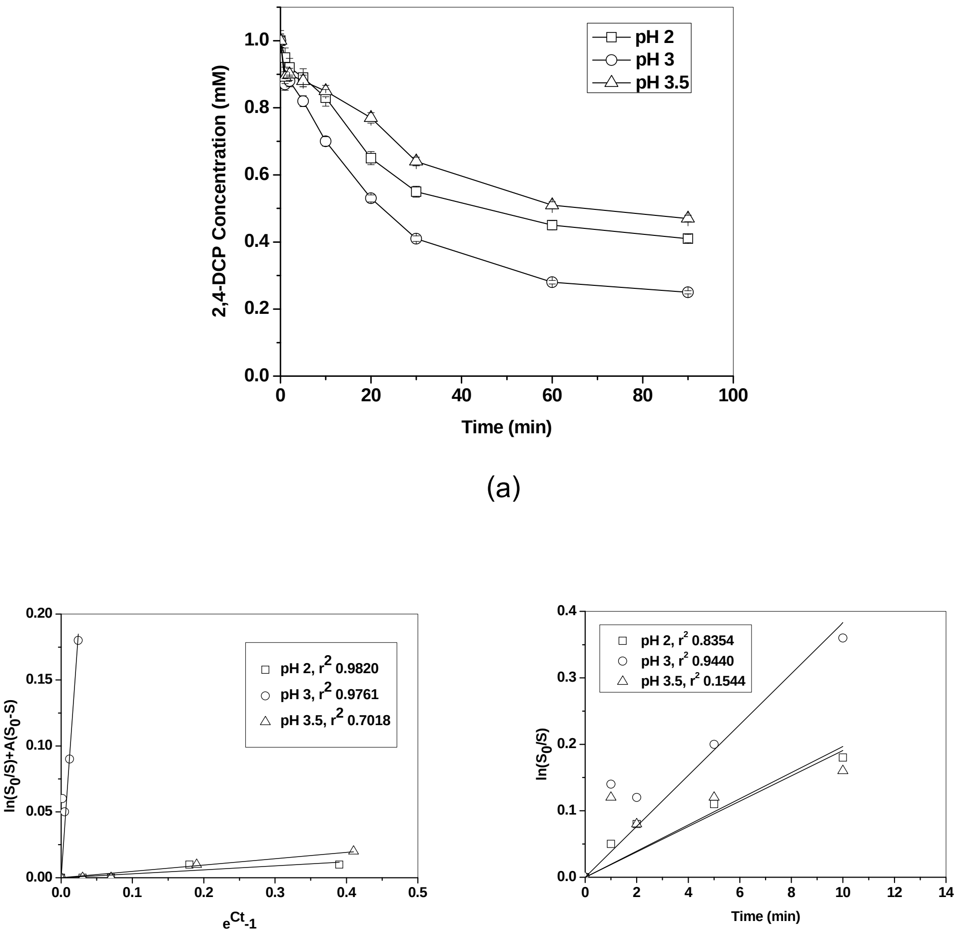

(a)

(b)

(c)

Figure 4.37 Effect of various constant pH on the kinetic of 2,4-DCP degradation (a) by novel kinetic model (b) and pseudo-first order model (c) plotted ([2,4-DCP] 1 mM, [Fe^{2+}] 0.1 mM, [H_2O_2] 1 mM, electrical current density of 0.05 mA cm^{-2})

Table 4.4 Effect of pH on kinetic constant of 2,4-DCP ([2,4-DCP] 1 mM, [Fe^{2+}] 0.1 mM, [H_2O_2] 1 mM (continuous feed 0.5 ml min^{-1}), electrical current of 0.05 mA cm^{-2})*

pH	Initial degradation rate (10^{-3} mM. min^{-1})	k (pseudo 1^{st}-order) (min^{-1})	$k_{\cdot OH \rightarrow 2,4\text{-}DCP}$ (Novel model) (10^9 $M^{-1}.s^{-1}$)
2.0	19.5	0.0195	0.07
3.0	34.4	0.0344	1.95
3.5	18.9	0.0189	0.05

*All data were calculated at 10 min. of reaction time.

4.3.3.2. Effect of current density on kinetics of 2,4-DCP removal by the electro-Fenton process

One of the most important parameters that affect the electro-Fenton process of the type ferrous regeneration is the amount of DC current supplied to the electrodes (Chen et al., 2011). The experimental condition of initial Fe^{2+} of 0.1 mM and H_2O_2 of 1 mM (continuous feeding) at constant pH 3 was performed to study the effect of current densities on the kinetics of the process. The current density, 0.01, 0.05, 0.10, 0.25, and 0.50 mA cm^{-2}, was varied to investigate the effect of current density on the amount of ferrous concentration and the kinetics of the process. The remaining of ferrous concentration in terms of natural logarithm ($\ln(Fe^{2+}/Fe_0^{2+})$) depended significantly on the current density as shown in Figure 4.38. The results also show that a higher ferrous concentration remaining ratio was found when increasing the current density might cause the higher current force to support the continuous regeneration of [Fe^{3+}] to [Fe^{2+}] to the system. The rate constant of 2,4-DCP with hydroxyl radical in various conditions of current density variation was determined by data plotted compared to the pseudo-first order model as shown in Figure 4.39, and using equation 9 with the novel model analysis as reported in Table 4.5. The rate constants obtained from various current densities were found to be in the range of 0.99×10^9 to 1.95×10^9 $M^{-1}s^{-1}$. The data from

Table 4.5 indicates that when increasing the current density, our novel model (plotted $[\ln(S_0/S)+A(S_0-S)]$ vs. $[e^{Ct}-1]$) could give higher correlation coefficients compared to the former pseudo-first order model. This suggests that the novel model of electro-Fenton process of the type ferrous regeneration is suitable and better for kinetic investigation than the pseudo-first order model since the current density is also considered a significant parameter to be included in the kinetic determination of electro-Fenton process of the type ferrous regeneration.

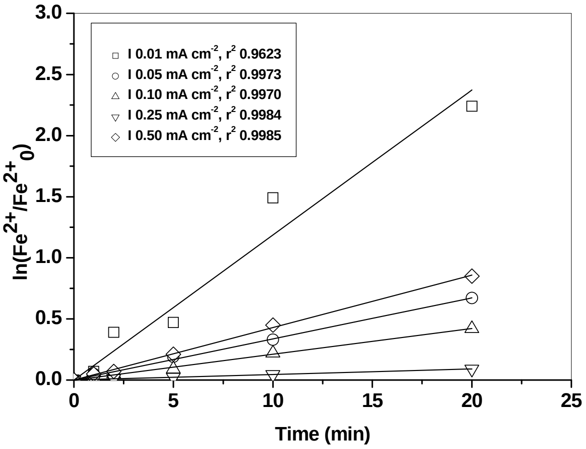

Figure 4.38 Effect of various current densities on ferrous concentration remaining ratio ([2,4-DCP] 1 mM, $[Fe^{2+}]$ 0.1 mM, $[H_2O_2]$ 1 mM, pH 3, electrical current densities of 0.01-0.50 mA cm^{-2})

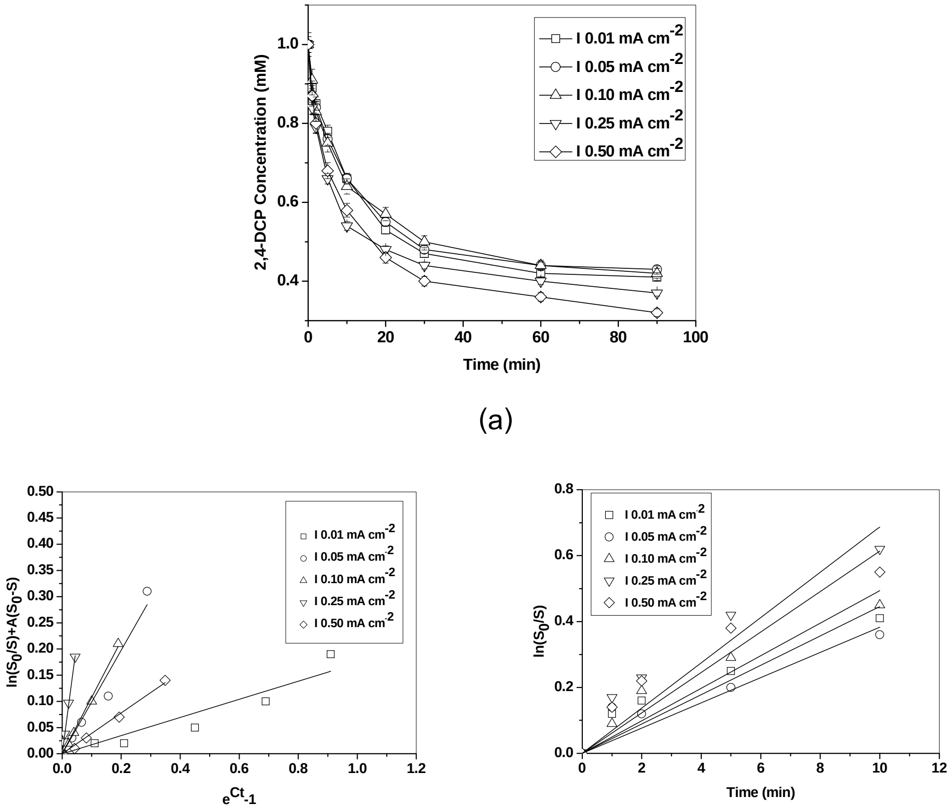

(a)

(b) (c)

Figure 4.39 Effect of various current densities on the kinetic of 2,4-DCP degradation (a) by novel kinetic model (b) and pseudo-first order model (c) plotted ([2,4-DCP] 1 mM, [Fe^{2+}] 0.1 mM, [H_2O_2] 1 mM, pH 3, electrical current densities of 0.01-0.50 mA cm^{-2})

4.3.3.3 Effect of hydrogen peroxide concentration on kinetics of 2,4-DCP removal by the electro-Fenton process

The most important reagent playing the role of an oxidizing agent in the Fenton process and also in the electro-Fenton process of the type ferrous regeneration is hydrogen peroxide (H_2O_2). In this experiment, the H_2O_2 concentration was varied to determine the relationship between the amount of ferrous concentration and kinetics in the electro-Fenton process of the type ferrous regeneration. A ferrous concentration (Fe^{2+}) of 0.1 mM and current density of 0.05 and 0.10 mA cm^{-2} were used at constant pH

3 and H_2O_2 was continuously fed at different total concentrations of 1, 3, and 5 mM for the kinetic investigation experiment. The experiment was studied using both the pseudo-first order kinetic model and our novel model together. The relationship between the H_2O_2 concentrations and remaining amount of Fe^{2+} is shown in Figure 4.40. The result of the Fe^{2+} remaining ratio in this process suggests that increasing the H_2O_2 could affect the rate of the remaining ferrous concentration. The data of H_2O_2 variation from Table 4.5 shows that the initial degradation rate of 2,4-DCP removal depended on an increase in hydroxyl radical concentration resulting from H_2O_2 addition. However, at a higher dosage of H_2O_2 with the current density increasing, the degradation rate decreased because the hydroxyl radicals were scavenging the effect of H_2O_2 (Reaction (R7)) and the recombination of the hydroxyl radicals. It can be seen that higher rates of 2,4-DCP degradation and ferrous regeneration were achieved when the optimum H_2O_2 concentration was used. The profile of concentration of 2,4-DCP behavior was demonstrated in Figure 4.41. The rate constants obtained from various H_2O_2 concentrations were plotted for the novel model compared to the pseudo-first order model as shown in Figure 4.42. The rate constants for various H_2O_2 concentrations were found to be between 0.76×10^9 and 1.82×10^9 $M^{-1}s^{-1}$ as shown in Table 4.5. The data from the table shows that at a low current density with different H_2O_2 concentrations, the linear correlation coefficients in the novel model gave a fitting similar to the pseudo-first order model. However, it seems to be a better fit with the novel model than the pseudo-first order model when a higher current density was applied. This suggests that the rate constant of the electro-Fenton process of the type ferrous regeneration depends significantly on H_2O_2 concentrations and also current density. All data confirms that the novel model is a good application for determining the hydroxyl radical kinetic rate constant of the electro-Fenton process of the type ferrous regeneration.

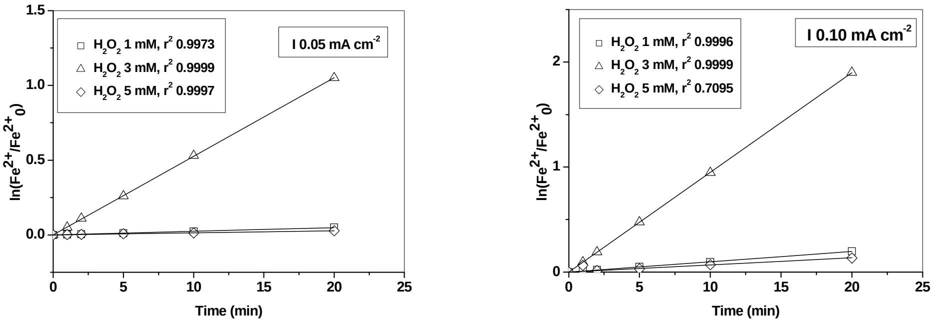

(a) (b)

Figure 4.40 Effect of various H_2O_2 on ferrous concentration remaining ratio ([2,4-DCP] 1 mM, [Fe^{2+}] 0.1 mM, [H_2O_2] 1-5 mM, pH 3, electrical current density of 0.05 (a) and 0.10 (b) mA cm^{-2})

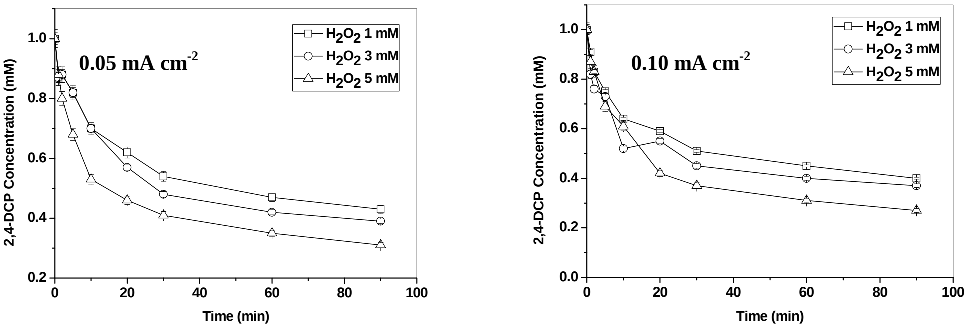

(a) (b)

Figure 4.41 Effect of various H_2O_2 on kinetic of 2,4-DCP degradation ([2,4-DCP] 1 mM, [Fe^{2+}] 0.1 mM, [H_2O_2] 1-5 mM, pH 3, electrical current density of 0.05 (a) and 0.10 mA cm^{-2} (b))

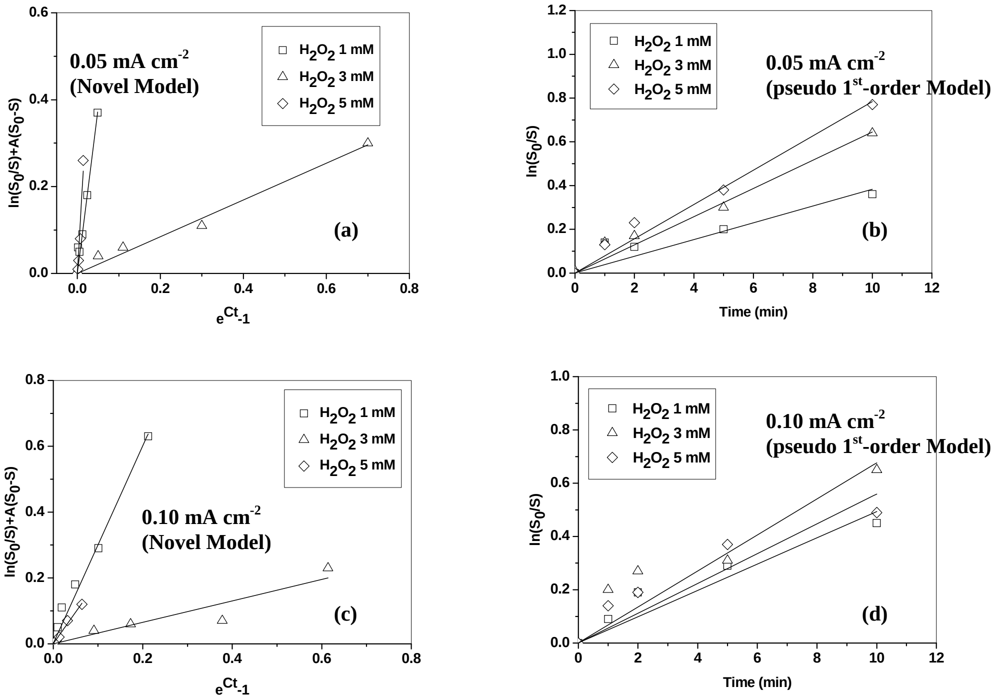

Figure 4.42 Effect of various H_2O_2 on novel kinetic model (a) and pseudo-first order model (b) plotted ([2,4-DCP] 1 mM, [Fe^{2+}] 0.1 mM, [H_2O_2] 1-5 mM, pH 3, electrical current density of 0.05 and 0.10 mA cm^{-2})

4.3.3.4 Rate constant of 2,4-DCP with hydroxyl radical

With reference to the novel model expressed in equation (9), the rate constant of 2,4-DCP used as an organic representative with hydroxyl radical is summarized in Table 4.5. As shown in the table results, the range of rate constants were between 0.76 x 10^9 to 1.95 x 10^9 $M^{-1}s^{-1}$; the average value of the rate constant in this experiment was 1.437 x 10^9 $M^{-1}s^{-1}$ with a standard deviation of 0.494. These result was received by the validation of the experiments on degradation of 2,4-DCP as an organic representative at initial Fe^{2+} of 0.1 mM, H_2O_2 of 1-5 mM (continuous feeding) and constant pH 3, with different current densities (0.01, 0.05, 0.10, 0.25 and 0.50 mA cm^{-2}). For the accuracy of the model comparison, the experimental data was plotted by using both our novel model and the pseudo-first order model, respectively. Table 4.5 presents the fitting results in linear form for our novel model and the pseudo-first order model. It is apparent that the correlation coefficients for the fit of our novel model are significantly greater than those of the pseudo-first order model. Although the conventional pseudo-first order model is the simplest model to describe a variety of chemical reactions and has been widely applied to several of water and wastewater treatment processes, it is difficult to accurately describe the reaction kinetic of the electro-Fenton process of the type ferrous regeneration precisely. It should be noted that the novel model can clearly identify the kinetics of the electro-Fenton process of the type ferrous regeneration and that the prediction in organic degradation and the phenomena of the ferrous concentration in the process can be derived more accurately than the pseudo-first order model.

Table 4.5 Summary of rate constant of 2,4-DCP with hydroxyl radical by novel model under various conditions*

Fe^{2+} (mM)	H_2O_2 (mM)	Current Density (mA cm^{-2})	Initial degradation rate (10^{-3} mM min^{-1})	C	$k_{\cdot OH \rightarrow 2,4\text{-}DCP}$ (Novel Model) (10^9 $M^{-1}.s^{-1}$)	r^2 (Novel Model)	r^2 (pseudo 1^{st}-order Model)
0.1	1	0.01	34.0	0.119	1.23	0.897	0.875
		0.05	34.4	0.034	1.95	0.963	0.944
		0.10	45.9	0.021	1.33	0.996	0.970
		0.25	68.3	0.004	1.12	0.999	0.869
		0.50	61.3	0.042	0.99	0.997	0.867
0.1	1	0.05	34.4	0.002	1.07	0.976	0.944
	3		64.3	0.052	1.29	0.986	0.970
	5		78.3	0.001	1.36	0.948	0.976
0.1	1	0.10	45.9	0.009	1.75	0.983	0.970
	3		67.6	0.095	1.82	0.885	0.827
	5		56.4	0.006	0.76	0.988	0.821

*All of data were calculated at 10 min. of reaction time.

4.3.4 Kinetics of triclosan removal by the electro-Fenton process

4.3.4.1 Effect of different operating pH on kinetics of triclosan removal by the electro-Fenton process

The productivity of hydroxyl radical and ferrous ions concentration were controlled by pH solution of the electro-Fenton process. Hence, pH is also an important parameter for the electro-Fenton process of the type ferrous regeneration. Currently, it is well known that the reaction of both Fenton and electro-Fenton process have the highest efficiency when the pH is around 2-4 (Duesterberg et al., 2008). In this experiment, constant pH 2, 3, 3.5 were used for investigating the effect of pH on the kinetic of electro-Fenton process of the type ferrous regeneration. The experiment was conducted, using both the pseudo-first order kinetic model and the novel model for kinetic constant determination as shown in Figure 4.43. The result of both models indicated that pH 3 was the best condition in triclosan removal by the electro-Fenton process of the type ferrous regeneration with confirmation by a higher initial degradation rate than any other pH reported in Table 4.6. From Table 4.6, the results indicate that the rate constant was depended on the pH of the solution. At pH over 3.0, the decreasing oxidation potential of ·OH affected the reduction of the decomposition rate, and also the increasing of pH induced a decrease in the fraction of dissolved iron species. While at pH under 3.0, the electro-generated hydrogen peroxide solvates a proton to form an oxonium ion ($H_3O_2^+$) which enhances its stability and reduces the reactivity with ferrous ions and consequently less hydroxyl radicals are produced by reaction (4.7) (Kwon et al., 1999).

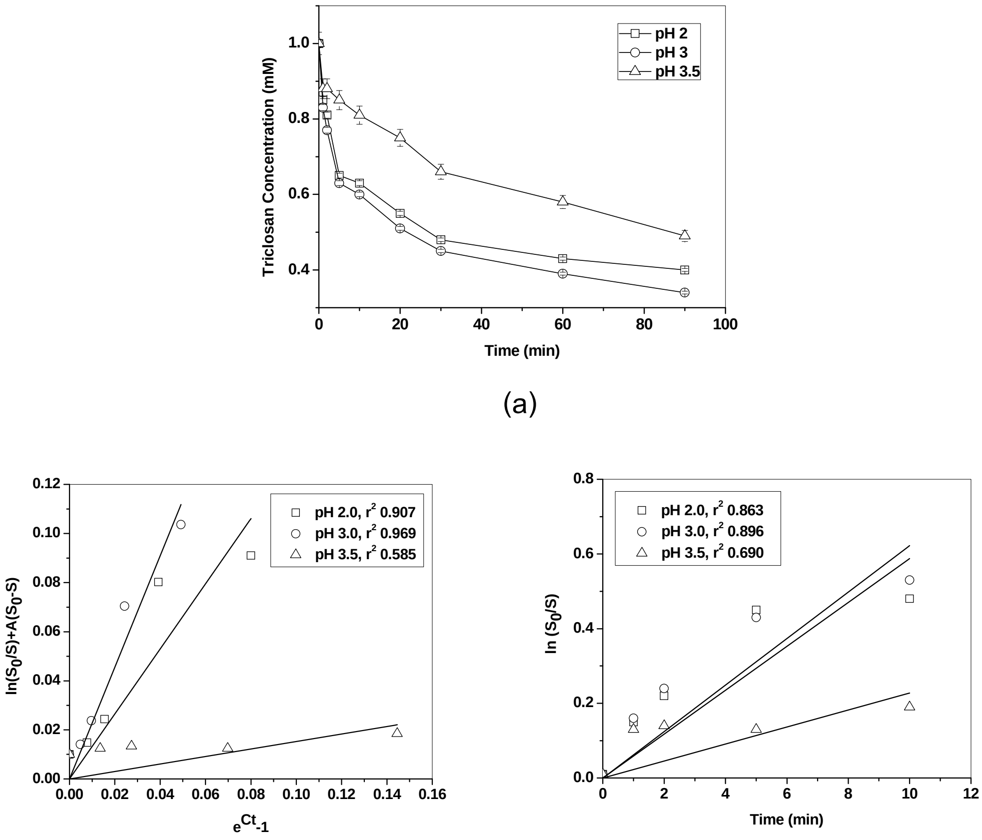

(a)

(b) (c)

Figure 4.43 Effect of various constant pH on kinetic of triclosan degradation (a) by novel kinetic model (b) and pseudo-first order model (c) plotted ([Triclosan] 1 mM, [Fe^{2+}] 0.1 mM, [H_2O_2] 1 mM, electrical current density of 0.15 mA cm^{-2})

Table 4.6 Effect of pH on kinetic constant of triclosan ([Triclosan] 1 mM, [Fe^{2+}] 0.1 mM, [H_2O_2] 1 mM (continuous feed), electrical current density of 0.15 mA cm^{-2})*

pH	Initial degradation rate (10^{-3} mM. min^{-1})	k (pseudo 1^{st}-order) (min^{-1})	$k_{\cdot OH \rightarrow Triclosan}$ (Novel model) (10^9 $M^{-1}.s^{-1}$)
2.0	58.7	0.0587	0.71
3.0	62.2	0.0622	5.34
3.5	22.0	0.0220	0.16

*All data were calculated at 10 min. of reaction time.

4.3.4.2. Effect of current density on kinetics of triclosan removal by the electro-Fenton process

One of the most important parameters affecting the electro-Fenton process of the type ferrous regeneration is the amount of DC current supplied to the electrodes (Chen et al., 2011). The experimental condition of initial Fe^{2+} of 0.1 mM and H_2O_2 of 1 mM (continuous feeding) at constant pH 3 was performed to study the effect of current densities on the kinetics of the process. The current density, 0.01, 0.15, 0.24, 0.35, and 0.50 mA cm^{-2}, was varied to investigate the effect of current density on the amount of ferrous concentration and the kinetics of the process. The remaining of ferrous concentration in terms of natural logarithm ($\ln(Fe^{2+}/Fe_0^{2+})$) depended significantly on the current density as shown in Figure 4.44. The results also show that a higher ferrous concentration remaining ratio found when increasing current density might cause the higher current force to support the continuous regeneration of [Fe^{3+}] to [Fe^{2+}] to the system. The rate constant of triclosan with hydroxyl radical with various current densities was determined by data plotted compared to the pseudo-first order model as shown in Figure 4.45, and using equation 9 with the novel model analysis as reported in Table 4.7. The rate constants obtained from various current densities were found to be in the range of 4.15×10^9 to 6.54×10^9 $M^{-1}s^{-1}$. The data from Table 4.7 indicates that when increasing current density, our novel model (plotted [ln(S_0/S)+A(S_0-S)] vs. [e^{Ct}-1]) could give higher correlation coefficients compared to the former pseudo-first order model. This suggests that the novel model of the electro-Fenton process of the type ferrous regeneration is suitable and better for kinetic investigation than the pseudo-first order model since the current density is also considered a significant parameter to be included in the kinetic determination of the electro-Fenton process of the type ferrous regeneration.

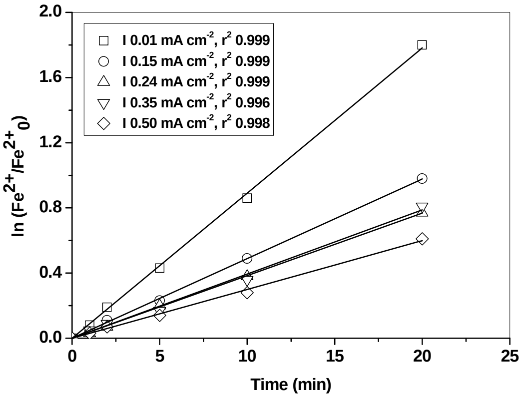

Figure 4.44 Effect of various current densities on ferrous concentration remaining ratio ([Triclosan] 1 mM, [Fe^{2+}] 0.1 mM, [H_2O_2] 1 mM, pH 3, electrical current densities of 0.01-0.50 mA cm^{-2})

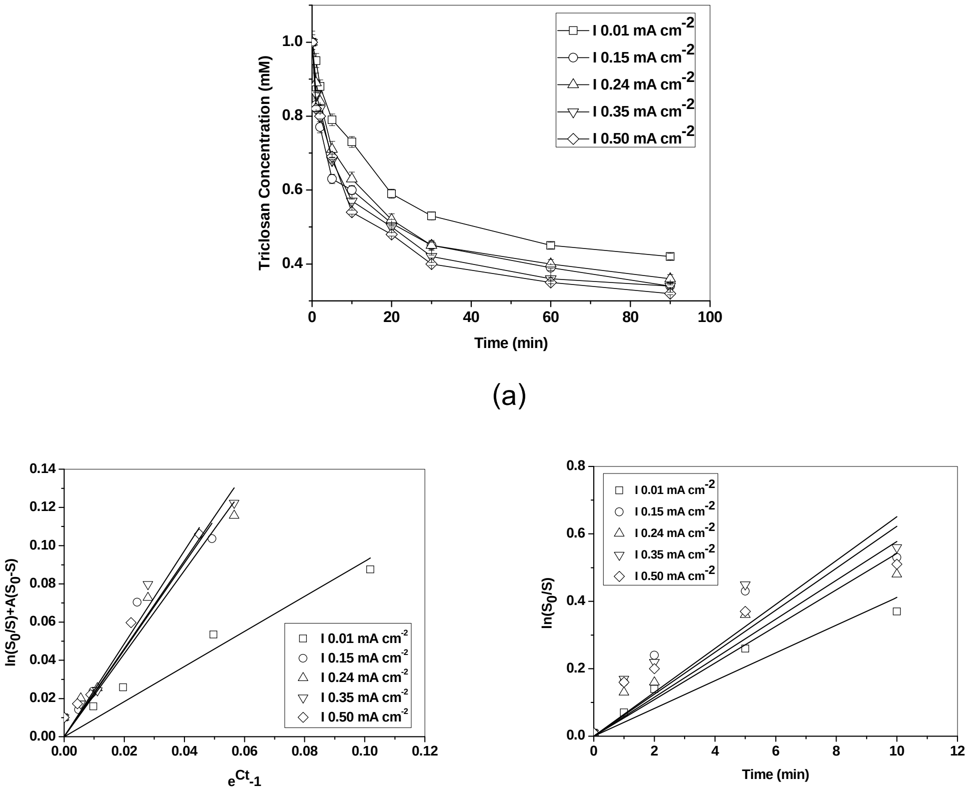

(a)

(b) (c)

Figure 4.45 Effect of various current densities on kinetic of triclosan degradation (a) by novel kinetic model (b) and pseudo-first order model (c) plotted ([Triclosan] 1 mM, [Fe^{2+}] 0.1 mM, [H_2O_2] 1 mM, pH 3, electrical current densities of 0.01-0.50 mA cm^{-2})

4.3.4.3 Effect of hydrogen peroxide concentration on kinetics of triclosan removal by the electro-Fenton process

The most important reagent playing the role of an oxidizing agent in Fenton and also in the electro-Fenton process of the type ferrous regeneration is hydrogen peroxide (H_2O_2). In this experiment, H_2O_2 concentration was varied to determine the relationship between the amount of ferrous concentration and kinetics in the electro-Fenton process of the type ferrous regeneration. Ferrous concentration (Fe^{2+}) of 0.1 mM and current densities 0.05 and 0.10 mA cm^{-2} were used at constant pH 3 and H_2O_2 was continuously fed at different total concentrations of 1, 3, and 5 mM for the kinetic investigation experiment. The experiment was studied using both the pseudo-first order kinetic model and our novel model together. The relationship between the H_2O_2 concentrations and remaining amount of Fe^{2+} is shown in Figure 4.46. The result of remaining Fe^{2+} ratio in this process suggests that increasing the H_2O_2 could affect the rate of the remaining ferrous concentration. The data of H_2O_2 variation from Table 4.7 shows that an initial degradation rate of triclosan removal depended on an increase in hydroxyl radical concentration resulting from H_2O_2 addition. However, at a higher dosage of H_2O_2 with an increasing current density, the degradation rate decreased because the hydroxyl radicals were scavenging the effect of H_2O_2 (Reaction (R7)) and the hydroxyl radicals recombined. It can be seen that the higher rates of triclosan degradation and ferrous regeneration were achieved when the optimum H_2O_2 concentration was used. The profile of concentration of triclosan behavior was demonstrated in Figure 4.47. The rate constants obtained from various H_2O_2 concentrations were plotted for the novel model compared to the pseudo-first order model as shown in Figure 4.48. The rate constants for various H_2O_2 concentrations were found to be between $4.21\text{x}10^9$ and $6.90\text{x}10^9$ $M^{-1}s^{-1}$ as shown in Table 4.7. The data from the table shows that at a low current density with different H_2O_2 concentrations, the linear correlation coefficients in the novel model gave a fitting similar to the pseudo-first order model. However, it seems to fit better with the novel model than the pseudo-first order model when a higher current density was applied. This suggests that the rate constant of the electro-Fenton process of the type ferrous regeneration depends significantly on H_2O_2 concentrations and also current density. All the data confirms that the novel model is a good application for determining the hydroxyl radical kinetic rate constant of the electro-Fenton process of the type ferrous regeneration.

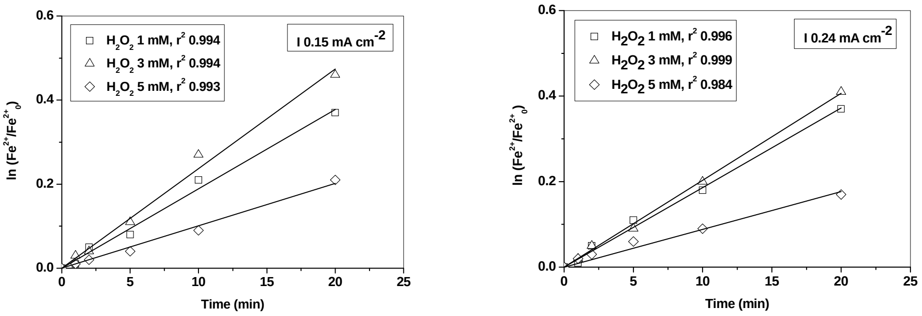

(a) (b)

Figure 4.46 Effect of various H_2O_2 on ferrous concentration remaining ratio ([Triclosan] 1 mM, [Fe^{2+}] 0.1 mM, [H_2O_2] 1-5 mM, pH 3, electrical current 0.15 (a) and 0.24 (b) mA cm^{-2})

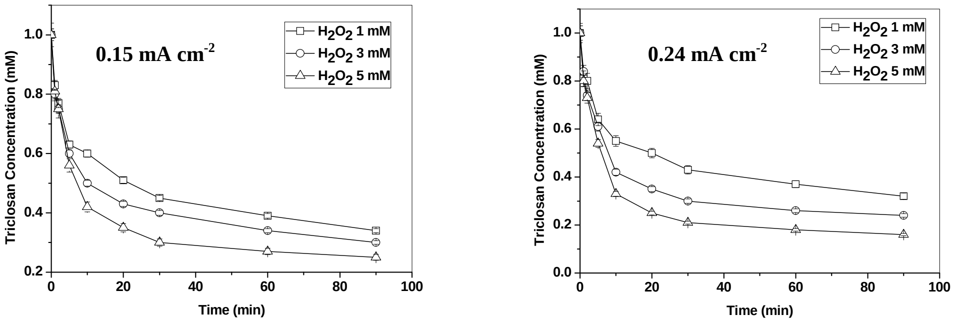

(a) (b)

Figure 4.47 Effect of various H_2O_2 on kinetic of triclosan degradation ([Triclosan] 1 mM, [Fe^{2+}] 0.1 mM, [H_2O_2] 1-5 mM, pH 3, electrical current density of 0.15 (a) and 0.24 mA cm^{-2} (b))

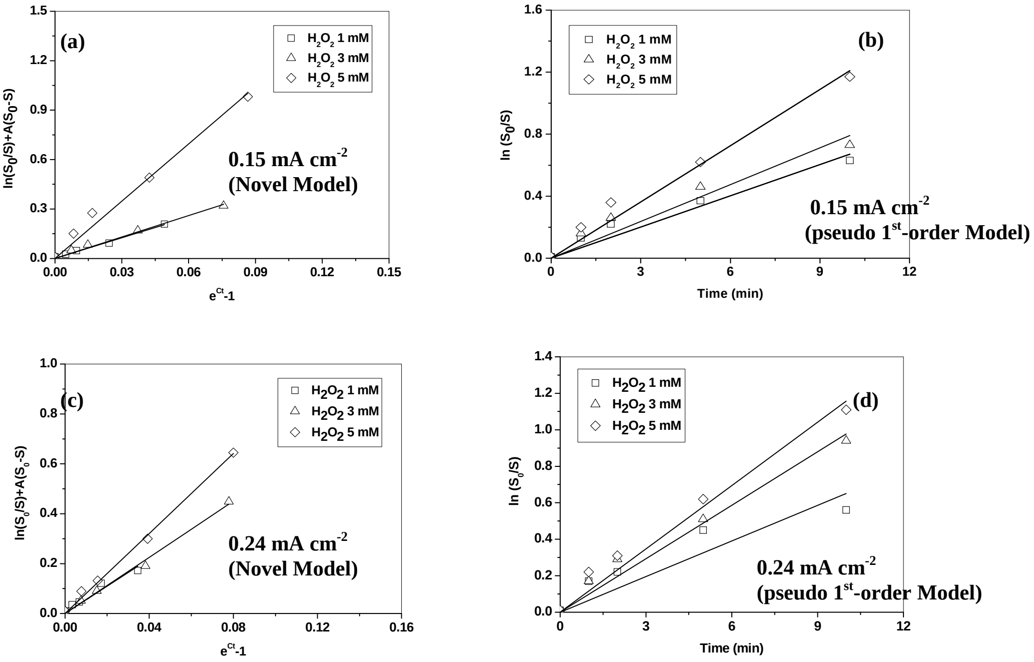

Figure 4.48 Effect of various H_2O_2 on novel kinetic model (a) and pseudo-first order model (b) plotted ([Triclosan] 1 mM, [Fe^{2+}] 0.1 mM, [H_2O_2] 1-5 mM, pH 3, electrical current density of 0.15 and 0.24 mA cm^{-2})

4.3.4.4 Rate constant of triclosan with hydroxyl radical

With reference to the novel model expressed in equation (9), the rate constant of triclosan used as an organic representative with hydroxyl radical is summarized in Table 4.7. As shown in the table results, the range of rate constants was between 4.15 x 10^9 to 6.90 x 10^9 $M^{-1}s^{-1}$; which is close to a previous study reported by Sir’es (Sir’es et al., 2007) and the average value of rate constant in this experiment was 5.434 x 10^9 $M^{-1}s^{-1}$ with a standard deviation of 0.993. These result was received by the experiments of the degradation of triclosan as an organic representative at initial Fe^{2+} of 0.1 mM, H_2O_2 of 1-5 mM (continuous feeding) and constant pH 3, with different current densities (0.01, 0.15, 0.24, 0.35 and 0.50 mA cm^{-2}). For the accuracy of the model comparison, the experimental data were plotted by using both our novel model and the pseudo-first order model, respectively. Table 4.7 presents the fitting results in linear form for our novel model and the pseudo-first order model. Apparently, the correlation coefficients for the fitting of our novel model are significantly greater than those of the pseudo-first order model. Although the conventional pseudo-first order model is the simplest model to describe a variety of chemical reactions and has been widely applied to several water and wastewater treatment processes, it is difficult to accurately describe the reaction kinetic of the electro-Fenton process of the type ferrous regeneration precisely. It should be noted that the novel model can clearly identify the kinetics of the electro-Fenton process of the type ferrous regeneration and that the prediction in organic degradation and the phenomena of the ferrous concentration in the process can be derived more accurately than the pseudo-first order model.

Table 4.7 Summary of rate constant of triclosan with hydroxyl radical by novel model under various conditions*

Fe^{2+} (mM)	H_2O_2 (mM)	Current Density (mA cm^{-2})	Initial degradation rate (10^{-3} mM min^{-1})	C	$k_{\cdot OH \rightarrow Triclosan}$ (Novel Model) (10^9 $M^{-1}.s^{-1}$)	r^2 (Novel Model)	r^2 (pseudo 1^{st}-order Model)
0.1	1	0.01	41.1	0.089	4.81	0.967	0.951
		0.15	62.2	0.049	6.54	0.969	0.896
		0.24	54.2	0.038	4.85	0.977	0.937
		0.35	65.1	0.039	5.28	0.976	0.909
		0.50	57.8	0.030	4.15	0.985	0.922
0.1	1	0.15	62.5	0.019	4.67	0.994	0.970
	3		79.1	0.023	5.82	0.992	0.962
	5		120.9	0.010	6.75	0.990	0.985
0.1	1	0.24	54.3	0.018	5.80	0.961	0.909
	3		97.6	0.020	6.90	0.995	0.984
	5		115.6	0.009	4.21	0.997	0.985

*All of data were calculated at 10 min. of reaction time.

4.3.5 The rate constant of hydroxyl radical with 2,4-dicholrophenol and triclosan confirmation by competitive technique analysis

4.3.5.1 Validation of competitive technique

In this research, the intrinsic pseudo-second order rate constant of the reaction between 2,4-DCP and triclosan with •OH were confirmed by using a technique of competitive kinetics between 2,4-DCP and triclosan with a reference compound in the presence of •OH. This reference compound has to have the intrinsic rate constant with •OH reported. Buxton et al, (1988) have compiled many rate constants between various organic compounds and •OH some of which were used in this study. Methanol and ethanol were selected as the reference compound with the rate constant with •OH of 0.97×10^{9} M^{-1} s^{-1} and 1.90×10^{9} M^{-1} s^{-1}, respectively (Buxton et al., 1988). The competitive kinetics as described later is a very useful yet simple tool to estimate the unknown rate constant of a compound without any complexity in experimental setup and equipments. It is well established that •OH will react with any compound in a pseudo second order manner. Hence, the reaction rate in a batch operation could be written as shown in Equations (4.36), (4.37) and (4.38) which could be further derived for the competition reaction manner as illustrated below (Boonrattanakij et al., 2009):

$$\frac{dS}{dt}=k_S[\bullet OH][S] \qquad (4.36)$$

$$\frac{dR}{dt}=k_R[\bullet OH][R] \qquad (4.37)$$

$$\ln(\frac{S_0}{S_t})=\frac{k_S}{k_R}\ln(\frac{R_0}{R_t}) \qquad (4.38)$$

where S_0 and S_t are the concentrations of target organic compound at the beginning and specific time, respectively. R_0 and R_t are the concentrations of reference organic compound at the beginning and specific time, respectively. [•OH] is the concentration of hydroxyl radical. k_S and k_R are the rate constants of hydroxyl radical reacting with target organic compound and reference organic compound, respectively.

4.3.5.2 Intrinsic rate constant of 2,4-dichlorophenol (2,4-DCP) with hydroxyl radical

The behavior of 2,4-DCP competitive with methanol and ethanol were demonstrated in Figure 4.49. The rate constant of 2,4-DCP with hydroxyl from competitive technique experiment was shown in Figure 4.50 and summarized in Table 4.8. The result showed that the average rate constant of hydroxyl radical with 2,4-DCP in condition of 2,4-DCP competitive with methanol is 1.423 x 10^9 $M^{-1}s^{-1}$. In addition the average rate constant of hydroxyl radical with 2,4-DCP in condition of 2,4-DCP competitive with ethanol is 1.457 x 10^9 $M^{-1}s^{-1}$. The result from competitive technique experiment also showed that the kinetic rate constant which received from this experiment is closely with receiving from the novel kinetic model. It can conclude from this experiment that the rate constant of hydroxyl radical with 2,4-DCP is around 1.4 x 10^9 $M^{-1}s^{-1}$ which are confirmed by both the competitive technique experiment and the novel kinetic model experiment.

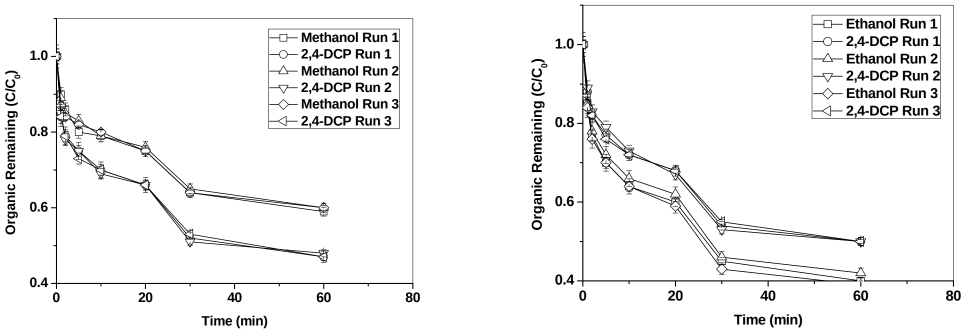

(a) (b)

Figure 4.49 The triplicate removal of 2,4-DCP-methanol (a) and 2,4-DCP-ethanol (b) by electro-Fenton process ([2,4-DCP] 1 mM, [methanol] 1 mM, [ethanol] 1 mM, pH 3, current densities 0.05 mA cm^{-2}, [Fe^{2+}] 0.1 mM, [H_2O_2] 3 mM, Temp 25±0.2 °C)

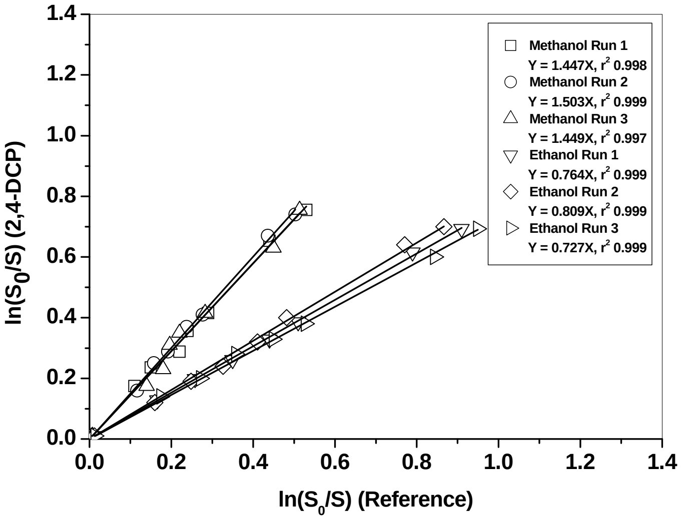

Figure 4.50 The triplicate intrinsic rate constant of 2,4-DCP removal by electro-Fenton process ([2,4-DCP] 1 mM, [methanol] 1 mM, [ethanol] 1 mM, pH 3, current densities 0.05 mA cm^{-2}, [Fe^{2+}] 0.1 mM, [H_2O_2] 3 mM, Temp 25±0.2 °C)

Table 4.8 pseudo-second order intrinsic rate constant between 2,4-DCP and hydroxyl radical in electro-Fenton process

Run	2,4-DCP (mM)	Methanol (mM)	Ethanol (mM)	Slope	r^2	$k_{\cdot OH \rightarrow 2,4\text{-DCP}}$ (10^9 M^{-1} s^{-1})*
1	1	1	-	1.447	0.998	1.404
2				1.503	0.999	1.458
3				1.449	0.997	1.406
Avg.						1.423±0.03
1	1	-	1	0.764	0.999	1.452
2				0.809	0.999	1.537
3				0.727	0.999	1.381
Avg.						1.457±0.08

* Based on k methanol with ·OH 0.97×10^9 M^{-1} s^{-1} and k ethanol with ·OH 1.90×10^9 M^{-1} s^{-1} (Buxton et al., 1988)

4.3.5.3 Intrinsic rate constant of triclosan with hydroxyl radical

The behavior of triclosan competitive with methanol and ethanol were demonstrated in Figure 4.51. The rate constant of triclosan with hydroxyl from competitive technique experiment was shown in Figure 4.52 and summarized in Table 4.9. The result showed that the average rate constant of hydroxyl radical with triclosan in condition of triclosan competitive with methanol is 5.218 x 10^9 $M^{-1}s^{-1}$. In addition the average rate constant of hydroxyl radical with triclosan in condition of triclosan competitive with ethanol is 5.390 x 10^9 $M^{-1}s^{-1}$. The result from competitive technique experiment also showed that the kinetic rate constant which received from this experiment is closely with receiving from the novel kinetic model. It can conclude from this experiment that the rate constant of hydroxyl radical with triclosan is around 5.3 x 10^9 to 5.4 x 10^9 $M^{-1}s^{-1}$ which are confirmed by both the competitive technique experiment and the novel kinetic model experiment.

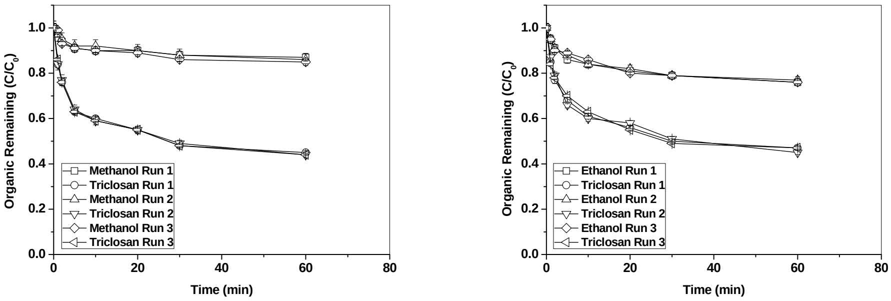

(a) (b)

Figure 4.51 The triplicate removal of triclosan-methanol (a) and triclosan-ethanol (b) by electro-Fenton process ([Triclosan] 1 mM, [methanol] 1 mM, [ethanol] 1 mM, pH 3, current densities 0.12 mA cm^{-2}, [Fe^{2+}] 0.1 mM, [H_2O_2] 4 mM, Temp 25±0.2 °C)

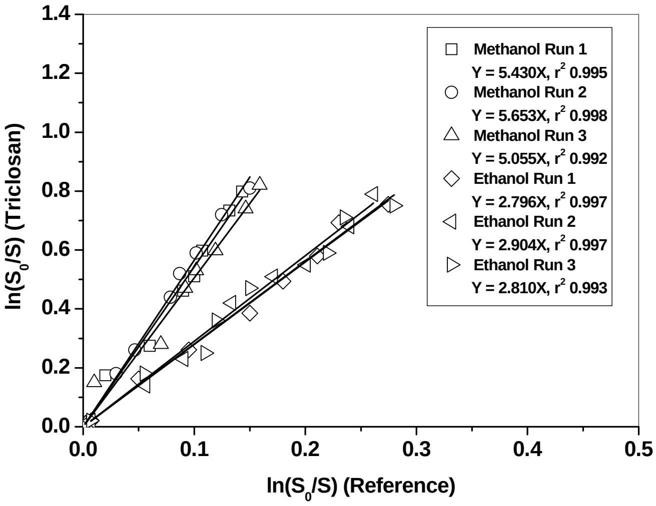

Figure 4.52 The triplicate intrinsic rate constant of triclosan removal by electro-Fenton process ([Triclosan] 1 mM, [methanol] 1 mM, [ethanol] 1 mM, pH 3, current densities 0.12 mA cm^{-2}, [Fe^{2+}] 0.1 mM, [H_2O_2] 4 mM, Temp 25±0.2 °C)

Table 4.9 pseudo-second order intrinsic rate constant between triclosan and hydroxyl radical in electro-Fenton process

Run	Triclosan (mM)	Methanol (mM)	Ethanol (mM)	Slope	r^2	$k_{\cdot OH \rightarrow triclosan}$ (10^9 M^{-1} s^{-1})*
1	1	1	-	5.430	0.995	5.267
2				5.653	0.998	5.483
3				5.055	0.992	4.903
Avg.						5.218±0.29
1	1	-	1	2.796	0.997	5.312
2				2.904	0.997	5.518
3				2.810	0.993	5.339
Avg.						5.390±0.11

* Based on k methanol with ·OH 0.97×10^9 M^{-1} s^{-1} and k ethanol with ·OH 1.90×10^9 M^{-1} s^{-1} (Buxton et al., 1988)

4.4 Proposed reaction pathways and evolution of intermediates from oxidation organic compounds by the electro-Fenton process

4.4.1 Oxidation mechanisms of 2,4-dichlorophenol (2,4-DCP)

4.4.1.1 Evolution of intermediates in 2,4-dichlorophenol (2,4-DCP) oxidation

High performance liquid chromatography (HPLC) and ion chromatography (IC) were applied to investigate and classify the types of various intermediates which were confirmed by GC-MS analysis. The carboxylic acid group was examined by an ion chromatograph (Dionex DX-120). For this experiment, the condition of 112 mg L^{-1} of 2,4-DCP was used to its intermediate investigation under the conditions of initial Fe^{2+} of 0.10 mM, H_2O_2 of 3 mM at pH 3.0 in the electro-Fenton process with the current densities of 0.05 mA cm^{-2}. The peak of the intermediate of 2,4-DCP oxidation by the electro-Fenton process were 2-chlorophenol at 6.36 minutes, phenol at 4.64 minutes, hydroquinone at 3.14 minutes, p-benzoquinone at 3.5 minutes and the carboxylic acid group. The detection time of the carboxylic acid group included acetic acid at 2.9 minutes, maleic acid at 9.79 minutes, formic acid at 3.58 minutes and oxalic acid at 10.64 minutes.

The evolution of aromatic intermediates in 2,4-DCP oxidation is illustrated in Figure 4.53 (a). The results showed that the evolution of 2-chlorophenol and phenol were similar in trend increasing at the beginning of the process and decreasing after the reaction time passed 30 minutes, which was related to the decay of 2,4-DCP in this experiment. The evolution of hydroquinone and p-benzoquinone were following up to increase at the reaction time of 20 minutes. For this experiment the highest concentration of hydroquinone was detected at 60 minutes and decreased to close to zero at near 90 minutes, whereas the p-benzoquinone was still continuing to increase at the same time. This phenomenon was occurring in the condition of initial H_2O_2 feeding. In contrast, the p-benzoquinone was not generated in the condition of the H_2O_2 step feeding which generated continuous ·OH; therefore, the dehydrogenation of hydroquinone to p-benzoquinone was prohibited.

The carboxylic acid group evolutions are shown in Figure 4.53 (b). The results showed that the maleic acid was the first that could be detected. Maleic acid started to be generated after 10 minutes of the process reaction time and increased to the maximum concentration in this experiment when the time passed 90 minutes, possibly decreasing after that. Acetic acid, oxalic acid and formic acid were similar, being generated at around 10-20 minutes in the same manner as maleic acid evolution. These were the most successive organic products prior to conversion to CO_2 which were accumulated in the solution. This implies that under the studied condition within 90 minutes of the reaction time, 2,4-DCP could not be completely mineralized to CO_2. This is in agreement with the total organic carbon profile in which only 10% of initial organic carbon was converted to CO_2. Considering the carbon balance at the end of the reaction period, it can be seen that approximately 80-90% of the organic carbon could be quantified from the identified intermediates.

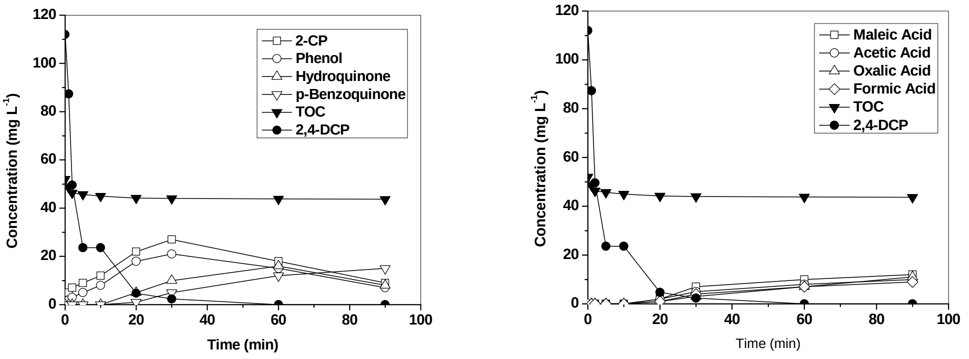

(a) (b)

Figure 4.53 Aromatic intermediate products evolution with TOC profiles (a) and carboxylic acid evolution (b) of 2,4-DCP oxidation by electro-Fenton process

For complete in mineralization, the evolution of aromatic intermediates in 2,4-DCP oxidation is illustrated in Figure 4.54. The result showed that the evolution of only one aromatic intermediate hydroquinone was following up to increase at the first minute of experiment. For this experiment the highest concentration of hydroquinone was detected at 2 minutes. It decreased to closed zero at near 10 minutes. This phenomenon was occurring in the condition of initial H_2O_2 feeding.

The carboxylic acid group evolutions are shown as Figure 4.54 (b). The result showed that the group of carboxylic acids started to generate at first minutes of process reaction time and increasing to the maximum concentration of this experiment when the time pass through 10 minutes and might be decreasing after that. Maleic acid and acetic acid were the earlier and more abundant products of carboxylic acid group at the initial stage. It can be referred that these compounds are the primary products indicator of the ring cleavage of aromatic intermediates. Acetic acid, oxalic acid and formic acid were similar to generate at the time around 10 minutes as similar as maleic acid evolution. These are the most successive organic products prior to conversion to CO_2 which were accumulated in the solution. This implies that under the studied condition within 90 minutes of reaction time, 2,4-DCP could be nearly completely mineralized to CO_2. This is in agreement with the total organic carbon profile in which 50% of initial organic carbon was converted to CO_2. Considering the carbon balance at the end of the reaction period, it can be seen that approximately 50% of the organic carbon could be quantified from the identified intermediates.

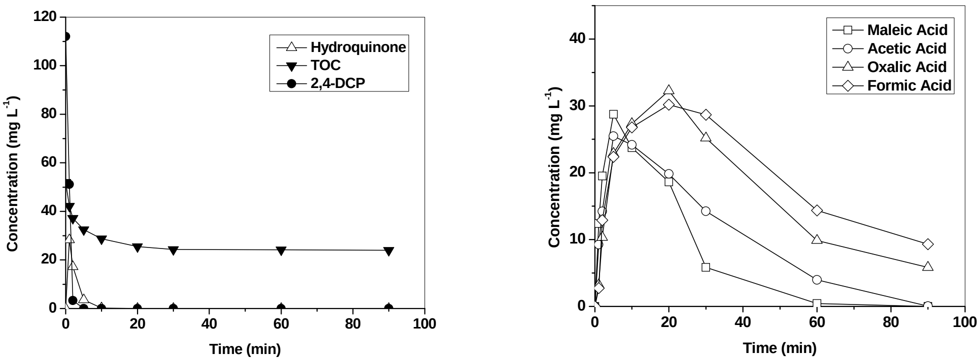

(a) (b)

Figure 4.54 Aromatic intermediate products evolution with TOC profiles (a) and carboxylic acid evolution (b) of 2,4-DCP mineralization by electro-Fenton process

4.4.1.2 Proposed reaction pathways of 2,4-dichlorophenol (2,4-DCP) oxidation

The reaction pathway of 2,4-DCP oxidation by the electro-Fenton process of the type electro-regeneration of ferrous ion is proposed here. High performance liquid chromatography (HPLC) and ion chromatography (IC) were applied to identify and propose the intermediates that might occur among the reactions. The degradation pathway and occurrence of intermediates are presented in Figure 4.55. The pathway can be proposed as follows; 2,4-DCP was oxidized to hydroquinone or p-benzoquinone by hydroxyl radical majority. This intermediate was similar as found in formation of chlorohydroquinone in photo-Fenton-like process by Chu et al., 2005. In the other way, 2,4-DCP might be de-chlorinated to 2-chlorophenol, which was further de-chlorinated to phenol. The same intermediates were found in electrochemical process by Wang et al., 2010. These conditions might be generated due to the effect of reduction mechanism by electrical current at nearly electrode of the process. It was the minor mechanism of intermediate in this process as can be proposed by dash line of this pathway. After that, phenol was oxidized to hydroquinone by hydroxylation on the C(4)-position of phenol. The formation of hydroquinone might have occurred by de-chlorinated and hydroxylation from 2-chlorophenol at the same time. Hydroquinone was subsequently dehydrogenated to p-benzoquinone which is known to be a toxic compound at the initial H_2O_2 feeding. In the initial feeding condition, •OH may be empty during the degradation pathway, therefore the dehydrogenation of hydroquinone to p-benzoquinone dominated. On the other hand, hydroquinone could directly oxidize to form the aliphatic carboxylic acid that occurred in the H_2O_2 step feed condition. It has been confirmed from this pathway that the step feeding of H_2O_2 might reduce the toxicity possibility from intermediate rather than initial H_2O_2 feeding. After that the ring cleavage to the formation of maleic acid, the degradation may separate in a two-way direction. The first direction is the way of acetic acid formation. The second direction is to form oxalic acid and formic acid by hydrogen abstraction. In both degradation pathways, organic acids are directly converted to carbon dioxide and water as final products.

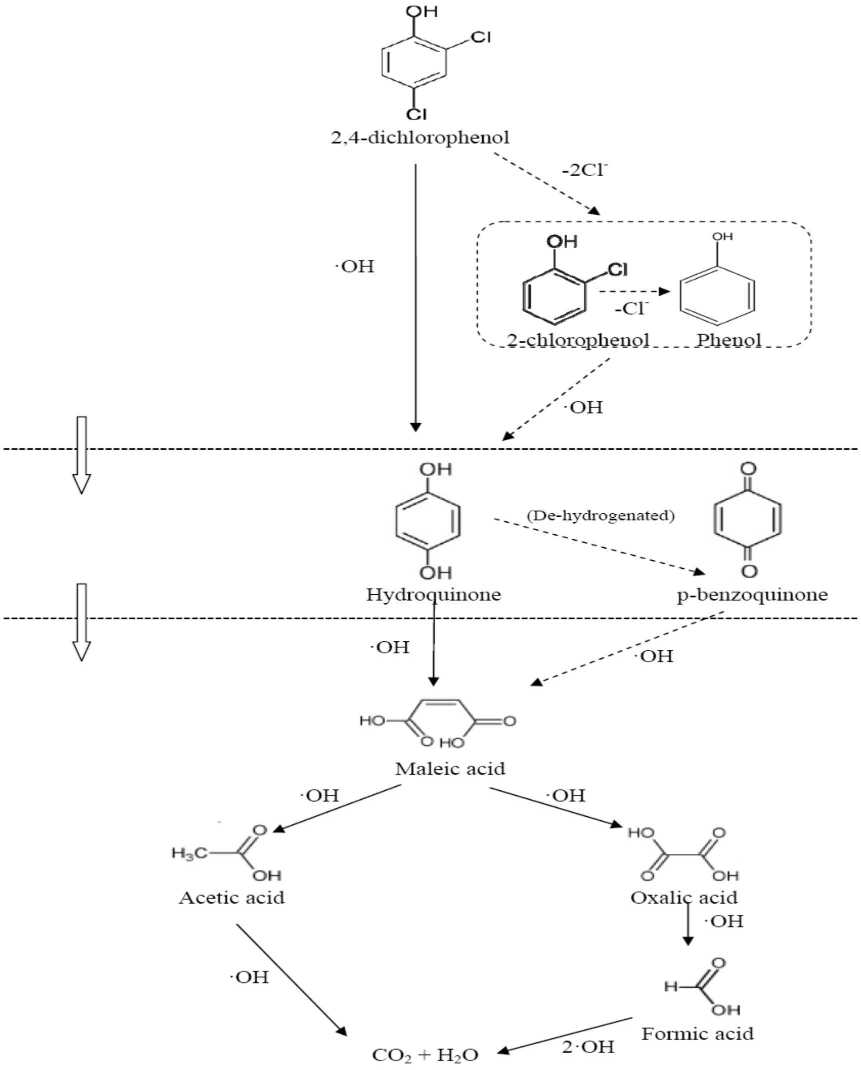

Figure 4.55 Proposed reaction pathways of 2,4-DCP degradation by the electro-Fenton process

4.4.2 Oxidation mechanisms of triclosan

4.4.2.1 Evolution of intermediates in triclosan oxidation

High performance liquid chromatography (HPLC) and ion chromatography (IC) were applied to investigate and classify the type of various intermediates which were confirmed by GC-MS analysis. The carboxylic acid group was examined by ion chromatograph (Dionex DX-120). For this experiment, the condition of 284 mg L^{-1} of triclosan was used for intermediate investigation under the conditions of initial Fe^{2+} of 0.10 mM, H_2O_2 of 4 mM at pH 3.0 in the electro-Fenton process with the current density 0.15 mA cm^{-2}. The peak of intermediate of triclosan oxidation by the electro-Fenton process were 2,4-dichlorophenol at 10.49 minutes, 4-chlorocatechol at 4.20 minutes, phenol at 5.60 minutes, hydroquinone at 3.14 minutes, p-benzoquinone at 3.52 minutes and the carboxylic acid group. The detection time of carboxylic acid group included acetic acid at 2.90 minutes, maleic acid at 9.79 minutes, formic acid at 3.58 minutes and oxalic acid at 10.64 minutes.

The evolution of intermediates in triclosan oxidation is shown in Figure 4.56. The results showed that the evolution of 2,4-dichlorophenol and 4-chlorocatechol were of a similar trend which were generated and increased at the initial phase of the experimental process and decreased after the reaction time passed 5 minutes which was related to the decay of triclosan in this experiment. The evolution of the phenol was following up to increase at the same reaction time and continued to be the highest concentration at 30 minutes and decreased to close to zero at nearly 90 minutes. The hydroquinone and/or p-benzoquinone occurred among the processes depending on the mode of H_2O_2 feeding in this experiment as mentioned in the proposed pathway section. It might be inferred that hydroquinone and/or p-benzoquinone were generated from 2,4-dichlorophenol and also that phenol was oxidized by ·OH in the parallel oxidation reaction of this process. The evolution of these intermediates in this experiment began to be generated at around a reaction time of 5-10 minutes and continued on a similar trend to increase up to 60 minutes. After 60 minutes, the evolution of hydroquinone tended to decrease whereas p-benzoquinone still increased until 90 minutes. This phenomenon occurred in the condition of initial H_2O_2 feeding. In contrast the p-benzoquinone was not generated in the condition of H_2O_2 step feeding which generated continuous ·OH; therefore, the dehydrogenation of hydroquinone to p-benzoquinone was prohibited.

The carboxylic acid group evolutions are shown in Figure 4.57. The results showed that the maleic acid was the first that could be detected. Maleic acid started to be generated at 10 minutes into the process reaction time and increased to the maximum concentration of this experiment after 90 minutes and possibly decreasing after that. Acetic acid, oxalic acid and formic acid were similar in being generated at around 20 minutes like maleic acid evolution. These are the most successive organic products prior to conversion to CO_2 which were accumulated in the solution. This implies that under the studied conditions within 90 minutes of reaction time, triclosan could not be completely mineralized to CO_2. This is in agreement with the total organic carbon profile in which only 7% of initial organic carbon was converted to CO_2. Considering the carbon balance at the end of the reaction period, it can be seen that approximately 90% of the organic carbon could be quantified from the identified intermediates.

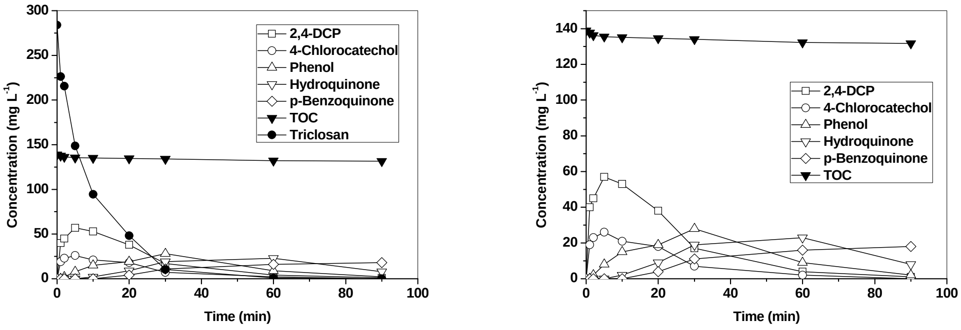

(a) (b)

Figure 4.56 Intermediate products evolution and TOC profiles of triclosan oxidation by the electro-Fenton process ((a) intermediate products, triclosan and TOC profiles, (b) TOC and intermediate products profiles)

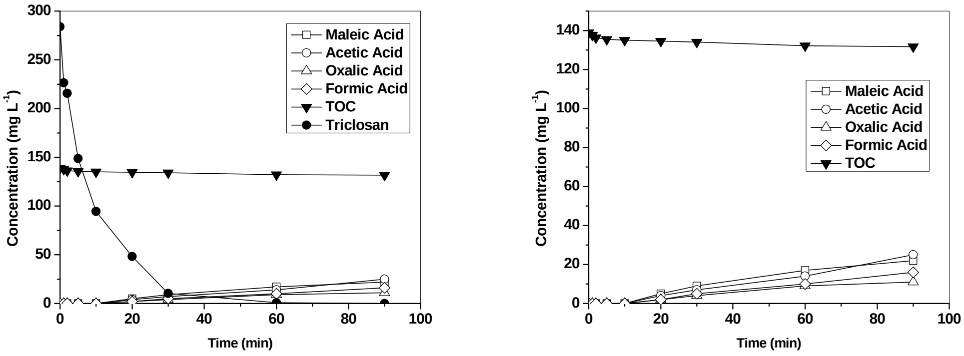

(a) (b)

Figure 4.57 Carboxylic acid evolution and TOC profiles of triclosan oxidation by the electro-Fenton process ((a) carboxylic acids, triclosan and TOC profiles, (b) TOC and carboxylic acids profiles)

For complete mineralization, the evolution of aromatic intermediates in triclosan oxidation is illustrated in Figure 4.58. The result showed that the evolution of only one aromatic intermediate hydroquinone was following up to increase at the first minute of experiment. For this experiment the highest concentration of hydroquinone was detected at 2 minutes. It decreased to closed zero at near 10 minutes. This phenomenon was occurring in the condition of initial H_2O_2 feeding.

The carboxylic acid group evolutions are shown as Figure 4.58 (b). The result showed that the group of carboxylic acids started to generate at first minutes of process reaction time and increasing to the maximum concentration of this experiment when the time pass through 10 minutes and might be decreasing after that. Maleic acid and acetic acid were the earlier and more abundant products of carboxylic acid group at the initial stage. It can be referred that these compounds are the primary products indicator of the ring cleavage of aromatic intermediates. Acetic acid, oxalic acid and formic acid were similar to generate at the time around 10 minutes as similar as maleic acid evolution. These are the most successive organic products prior to conversion to CO_2 which were accumulated in the solution. This implies that under the studied condition within 90 minutes of reaction time, triclosan could be nearly completely mineralized to CO_2. This is in agreement with the total organic carbon profile in which 50% of initial organic carbon was converted to CO_2. Considering the carbon balance at the end of the reaction period, it can be seen that approximately 50% of the organic carbon could be quantified from the identified intermediates.

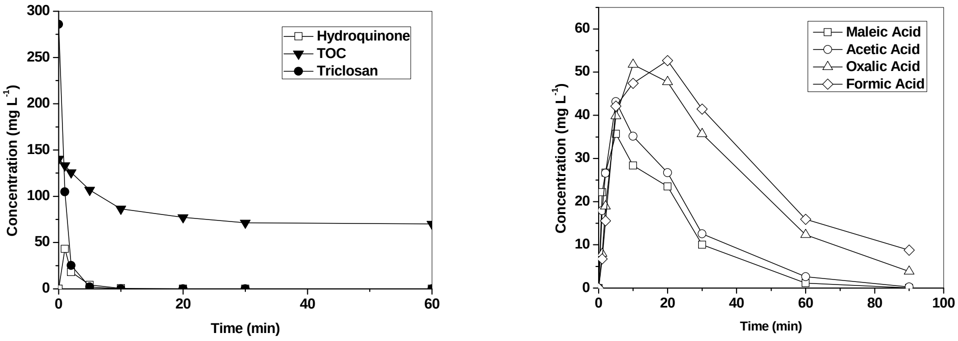

(a) (b)

Figure 4.58 Aromatic intermediate products evolution with TOC profiles (a) and carboxylic acid evolution (b) of triclosan mineralization by electro-Fenton process

4.4.2.2 Proposed reaction pathways of triclosan oxidation

The reaction pathway of triclosan oxidation by the electro-Fenton process of the type ferrous regeneration is proposed here. High performance liquid chromatography (HPLC) and ion chromatography (IC) were applied to identify and propose the intermediates that might occur among the reactions. The degradation pathway and occurrence of the intermediates are presented in Figure 4.59. The following pathway can be proposed; triclosan was separated into a two-way direction in majority. Firstly forming 2,4-dichlorophenol which can be oxidized to hydroquinone in the next step. Secondly the 4-chloro-catechol formed which also continued to oxidize to hydroquinone at the same way. The 4-chloro-catechol might be dechlorinated and oxidized to phenol at the same time. It was occurring due to the effect of reduction mechanism by electrical current at nearly electrode of the process. It was the minor mechanism of intermediate in this process as can be proposed by dash line of this pathway. Phenol might be oxidized to hydroquinone by hydroxylation on the C(4)-position of phenol. Additionally, the reaction might be dehydrogenated from 2,4-dichlorophenol or 4-chloro-catechol or phenol to p-benzoquinone, which is known as a toxic compound, and was received in the initial H_2O_2 feeding condition. For this condition, •OH might be empty during the degradation pathway; therefore, the dehydrogenation of hydroquinone to p-benzoquinone dominated. On the other hand, the formation of hydroquinone, which can continuously oxidize to form aliphatic carboxylic acid directly, occurred in the step feed of H_2O_2 condition. It can be inferred from this pathway that the step feeding of H_2O_2 might reduce the toxicity possibility from intermediate rather than the initial H_2O_2 feeding. After the ring cleavage to the formation of maleic acid, the degradation may separate in a two-way direction. The first direction is acetic acid formation. The second direction is to form oxalic acid and formic acid by hydrogen abstraction. In both degradation pathways, organic acids are directly converted to carbon dioxide and water as final products.

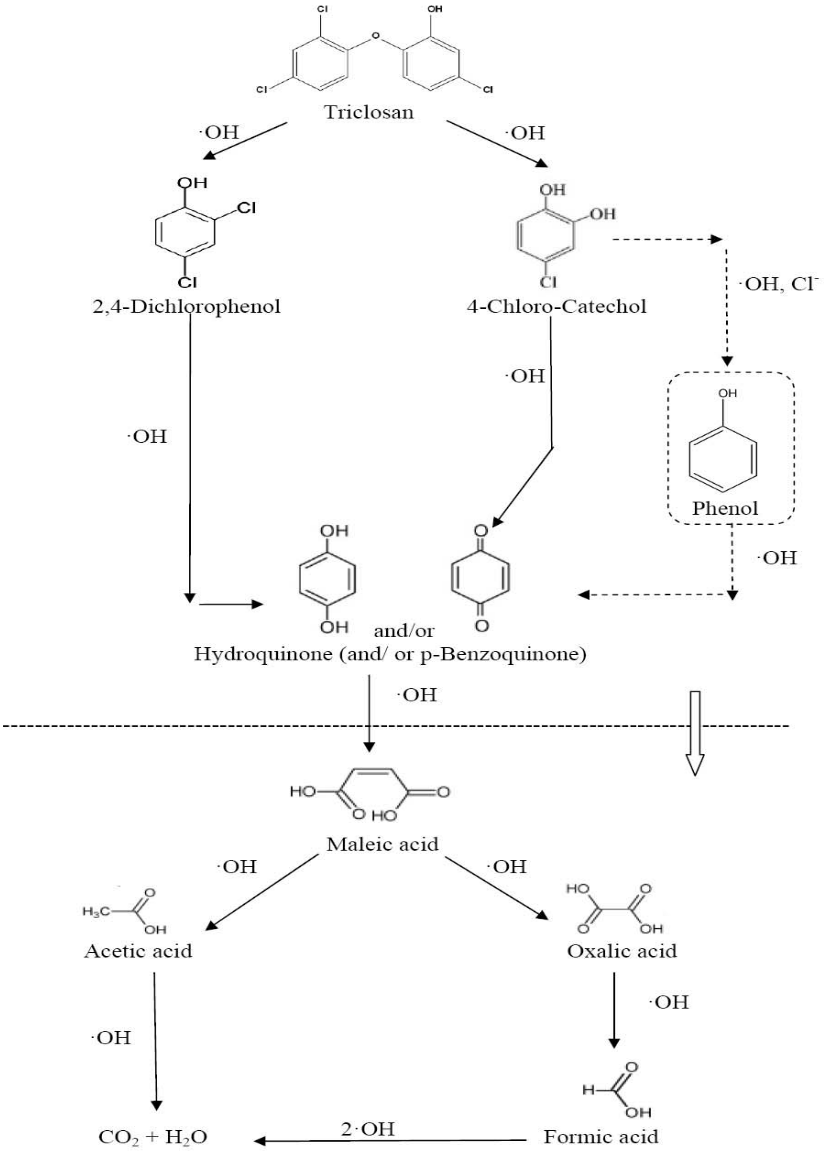

Figure 4.59 Proposed reaction pathway and evaluation of intermediate detection on triclosan degradation by the electro-Fenton process

4.5 Comparison of 2,4-dichlorophenol (2,4-DCP) and triclosan degradation by Fenton and electro-Fenton processes

This research was study the removal of 2,4-dichlorophenol (2,4-DCP) and triclosan by Fenton and electro-Fenton process. 2,4-DCP and triclosan were identified as endocrine disruption organic compound. 2,4-DCP is lower in molecular weight and Cl content whereas higher in water solubility than triclosan. The Fenton and electro-Fenton processes were selected for remove these compounds. The optimization of Fenton and electro-Fenton process for remove 2,4-DCP-and triclosan was demonstrated in Table 4.10. From this table the removal efficiencies of both processes indicated that the molecular weight had affect with the amount of operating parameters such as pH, H_2O_2/Fe^{2+} ratio and also current density. The same of removal efficiency was received under higher concentration of operating parameters at the higher molecular weight compound (triclosan) than the lower molecular weight compound (2,4-DCP).

For the Fenton process, the wellness efficiency came with the higher amounts of Fenton's reagents than electro-Fenton process for keep the nearly H_2O_2/Fe^{2+} ratio. In addition, the generation of sludge from ferric hydroxide, which low activity with H_2O_2, was become to the limitation of removal efficiency in this process. The change of H_2O_2 operational feeding did not affected with the process because of the low rate in Fenton's reagents regeneration was not support with the increasing efficiency by H_2O_2 feeding development. The efficiency of the process was depended on only the amount of Fenton's reagents for both of 2,4-DCP and triclosan removal.

Table 4.10 Comparison of 2,4-dichlorophenol (2,4-DCP) and triclosan degradation by Fenton and electro-Fenton processes at optimum pH 3

Organic Pollutants	Process	H_2O_2/Fe^{2+} (H/F) (H_2O_2 : Fe^{2+})	Current Density (mA cm^{-2})	%Pollutants Removal		
				Organic	COD	TOC
2,4-DCP 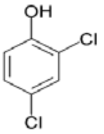 - $C_6H_4Cl_2O$ - MW 163.00 g mol^{-1} - Cl 2 atoms - Solubility 4500 mg L^{-1}	Fenton	16 (5 : 0.3)	-	78	40	5
	Electro-Fenton	10 (1 : 0.1)	0.05	100	40	17
		20 (20 : 1)	0.05	100	60	38
		20 (20 : 1)	0.12	100	80	50
Triclosan 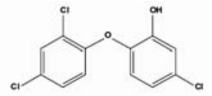 - $C_{12}H_7Cl_3O_2$ - MW 289.54 g mol^{-1} - Cl 3 atoms - Solubility 4.6 mg L^{-1}	Fenton	50 (5 : 0.1)	-	75	38	3
	Electro-Fenton	40 (4 : 0.1)	0.15	100	53	15
		50 (50 : 1)	0.15	100	59	33
		50 (50 : 1)	0.24	100	70	47

For the electro-Fenton process, the higher removal efficiency and chemical economize was received than Fenton process at the same organic compound as confirmed by the results of optimization processes that mentioned in Table 4.10 and previous section. The higher of removal efficiency of electro-Fenton than Fenton process was due to the current density which applied to the process for continuously generating hydroxyl radical into the process. Moreover the regeneration of Fenton’s reagents in electro-Fenton process that rapidly than Fenton process was also promoted in higher process efficiency. The main operating parameter that affect with the efficiency of the process was the current density. The increasing of current density could support the process efficiency increasing more than increasing of Fenton’s reagents. The important of current density can be seen in the increasing of process efficiency of 2,4-DCP and triclosan removal at previous section. The other operating parameter which had the role for increase removal efficiency was the H_2O_2 operation feeding mode. The operation feeding mode in term of step feeding operation was found to higher removal efficiency and reduced the possibility of toxic formation intermediate compounds generation than initial feeding operation, so call original feeding. The wellness of step feeding to the efficiency of processes was due to the continuously regenerated in Fenton’s reagents for hydroxyl radical generation into the process than initial feeding.

The kinetic of electro-Fenton process for 2,4-DCP and triclosan removal were studied in term of initial degradation rate and novel kinetic model which proposed in this experiment. The initial degradation rate was developed for using to describe the organic degradation of process and indicate the process optimization. The novel kinetic model was developed and proposed to identify the kinetic rate constant of hydroxyl radical with chlorinated pollutant organic compound. It was proposed to be an option in kinetic determination which higher accuracy of kinetic constant investigation as confirmed by the results of competitive technique experiment that mentioned in the previous section. However, the novel kinetic model that proposed was only validated by the experiments of 2,4-DCP and triclosan. Further studies for apply this kinetic model in degradation of other organics becomes necessary.

The evolution of intermediate compounds in the condition of only 2,4-DCP or triclosan oxidation had both of aromatic intermediate compounds evolution and carboxylic acid evolution. The evolution of intermediate compounds in the condition of 2,4-DCP or triclosan mineralization had a few of hydroquinone as aromatic intermediates compounds and the much of carboxylic acids which indicated to the mineralization of process with TOC removal efficiency 50% or much more. For all of conditions, it can be seen that the characteristic of aromatic intermediate compounds evolution and carboxylic acid evolution were depended the amounts of operating parameters in process that confirmed by the difference of detected intermediate compounds between oxidation process and mineralization process. The degradation pathway of 2,4-DCP and triclosan by electro-Fenton process were proposed based on the intermediate compounds that can be detected. The mechanism of both compounds degradation had the oxidation mechanism in majority and some of reduction due to the effect of electrical current at electrode in minority. The level of degradation pathways was depended on the amounts of operating parameters as can be confirmed by the difference concentration of current density and Fenton’s reagents between oxidation process and mineralization process as mentioned in previous.

CHAPTER V

CONCLUSIONS AND SUGGESTIONS FOR FUTURE WORK

5.1 Conclusions

1. It is obvious from the study that both the Fenton and electro-Fenton processes were able to degrade wastewater containing 2,4-dichlorophenol and triclosan.

2. The electro-Fenton process could give a higher performance in 2,4-DCP and triclosan degradation than the Fenton process and could reduce the possibility of sludge formation effectively which can extend the effective performance of Fenton's reagents over a longer periods by the electrochemical regeneration of ferrous ions.

3. Optimum operating pH, ferrous ion concentration, hydrogen peroxide concentration, applied electrical current densities and hydrogen peroxide feeding mode are important factors in the degradation of 2,4-dichlorophenol and triclosan by electro-Fenton process.

4. The wellness operating condition for 1 mM 2,4-DCP and triclosan removal was found at same operating pH of 3. The current density at 0.05 mA cm^{-2} and the H_2O_2 to Fe^{2+} ratio at 30 were good operating conditions for 2,4-DCP. For triclosan degradation, the current densities 0.15 mA cm^{-2} and the H_2O_2 to Fe^{2+} ratio at 40 were found to be the wellness operating conditions in this process.

5. Development of the operation feeding mode from the original one-time initial H_2O_2 feeding to the step feeding condition could give higher mineralization efficiency. The step feeding operation could reduce the scavenging effect on the reaction process and decrease the possibility of toxic compound formation from intermediates.

6. A novel kinetic model of the electro-Fenton process is proposed for being used as a tool to investigate the rate constant between hydroxyl radical (·OH) and chlorinated organic compounds.

7. The experiments data confirmed that the novel model could be applied to the electro-Fenton rate constant determination and could clearly identify the kinetics of the electro-Fenton process more accurately than the pseudo-first order model.

8. The rate constant of the reaction between 2,4-DCP and ·OH in the electro-Fenton process obtained by our novel model was reported between 0.76×10^{9} and 1.95×10^{9} $M^{-1}s^{-1}$ with an average of 1.437×10^{9} $M^{-1}s^{-1}$.

9. The rate constant of reaction between triclosan and ·OH in the electro-Fenton process obtained by our novel model was reported between 4.15×10^{9} and 6.90×10^{9} $M^{-1}s^{-1}$ with an average of 5.434×10^{9} $M^{-1}s^{-1}$.

10. A degradation pathway for 2,4-DCP and triclosan oxidation by the electro-Fenton process was proposed on the basis of intermediate compounds that be detected. The occurring intermediates in this experiment depended on the mode of H_2O_2 feeding to the process in majority.

11. 2-chlorophenol and phenol were the products of de-chlorination while hydroquinone, p-benzoquinone, maleic, acetic, oxalic, and formic acids were found to be the main oxidation intermediates in 2,4-DCP degradation by the electro-Fenton process.

12. 2,4-DCP, 4-chlorocatechol, phenol, hydroquinone, p-benzoquinone, maleic, acetic, oxalic, and formic acids were found to be the main oxidation intermediates in triclosan degradation by the electro-Fenton process.

5.2 Suggestions for future work

- The behavior of the electro-Fenton process under continuous operation should be investigated.

- Real wastewater should be applied in the study of other parameters in real wastewater which can affect degradation behavior.

- The effect of anion (such as Cl^-, NO_3^- and SO_4^{2-}) on the performance and kinetics of the electro-Fenton process should be investigated.

- The rate constant of 2,4-DCP and triclosan with hydroxyl radicals should be determined by using other advanced oxidation processes and compared with the values obtained from this study.

- The effect of temperature on the rate constant between 2,4-DCP and triclosan with hydroxyl radicals should be determined via the Arrhenius equation so that the rate constant can be applied in practice field for the required temperature.

REFERENCES

Achari, R.G., Chin, D. 1981. HPLC analysis of some bacteriostats in deodorant sticks and soaps. Journal of the Society of Cosmetic Chemists 32: 163–173.

Adolfsson-Erici, M., Pettersson, M., Parkkonen, J., Sturve, J., 2002. Triclosan, a commonly used bactericide found in human milk and in the aquatic environment in Sweden. Chemosphere 46: 1485–1489.

Agency for Toxic Substances and Disease Registry (ATSDR). 1999. Toxicological profile for chlorophenols U.S., Department of Health and Human Services, Public Health Services Agency for Toxic Substances and Disease Registry. Atlanta, Georgia.

Aglera, A., Fernandez-Alba, A.R., Piedra, L., Muzcua, M., Gomez, M.J., 2004. Evaluation of triclosan and biphenylol in marine sediments and urban wastewaters by pressurized liquid extraction and solid phase extraction followed by gas chromatography mass spectrometry and liquid chromatography mass spectrometry. Analytical Chimica Acta 480: 193–250.

Ahlborg, U.G. and Victori, K. 1987. Impact on health of chlorinated dioxins and other trace organic emissions. Waste Management & Research 5: 203-224.

Alum, A., Yoon, Y., Westerhoff, P., Abbaszadegan, M. 2004. Oxidation of bisphenol A, 17b-estradiol, and 17a-ethynyl estradiol and byproduct estrogenicity. Environmental Toxicology 19: 257–264.

Andersson, T., Forlin, L., Harig, I., Larsson, A., 1988. Physiological disturbances in fish living in coastal water polluted with bleached kraft mill effluents. Canadian Journal of Fisheries and Aquatic Sciences 45: 1525–1536.

Anotai, J., Lu, M.-C., Chewpreecha, P. 2006. Kinetics of Aniline degradation by Fenton and Electro-Fenton processes. Water Research 40: 1841-1847.

Anotai, J., Su, C.-C., Tsai, Y.-C., Lu, M.-C. 2010. Effect of hydrogen peroxide on aniline oxidation by electro-Fenton and fluidized-bed Fenton processes. Journal of Hazardous Materials 183: 888-893.

Baronti, C., Curini, R., D'Ascenzo, G., Di Corcia, A., Gentili, A., Samperi, R. 2000. Monitoring Natural and Synthetic Estrogens at Activated Sludge Sewage Treatment Plants and in a Receiving River Water. Environmental Science and Technology 34: 5059-5066.

Behera, S. K., Oh, S.-Y., Park, H.-S. 2010. Sorption of triclosan onto activated carbon, kaolinite and montmorillonite: Effects of pH, ionic strength, and humic acid. Journal of Hazardous Materials 179: 684-691.

Belfroid, A.C., Van der Horst, A., Vethaak, A.D., Schaufer, .J., Rijs, G.B.J., Wegener, J., Cofino, W.P., 1999. Analysis and occurrence of estrogenic hormones and their glucuronides in surface water and wastewater in The Netherlands. Science of the Total Environment 225: 101–108.

Bell, L.S., Devlin J.F., Gillham R.W. and Binning, P. J. 2003. A sequential zero valent iron and aerobic biodegradation treatment system for nitrobenzene. Journal of Contaminant Hydyology 66: 201- 207.

Bester, K. 2003. Triclosan in a sewage treatment process—balances and monitoring data. Water Research 37: 3891–3896.

Boonrattanakij, N., Lu, M.C., Anotai, J. 2009. Kinetics and mechanism of 2,6-dimethyl-aniline degradationby hydroxyl radicals. Journal of Hazardous Materials 172 (2-3): 952–957.

Boye, B., Dieng, M.M. and Brillas, E. 2003. Anodic Oxidation, Electro-Fenton and Photo electro- Fenton Treatment of 2,4,5-Trichlorophenoxyacetic acid. Journal of Electroanalytical Chemistry 557:135-146.

Brillas, E., Bastida, R.M., Llosa, E., Casado, J. 1995. Electrochemical destruction of aniline and 4-chloroaniline for wastewater treatment using a carbon-PTFE O_2-fed cathode. Journal of The Electrochemical Society 142:1733.

Brillas, E., Mur, E., Sauleda, R., Sanchez, L., Pera, J., Doenech, X. and Casado, J. 1998. Aniline mineralization by AOP's: anodic, photocatalysis, electro-Fenton and photoelectro-Fenton processes. Applied Catalysis B: Environmental 16: 31-42.

Brillas, E. and Casado, J. 2001. Aniline degradation by electro-Fenton and Peroxi-Coagulation processes using a flow reactor for wastewater. Chemosphere 47(3): 241-248.

Brillas, E., Banos, M.A. and Garrido, J.A. 2003. Mineralization of Herbicide 3,6-Dichloro-2- Methoxybenzoic acid in aqueous medium by anodic oxidation, electro-Fenton and photoelectro-Fenton. Electrochemica Acta 48: 1697-1705.

Brillas, E., Boye, B., Banos., M.A., Calpe, J.C. and Garrido, J.A. 2003. Electrochemical degradation of chlorophenoxy and chlorobenzoic herbicide in acid aqueous medium by the peroxi-coagulation method. Chemosphere 51: 227-235.

Brillas, E., Calpe, J.C., Casado, J. 2000. Minerallization of 2,4-D by advanced electrochemical oxidation process. Water Research 34: 2253–2262.

Brillas, E., Sauleda, R., Casado, J. 1998. Degradation of 4- chlorophenol by anodic oxidation, electro-Fenton, photoelectro- Fenton and peroxi-coagulation processes. Journal of Electrochemical Society 145: 759–765.

Buxton, G.V., Greenstock, C.L. 1988. Critical review of rate constants for reactions of hydrated electrons. Journal of Physical Chemistry Reference Data 17 (2): 513-886.

Casado, J., Fornaguera, J. and Galan, M.I. 2005. Mineralization of aromatics in water by sunlight-assisted electro-Fenton technology in a pilot reactor. Environmental Science and Technology 39(6): 1843-1847.

Casado, J., Fornaguera, J., Galan, M.I. 2006. Pilot scale mineralization of organic acid by electro-fenton process plus sunlight exposure. Water Research 40(13): 2511-2516.

Chan, K.H., Chu, W. 2005. Atrazine removal by catalytic oxidation processes with or without UV irradiation, Part I – quantification and rate enhancement via kinetic study. Applied Catalysis B 58: 157–163.

Chang, P.H. 2001. Treatment of non-biodegradable wastewater by electro-Fenton method. Water Science & Technology 49 (4):213-218.

Chen, J.-L., Wang, J.-Y., Wu, C.-C., Chiang, K.-Y. 2011. Electrocatalytic degradation of 2,4-dichlorophenol by granular graphite electrodes. Colloid Surface. A.: Physicochemical Engineering Aspects 379 (1-3): 163-168.

Chou, S., Huane, Y., Lee, S., Huang, G., Huang, C. 1999. Treatment of high strength Hexamine containing wastewater by electro-Fenton method. Water Research 33(3): 751-759.

Chu, S., Metcalfe, C.D. 2007. Simultaneous determination of triclocarban and triclosan in municipal biosolids by liquid chromatography tandem mass spectrometry. Journal of Chromatography A 1164: 212–218.

Chu, W., Kwan, C.Y., Chan, K.H. and Kam, S.K. 2005. A study of kinetic modelling and reaction pathway of 2,4-dichlorophenol transformation by photo-fenton-like oxidation. Journal of Hazardous Materials B121: 119–126.

Chun, H. 2002. Performances of three-phase three-dimensional electrode rector and its application to the degradation of aniline, Master of engineering Thesis, Chemical Engineering Programe, Faculty of Engineering, Zhongshan University.

Contreras, S., Rodriguez, M., Chamarro, E. And Esplugas, S. 2001. UV-and UV/Fe(III)-Enhanced ozonation of nitrobenzene in aqueous solution. Journal of Photochemistry and Photobiology A: Chemistry 142: 79-83.

Cronin, M.T., Manga, N., Seward, J.R., Sinks, G.D., Schultz, T.W. 2001. Relation between physicochemical properties of phenols and their toxicity and accumulation in fish. Chemical Research Toxicology 14: 1498-505.

D'Ascenzo, G., Di Corcia, A., Gentili, A., Manzini, R., Mastropasqua, R., Nazzari, M., Samperi, R., 2003. Fate of estrogen conjugates in municipal sewage transport and treatment facilities. Science of the Total Environment 302: 199–209.

Deborde, M., Rabouan, S., Duguet, J.P., Legube, B., 2005. Kinetics of aqueous ozone-induced oxidation of some endocrine disruptors. Environmental Science and Technology 39: 6086–6092.

DeKruijf, N., Schouten, A., Rijk, M.A.H. Pranoto- Soetardhi, L.A. 1989. Determination of preservatives in cosmetic products II. High-performance liquid chromatographic identification. Journal of Chromatography A 469: 317–328.

Demkowicz, M.P., Chanhan, V., Stern, D.A., Vasquez, F.G. 1994. Simultaneous determination of anions and triclosan in dentifrices by gradient ion chromatography and isocratic high-performance liquid chromatography interfaced with conductivity and ultraviolet detection. Journal of Chromatography A 671: 351–357.

Diagne, M., Oturan, N. and Oturan, M.A. 2007. Removal of methyl parathion from water by electrochemically generated Fenton's reagent. Chemosphere 66: 841-848.

Directive 2000/60/EC. 2000. Establishment and framework for community action in the field of water policy. Luxembourg, Luxembourg; European Parliament and the Council of the European Union.

Doocey, J.D. and Sharratt, N.P. 2004. Zeolite-mediated advanced oxidation of model chlorinated phenolic aqueous waste Part 1: Aqueous Phase Fenton Catalysis. Trans I Chemical E82(B5): 352-358.

Duesterberg, C.K. and Waite, T.D. 2006. Process optimization of Fenton oxidation using kinetic modeling. Environmental Science and Technology 40: 4189-4195.

Duesterberg, C.K., Mylon, S.E. and Waite, T.D. 2008. pH effects on iron-catalyzed oxidation using Fenton's reagent, Environmental Science and Technology 42: 8522–8527.

Duran, M.A., Frontana-Uribe, B.A. and Ramirez Zamora, R.M. 2004. Electro-Fenton as a feasible advanced treatment process reclaimed water. Water Science & Technology 50(2): 83-90.

Fenner-Crisp, P.A. 1997. Endocrine disruptor risk characterization: An EPA perspective. Regul. Toxicol. Pharmacol 26: 70-73

Fenton, H.J.H. 1884. Oxidative Properties of the H_2O_2/Fe^{2+} System and its Application. Journal of Chemical Sources 65: 889-899.

Fry, D.M., Toone, C.K., Speich, S.M., Peard, R.J., 1987. Sex ratio skew and breeding patterns of gulls: demographic and toxicological considerations. Studies in Avian Biology 10: 26–43.

Gagliardi, L., Amato, A., Basili, A., Cavazzuti, G., Gattavecchia, E., Tonelli, D. 1985. Determination of preservatives in cosmetic products by reversed-phase high-performance liquid chromatography. II. Journal of Chromatography A. 325: 353–358.

Gagliardi, L., Cavazzuti, G., Turchetto, L., Manna, F., Tonelli, D. 1990. Determination of preservatives in cosmetic products by reversed phase high-performance liquid chromatography. IV. Journal of Chromatography A. 508: 252–258.

Gagliardi, L.D., De Orsi, D.L., Manna, L.D. Tonelli, D. 1997. Simultaneous determination of antioxidants and preservatives in cosmetics and pharmaceutical preparations by reversed-phase HPLC. J. Liq. Chrom. Rel. Technol 20: 1797–1808.

Glaze, W.H., Kang, J.W. and Chapin, D.H. 1987. The Chemistry of water treatment processes involving ozone. Science Engineering 9: 335-352.

Gözman, B., Oturan. M.A., Oturan, N. and Erbatur, O. 2003. Indirect electrochemical treatment of bisphenol A in water via electrochemically generated Fenton's reagent. Environmental Science& Technology 37 (16): 3716-3723.

Gomes, R.L., Lester, J.N., 2003. Endocrine disruptors in receiving Waters. In: Birkett, J.W., Lester, J.N. (Eds.), Endocrine Disruptors in Wastewater and Sludge Treatment Processes, pp. 177–217. Boca Raton, FL.: CRC Press Inc.

Guillette Jr., L.J., Gross, T.S., Masson, G.R., Matter, J.M., Percival, H.F., Woodward, A.R., 1994. Developmental abnormalities of the gonad and abnormal sex hormone concentrations in juvenile alligators form contaminated and control lakes. Environmental Health Perspectives 102: 680–688.

Halden, R. U., Paull, D. H., 2005. Co-occurrence of triclocarbon and triclosan in U.S. water resources. Environmental Science and Technology 39(6): 1420-1426.

Heath, R.J., Rubin, J.R., Holland, D.R., Zhang, E., Snow, M.E., Rock, C.O., 1999. Mechanism of triclosan inhibition of bacterial fatty acid synthesis. Journal of Biological Chemistry 274: 11110–11114.

Herbst, A.L., Senekjian, E.K., Frey, K., 1989. Abortion and pregnancy loss among diethylstilbestrol-exposed women. Seminars in Reproductive Endocrinology 7: 124–129.

Hu, C., Wang, G., Wu, C., Li, P. and Wei, C. 2003. Oxidation treatment of formaldehyde-containing wastewater by electro-Fenton method. Huan Jing Ke Xue 24(6): 106-111.

Hua, W., Bennett, E.R., Letcher, R.J., 2005. Triclosan in waste and surface waters from the upper Detroit River by liquid chromatography–electrospray–tandem quadrupole mass spectrometry. Environ. Int. 31: 621–630.

Huang, Y.H., Chen, C., Huang, G.H. and Chou, S.S. 2001. Comparison of a novel electro-Fenton method with Fenton's reagent in treating a highly contaminated wastewater. Water Science & technology 43(2): 17-24.

Hutchinson, T.H., Brown, R., Brugger, K.E., Campbell, P.M., Holt, M., Lange, R., McCahon, P.,Tattersfield, L.J., van Egmond, R. 2000. Ecological risk assessment of endocrine disruptors. Environ. Health Prespect 108: 1007-1014.

Ingerslev, F., Vaclavik, E. and Halling-Sorenson, B. 2003. Pharmaceuticals and personal care products: a source of endocrine disruption in the environment. Pure and Applied Chemistry 75: 1881–1893.

International Agency for Research on Cancer (IARC).1999. Polychlorophenols and their Sodium Salts Group 2B) [Online]. Available from: http://monographs.iarc.fr/ENG/Monographs/vol71/volume71.pdf [2008, July 17]

International Chemical Safety Cards (WHO/IPCS/ILO)/ CDC/NIOSH.1997. 2,4-dichlrophenol [Online]. Available from: http://www.cdc.gov/niosh/ipcsneng/neng0438. html [2008, June 2]

Jintelmann, J., Katayama, A., Kurihara, N., Shore, L., Wenzel, A., 2003. Endocrine disruptors in the environment. Pure and Applied Chemistry 75: 631–681.

Kang, N., Lee, D.S., Yoon, J. 2002. Kinetic model of Fenton oxidation of phenol and monochlorophenols. Chemosphere 47: 915-924.

Kuo WG. 1992. Decolorizing dye waste-water with Fenton reagent. Water Research 26: 881-886.

Kwon, B.G., Lee, D.S., Kang, N. and Yoon, J. 1999. Characteristic of p-chlorophenol oxidationby Fenton’s reagent. Water Research 33: 2110-2118.

Kwon, B.G., Ryu, S., Yoon, J. 2009. Determination of hydroxyl radical rate constants in a continuous flow system using competition kinetics. Journal of Industrial and Engineering Chemistry 15 (6): 809-812.

Langford, K.H., Lester, J.N. 2002. Fate and behaviour of endocrine disrupters in wastewater treatment processes. In: Brikett JW, Lester JN, editors, Endocrine disrupters in wastewater and sludge treatment processes. Boca Raton, USA: CRC Press Inc.

Latch, D.E., Packer, J.L., Arnold, W.A., McNeill, K., 2003. Photochemical conversion of triclosan to 2,8-dichlorodibenzo-p-dioxin in aqueous solution. J. Photochem. Photobiol. A Chem. 158: 63–66.

Levy, C.W., Roujeinikova, A., Sedelnikova, S., Baker, P.J., Stuitje, A.R., Slabas, A.R., Rice, D.W., Rafferty, J.B., 1999. Molecular basis of triclosan activity. Nature 398: 383–384.

Li, X.Z., Zhao, B.X. and Wang, P. 2007. Degradation of 2,4-dichlorophenol in aqueous solution by hybrid oxidation process. Journal of Hazardous Materials 147: 281-287.

Lin, S.H. and Chang, C.C. 2000. Treatment of landfill leachate by conbined electro-Fenton oxidation and sequencing batch reactor method. Water Research 34(17): 4243-4249.

Liou, M.J. and Lu, M.C. 2007. Catalytic degradation of nitroaromatic explosives with Fenton’s reagents. Journal of Molecular Catalysis. A: Chemical 277: 155–163.

Liu, H., Li, X.Z., Leng, Y.J., Wang, C. 2007. Kinetic modeling of electro-Fenton reaction in aqueous solution. Water Research 41: 1161 – 1167.

Liu, D.X., Liu, J., Wen, J. 1999. Elevation of hydrogen peroxide after spinal cord injury detected by using the Fenton reaction. Free Radic. Biol. Med. 27: 478–482.

Lorenc, J.L., Scheffer, G. 2003. Alkylphenols W. Kirk–Othmer encyclopaedia of chemical technology. [Online] Available from: http://www.mrw.interscience.wiley.com/emrw/9780471238966/kirk/article/alkylore.a01/current/html [2008, June 3]

Lu, M.C., Chen, J.N. and Chang, P. 1997. Effect of inorganic ions on the oxidation of dichlorvos insecticide with Fenton's reagent. Chemosphere 35: 2285-2293.

Lu, M.C., Chen, J.N. and Chang, .P. 1999. Oxidation of dichlorvos with hydrogen peroxide using ferrous ion as catalyst. Journal of Hazardous Materials B65: 277-288.

Lussier, S.M., Champlin, D,, LiVolsi, J., Poucher, S., Pruella, R.J. 1999. Acute toxicity of paranonylphenol to saltwater animals. Environ. Toxicol. Chem. 19: 617–621.

Ma, W.T., Fu, K.K., Cai, Z.W., Jiang, G.B., 2003. Gas chromatography/mass spectrometry applied for the analysis of triazine herbicides in environmental waters. Chemosphere 52: 1627–1632.

Martinez, N, Fernandez J, Segura X, Ferrer A., 2003. Pre-oxidation of an Extremely Polluted Industrial Wastewater by the Fenton's Reagent. Journal of Hazardous Materials B101: 315-322.

Masomboon, N., Lu, M.-C., Ratanatamskul, C., 2009. Chemical oxidation of 2,6-dimethylaniline in Fenton process. Environmental Science and Technology 43(22): 8629-8634.

Masomboon, N., Ratanatamskul, C., Lu, M.-C., 2010. Mineralization of 2,6-dimethylaniline by photoelectron-Fenton process. Applied Catalysis A: General 384: 128-135.

McAvoy, D.C., Schatowitz, B., Jacob, M., Hauk, A., Eckhoff, W.S., 2002. Measurement of triclosan in wastewater treatment systems. Environ. Toxicol. Chem. 21: 1323–1329.

Metzler, M., Pfeiffer, E., 2001. Chemistry of natural and antropogenic endocrine active compounds. In: Metzler, M. (Ed.), Endocrine Disruptors Part I. Springer, Germany, pp. 63–80.

Mijangos, F., Varona, F. and Villota, N. 2006. Changes in solution color during phenol oxidation by Fenton reagent. Environmental Science and Technology 40 (17): 5538–5543.

Mocarelli, P., Brambilla, P., Gerthoux, P.M., Patterson Jr., D.G., Needham, L.L., 1996. Change in sex ratio with exposure to dioxin. The Lancet 348: 401–416.

Momani, A.F., Sans, C. and Esplugas, S. 2004. A comparative study of the advanced oxidation of 2,4-dichlorophenol. Journal of Hazardous Materials B107: 123-129.

Morrall, D., McAvoy, D., Schatowitz, B., Inauen, J., Jacob, M., Hauk, A., Eckhoff, W., 2004. A field study of triclosan loss rates in river water (Cibolo Creek, TX). Chemosphere 54: 653–660.

Morrison, P.A., Leatherland, J.F., Sonstegard, R.A., 1985. Plasma cortisol and sex steroid levels in great lakes coho salmon (Oncorhynchus kisutch walbaum) in relation to fecundity and egg survival. Comparative Biochemistry and Physiology 80A: 61–68.

Mu, Y., Yu, H.Q., Zheng, J.C., Zhang, S.J. and Sheng, G.P. 2004. Reductive degradation of nitrobenzene in aqueous solution by zero-valent iron. Chemosphere 54: 789-794.

Muller, S., Schlatter, C. 1998. Oestrogenic potency of nonylphenol in vivo: a case study to evaluate the relevance of human non-occupational exposure. Pure Appl Chem. 70: 1847–1853.

Muzcua, M., Gomez, M.J., Ferrer, I., Agrera, A., Hernando, M.D., Fernandez-Alba, A.R., 2004. Evidence of 2,7/2,8-dibenzodichloro-p-dioxin as a photo degradation product of triclosan in water and wastewater samples. Analytical Chimica Acta 524: 241–247.

Nakada, N., Tanishima, T., Shinohara, H., Kiri, K., Takada, H. 2006. Pharmaceutical chemicals and endocrine disrupters in municipal wastewater in Tokyo and their removal during activated sludge treatment. Water Research 40: 3297–3303.

National Toxicology Program (NTP). 1989. Toxicology and carcinogenesis studies of 2,4- Dichlorophenol in F344/N rats and BC3F1 mice. (Feed Studies).Technical Report Series 353.

Naylor, C.G. 1993. Textile Chemist and Colorist, April 1993, American Chemical Society Southwest Regional Meeting.

Naylor, C.G. 1996. Presented at the 17th Annual Meeting of the Society of Environmental Toxicology and Chemistry, San Francisco.

Neyen E., Baeyens J. 2003. A review of classic Fenton’s peroxidation as an advanced oxidation technique. Journal of Hazardous Materials B98: 33-50.

Nguyen, M.H., Sigoillot, J.C. 1997. Isolation from coastal sea water and characterization of bacterial strains involved in non-ionic surfactant degradation. Biodegradation 7: 369–375.

Nice, H.E., Crane, M., Morritt, D., Thorndyke, M. 2001. Endocrine disrupters, critical windows and developmental success in oyster larvae In: Atckninson D, Thorndyke M eds. Environment and Animal Development: Genes, Life History and Plasticity. Bios Scientific publishers 203-217.

Nilsson, R. 2000. Endocrine modulators in the food chain and environment. Toxicol. Pathol. 28. 420-431.

Okumura, T., Nishikawa, Y., 1996. Gas chromatography–mass spectrometry determination of triclosans in water, sediment and fish samples via methylation with diazomethane. Analytical Chimica Acta 325: 175–184.

Oturan, M.A., Oturan, N., Lahitte, C. and Trevin, S. 2001. Production of hydroxyl radical by electrochemically assisted Fenton’s reagent: application to the mineralization of an organic micropollutant, Pentachlorophenol. Journal of Electroanalytical Chemistry 507: 69-102.

Panizza, M. and Cerisola, G. 2001. Removal of organic pollutants from industrial wastewater by electro generated Fenton's reagent. Water Research 35(16): 3987-3992.

Panter, G.H., Thompson, R.S., Beresford, N., Sumpter, J.P., 1999. Transformation of non oestrogenic steroid metabolite to an estrogenically active substance by minimal bacterial activity. Chemosphere 38: 3579–3596.

Pera-Titus, M. Garcia-Molina, V. Banos, M.A. Gimenez, J. and Esplugas, S. 2004. Degradation of chlorophenols by means of advanced oxidation processes: A General Review, Applied Catalysis B 47: 219-256.

Petrovic, M., Fernandez-Alba, A.R., Borrull, F., Marce, R.M., Mazo, E.G., Barcelo, D. 2002a. Occurrence and distribution of nonionic surfactants, their degradation products, and linear alkylbenzene sulfonates in coastal waters and sediments in Spain. Environ Toxicol Chem. 21: 37–46.

Petrovic, M., Sole, M., De Alda, M.J.L., Barcelo, D. 2002. Endocrine disruptors in sewage treatment plants, receiving river waters, and sediments: integration of chemical analysis and biological effects on feral carp. Environ Toxicol Chem. 21:2146–2156.

Piccinini, P., Minero, C., Vincenti, M. And Pelizzetti, E. 1997. Photocatalytic mineralization of nitrogen-containing benzene derivatives. Catalysis Today 39: 187-195.

Piccoli, A. 2002. Determination of triclosan in personal health care products by liquid chromatography (HPLC). Il Farmaco 57: 369–372.

Pignatello, J.J. 1992. Dark and photoassisted Fe^{3+}-catalysed degradation of Chlorophenoxy herbicides by hydrogen peroxide. Environmental Science and Technology 26: 944-951.

Pimentel, M., Oturan, N., Dezotti, M., Oturan, M. A. 2008. Phenol degradation by advanced electrochemical oxidation process electro-Fenton using a carbon felt cathode. Applied Catalysis B: Environmental.83: 140–149.

Plomley, J.B., Lausevic, M., March, R.E., 2000. Determination of dioxins/furans and PCBs by quadrupole ion-trap gas chromatography–mass spectrometry. Mass Spectrom 19: 305–365.

Qiang, Z., Chang, J. and Huang, C. 2002. Electrochemical generation of hydrogen peroxide from dissolved oxygen in acidic solution. Water Research 36: 85-94.

Qiang, Z., Chang, J. and Huang, C. 2003. Electrochemical generation of Fe^{2+} in Fenton oxidation processes. Water Research 37: 1308-1319.

Recchia, A.G., Vivacqua, A., Gabriele, S., Carpino, A., Fasanella, G., Rago, V., Bonofiglio, D.,Maggiolini, M. 2004. Xenoestrogens and the induction of proliferative effects in breast cancer cells via direct activation of oestrogen receptor alpha. Food Addit. Contam 21: 134-44.

Reed, H.W.B. 1978. Alkylphenols. In: Grayson M and EcKroth D eds. Kirk-Othmer, Encyclopedia of Chemical Technology, pp. 72-96. 3rd. Ed. Vol. 2. John Wiley and Sons. New York.

Renner, R. 1997. European bans on surfactant trigger transatlantic debate. Environmental Science and Technology 31: A316–320.

Richard, J.W. 1998. Hazardous Waste Sources Pathway Receptors, John Wiley & Sons, U.S.A.

Rios-Enriquez M., Shahin N., Durán-de-Bazúa C., Lang J., Oliveros E., Bossmann S.H., Braun A.M. Optimization of the heterogeneous Fenton-oxidation of the model pollutant 2,4-xylidine using the optimal experimental design methodology. Solar Energy 77(2004): 491-501.

Rodgers, J.D. and Bunce, N.J. 2001. Review Paper, Treatment methods for the remediation of nitroaromatic explosives. Water Research 35(9): 2101-2111.

Saarikoski, J., Viluksela, M. 1982. Relation between physicochemical properties of phenols and their toxicity and accumulation in fish. Ecotóxicology Environmental and Safety 6: 501-512.

Safe, S.H. 2000. Endocrine disruptor and human health, is there a problem? Environ. Health Prespect 108: 487-493.

Sauleda, R. and Brillas, E. 2001. Mineralization of aniline and 4-chlorophenol in acidic solution by ozonation catalyzed with Fe^{2+} and UV-A light. Applied Catalysis B: Environmental 29:135-145.

Scalia, S., Guarneri, M., Menegatti, E. 1994. Assay of triclosan in deodorant sticks and soaps by supercritical fluid extraction and HPLC. Journal of the Society of Cosmetic Chemists 45: 35–42.

Schroder, H.F. 2001. Tracing of surfactants in the biological wastewater treatment process and the identification of their metabolites by flow injection-mass spectrometry and liquid chromatography-mass spectrometry and-tandem mass spectrometry. Journal of Chromatography A 926: 127–150.

Schweizer, H.P., 2001. Triclosan: a widely used biocide and its link to antibiotics. FEMS Microbiol. Lett. 202: 1–7.

Scrimshaw, M.D., Lester, J.N. 2002. Fate and behaviour of endocrine disrupters in sludge treatment and disposal. In: Brikett JW, Lester JN, editors. Endocrine disrupters in wastewater and sludge treatment processes. Boca Raton, USA: CRC Press Inc.

Singer, H., Muller, S., Tixier, C., Pillonel, L., 2002. Triclosan: occurrence and fate of a widely used biocide in the aquatic environment: field measurements in wastewater treatment plants, surface waters, and lake sediments. Environmental Science and Technology 36: 4998–5004.

Sir´es, I., Arias, C., Cabot, P.L., Centellas, F., Garrido, J.A., Rodriquez, R.M. and Brillas, E. 2007. Degradation of clofibric acid in acidic aqueous medium by electro-Fenton and photoelectro-Fenton. Chemosphere. 66: 1660-1669.

Sir´es, I., Oturan, N., Oturan, M.A., Rodr´ıguez, R.M., Garrido, J.A., Brillas, E. 2007. Electro-Fenton degradation of antimicrobials triclosan and triclocarban. Electrochimica Acta 52: 5493–5503.

Skakkebaek, N.E., Rajpert-De Meyts, E., Jorgensen, N., Carlsen, E., Petersen, P.M., Giwercman, A., Andersen, ,A.G., Jensen, T., Andersson, A.M., Muller, J. 1998. Germ cell cancer and disorders of spermatogenesis: An environmental connection. Acta Pathol. Microbiol. Immunol. Scandinavica 106: 3-12.

Soares, A., Vijayram, I.A., Guieysse, B., Murto, M., Guieysse, B., Mattiasson, B. 2005. Degradation of non-ionic surfactants under anaerobic conditions. In: Rittmann BE, van LoosdrechtMCM, editors. Third IWAleading-edge conference on water and wastewater treatment technologies. Sapporo, Japan: IWA Publishing.

Sole, M., Lopez de Alda, M.J., Castillo, M., Porte, C., Ladegaard-Pedersen, K., Barcelo, D. 2000. Estrogenicity determination in sewage treatment plants and surface waters from Catalonian area (NE Spain). Environmental Science and Technology 34: 5076-5083.

Song-hu, Y. and Xiao-hua, L. 2005. Comparison treatment of various chlorophenols by electro-Fenton method: relationship between chlorine content and degradation. Journal of Hazardous Materials 118(1-3): 85-92.

Soto, A.M., Justicia, H., Wray, J.W., Sonnenschein, C. 1991. P-Nonylphenol: an estrogenic xenobiotic released from “modified” polystyrene. Environmental Health Perspective 92: 167–173.

Suarez, S., Dodd, M.C., Omil, F., Gunten, U.V. 2007. Kinetics of triclosan oxidation by aqueous ozone and consequent loss of antibacterial activity: Relevance to municipal wastewater ozonation. Water Research 41: 2481 – 2490.

Sun, J.-H., Sun, S.-P., a, Fan, M.-H., Guo, H.-Q., Qiao, L.-P., Sun, R.-X. 2007. A kinetic study on the degradation of *p*-nitroaniline by Fenton oxidation process. Journal of Hazardous Materials 148: 172–177.

Synder, S.A., Westerhoff, P., Yoon, Y., Sedlak, D.L., 2003. Pharmaceuticals, personal care products, and endocrine disruptors in water: implications for the water industry. Environmental Engineering Science 20 (5): 449–469.

Tang, W.Z. and Huang, C.P. 1996. Effect of chlorine content of chlorinated phenols on their oxidation kinetics by Fenton’s reagent, Chemosphere 33 (8): 1621-1635.

Tang, Z. and Tassos, S. 1997. Oxidation kinetics and mechanism of Trihalomethanes by Fenton's reagent. Water Research. 31(5): 1117-1125.

Tatarazako, N., Ishibashi, H., Teshima, K., Kishi, K. and Arizono, K. 2004. Effects of triclosan on various aquatic organisms, Environmental Science and Technology 11: 133–140.

Ternes, T.A., Kreckel, P., Mueller, J., 1999. Behaviour and occurrence of oestrogens in municipal sewage treatment plants-II. Aerobic batch experiments with activated sludge. Science of the Total Environment 225: 91–99.

Ting, W. P., Lu, M. C., Huang, Y. H. 2008. The reactor design and comparison of Fenton, electro-Fenton and photoelectro-Fenton processes for mineralization of benzene sulfonic acid (BSA). Journal of Hazardous Materials 156: 421-427.

Ting, W. P., Lu, M. C., Huang, Y. H. 2009. Kinetic of 2,6-dimethylaniline degradation by electro-Fenton process, Journal of Hazardous Materials 161: 1484–1490.

Tixier, C., Singer, H.P., Canonica, S., Mueller, S.R., 2002. Phototransformation of triclosan in surface waters: a relevant elimination process for this widely used biocide-laboratory studies, field measurements, and modeling. Environmental Science and Technology 36: 3482–3489.

U.S. Environmental Protection Agency. 2001. Removal of endocrine disruptor chemicals using water treatment processes, 625/R-00/015. Washington DC.

U.S. Environmental Protection Agency [U.S. EPA]. 2008. 2,4-Dichlorophenol; CASRN 120- 83-2 [Online]. Available from: http://www.epa.gov/iris/subst/0041.htm [2008, June 2]

Van Stee, L.L.P., Leonards, P.E.G., Vreuls, R.J.J., Brinkman, U.A.T., 1999. Identification of non-target compounds using gas chromatography with simultaneous atomic emission and mass spectrometric detection (GC–AED/MS): analysis of municipal wastewater. Analyst 124: 1547–1552.

Ventura, A., Jacquet, G., Bermond, A. and Camel, V. 2002. Electrochemical generation of the Fenton's reagent : application to atrazine degradation. Water Research 36: 3517-3522.

Walling C. 1975. Fenton's reagent revised. Accounts of Chemical Research 8: 125-131.

Wang, Q.Q. and Lemley, A.T. 2001. Kinetic model and optimization of 2,4-D degradation by anodic Fenton treatment. Environmental Science and Technology 35: 4509–4514.

Wang, S. 2008. A comparative study of Fenton and Fenton-like reaction kinetics in decolourisation of wastewater. Dyes and Pigments 76 (3): 714-720.

Wang, Y., Shen, Z., Li, Y. and Niu, J. 2010. Electrochemical properties of the erbium-chitosan-fluorine-modified PbO_2 electrode for the degradation of 2,4-dichlorophenol in aqueous solution. Chemosphere 79: 987-996.

Widera, J. and Cox, J.A. 2002. Electrochemical Oxidation of aniline in a silica sol-gel matrix. Electrochemistry Communications 4: 118-122.

Witorsch, R.J. 2002. Endocrine disruptors: can biological effects and environmetal risk be predicted. Regul. Toxicol. Pharmacol. 36: 118-130.

Yadetie, F., Arukwe, A., Gokoyr, A., Male, R. 1999. Induction of hepatic estrogen receptor in juvenile Atlantic salmon in vivo by the environmental estrogen, 4-nonylphenol. Science of the Total Environment 233: 201-210.

Ying, G.G., Kookana, R.S., Ru, Y.J., 2002a. Occurence and fate of hormone steroids in the environment. Environment International 28: 545–551.

Yuan, S., Tian, M., Cui, Y., Lin, L. and Lu, X. 2006. Treatment of nitrophenols by cathode reduction and electro-Fenton methods. Journal of Hazardous Materials 137: 573-580.

Zhang, H., Zhang, D. and Zhou, J. 2006. Removal of COD from landfill leachate by Electro-Fenton method. Journal of Hazardous Materials B135 : 106-111.

Zhao, B.X., Li, X.Z. and Wang, P. 2007. Degradation of 2,4-dichlorophenol with a novel TiO2/ Ti-Fe graphite felt photoelectrocatalytic oxidation process. Journal of Environmental Sciences 19: 1020-1024.

Zhou, T., Li, Y., Wong S.F. and Lu, X. 2008. Enhanced degradation of 2,4-dichlorophenol by ultrasound in a new Fenton-like system (Fe/EDTA) at ambient circumstance. Ultrasonics Sonochemistry 15: 782-790.

APPENDICES

APPENDIX A

Analytical Methods

Appendix A1
Analysis of 2,4-dichlorophenol and triclosan

2,4-dichlorophenol (2,4-DCP)

The sample were filtered with 0.20 µm micro-filters to separate the iron from the solution before analysis 2,4-DCP concentration. 2,4-DCP concentration was determined by High Performance Liquid Chromatograph (HPLC) (Thermo SCIENTIFIC Model) equipped with a UV detector (FINNIGAN SPECTRA SYSTEM UV1000). The UV wavelength for detection was 285 nm. The retention time for 2,4-DCP was 10 min and injected volume was 20 µL. The separation column was a reverse-phase column (Shodex Asahipak, ODP-506D 6 mm × 150 mm × 5 µm) equipped with Spectra SYSTEM SN4000 model pump at the operating flow rate 1ml min^{-1}. The column was operated at temperature between 18 and 22 ^{o}C. The mobile phase consisted of acetonitrile : water : acetic acid (69 : 30 : 1).

Apparatus

1. High Performance Liquid Chromatograph (HPLC) (Thermo SCIENTIFIC Model) equipped with a UV detector (FINNIGAN SPECTRA SYSTEM UV1000) 50 ml Erlenmeyer flask. The separation column was a reverse-phase column (Shodex Asahipak, ODP-506D 6 mm × 150 mm × 5 µm) equipped with Spectra SYSTEM SN4000 model pump at the operating flow rate 1ml min^{-1}. The mobile phase consisted of acetonitrile : water : acetic acid (69 : 30 : 1).
2. Medicine syringe

Preparing for Calibration Curve

The standard 2,4-DCP solution were prepared in the range of 0 to 1.0 mM as 2,4-DCP

1. 16.3 mg of 2,4-DCP was prepared in 100 ml volumetric flasks with vigorous stirring for 1 mM stock solution of 2,4-DCP..
2. The samples were diluted to 0.01, 0.05, 0.10, 0.25, 0.50 mM with RO water, mixed thoroughly. After that, it has to stand for 10 min.
3. Measured samples by High Performance Liquid Chromatograph (HPLC) at 285 nm.

Calculation

$Y = 2.497X$

$r^2 = 0.999$

Where X = Area, Y = 2,4-DCP concentration (mM)

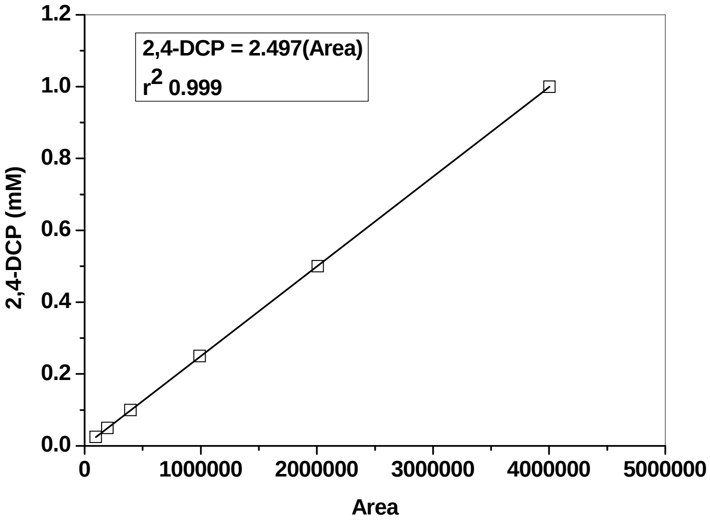

Triclosan (Piccoli et al. 2002; Behera et al., 2010)

The sample was filtered with 0.20 µm micro-filters to separate the iron from the solution before analysis triclosan concentration. Triclosan concentration was determined by High Performance Liquid Chromatograph (HPLC Thermo SCIENTIFIC Model) equipped with a UV detector (FINNIGAN SPECTRA SYSTEM UV1000). The UV wavelength for detection was 220 nm. The retention time for triclosan was 5 min. A sample injection volume of 50 µL was used. The separation column is a reverse-phase column (Zorbax XDB-C18 4.6 mm × 250 mm, 5 µm), the flow rate was set at 1 mL min^{-1}. The column temperature was maintained at 25 °C. A mobile phase was consists of acetonitrile : water (70 : 30).

Apparatus

1. High Performance Liquid Chromatograph (HPLC Thermo SCIENTIFIC Model) equipped with a UV detector (FINNIGAN SPECTRA SYSTEM UV1000) 50 ml Erlenmeyer flask. The separation column is a reverse-phase column (Zorbax XDB-C18 4.6 mm × 250 mm, 5 µm), the flow rate was set at 1 mL min^{-1}. The mobile phase consisted of acetonitrile : water (70 : 30).
2. Medicine syringe

Preparing for Calibration Curve

The standard triclosan solution were prepared in the range of 0 to 1.0 mM as triclosan

1. The RO water was adjust pH by NaOH to 10 for dissolve triclosan 1 mM
2. 28.9 mg of triclosan was prepared in 100 ml volumetric flasks with the RO water pH 10 with vigorous stirring for 1 mM stock solution of triclosan.

3. The samples were diluted to 0.01, 0.05, 0.10, 0.25, 0.50 mM with RO water, mixed thoroughly and adjust pH to normally 6-7. After that, it has to stand for 10 min.
4. Measured samples by High Performance Liquid Chromatograph (HPLC) at 220 nm.

Calculation

$Y = 4.90X$

$r^2 = 0.990$

Where X = Area, Y = triclosan concentration (mM)

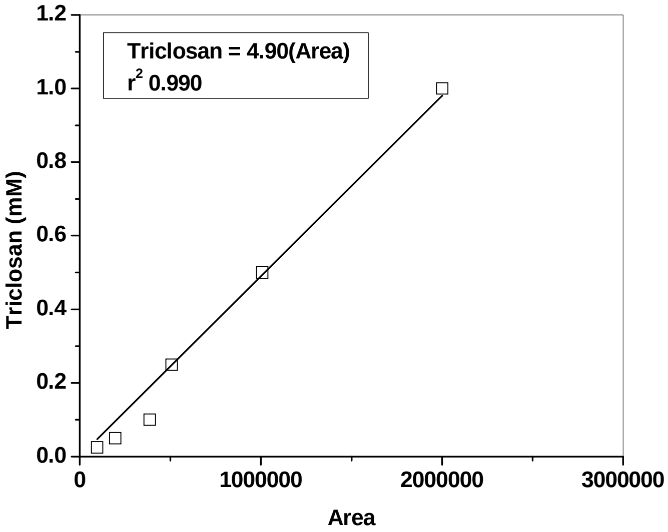

Appendix A2

Analysis of Chemical Oxygen Demand (COD)

(Closed-reflux titrimetric method based on the Standard methods, APHA, 1992).

1. General Discussion

The chemical oxygen demand (COD) test is commonly used to indirectly measure the amount of organic compounds in water. Most applications of COD determine the amount of organic pollutants found in surface water (e.g. lakes and rivers), making COD a useful measure of water quality. It is expressed in milligrams per liter (mg L^{-1}), which indicates the mass of oxygen consumed per liter of solution. Older references may express the units as parts per million (ppm). The basis for the COD test is that nearly all organic compounds can be fully oxidized to carbon dioxide with a strong oxidizing agent under acidic conditions.

For many years, the strong oxidizing agent potassium permanganate ($KMnO_4$) was used for measuring chemical oxygen demand. Measurements were called oxygen consumed from permanganate, rather than the oxygen demand of organic substances. Potassium permanaganate's effectiveness at oxidizing organic compounds varied widely, and in many cases biochemical oxygen demand (BOD) measurements were often much greater than results from COD measurements. This indicated that potassium permanganate was not able to effectively oxidize all organic compounds in water, rendering it a relatively poor oxidizing agent for determining COD. Since then, other oxidizing agents such as ceric sulfate, potassium iodate, and potassium dichromate have been used to determine COD. Of these, potassium dichromate ($K_2Cr_2O_7$) has been shown to be the most effective: it is relatively cheap, easy to purify, and is able to nearly completely oxidize almost all organic compounds.

For all organic matter to be completely oxidized, an excess amount of potassium dichromate (or any oxidizing agent) must be present. Once oxidation is complete, the amount of excess potassium dichromate must be measured to ensure that the amount of

Cr^{3+} can be determined with accuracy. To do so, the excess potassium dichromate is titrated with ferrous ammonium sulfate (FAS) until all of the excess oxidizing agent has been reduced to Cr^{3+}. Typically, the oxidation-reduction indicator Ferroin is added during this titration step as well. Once all the excess dichromate has been reduced, the Ferroin indicator changes from blue-green to reddish-brown. The amount of ferrous ammonium sulfate added is equivalent to the amount of excess potassium dichromate added to the original sample

2. Apparatus

The reagent uses in COD measurement are:

$K_2Cr_2O_7$ (0.1 N) : 167 ml H_2SO_4 add into 1000 ml volumetric flask and then add 200 ml of DI water. After that 4.913 gram of $K_2Cr_2O_7$ was added and then 33.3 ml of $HgSO_4$. Then DI water was adjusted up-to 1 liter.

H_2SO_4 solution: prepared by added 25.3 gram of Ag_2SO_4 into 2.5 liter of H_2SO_4

FAS (0.025 N): 9.8 gram of $FeSO_4(NH_4)SO_4.6H_2O$ was put into 1 liter volumetric flask and then 20 ml of H_2SO_4 was added. Then the DI water was poured until 1 liter.

Ferroin Indicator: 1 drop

3. Procedure

The sample 2.5 ml was put into tube and then 1.5 ml of $K_2Cr_2O_7$ (0.1 N), 3.5 ml of H_2SO_4 reagent were added. After that the mixed chemical was incubate at 150 $^{\circ}$C for 2 hours. Then the chemical was put outside at room temperature to cool down the temperature. After that, 1 drop of Ferroin indicator was added and titrated by using FAS.

4. Calculation

The following formula is used to calculate COD:

$$\mathrm{COD} = \frac{(\mathit{blank} - \mathit{sample}) * \mathrm{FAS\ conc.} * 8000}{2.5}$$

$$\mathrm{FAS\ conc.} = \frac{0.1 * 1.5}{V_{\mathrm{FAS\ (normal)}}}$$

Where blank is the volume of FAS used in the blank sample, sample is the volume of FAS in the original sample, and FAS conc. is the normality of FAS. If milliliters are used consistently for volume measurements, the result of the COD calculation is given in mg L^{-1}.

Appendix A3

Analysis of ferrous ions (APHA, 1992)

Principle

The phenanthroline method is the preferred standard procedure for the measurement of iron in water at the present time, except when color, turbidity, phosphate, or heavy metal interferences are present. The method depends upon the fact that 1,10-phenanthroline combine with ferrous to form a complex iron that is orange-red in color. Three molecules of 1,10-phenanthroline are required to sequester or form a complex ion with each ferrous ion. The reaction may be represented as shown in the following equation:

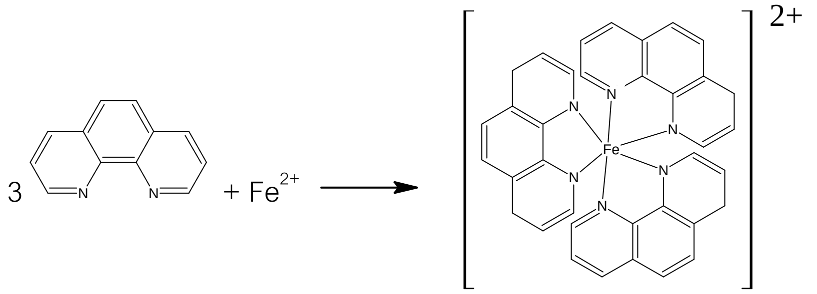

(A-1)

Reagents

1. Hydrochloric acid, HCl: 20 ml of concentration hydrochloric acid is diluted to 1,000 ml with RO water.
2. Ammonium acetate buffer solution: 500 g of $NH_4C_2H_3O_2$ is dissolved in 300 ml of RO water. Then 1,400 ml of concentration acetic acid was filled up to the mark of 2,000 ml.
3. Phenanthroline solution: dissolve 5 g of 1,10-phenanthroline hydrochloride ($C_{12}H_8N_2$•HCl+H_2O) into 1,000 ml of RO water.

Apparatus

3. Spectrophotometer (Shimadsu UV-1201) The absorbance used for ferrous ion analysis was 510 nm.
4. 50 ml Erlenmeyer flask
5. Medicine dropper

Procedure

1. 25 ml of HCl from stock solution was prepared in 50 ml volumetric flask. Then, 10 ml of phenanthroline solution and 5 ml of ammonium acetate solution are added with vigorous stirring.
2. 1 ml of sample is filled and diluted to 50 ml with RO water. After that, it has to stand for 10 min. do not expose to sunlight. (Color develop was rapid in the presence of excess phenanthrolines.)
3. Measured samples by spectrophotometer at 510 nm.

Preparing for Calibration Curve

The standard ferrous solution were prepared in the range of 0 to 2.0 mM as Fe^{2+}

1. 25 ml of HCl from stock solution was prepared in five 50 ml volumetric flasks. Then, 10 ml of phenanthroline solution and 5 ml of ammonium acetate solution are added with vigorous stirring.
2. 1 ml of 0, 0.5, 1, and 2 mg L^{-1} as Fe^{2+} standard solution are pipetted, respectively.
3. The samples were diluted to 50 ml with RO water, mixed thoroughly. After that, it has to stand for 10 min.
4. Measured samples by spectrophotometer at 510 nm.

Calculation

Y = 4.9839X

Where X = absorbance at 510 nM, Y = Fe^{2+} concentration (mM)

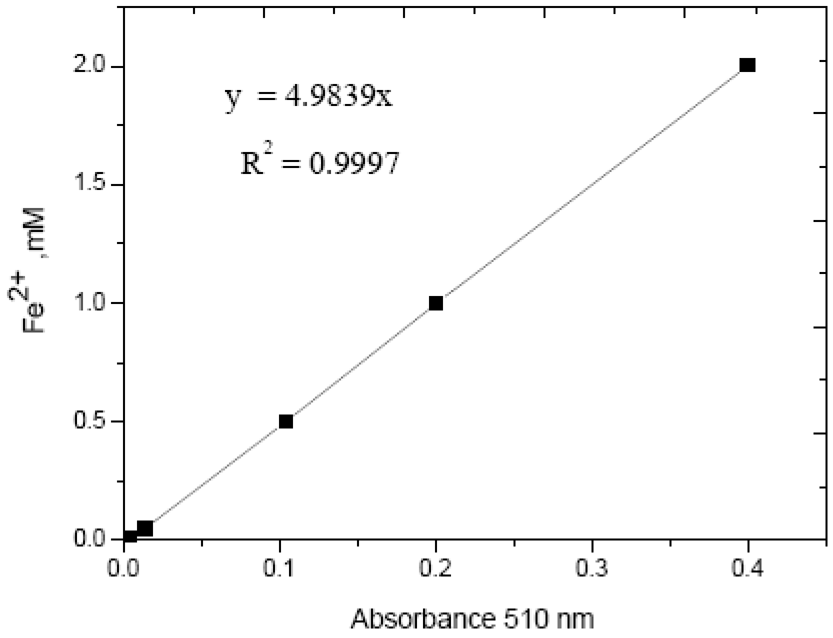

Appendix A4

Spectrophotometric determination of hydrogen peroxide

(Eisenberg, 1943 and Sellers, 1980)

Principle

The method is based on photoelectric measurement of color intensities of hydrogen peroxide solution treated with potassium titanium (IV) oxalate reagent in the acid solution. The yellow color produced in the reaction due to the formation of pertitanic acid complex as $TiO_2.H_2O_2$, showing a true peroxide structure. The reaction equation is usually written:

$Ti^{4+} + H_2O_2 + 2H_2O\ H_2TiO_4 + 4H^+$

Reagents

Potassium titanium (IV) oxalate solution is prepared by mixed 27.2 mL of concentrated sulfuric acid (H_2SO_4 (conc.)) with about 300 mL of dionized water, then dissolve in this mixture 35.4 g of potassium titanium (IV) oxalate ($K_2TiO(C_2O_4)_2{\cdot}2H_2O$) and make up to 1 L with dionized water.

Apparatus

1. Spectrophotometer capable of measuring absorption at a wavelength of 400 nm and fitted with 10 mm and 40 mm path length glass cells.
2. 25 ml Erlenmeyer flask
3. Medicine dropper

Procedure

1. 5 mL of titanium oxalate reagent was prepared into 25 mL volumetric flask.
2. Transfer 1 mL of sample to 25 mL Erlenmeyer flask.
3. Adjust the volume to 25 mL with DI water, mixed thoroughly. After that, it had to stand for 15 min for the stable coloration.
4. Measured the absorbance of samples by spectrophotometer at 400 nm.

Preparing for Calibration Curve

The standard ferrous solution were prepared in the range of 0 to 20 mM

1. 5 ml of titanium oxalate reagent was prepared into 25 ml volumetric flasks.

2. 1 ml of 0.1, 0.5, 1, 5, 10 and 20 mM of H_2O_2 concentration were pipetted, respectively.

3. The samples were diluted to 25 ml with DI water, mixed thoroughly. After that, it had to stand for 15 min for the stable coloration.

4. Measured the absorbance of samples by spectrophotometer at 400 nm.

Calculation

Y = 27.213X

Where X = absorbance at 400 nM, Y = H_2O_2 (mM)

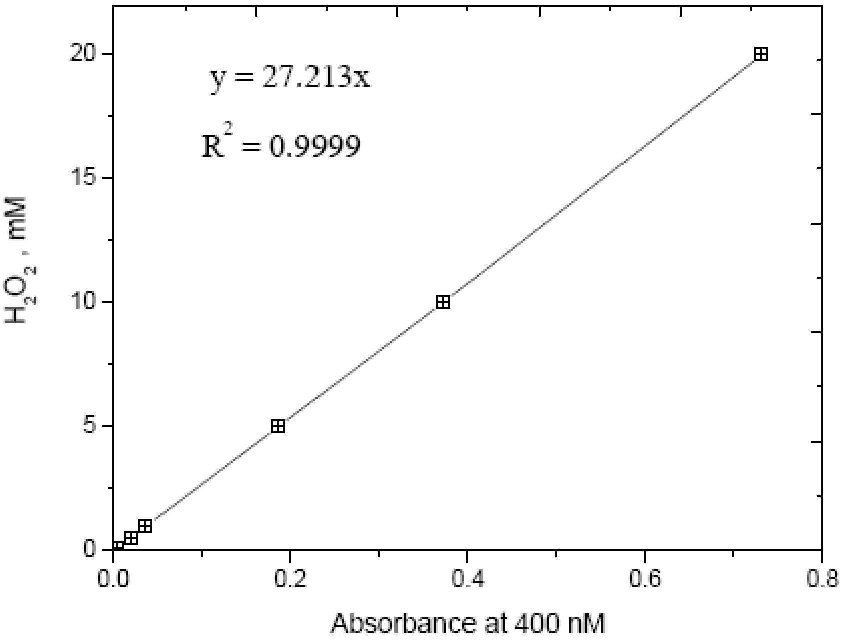

Appendix A5

Theory of Reaction Rates, first order theory and initial rate investigation

The rate of a chemical reaction depends upon many factors, such as concentration of reactants, temperature, and the presence of a catalyst. The rate of a reaction is usually dependent on the concentration of reactants. The rate decreases as concentration decreases. We can write a rate law equation to show this relationship. The rate law equation relates the rate of a reaction to the concentration of each reactant. Consider the general reaction below:

$$a\,A + b\,B \longrightarrow c\,C \text{ and } d\,D + \ldots \tag{1}$$

The small letters represent the stoichiometric coefficients. We can express the general rate of reaction in terms of the disappearance of the reactants or appearance of the products.

$$Rate = -\frac{\Delta A}{\Delta t}\ or\ -\frac{\Delta[B]}{\Delta t}\ or\ \frac{\Delta[C]}{\Delta t}\ or\ \frac{\Delta[D]}{\Delta t} \tag{2}$$

Here Δ[A] is the change in the molar concentration of reactant A over time, Δt. The reaction rate will have units of M/time. By convention, the minus sign for reactants ensures a positive value for the rate since a change in concentration of a reactant with time, (Δ[A]/Δt), is a negative value.

An empirical formula (rate law equation or rate equation) has been found from experiment that relates rate to the concentration of each reactant at any time in the reaction. The rate law equation has the form

$$Rate = k[A]^m[B]^n \tag{3}$$

In the rate law equation, [A] and [B] are the molarities of each reactant in the balanced equation at some time t. Here k is the rate constant (depends only on temperature), and m and n are the orders of the reaction with respect to A and B. Important: m and n are not related to the stoichiometric coefficients in the balanced equation! Reaction orders must be determined by experiment! Reaction orders are usually integers of value 0, 1, or 2. The rate constant, k, is also determined by experiment.

If the initial concentration of the reactant A is a few or constant difference of its concentration (steady state condition) with reaction time than the reactant B concentration, the concentration of A will not change appreciably during the course of the reaction. It can define this condition as psudo-steady state reaction. Thus the rate's dependence on reactant B can be isolated and the rate law can be written

$$Rate = \frac{dC}{dt} = k[A]^m[B]^n = k'[B]^n \tag{4}$$

Where k' is k[A]

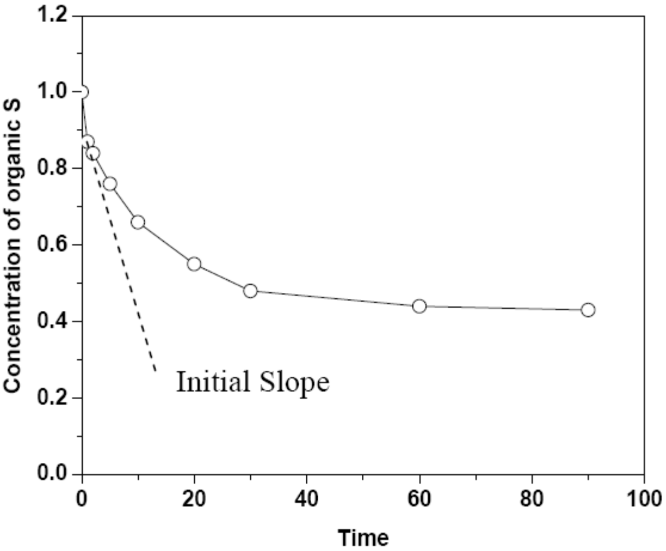

For Fenton and electro-Fenton processes, the hydroxyl radical is react with organic S as shown in equation (5)-(9) in order of pseudo-first order reaction.

$$\bullet OH + S \xrightarrow{k} products \tag{5}$$

$$Rate = \frac{dS}{dt} = k[\bullet OH][S] \ = k'[S] \tag{6}$$

Where k' is k[•OH]

$$\frac{1}{[S]} dS = k'dt \tag{7}$$

$$\int_{S_0}^{S} \frac{1}{[S]} dS = \int_{0}^{t} k'dt \tag{8}$$

$$\ln\left(\frac{[S]}{[S_0]}\right) = k't \tag{9}$$

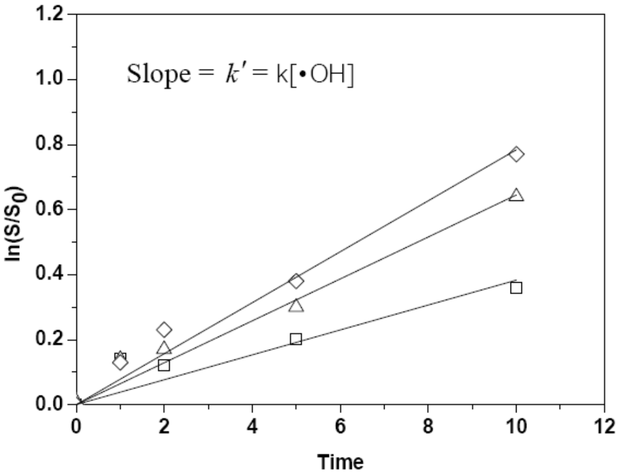

$$Initial\ Rate = k'[S_0] \tag{10}$$

For k' investigation, the slope of graphical plot between ln(S/S_0) versus time at initial time (0-20 minutes approximately) was determined. The slope or k' is used to find the initial rate by substitution of the slope or k' value for multiply with initial concentration S_0 in equation (10).

APPENDIX B

Experimental Apparatus Figures

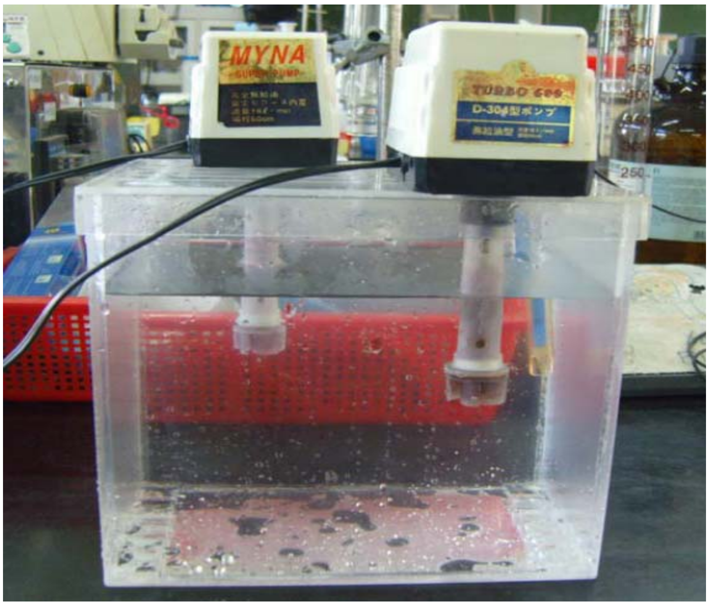

Figure B.1. Fenton reactor setup

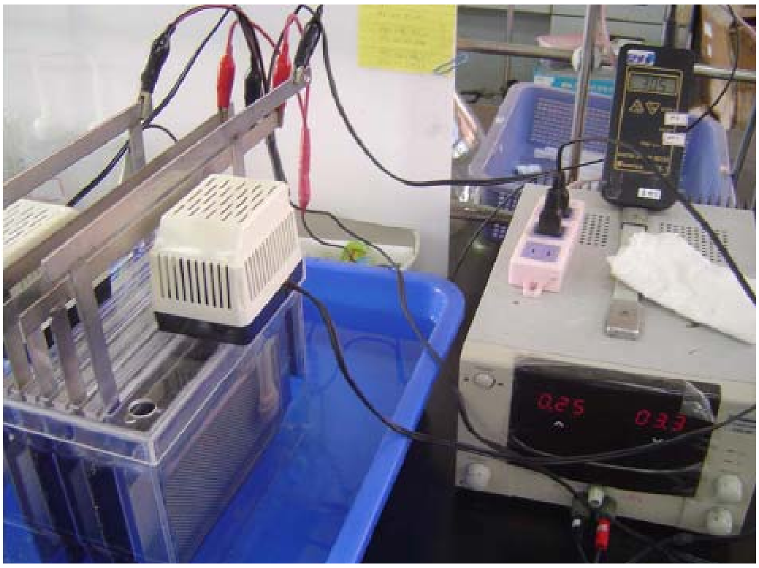

Figure B.2. Electro-Fenton reactor setup

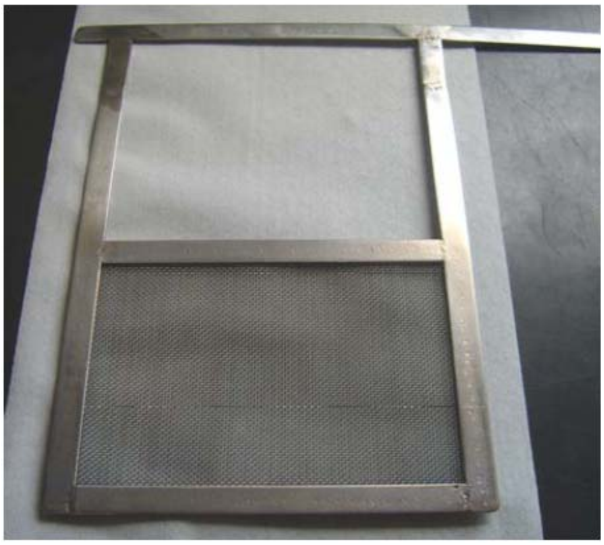

Figure B.3. Cathode electrode of electro-Fenton reactor

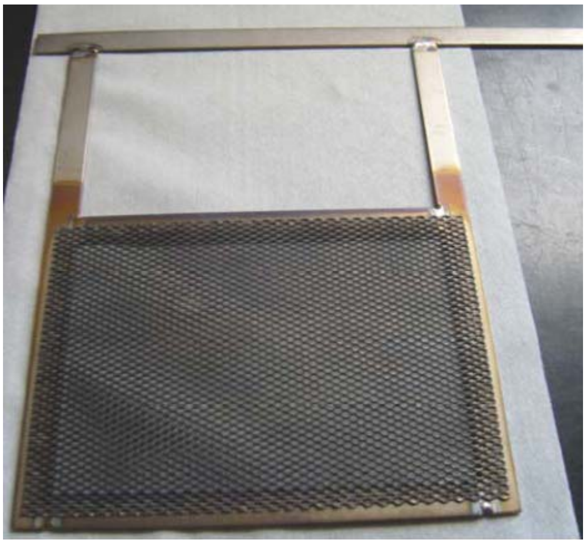

Figure B.4. Anode electrode of electro-Fenton reactor

Figure B.5. Thermal Controller

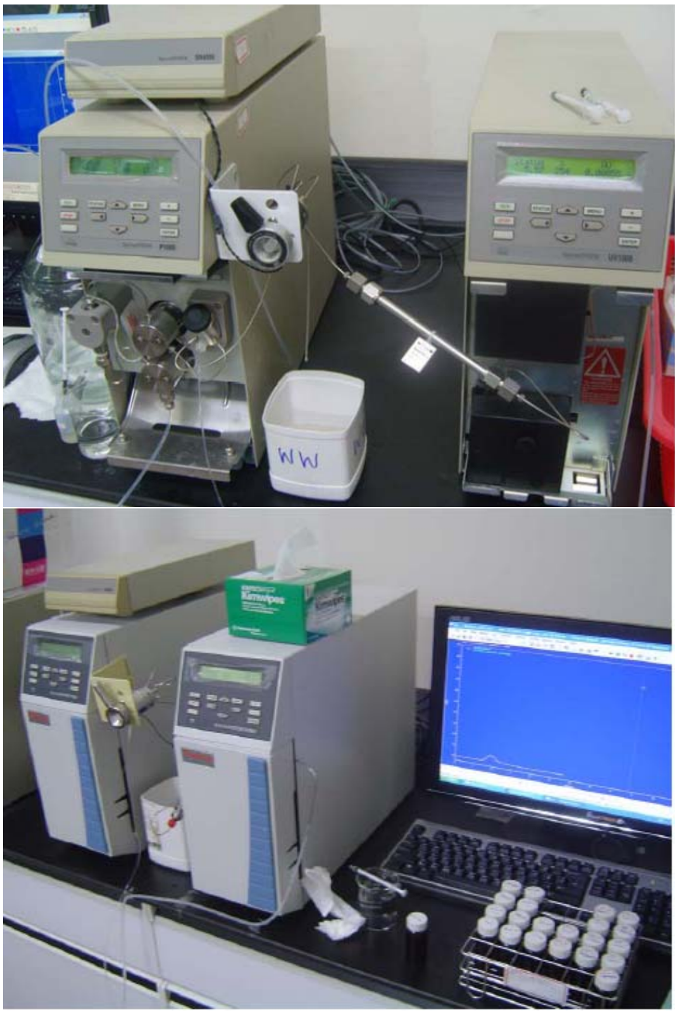

Figure B.6. High Performance Liquid Chromatography (HPLC) Instrument

Figure B.7. Total Organic Carbon (TOC) Analyzer Instrument

Figure B.8. Liquid Ion Chromatography (IC) Instrument

Figure B.9. Demineralization Water Production Instrument

Figure B.10. pH Meter Instrument

Figure B.11. Filter Instrument Set

Figure B.12. Ultrasonic Cleaner Instrument

Figure B.13. Hydrogen Peroxide Feeding Pump Instrument

APPENDIX C

Experimental Data

2,4-Dichlorophenol (2,4-DCP) Experiments

Control Experiments

2,4-DCP volatilization control experiment

Time (minute)	2,4-DCP Remaining (mM)				
	pH 2	pH 3	pH 3.5	pH 7.8	pH 9
0	1.01	1.02	0.99	0.99	1.02
1	0.99	0.99	0.99	0.99	0.99
2	0.96	0.97	0.97	0.98	0.98
5	0.95	0.94	0.94	0.97	0.99
10	0.91	0.94	0.93	0.97	0.98
20	0.89	0.93	0.92	0.95	0.97
30	0.86	0.92	0.93	0.93	0.97
60	0.85	0.90	0.92	0.93	0.95
90	0.84	0.89	0.91	0.93	0.95
120	0.84	0.89	0.91	0.92	0.94

Electrolysis control experiment

Time (minute)	2,4-DCP Remaining (mM)				
	Current Density 0.01 mA cm^{-2}	Current Density 0.05 mA cm^{-2}	Current Density 0.12 mA cm^{-2}	Current Density 0.25 mA cm^{-2}	Current Density 0.50 mA cm^{-2}
0	0.97	1.00	0.99	0.99	1.05
1	0.99	0.97	0.96	0.97	0.96
2	0.99	0.96	0.96	0.96	0.97
5	0.97	0.96	0.96	0.96	0.96
10	0.98	0.97	0.93	0.95	0.95
20	0.97	0.98	0.91	0.93	0.92
30	0.97	0.94	0.91	0.90	0.91
60	0.97	0.95	0.91	0.90	0.91
90	0.95	0.93	0.91	0.90	0.90

Various process control experiments

Time (minute)	2,4-DCP Remaining (mM)			
	Current Density 0.05 mA cm^{-2}	Current Density 0.12 mA cm^{-2}	Fenton Process (No Current)	Electro-Fenton Process (Current Density 0.05 mA cm^{-2})
0	1.00	0.99	1.01	1.02
1	0.97	0.96	0.92	0.87
2	0.96	0.96	0.89	0.88
5	0.96	0.96	0.85	0.82
10	0.97	0.93	0.77	0.69
20	0.98	0.91	0.63	0.51
30	0.94	0.91	0.48	0.39
60	0.95	0.91	0.42	0.29
90	0.93	0.91	0.40	0.29

Fenton Process Experiments

Effect of pH on 2,4-DCP removal by Fenton's experiment

2,4-DCP concentrations remaining in effect of pH on 2,4-DCP removal by Fenton's experiment

Time (minute)	2,4-DCP Remaining (mM)		
	pH 2	pH 3	pH 3.5
0	0.99	1.01	0.99
1	0.94	0.90	0.94
2	0.93	0.89	0.92
5	0.90	0.83	0.90
10	0.83	0.71	0.88
20	0.64	0.52	0.80
30	0.59	0.47	0.76
60	0.52	0.41	0.61
90	0.48	0.37	0.56

COD concentrations remaining in effect of pH on 2,4-DCP removal by Fenton’s experiment

Time (minute)	COD Remaining ($mg\ L^{-1}$)		
	pH 2	pH 3	pH 3.5
0	198.00	202.06	203.12
1	188.10	185.89	195.99
2	182.16	181.85	187.91
5	174.24	171.75	175.79
10	168.30	167.70	171.75
20	160.38	155.58	165.68
30	156.42	147.50	161.65
60	150.48	141.44	153.56
90	144.54	135.38	151.54

TOC concentrations remaining in effect of pH on 2,4-DCP removal by Fenton’s experiment

Time (minute)	TOC Remaining ($mg\ L^{-1}$)		
	pH 2	pH 3	pH 3.5
0	50.15	52.24	49.72
1	49.65	51.72	49.23
2	49.65	51.71	49.23
5	49.64	50.67	49.22
10	49.14	50.16	49.22
20	49.64	50.16	48.73
30	49.64	50.15	48.72
60	49.63	50.15	48.23
90	49.63	49.63	48.22

Fe^{2+} concentrations remaining in effect of pH on 2,4-DCP removal by Fenton's experiment

Time (minute)	Fe^{2+} Remaining ($mg\ L^{-1}$)		
	pH 2	pH 3	pH 3.5
0	5.49	5.53	5.51
1	3.84	3.43	4.02
2	3.56	3.21	4.68
5	3.29	3.59	4.24
10	3.18	3.48	3.96
20	2.85	3.26	3.75
30	2.19	2.43	3.47
60	2.14	2.15	3.14
90	1.81	1.71	2.69

H_2O_2 concentrations remaining in effect of pH on 2,4-DCP removal by Fenton's experiment

Time (minute)	H_2O_2 Remaining ($mg\ L^{-1}$)		
	pH 2	pH 3	pH 3.5
0	30.21	30.75	29.94
1	28.69	30.13	29.64
2	28.09	29.21	28.44
5	27.18	27.36	27.54
10	25.67	25.52	26.04
20	21.75	23.37	24.85
30	20.24	19.98	22.75
60	16.91	15.68	20.65
90	15.70	14.45	19.16

Effect of Fe^{2+} concentration on 2,4-DCP removal by Fenton's experiment

2,4-DCP concentrations remaining in effect of Fe^{2+} concentration on 2,4-DCP removal by Fenton's experiment

Time (minute)	2,4-DCP Remaining (mM)				
	Fe^{2+} 0.10 mM	Fe^{2+} 0.20 mM	Fe^{2+} 0.30 mM	Fe^{2+} 0.40 mM	Fe^{2+} 0.50 mM
0	1.01	0.98	0.99	0.98	1.01
1	0.90	0.87	0.86	0.85	0.86
2	0.89	0.80	0.80	0.79	0.80
5	0.83	0.74	0.74	0.71	0.72
10	0.71	0.65	0.65	0.62	0.64
20	0.52	0.49	0.50	0.57	0.59
30	0.47	0.46	0.46	0.51	0.54
60	0.41	0.42	0.39	0.47	0.50
90	0.37	0.35	0.39	0.45	0.47

COD concentrations remaining in effect of Fe^{2+} concentration on 2,4-DCP removal by Fenton's experiment

Time (minute)	COD Remaining (mg L^{-1})				
	Fe^{2+} 0.10 mM	Fe^{2+} 0.20 mM	Fe^{2+} 0.30 mM	Fe^{2+} 0.40 mM	Fe^{2+} 0.50 mM
0	202.06	211.35	208.79	211.54	212.76
1	185.89	209.23	202.52	209.42	208.50
2	181.85	198.66	185.82	198.84	197.86
5	171.75	202.89	192.08	194.61	191.48
10	167.70	192.32	183.73	179.80	189.35
20	155.58	185.98	175.38	175.57	178.71
30	147.50	177.53	158.68	167.11	168.08
60	141.44	166.96	144.06	154.42	155.31
90	135.38	156.39	144.05	143.84	151.05

TOC concentrations remaining in effect of Fe^{2+} concentration on 2,4-DCP removal by Fenton's experiment

Time (minute)	TOC Remaining (mg L^{-1})				
	Fe^{2+} 0.10 mM	Fe^{2+} 0.20 mM	Fe^{2+} 0.30 mM	Fe^{2+} 0.40 mM	Fe^{2+} 0.50 mM
0	52.24	53.44	52.67	52.54	52.07
1	51.72	52.90	52.14	52.01	51.54
2	51.71	52.90	52.12	51.48	50.51
5	50.67	52.37	51.62	50.96	50.50
10	50.16	51.83	51.61	50.44	49.47
20	50.16	51.30	51.10	50.43	49.46
30	50.15	51.61	51.09	49.91	48.95
60	50.15	51.30	51.09	49.89	48.42
90	49.63	51.29	51.07	49.88	48.42

Fe^{2+} concentrations remaining in effect of Fe^{2+} concentration on 2,4-DCP removal by Fenton's experiment

Time (minute)	Fe^{2+} Remaining (mg L^{-1})				
	Fe^{2+} 0.10 mM	Fe^{2+} 0.20 mM	Fe^{2+} 0.30 mM	Fe^{2+} 0.40 mM	Fe^{2+} 0.50 mM
0	5.53	10.40	15.50	19.20	23.40
1	3.43	8.00	12.55	15.26	18.15
2	3.21	7.07	11.47	14.58	16.74
5	3.59	6.55	9.61	13.02	15.21
10	3.48	6.24	9.14	12.09	14.04
20	3.26	6.03	9.51	10.94	13.57
30	2.43	5.09	7.28	9.70	12.40
60	2.15	3.84	6.35	9.11	10.79
90	1.71	3.64	6.04	8.54	10.06

H_2O_2 concentrations remaining in effect of Fe^{2+} concentration on 2,4-DCP removal by Fenton's experiment

Time (minute)	H_2O_2 Remaining (mg L^{-1})				
	Fe^{2+} 0.10 mM	Fe^{2+} 0.20 mM	Fe^{2+} 0.30 mM	Fe^{2+} 0.40 mM	Fe^{2+} 0.50 mM
0	30.75	29.05	30.01	28.10	31.06
1	30.13	26.39	25.50	25.20	29.50
2	29.21	21.46	21.00	21.84	26.09
5	27.36	18.85	21.90	19.67	24.85
10	25.52	16.53	19.80	17.70	23.60
20	23.37	15.08	18.00	16.30	22.67
30	19.98	13.92	16.20	14.05	20.81
60	15.68	12.76	15.30	12.64	18.64
90	14.45	13.05	14.70	11.80	17.08

Effect of H_2O_2 concentration on 2,4-DCP removal by Fenton's experiment

2,4-DCP concentrations remaining in effect of H_2O_2 concentration on 2,4-DCP removal by Fenton's experiment

Time (minute)	2,4-DCP Remaining (mM)				
	H_2O_2 1 mM	H_2O_2 2 mM	H_2O_2 3 mM	H_2O_2 4 mM	H_2O_2 5 mM
0	1.01	1.04	0.99	0.99	1.05
1	0.90	0.78	0.77	0.74	0.69
2	0.89	0.69	0.67	0.69	0.56
5	0.83	0.54	0.56	0.53	0.53
10	0.71	0.53	0.47	0.48	0.45
20	0.52	0.46	0.39	0.43	0.32
30	0.47	0.40	0.32	0.29	0.24
60	0.41	0.36	0.31	0.26	0.22
90	0.37	0.35	0.31	0.25	0.21

COD concentrations remaining in effect of H_2O_2 concentration on 2,4-DCP removal by Fenton's experiment

Time (minute)	COD Remaining (mg L^{-1})				
	H_2O_2 1 mM	H_2O_2 2 mM	H_2O_2 3 mM	H_2O_2 4 mM	H_2O_2 5 mM
0	202.06	207.12	203.27	201.59	205.14
1	185.89	186.40	193.10	175.38	176.42
2	181.85	182.26	170.74	161.27	155.90
5	171.75	173.98	160.58	147.16	143.59
10	167.70	165.69	152.45	133.04	127.18
20	155.58	155.34	142.28	120.95	123.08
30	147.50	147.05	130.09	118.93	125.13
60	141.44	142.91	128.06	116.92	121.03
90	135.38	134.62	126.02	116.92	116.92

TOC concentrations remaining in effect of H_2O_2 concentration on 2,4-DCP removal by Fenton's experiment

Time (minute)	TOC Remaining (mg L^{-1})				
	H_2O_2 1 mM	H_2O_2 2 mM	H_2O_2 3 mM	H_2O_2 4 mM	H_2O_2 5 mM
0	52.24	55.01	50.12	49.67	54.26
1	51.72	54.46	49.62	49.17	53.72
2	51.71	54.45	49.12	48.67	52.63
5	50.67	53.91	49.11	48.18	52.09
10	50.16	53.90	48.62	48.17	51.00
20	50.16	53.36	48.11	47.68	50.47
30	50.15	53.35	48.11	47.19	50.46
60	50.15	52.81	47.61	47.18	50.45
90	49.63	52.80	47.61	47.18	50.45

Fe^{2+} concentrations remaining in effect of H_2O_2 concentration on 2,4-DCP removal by Fenton’s experiment

Time (minute)	Fe^{2+} Remaining ($mg\ L^{-1}$)				
	H_2O_2 1 mM	H_2O_2 2 mM	H_2O_2 3 mM	H_2O_2 4 mM	H_2O_2 5 mM
0	15.53	15.45	15.57	15.44	15.61
1	9.52	9.27	10.12	10.03	9.99
2	9.00	8.49	7.16	8.33	7.80
5	10.09	7.57	6.22	6.48	7.02
10	9.78	6.64	5.91	6.17	5.77
20	9.16	6.95	5.44	5.71	5.15
30	6.83	6.18	4.98	5.09	4.52
60	6.05	5.56	4.87	4.47	3.90
90	4.81	5.25	4.56	3.86	3.83

H_2O_2 concentrations remaining in effect of H_2O_2 concentration on 2,4-DCP removal by Fenton’s experiment

Time (minute)	H_2O_2 Remaining ($mg\ L^{-1}$)				
	H_2O_2 1 mM	H_2O_2 2 mM	H_2O_2 3 mM	H_2O_2 4 mM	H_2O_2 5 mM
0	30.75	65.37	98.87	131.53	162.14
1	30.13	62.75	93.92	121.00	154.03
2	29.21	56.87	89.97	110.48	141.06
5	27.36	55.56	81.07	98.64	129.72
10	25.52	52.29	75.14	88.12	118.36
20	23.37	47.72	69.20	78.92	103.76
30	19.98	43.79	64.26	76.28	95.66
60	15.68	36.60	57.34	73.65	94.04
90	14.45	32.68	53.38	72.34	94.03

Effect of H_2O_2 feeding modes on 2,4-DCP removal by Fenton's experiment

Initial feeding mode

2,4-DCP concentrations remaining in effect of H_2O_2 initial feeding modes on 2,4-DCP removal by Fenton's experiment

Time (minute)	2,4-DCP Remaining (mM)				
	H_2O_2 1 mM	H_2O_2 2 mM	H_2O_2 3 mM	H_2O_2 4 mM	H_2O_2 5 mM
0	1.01	1.04	0.99	0.99	1.05
1	0.90	0.78	0.77	0.74	0.69
2	0.89	0.69	0.67	0.69	0.56
5	0.83	0.54	0.56	0.53	0.53
10	0.71	0.53	0.47	0.48	0.45
20	0.52	0.46	0.39	0.43	0.32
30	0.47	0.40	0.32	0.29	0.24
60	0.41	0.36	0.31	0.26	0.22
90	0.37	0.35	0.31	0.25	0.21

Step feeding mode

2,4-DCP concentrations remaining in effect of H_2O_2 step feeding modes on 2,4-DCP removal by Fenton's experiment

Time (minute)	2,4-DCP Remaining (mM)				
	H_2O_2 1 mM	H_2O_2 2 mM	H_2O_2 3 mM	H_2O_2 4 mM	H_2O_2 5 mM
0	0.99	1.06	0.97	1.04	0.99
1	0.92	0.73	0.70	0.66	0.64
2	0.89	0.64	0.62	0.6	0.57
5	0.84	0.51	0.49	0.45	0.42
10	0.70	0.48	0.45	0.41	0.39
20	0.50	0.44	0.38	0.36	0.30
30	0.46	0.41	0.33	0.27	0.25
60	0.40	0.37	0.31	0.27	0.21
90	0.37	0.35	0.30	0.26	0.20

Electro-Fenton Process Experiments

Effect of pH on 2,4-DCP removal by electro-Fenton's experiment

2,4-DCP concentrations remaining in effect of pH on 2,4-DCP removal by electro-Fenton's experiment

Time (minute)	2,4-DCP Remaining (mM)				
	pH 1.5	pH 2	pH 2.5	pH 3	pH 3.5
0	0.99	0.97	0.99	1.02	0.98
1	0.95	0.94	0.94	0.87	0.89
2	0.94	0.92	0.93	0.88	0.92
5	0.91	0.90	0.89	0.82	0.88
10	0.87	0.83	0.85	0.69	0.85
20	0.83	0.68	0.79	0.51	0.78
30	0.75	0.55	0.65	0.39	0.66
60	0.70	0.46	0.60	0.29	0.54
90	0.67	0.45	0.58	0.29	0.49

COD concentrations remaining in effect of pH on 2,4-DCP removal by electro-Fenton's experiment

Time (minute)	COD Remaining (mg L^{-1})				
	pH 1.5	pH 2	pH 2.5	pH 3	pH 3.5
0	225.21	227.62	228.16	232.34	227.66
1	211.69	218.51	219.03	220.72	216.27
2	202.69	211.68	209.90	209.10	209.44
5	198.18	202.58	205.34	197.48	198.06
10	191.42	195.75	198.49	188.19	191.23
20	189.17	186.64	193.93	178.90	188.95
30	186.92	182.09	189.37	171.93	184.40
60	184.67	179.81	182.52	167.28	177.57
90	184.67	175.26	180.24	164.96	175.29

TOC concentrations remaining in effect of pH on 2,4-DCP removal by electro-Fenton's experiment

Time (minute)	TOC Remaining (mg L^{-1})				
	pH 1.5	pH 2	pH 2.5	pH 3	pH 3.5
0	56.21	55.77	54.93	55.31	55.76
1	55.65	55.21	54.38	54.75	55.20
2	55.64	54.65	53.83	54.20	54.65
5	55.63	54.65	53.28	53.65	54.64
10	55.08	54.65	53.28	52.54	54.64
20	55.08	54.09	52.73	51.99	54.09
30	54.52	54.08	52.72	51.44	54.08
60	54.52	52.98	52.18	51.44	53.53
90	54.52	52.97	52.17	50.88	53.52

Fe^{2+} concentrations remaining in effect of pH on 2,4-DCP removal by electro-Fenton's experiment

Time (minute)	Fe^{2+} Remaining (mg L^{-1})				
	pH 1.5	pH 2	pH 2.5	pH 3	pH 3.5
0	5.55	5.58	5.52	5.51	5.61
1	5.22	5.18	5.02	5.07	5.22
2	5.16	5.07	4.97	4.90	5.21
5	5.10	5.24	5.18	5.12	5.27
10	5.21	5.30	5.29	5.23	5.33
20	5.21	5.36	5.29	5.29	5.32
30	5.27	5.35	5.35	5.40	5.27
60	5.33	5.30	5.29	5.40	5.27
90	5.28	5.30	5.30	5.34	5.21

H_2O_2 concentrations remaining in effect of pH on 2,4-DCP removal by electro-Fenton's experiment

Time (minute)	H_2O_2 Remaining (mg L^{-1})				
	pH 1.5	pH 2	pH 2.5	pH 3	pH 3.5
0	33.26	30.94	32.17	32.15	33.21
1	26.27	23.51	24.77	24.11	26.90
2	21.61	20.11	19.30	20.25	24.57
5	17.96	15.47	13.51	12.21	18.93
10	14.30	11.75	8.68	7.72	21.58
20	8.98	9.59	5.79	2.25	17.60
30	5.99	6.81	2.25	0.65	12.28
60	2.99	5.25	1.29	0.00	7.97
90	2.33	2.47	0.00	0.00	5.31

Effect of current density on 2,4-DCP removal by electro-Fenton's experiment

2,4-DCP concentrations remaining in effect of current density on 2,4-DCP removal by electro-Fenton's experiment

Time (minute)	2,4-DCP Remaining (mM)				
	Current Density 0.01 $mAcm^{-2}$	Current Density 0.05 $mAcm^{-2}$	Current Density 0.12 $mAcm^{-2}$	Current Density 0.25 $mAcm^{-2}$	Current Density 0.50 $mAcm^{-2}$
0	0.99	1.02	1.01	0.98	0.99
1	0.88	0.87	0.90	0.85	0.87
2	0.85	0.88	0.82	0.80	0.80
5	0.78	0.82	0.70	0.66	0.68
10	0.66	0.69	0.55	0.54	0.58
20	0.54	0.51	0.45	0.46	0.47
30	0.47	0.39	0.42	0.43	0.41
60	0.43	0.29	0.39	0.37	0.39
90	0.44	0.29	0.36	0.35	0.39

COD concentrations remaining in effect of current density on 2,4-DCP removal by electro-Fenton’s experiment

Time (minute)	COD Remaining (mg L^{-1})				
	Current Density 0.01 $mAcm^{-2}$	Current Density 0.05 $mAcm^{-2}$	Current Density 0.12 $mAcm^{-2}$	Current Density 0.25 $mAcm^{-2}$	Current Density 0.50 $mAcm^{-2}$
0	228.46	232.34	225.93	234.17	230.57
1	223.89	220.72	221.41	231.82	223.65
2	221.60	209.10	214.63	229.48	216.73
5	221.60	197.48	207.85	224.80	209.81
10	217.03	188.19	203.33	215.43	202.90
20	212.46	178.90	198.81	208.41	195.98
30	205.61	171.93	192.04	199.04	184.45
60	198.76	167.28	178.48	189.67	177.53
90	194.19	164.96	176.22	180.31	175.23

TOC concentrations remaining in effect of current density on 2,4-DCP removal by electro-Fenton's experiment

Time (minute)	TOC Remaining ($mg\ L^{-1}$)				
	Current Density 0.01 $mAcm^{-2}$	Current Density 0.05 $mAcm^{-2}$	Current Density 0.12 $mAcm^{-2}$	Current Density 0.25 $mAcm^{-2}$	Current Density 0.50 $mAcm^{-2}$
0	54.51	55.31	56.37	53.13	52.36
1	53.96	54.75	55.80	52.60	51.83
2	53.96	54.20	55.24	52.59	51.31
5	53.96	53.65	54.67	52.06	50.79
10	53.41	52.54	54.67	51.55	50.26
20	53.41	51.99	54.11	52.06	50.25
30	52.87	51.44	54.11	51.54	49.74
60	52.87	51.44	53.55	51.54	49.74
90	52.87	50.88	53.55	51.52	49.74

Fe^{2+} concentrations remaining in effect of current density on 2,4-DCP removal by electro-Fenton's experiment

Time (minute)	Fe^{2+} Remaining ($mg\ L^{-1}$)				
	Current Density 0.01 $mAcm^{-2}$	Current Density 0.05 $mAcm^{-2}$	Current Density 0.12 $mAcm^{-2}$	Current Density 0.25 $mAcm^{-2}$	Current Density 0.50 $mAcm^{-2}$
0	5.32	5.51	5.59	5.27	5.21
1	5.26	5.07	5.19	5.00	5.15
2	5.26	4.90	4.80	4.90	5.05
5	5.21	5.12	4.97	4.95	4.94
10	5.16	5.23	5.25	5.11	4.89
20	5.05	5.29	5.42	5.05	5.00
30	4.89	5.40	5.47	5.00	5.05
60	4.89	5.40	5.42	5.01	5.10
90	4.84	5.34	5.42	5.06	5.10

H_2O_2 concentrations remaining in effect of current density on 2,4-DCP removal by electro-Fenton's experiment

Time (minute)	H_2O_2 Remaining (mg L^{-1})				
	Current Density 0.01 $mAcm^{-2}$	Current Density 0.05 $mAcm^{-2}$	Current Density 0.12 $mAcm^{-2}$	Current Density 0.25 $mAcm^{-2}$	Current Density 0.50 $mAcm^{-2}$
0	33.47	32.15	30.42	32.11	33.54
1	26.10	24.11	21.90	23.44	24.81
2	19.74	20.25	20.68	18.30	23.14
5	15.06	12.21	13.68	14.77	14.75
10	10.37	7.72	5.77	8.99	10.06
20	8.36	2.25	3.04	8.02	4.02
30	6.36	0.65	1.82	4.49	1.01
60	4.35	0.00	0.60	1.60	0.00
90	3.34	0.00	0.00	0.32	0.00

Effect of H_2O_2/Fe^{2+} ratio on 2,4-DCP removal by electro-Fenton's experiment

2,4-DCP concentrations remaining in effect of H_2O_2/Fe^{2+} ratio on 2,4-DCP removal by electro-Fenton's experiment

Time (minute)	2,4-DCP Remaining (mM)				
	H_2O_2/Fe^{2+} ratio 10	H_2O_2/Fe^{2+} ratio 20	H_2O_2/Fe^{2+} ratio 30	H_2O_2/Fe^{2+} ratio 40	H_2O_2/Fe^{2+} ratio 50
0	1.02	0.99	0.99	1.03	0.97
1	0.87	0.88	0.74	0.84	0.84
2	0.88	0.86	0.64	0.76	0.74
5	0.82	0.71	0.42	0.57	0.53
10	0.69	0.56	0.20	0.37	0.30
20	0.51	0.34	0.04	0.15	0.09
30	0.39	0.26	0.02	0.06	0.03
60	0.29	0.19	0.00	0.01	0.00
90	0.29	0.19	0.00	0.01	0.00

Effect of H_2O_2 to Fe^{2+} ratios (H/F) on Removal efficiency and Relative oxidation performance ratio

H_2O_2 to Fe^{2+} ratios (H/F)	2,4-DCP Removal efficiency (%)	2,4-DCP Removal per 1 mM H_2O_2 (mM)	Relative oxidation performance ratio
10	71	0.28	1.13
20	81	0.21	1.28
30	100	0.18	1.32
40	99	0.16	1.28
50	100	0.12	1.23

COD concentrations remaining in effect of H_2O_2/Fe^{2+} ratio on 2,4-DCP removal by electro-Fenton’s experiment

Time (minute)	COD Remaining (mg L^{-1})				
	H_2O_2/Fe^{2+} ratio 10	H_2O_2/Fe^{2+} ratio 20	H_2O_2/Fe^{2+} ratio 30	H_2O_2/Fe^{2+} ratio 40	H_2O_2/Fe^{2+} ratio 50
0	232.34	228.76	227.45	229.57	228.33
1	220.72	217.32	213.80	213.50	203.21
2	209.10	212.74	204.70	202.02	194.08
5	197.48	203.59	195.60	192.83	180.38
10	188.19	189.87	186.50	181.36	173.53
20	178.90	185.29	170.58	169.88	157.54
30	171.93	176.14	154.66	156.10	148.41
60	167.28	169.28	138.74	137.74	132.43
90	164.96	153.26	134.19	133.15	127.86

TOC concentrations remaining in effect of H_2O_2/Fe^{2+} ratio on 2,4-DCP removal by electro-Fenton’s experiment

Time (minute)	TOC Remaining (mg L^{-1})				
	H_2O_2/Fe^{2+} ratio 10	H_2O_2/Fe^{2+} ratio 20	H_2O_2/Fe^{2+} ratio 30	H_2O_2/Fe^{2+} ratio 40	H_2O_2/Fe^{2+} ratio 50
0	55.31	53.74	52.02	52.97	53.12
1	54.75	51.59	48.51	52.44	52.05
2	54.20	50.51	46.33	51.38	50.99
5	53.65	49.44	45.74	50.32	48.87
10	52.54	47.82	45.05	48.73	47.27
20	51.99	47.29	44.21	47.14	46.74
30	51.44	46.75	44.03	47.14	46.74
60	51.44	47.82	43.82	46.61	46.21
90	50.88	50.50	43.71	46.61	46.74

Fe^{2+} concentrations remaining in effect of H_2O_2/Fe^{2+} ratio on 2,4-DCP removal by electro-Fenton's experiment

Time (minute)	Fe^{2+} Remaining ($mg\ L^{-1}$)				
	H_2O_2/Fe^{2+} ratio 10	H_2O_2/Fe^{2+} ratio 20	H_2O_2/Fe^{2+} ratio 30	H_2O_2/Fe^{2+} ratio 40	H_2O_2/Fe^{2+} ratio 50
0	5.51	5.43	5.38	5.31	5.25
1	5.07	5.05	5.21	5.09	4.93
2	4.90	4.88	5.11	4.88	4.83
5	5.12	4.99	5.00	4.93	4.88
10	5.23	5.10	4.84	5.04	4.88
20	5.29	5.21	4.95	5.09	4.88
30	5.40	5.21	5.05	5.20	4.93
60	5.40	5.10	5.16	5.04	5.04
90	5.34	5.10	5.16	5.04	4.98

H_2O_2 concentrations remaining in effect of H_2O_2/Fe^{2+} ratio on 2,4-DCP removal by electro-Fenton's experiment

Time (minute)	H_2O_2 Remaining ($mg\ L^{-1}$)				
	H_2O_2/Fe^{2+} ratio 10	H_2O_2/Fe^{2+} ratio 20	H_2O_2/Fe^{2+} ratio 30	H_2O_2/Fe^{2+} ratio 40	H_2O_2/Fe^{2+} ratio 50
0	32.15	62.16	96.79	125.37	164.82
1	24.11	34.18	47.42	58.92	72.52
2	20.25	28.59	34.84	38.86	54.39
5	12.21	18.65	21.29	25.07	42.85
10	7.72	11.18	12.58	18.80	19.77
20	2.25	5.59	4.83	5.01	4.94
30	0.65	3.11	0.00	0.00	1.64
60	0.00	1.86	0.00	0.00	0.00
90	0.00	0.00	0.00	0.00	0.00

Effect of H_2O_2 feeding modes on 2,4-DCP removal by electro-Fenton's experiment

At current density 0.05 mA cm^{-2}

2,4-DCP concentrations remaining in effect of H_2O_2 feeding modes on 2,4-DCP removal by electro-Fenton's experiment at current density 0.05 mA cm^{-2}

Time (minute)	2,4-DCP Remaining (mM)			
	H_2O_2 2 mM		H_2O_2 3 mM	
	H_2O_2 Initial Feeding	H_2O_2 Step Feeding	H_2O_2 Initial Feeding	H_2O_2 Step Feeding
0	0.99	0.98	0.99	0.98
1	0.88	0.89	0.74	0.88
2	0.86	0.89	0.64	0.85
5	0.71	0.81	0.42	0.74
10	0.56	0.65	0.20	0.53
20	0.34	0.41	0.04	0.26
30	0.26	0.26	0.02	0.11
60	0.19	0.16	0.00	0.04
90	0.19	0.16	0.00	0.03

At current density 0.12 mA cm^{-2}

2,4-DCP concentrations remaining in effect of H_2O_2 feeding modes on 2,4-DCP removal by electro-Fenton’s experiment at current density 0.12 mA cm^{-2}

Time (minute)	2,4-DCP Remaining (mM)			
	H_2O_2 2 mM		H_2O_2 3 mM	
	H_2O_2 Initial Feeding	H_2O_2 Step Feeding	H_2O_2 Initial Feeding	H_2O_2 Step Feeding
0	1.02	0.98	0.99	0.99
1	0.84	0.90	0.93	0.82
2	0.81	0.72	0.85	0.76
5	0.62	0.81	0.72	0.74
10	0.44	0.51	0.50	0.52
20	0.31	0.41	0.30	0.22
30	0.22	0.27	0.19	0.10
60	0.17	0.14	0.08	0.02
90	0.16	0.13	0.08	0.02

TOC concentrations remaining in effect of H_2O_2 feeding modes on 2,4-DCP removal by electro-Fenton's experiment at current density 0.12 mA cm^{-2}

Time (minute)	TOC Remaining (mg L^{-1})			
	H_2O_2 2 mM		H_2O_2 3 mM	
	H_2O_2 Initial Feeding	H_2O_2 Step Feeding	H_2O_2 Initial Feeding	H_2O_2 Step Feeding
0	53.15	56.21	52.43	54.21
1	51.02	55.08	49.80	53.12
2	49.96	54.52	47.71	51.49
5	48.89	52.83	47.18	48.78
10	47.30	50.58	46.13	47.16
20	46.77	48.34	44.56	46.07
30	46.24	47.21	40.37	43.36
60	47.30	44.96	45.61	41.74
90	49.96	44.96	47.18	40.65

2,4,4'-trichloro-2'-hydroxydiphenyl ether ($C_{12}H_7O_2Cl_3$) (Triclosan) Experiments

Control Experiments

Electrolysis control experiment

Time (minute)	Triclosan Remaining (mM)				
	Current Density 0.01 mA cm^{-2}	Current Density 0.15 mA cm^{-2}	Current Density 0.24 mA cm^{-2}	Current Density 0.35 mA cm^{-2}	Current Density 0.50 mA cm^{-2}
0	0.99	0.99	1.01	1.02	1.02
1	0.99	0.99	0.99	0.99	0.99
2	0.99	0.99	0.99	0.98	0.98
5	0.99	0.98	0.98	0.98	0.98
10	0.98	0.99	0.98	0.97	0.97
20	0.98	0.98	0.97	0.97	0.97
30	0.98	0.98	0.98	0.96	0.97
60	0.98	0.97	0.97	0.96	0.96
90	0.98	0.97	0.96	0.96	0.96

Various process control experiments

Time (minute)	Triclosan Remaining (mM)			
	Current Density 0.15 mA cm^{-2}	Current Density 0.24 mA cm^{-2}	Fenton Process (No Current)	Electro-Fenton Process (Current Density 0.15 mA cm^{-2})
0	0.99	1.01	0.99	0.99
1	0.99	0.99	0.87	0.85
2	0.99	0.99	0.81	0.79
5	0.98	0.98	0.72	0.65
10	0.99	0.98	0.63	0.59
20	0.98	0.97	0.57	0.54
30	0.98	0.98	0.53	0.48
60	0.97	0.97	0.49	0.42
90	0.97	0.96	0.45	0.39

Fenton Process Experiments

Effect of pH on Triclosan removal by Fenton’s experiment

Triclosan concentrations remaining in effect of pH on Triclosan removal by Fenton’s experiment

Time (minute)	Triclosan Remaining (mM)		
	pH 2	pH 3	pH 3.5
0	1.02	0.99	0.99
1	0.85	0.80	0.87
2	0.83	0.77	0.85
5	0.69	0.66	0.84
10	0.61	0.57	0.81
20	0.54	0.52	0.77
30	0.48	0.49	0.65
60	0.45	0.44	0.56
90	0.44	0.42	0.55

COD concentrations remaining in effect of pH on Triclosan removal by Fenton's experiment

Time (minute)	COD Remaining ($mg\ L^{-1}$)		
	pH 2	pH 3	pH 3.5
0	388.74	395.17	391.33
1	365.41	375.41	375.67
2	349.86	351.70	352.19
5	338.20	331.94	340.45
10	326.54	312.18	320.89
20	310.99	296.37	309.15
30	299.32	280.57	305.23
60	283.78	268.71	301.32
90	276.00	264.76	301.32

TOC concentrations remaining in effect of pH on Triclosan removal by Fenton's experiment

Time (minute)	TOC Remaining ($mg\ L^{-1}$)		
	pH 2	pH 3	pH 3.5
0	139.56	138.24	135.08
1	138.16	136.85	133.73
2	138.15	136.85	133.72
5	138.14	134.09	133.70
10	136.77	132.71	133.71
20	136.75	131.32	132.37
30	133.97	132.70	131.03
60	135.37	132.69	132.37
90	136.77	129.94	132.35

Fe^{2+} concentrations remaining in effect of pH on Triclosan removal by Fenton's experiment

Time (minute)	Fe^{2+} Remaining ($mg\ L^{-1}$)		
	pH 2	pH 3	pH 3.5
0	5.47	5.53	5.56
1	3.88	3.37	4.00
2	3.44	3.26	3.33
5	3.34	3.15	3.44
10	3.01	2.93	3.28
20	2.84	3.04	3.39
30	2.41	2.87	3.16
60	2.07	2.59	3.15
90	1.91	2.10	2.89

H_2O_2 concentrations remaining in effect of pH on Triclosan removal by Fenton's experiment

Time (minute)	H_2O_2 Remaining ($mg\ L^{-1}$)		
	pH 2	pH 3	pH 3.5
0	31.18	33.21	30.77
1	28.37	32.21	29.53
2	27.43	29.88	28.30
5	26.50	28.22	27.38
10	25.87	27.23	26.15
20	22.13	24.57	25.23
30	21.20	22.25	22.76
60	17.46	17.60	20.30
90	17.15	16.60	18.76

Effect of Fe^{2+} concentration on Triclosan removal by Fenton's experiment

Triclosan concentrations remaining in effect of Fe^{2+} concentration on Triclosan removal by Fenton's experiment

Time (minute)	Triclosan Remaining (mM)				
	Fe^{2+} 0.10 mM	Fe^{2+} 0.20 mM	Fe^{2+} 0.30 mM	Fe^{2+} 0.40 mM	Fe^{2+} 0.50 mM
0	0.99	1.01	0.99	0.99	0.98
1	0.80	0.85	0.84	0.85	0.86
2	0.77	0.81	0.82	0.78	0.80
5	0.66	0.73	0.76	0.73	0.74
10	0.57	0.64	0.61	0.66	0.66
20	0.52	0.57	0.56	0.60	0.58
30	0.49	0.48	0.48	0.54	0.54
60	0.44	0.44	0.43	0.48	0.51
90	0.42	0.41	0.43	0.45	0.48

COD concentrations remaining in effect of Fe^{2+} concentration on Triclosan removal by Fenton's experiment

Time (minute)	COD Remaining (mg L^{-1})				
	Fe^{2+} 0.10 mM	Fe^{2+} 0.20 mM	Fe^{2+} 0.30 mM	Fe^{2+} 0.40 mM	Fe^{2+} 0.50 mM
0	395.17	403.36	397.42	392.64	395.86
1	375.41	391.25	389.47	380.86	376.06
2	351.70	375.12	357.67	365.15	364.19
5	331.94	363.24	333.83	341.59	348.35
10	312.18	350.92	321.91	325.89	336.48
20	296.37	346.88	317.93	310.18	324.60
30	280.57	330.75	298.06	314.11	304.81
60	268.71	310.58	278.19	282.70	277.10
90	264.76	298.48	270.24	270.92	277.10

TOC concentrations remaining in effect of Fe^{2+} concentration on Triclosan removal by Fenton's experiment

Time (minute)	TOC Remaining (mg L^{-1})				
	Fe^{2+} 0.10 mM	Fe^{2+} 0.20 mM	Fe^{2+} 0.30 mM	Fe^{2+} 0.40 mM	Fe^{2+} 0.50 mM
0	138.24	135.12	141.64	137.26	139.41
1	136.85	133.76	140.22	135.88	138.01
2	136.85	132.41	140.15	134.51	135.22
5	134.09	131.06	138.80	133.14	135.22
10	132.71	131.03	138.75	131.76	132.43
20	131.32	129.71	137.39	130.39	132.40
30	132.70	129.63	135.97	130.35	131.04
60	132.69	129.65	134.55	129.02	129.65
90	129.94	128.36	133.14	127.65	129.65

Fe^{2+} concentrations remaining in effect of Fe^{2+} concentration on Triclosan removal by Fenton's experiment

Time (minute)	Fe^{2+} Remaining (mg L^{-1})				
	Fe^{2+} 0.10 mM	Fe^{2+} 0.20 mM	Fe^{2+} 0.30 mM	Fe^{2+} 0.40 mM	Fe^{2+} 0.50 mM
0	5.53	9.98	15.80	21.34	27.12
1	3.37	7.38	12.32	16.85	22.23
2	3.26	6.86	11.37	16.21	20.34
5	3.15	6.18	10.11	14.72	18.17
10	2.93	5.78	9.63	13.65	16.54
20	3.04	5.28	9.16	11.95	15.45
30	2.87	4.69	8.37	11.31	14.91
60	2.59	4.09	7.42	10.45	14.10
90	2.10	3.89	6.63	10.02	13.83

H_2O_2 concentrations remaining in effect of Fe^{2+} concentration on Triclosan removal by Fenton's experiment

Time (minute)	H_2O_2 Remaining (mg L^{-1})				
	Fe^{2+} 0.10 mM	Fe^{2+} 0.20 mM	Fe^{2+} 0.30 mM	Fe^{2+} 0.40 mM	Fe^{2+} 0.50 mM
0	33.21	33.95	32.96	33.57	34.03
1	32.21	31.57	28.34	28.53	27.56
2	29.88	27.49	23.73	28.19	26.54
5	28.22	25.12	22.74	25.51	25.52
10	27.23	21.38	21.09	21.82	24.16
20	24.57	18.67	18.78	20.14	21.77
30	22.25	16.97	17.46	19.13	21.43
60	17.60	15.95	16.48	17.45	19.39
90	16.60	15.27	14.50	16.11	17.35

Effect of H_2O_2 concentration on Triclosan removal by Fenton's experiment

Triclosan concentrations remaining in effect of H_2O_2 concentration on Triclosan removal by Fenton's experiment

Time (minute)	Triclosan Remaining (mM)				
	H_2O_2 1 mM	H_2O_2 2 mM	H_2O_2 3 mM	H_2O_2 4 mM	H_2O_2 5 mM
0	0.99	1.04	0.98	0.99	1.02
1	0.80	0.77	0.76	0.74	0.70
2	0.77	0.68	0.68	0.66	0.64
5	0.66	0.55	0.54	0.54	0.55
10	0.57	0.52	0.48	0.47	0.45
20	0.52	0.45	0.41	0.42	0.40
30	0.49	0.40	0.34	0.32	0.31
60	0.44	0.37	0.32	0.28	0.23
90	0.42	0.35	0.31	0.28	0.21

COD concentrations remaining in effect of H_2O_2 concentration on Triclosan removal by Fenton's experiment

Time (minute)	COD Remaining (mg L^{-1})				
	H_2O_2 1 mM	H_2O_2 2 mM	H_2O_2 3 mM	H_2O_2 4 mM	H_2O_2 5 mM
0	395.17	402.65	399.54	397.88	403.46
1	375.41	374.46	375.56	354.11	346.97
2	351.70	354.33	343.60	334.21	318.73
5	331.94	330.17	319.63	302.38	290.49
10	312.18	318.09	303.65	270.55	258.21
20	296.37	306.01	291.66	250.66	234.00
30	280.57	281.85	263.69	234.74	225.93
60	268.71	277.82	251.71	226.79	221.90
90	264.76	265.74	251.69	226.73	221.90

TOC concentrations remaining in effect of H_2O_2 concentration on Triclosan removal by Fenton's experiment

Time (minute)	TOC Remaining (mg L^{-1})				
	H_2O_2 1 mM	H_2O_2 2 mM	H_2O_2 3 mM	H_2O_2 4 mM	H_2O_2 5 mM
0	138.24	139.34	140.43	139.56	141.11
1	136.85	137.95	139.02	138.16	139.69
2	136.85	137.92	137.62	136.76	136.87
5	134.09	136.55	137.59	135.37	135.46
10	132.71	136.49	136.21	133.97	134.05
20	131.32	135.15	134.81	132.58	132.65
30	132.70	133.76	134.78	131.18	132.61
60	132.69	132.37	133.40	131.12	132.60
90	129.94	130.97	133.38	131.09	131.23

Fe^{2+} concentrations remaining in effect of H_2O_2 concentration on Triclosan removal by Fenton's experiment

Time (minute)	Fe^{2+} Remaining (mg L^{-1})				
	H_2O_2 1 mM	H_2O_2 2 mM	H_2O_2 3 mM	H_2O_2 4 mM	H_2O_2 5 mM
0	5.53	5.43	5.51	5.47	5.44
1	3.37	3.36	3.47	3.33	3.26
2	3.26	3.14	2.97	3.00	2.93
5	3.15	2.71	2.64	2.51	2.55
10	2.93	2.38	2.31	2.40	2.23
20	3.04	2.49	1.98	2.24	1.95
30	2.87	2.11	1.81	1.91	1.63
60	2.59	2.06	1.76	1.75	1.46
90	2.10	2.00	1.76	1.58	1.41

H_2O_2 concentrations remaining in effect of H_2O_2 concentration on Triclosan removal by Fenton's experiment

Time (minute)	H_2O_2 Remaining (mg L^{-1})				
	H_2O_2 1 mM	H_2O_2 2 mM	H_2O_2 3 mM	H_2O_2 4 mM	H_2O_2 5 mM
0	33.21	64.76	97.88	129.83	167.64
1	32.21	62.81	92.00	118.14	159.25
2	29.88	56.98	89.07	112.95	140.81
5	28.22	54.39	81.24	102.56	127.40
10	27.23	52.45	77.32	92.17	115.67
20	24.57	46.62	72.43	84.38	108.95
30	22.25	44.03	65.57	76.59	95.55
60	17.60	36.91	59.70	71.40	90.52
90	16.60	33.02	54.81	68.80	90.50

Effect of H_2O_2 feeding modes on Triclosan removal by Fenton's experiment

Initial feeding mode

Triclosan concentrations remaining in effect of H_2O_2 initial feeding modes on Triclosan removal by Fenton's experiment

Time (minute)	Triclosan Remaining (mM)				
	H_2O_2 1 mM	H_2O_2 2 mM	H_2O_2 3 mM	H_2O_2 4 mM	H_2O_2 5 mM
0	0.99	1.04	0.98	0.99	1.02
1	0.80	0.77	0.76	0.74	0.70
2	0.77	0.68	0.68	0.66	0.64
5	0.66	0.55	0.54	0.54	0.55
10	0.57	0.52	0.48	0.47	0.45
20	0.52	0.45	0.41	0.42	0.40
30	0.49	0.40	0.34	0.32	0.31
60	0.44	0.37	0.32	0.28	0.23
90	0.42	0.35	0.31	0.28	0.21

Step feeding mode

Triclosan concentrations remaining in effect of H_2O_2 step feeding modes on Triclosan removal by Fenton's experiment

Time (minute)	Triclosan Remaining (mM)				
	H_2O_2 1 mM	H_2O_2 2 mM	H_2O_2 3 mM	H_2O_2 4 mM	H_2O_2 5 mM
0	0.99	1.01	0.98	1.01	0.99
1	0.82	0.79	0.76	0.71	0.72
2	0.78	0.71	0.70	0.65	0.64
5	0.69	0.54	0.53	0.52	0.57
10	0.57	0.50	0.46	0.44	0.49
20	0.53	0.42	0.40	0.37	0.36
30	0.48	0.39	0.35	0.30	0.30
60	0.42	0.36	0.30	0.28	0.21
90	0.42	0.34	0.30	0.27	0.20

Electro-Fenton Process Experiments

Effect of pH on Triclosan removal by electro-Fenton's experiment

Triclosan concentrations remaining in effect of pH on Triclosan removal by electro-Fenton's experiment

Time (minute)	Triclosan Remaining (mM)				
	pH 1.5	pH 2	pH 2.5	pH 3	pH 3.5
0	1.03	0.98	0.99	0.99	0.98
1	0.95	0.86	0.87	0.85	0.88
2	0.94	0.80	0.82	0.79	0.87
5	0.91	0.64	0.68	0.65	0.88
10	0.87	0.62	0.60	0.59	0.83
20	0.83	0.54	0.56	0.54	0.78
30	0.75	0.50	0.52	0.48	0.66
60	0.70	0.45	0.46	0.42	0.57
90	0.67	0.41	0.43	0.39	0.51

COD concentrations remaining in effect of pH on Triclosan removal by electro-Fenton's experiment

Time (minute)	COD Remaining (mg L^{-1})				
	pH 1.5	pH 2	pH 2.5	pH 3	pH 3.5
0	402.47	405.33	397.86	399.35	399.47
1	390.39	374.29	385.92	371.39	391.48
2	374.29	362.22	373.98	347.43	375.50
5	358.19	338.07	346.13	335.45	355.52
10	338.07	326.00	326.24	315.48	339.54
20	305.87	309.90	298.39	291.52	323.57
30	285.75	293.80	278.50	267.56	307.59
60	265.63	273.67	266.56	255.58	307.50
90	269.65	273.62	262.58	247.59	291.61

TOC concentrations remaining in effect of pH on Triclosan removal by electro-Fenton's experiment

Time (minute)	TOC Remaining (mg L^{-1})				
	pH 1.5	pH 2	pH 2.5	pH 3	pH 3.5
0	140.48	138.62	140.85	139.22	139.21
1	139.07	137.23	139.44	137.82	137.81
2	138.98	137.18	138.03	136.43	137.78
5	137.67	137.16	137.96	135.04	137.75
10	137.62	135.84	137.95	133.65	137.75
20	137.59	135.79	136.62	133.65	137.73
30	136.26	135.75	136.57	132.26	136.42
60	136.22	134.46	135.21	132.25	136.35
90	134.86	134.41	135.16	132.24	136.33

Fe^{2+} concentrations remaining in effect of pH on Triclosan removal by electro-Fenton's experiment

Time (minute)	Fe^{2+} Remaining ($mg\ L^{-1}$)				
	pH 1.5	pH 2	pH 2.5	pH 3	pH 3.5
0	5.58	5.52	5.51	5.47	5.37
1	5.35	5.35	5.34	5.14	5.15
2	5.30	5.31	5.12	5.30	4.94
5	4.91	5.24	5.28	5.08	4.29
10	5.07	4.80	5.23	4.92	4.24
20	5.24	4.91	5.17	5.19	4.51
30	4.96	5.07	4.73	5.03	4.29
60	4.74	4.80	4.40	4.81	4.14
90	4.57	4.69	4.33	4.75	4.09

H_2O_2 concentrations remaining in effect of pH on Triclosan removal by electro-Fenton's experiment

Time (minute)	H_2O_2 Remaining ($mg\ L^{-1}$)				
	pH 1.5	pH 2	pH 2.5	pH 3	pH 3.5
0	31.98	32.56	33.42	32.34	33.27
1	30.38	29.30	31.41	28.78	31.93
2	29.42	26.37	28.74	24.90	28.27
5	27.82	22.14	24.06	17.46	25.95
10	23.34	14.97	15.03	9.05	21.95
20	17.26	8.46	9.02	2.91	16.30
30	11.51	5.53	4.67	0.00	11.31
60	4.79	1.30	0.00	0.00	5.32
90	0.31	0.00	0.00	0.00	0.99

Effect of current density on Triclosan removal by electro-Fenton’s experiment

Triclosan concentrations remaining in effect of current density on Triclosan removal by electro-Fenton’s experiment

Time (minute)	Triclosan Remaining (mM)				
	Current Density 0.01 mAcm^{-2}	Current Density 0.15 mAcm^{-2}	Current Density 0.24 mAcm^{-2}	Current Density 0.35 mAcm^{-2}	Current Density 0.50 mAcm^{-2}
0	0.99	0.99	0.98	1.02	0.99
1	0.93	0.85	0.88	0.84	0.85
2	0.87	0.79	0.85	0.8	0.82
5	0.77	0.65	0.70	0.64	0.69
10	0.69	0.59	0.62	0.57	0.60
20	0.60	0.54	0.54	0.52	0.55
30	0.56	0.48	0.47	0.44	0.48
60	0.50	0.42	0.43	0.40	0.43
90	0.47	0.39	0.41	0.38	0.41

COD concentrations remaining in effect of current density on Triclosan removal by electro-Fenton's experiment

Time (minute)	COD Remaining ($mg\ L^{-1}$)				
	Current Density 0.01 $mAcm^{-2}$	Current Density 0.15 $mAcm^{-2}$	Current Density 0.24 $mAcm^{-2}$	Current Density 0.35 $mAcm^{-2}$	Current Density 0.50 $mAcm^{-2}$
0	398.85	399.35	403.42	401.67	402.86
1	390.87	371.39	395.35	397.65	390.77
2	386.88	347.43	383.24	393.63	378.68
5	386.82	335.45	371.14	385.60	366.60
10	378.90	315.48	363.07	369.53	354.51
20	370.93	291.52	355.00	357.48	342.43
30	358.96	267.56	342.90	341.41	322.28
60	346.99	255.58	318.70	325.35	310.20
90	339.02	247.59	314.66	309.28	290.05

TOC concentrations remaining in effect of current density on Triclosan removal by electro-Fenton’s experiment

Time (minute)	TOC Remaining (mg L^{-1})				
	Current Density 0.01 $mAcm^{-2}$	Current Density 0.15 $mAcm^{-2}$	Current Density 0.24 $mAcm^{-2}$	Current Density 0.35 $mAcm^{-2}$	Current Density 0.50 $mAcm^{-2}$
0	139.77	139.22	138.86	140.24	141.12
1	138.37	137.82	136.08	138.83	138.29
2	138.29	136.43	135.97	138.77	139.50
5	138.27	135.04	134.69	137.43	136.88
10	138.27	133.65	134.41	137.38	136.79
20	136.97	133.65	133.30	137.35	135.45
30	136.93	132.26	131.92	136.03	134.06
60	136.87	132.25	131.90	135.97	133.92
90	136.85	132.24	131.87	135.95	132.65

Fe^{2+} concentrations remaining in effect of current density on Triclosan removal by electro-Fenton's experiment

Time (minute)	Fe^{2+} Remaining ($mg\ L^{-1}$)				
	Current Density 0.01 $mAcm^{-2}$	Current Density 0.15 $mAcm^{-2}$	Current Density 0.24 $mAcm^{-2}$	Current Density 0.35 $mAcm^{-2}$	Current Density 0.50 $mAcm^{-2}$
0	5.41	5.47	5.55	5.59	5.64
1	4.92	5.14	5.05	5.25	5.47
2	4.65	5.30	5.32	5.14	4.96
5	4.76	5.08	4.77	5.42	5.18
10	5.08	4.92	5.27	5.36	5.41
20	4.54	5.19	5.16	5.31	5.30
30	3.89	5.03	4.82	5.03	5.01
60	3.62	4.81	4.99	5.19	4.79
90	3.40	4.75	4.93	5.08	4.85

H_2O_2 concentrations remaining in effect of current density on Triclosan removal by electro-Fenton’s experiment

Time (minute)	H_2O_2 Remaining ($mg\ L^{-1}$)				
	Current Density 0.01 $mAcm^{-2}$	Current Density 0.15 $mAcm^{-2}$	Current Density 0.24 $mAcm^{-2}$	Current Density 0.35 $mAcm^{-2}$	Current Density 0.50 $mAcm^{-2}$
0	33.75	32.34	34.03	32.87	33.54
1	29.36	28.78	31.64	28.92	28.17
2	25.65	24.90	25.18	22.35	24.14
5	19.57	17.46	17.01	13.47	17.10
10	16.53	9.05	8.84	6.57	11.73
20	11.47	2.91	6.12	6.90	11.40
30	10.46	0.00	1.70	1.31	6.03
60	7.42	0.00	0.68	0.00	4.02
90	7.37	0.00	0.00	0.00	0.67

Effect of H_2O_2/Fe^{2+} ratio on Triclosan removal by electro-Fenton's experiment

Triclosan concentrations remaining in effect of H_2O_2/Fe^{2+} ratio on Triclosan removal by electro-Fenton's experiment

Time (minute)	Triclosan Remaining (mM)				
	H_2O_2/Fe^{2+} ratio 10	H_2O_2/Fe^{2+} ratio 20	H_2O_2/Fe^{2+} ratio 30	H_2O_2/Fe^{2+} ratio 40	H_2O_2/Fe^{2+} ratio 50
0	0.99	1.02	0.99	0.99	1.01
1	0.85	0.89	0.85	0.8	0.82
2	0.79	0.86	0.77	0.75	0.70
5	0.65	0.66	0.63	0.54	0.54
10	0.59	0.54	0.48	0.33	0.31
20	0.54	0.44	0.35	0.17	0.19
30	0.48	0.37	0.29	0.04	0.10
60	0.42	0.29	0.19	0.00	0.03
90	0.39	0.27	0.15	0.00	0.02

Effect of H_2O_2 to Fe^{2+} ratios (H/F) on Removal efficiency and Relative oxidation performance ratio

H_2O_2 to Fe^{2+} ratios (H/F)	Triclosan Removal efficiency (%)	Triclosan Removal per 1 mM H_2O_2 (mM)	Relative oxidation performance ratio
10	67	0.23	1.06
20	73	0.17	1.16
30	85	0.14	1.28
40	100	0.10	1.30
50	98	0.07	1.21

COD concentrations remaining in effect of H_2O_2/Fe^{2+} ratio on Triclosan removal by electro-Fenton's experiment

Time (minute)	COD Remaining (mg L^{-1})				
	H_2O_2/Fe^{2+} ratio 10	H_2O_2/Fe^{2+} ratio 20	H_2O_2/Fe^{2+} ratio 30	H_2O_2/Fe^{2+} ratio 40	H_2O_2/Fe^{2+} ratio 50
0	399.35	403.15	402.41	405.68	401.32
1	371.39	366.86	366.19	365.11	361.18
2	347.43	338.64	329.97	340.77	329.08
5	335.45	322.52	317.90	308.31	296.97
10	315.48	306.39	297.78	283.97	280.92
20	291.52	282.20	273.63	263.69	264.87
30	267.56	262.04	257.54	247.46	240.79
60	255.58	245.92	237.42	215.01	216.71
90	247.59	241.89	225.34	190.66	196.64

TOC concentrations remaining in effect of H_2O_2/Fe^{2+} ratio on Triclosan removal by electro-Fenton's experiment

Time (minute)	TOC Remaining (mg L^{-1})				
	H_2O_2/Fe^{2+} ratio 10	H_2O_2/Fe^{2+} ratio 20	H_2O_2/Fe^{2+} ratio 30	H_2O_2/Fe^{2+} ratio 40	H_2O_2/Fe^{2+} ratio 50
0	139.22	140.26	138.24	138.93	138.76
1	137.82	137.45	136.85	137.73	131.82
2	136.43	136.05	134.09	136.33	131.74
5	135.04	133.24	131.32	135.58	131.70
10	133.65	133.18	130.96	135.07	130.43
20	133.65	131.84	128.56	134.65	126.27
30	132.26	131.72	127.73	134.04	124.88
60	132.25	130.44	124.41	132.27	119.33
90	132.24	130.02	123.03	131.75	118.92

Fe^{2+} concentrations remaining in effect of H_2O_2/Fe^{2+} ratio on Triclosan removal by electro-Fenton's experiment

Time (minute)	Fe^{2+} Remaining (mg L^{-1})				
	H_2O_2/Fe^{2+} ratio 10	H_2O_2/Fe^{2+} ratio 20	H_2O_2/Fe^{2+} ratio 30	H_2O_2/Fe^{2+} ratio 40	H_2O_2/Fe^{2+} ratio 50
0	5.47	5.49	5.51	5.52	5.48
1	5.14	5.05	5.06	4.85	4.98
2	5.30	5.21	5.12	4.69	4.87
5	5.08	5.27	5.23	4.52	4.98
10	4.92	5.05	4.95	4.41	5.04
20	5.19	4.94	4.90	4.74	4.76
30	5.03	4.83	4.73	4.63	4.65
60	4.81	4.66	4.57	4.47	4.71
90	4.75	4.57	4.51	4.41	4.63

H_2O_2 concentrations remaining in effect of H_2O_2/Fe^{2+} ratio on Triclosan removal by electro-Fenton's experiment

Time (minute)	H_2O_2 Remaining (mg L^{-1})				
	H_2O_2/Fe^{2+} ratio 10	H_2O_2/Fe^{2+} ratio 20	H_2O_2/Fe^{2+} ratio 30	H_2O_2/Fe^{2+} ratio 40	H_2O_2/Fe^{2+} ratio 50
0	32.34	59.97	97.45	127.85	164.21
1	28.78	47.97	75.03	89.49	108.37
2	24.90	40.77	61.39	69.03	82.10
5	17.46	31.78	47.75	54.97	62.39
10	9.05	11.99	20.46	14.06	16.42
20	2.91	0.59	1.95	0.00	0.00
30	0.00	0.00	0.00	0.00	0.00
60	0.00	0.00	0.00	0.00	0.00
90	0.00	0.00	0.00	0.00	0.00

Effect of H_2O_2 feeding modes on Triclosan removal by electro-Fenton's experiment

At current density 0.15 mA cm^{-2}

Triclosan concentrations remaining in effect of H_2O_2 feeding modes on Triclosan removal by electro-Fenton's experiment at current density 0.15 mA cm^{-2}

Time (minute)	Triclosan Remaining (mM)			
	H_2O_2 3 mM		H_2O_2 4 mM	
	H_2O_2 Initial Feeding	H_2O_2 Step Feeding	H_2O_2 Initial Feeding	H_2O_2 Step Feeding
0	0.99	0.98	0.99	1.02
1	0.85	0.86	0.8	0.78
2	0.77	0.75	0.75	0.74
5	0.63	0.61	0.54	0.55
10	0.48	0.46	0.33	0.32
20	0.35	0.35	0.17	0.16
30	0.29	0.28	0.04	0.05
60	0.19	0.17	0.00	0.00
90	0.15	0.16	0.00	0.00

At current density 0.24 mA cm^{-2}

Triclosan concentrations remaining in effect of H_2O_2 feeding modes on Triclosan removal by electro-Fenton's experiment at current density 0.24 mA cm^{-2}

Time (minute)	Triclosan Remaining (mM)			
	H_2O_2 3 mM		H_2O_2 4 mM	
	H_2O_2 Initial Feeding	H_2O_2 Step Feeding	H_2O_2 Initial Feeding	H_2O_2 Step Feeding
0	1.01	0.99	0.99	0.98
1	0.82	0.79	0.81	0.80
2	0.75	0.70	0.73	0.69
5	0.61	0.60	0.50	0.44
10	0.48	0.45	0.29	0.27
20	0.33	0.30	0.15	0.12
30	0.28	0.25	0.02	0.00
60	0.17	0.12	0.00	0.00
90	0.16	0.09	0.00	0.00

TOC concentrations remaining in effect of H_2O_2 feeding modes on Triclosan removal by electro-Fenton’s experiment at current density 0.24 mA cm^{-2}

Time (minute)	TOC Remaining ($mg\ L^{-1}$)			
	H_2O_2 3 mM		H_2O_2 4 mM	
	H_2O_2 Initial Feeding	H_2O_2 Step Feeding	H_2O_2 Initial Feeding	H_2O_2 Step Feeding
0	138.06	139.17	138.25	139.43
1	136.67	137.77	136.86	135.24
2	136.67	134.99	135.48	131.06
5	133.91	132.21	132.72	132.45
10	127.01	128.03	128.57	122.66
20	121.49	121.07	121.66	119.90
30	120.11	115.51	117.51	110.14
60	124.23	111.33	122.94	107.36
90	122.87	108.55	124.40	101.78

Kinetic of electro-Fenton experiment

Kinetic of 2,4-DCP removal by electro-Fenton process

Effect of pH on 2,4-DCP kinetic removal by electro-Fenton's experiment

2,4-DCP concentration remaining in effect of pH on kinetic of 2,4-DCP removal by electro-Fenton's experiment

Time (minute)	2,4-DCP Concentration (mM)		
	pH 2	pH 3	pH 3.5
0	0.99	0.98	0.99
1	0.95	0.87	0.89
2	0.92	0.88	0.90
5	0.89	0.82	0.88
10	0.83	0.70	0.85
20	0.65	0.53	0.77
30	0.55	0.41	0.64
60	0.45	0.28	0.51
90	0.41	0.25	0.47

Fe^{2+} concentration remaining in effect of pH on kinetic of 2,4-DCP removal by electro-Fenton's experiment

Time (minute)	Fe^{2+} Remaining (C/C_0)		
	pH 2	pH 3	pH 3.5
0	1	1	1
1	0.97	1.02	1.01
2	1.02	1.05	0.99
5	1.05	1.11	1.05
10	1.01	1.32	1.09
20	1.16	2.17	1.33

Effect of current density on 2,4-DCP kinetic removal by electro-Fenton's experiment

2,4-DCP concentration remaining in effect of current density on kinetic of 2,4-DCP removal by electro-Fenton's experiment

Time (minute)	2,4-DCP Concentration (mM)				
	Current Density 0.01 $mAcm^{-2}$	Current Density 0.05 $mAcm^{-2}$	Current Density 0.10 $mAcm^{-2}$	Current Density 0.25 $mAcm^{-2}$	Current Density 0.50 $mAcm^{-2}$
0	0.99	0.99	0.98	1.03	0.99
1	0.89	0.87	0.91	0.84	0.87
2	0.85	0.84	0.83	0.79	0.80
5	0.78	0.76	0.75	0.66	0.68
10	0.66	0.66	0.64	0.54	0.58
20	0.53	0.55	0.57	0.48	0.46
30	0.47	0.48	0.50	0.44	0.40
60	0.42	0.44	0.44	0.40	0.36
90	0.41	0.43	0.42	0.37	0.32

Fe^{2+} concentration remaining in effect of current density on kinetic of 2,4-DCP removal by electro-Fenton's experiment

Time (minute)	Fe^{2+} Remaining (C/C_0)				
	Current Density 0.01 $mAcm^{-2}$	Current Density 0.05 $mAcm^{-2}$	Current Density 0.10 $mAcm^{-2}$	Current Density 0.25 $mAcm^{-2}$	Current Density 0.50 $mAcm^{-2}$
0	1	1	1	1	1
1	0.94	0.95	0.98	0.99	0.95
2	0.69	0.93	0.95	0.98	0.93
5	0.65	0.85	0.91	0.97	0.81
10	0.24	0.74	0.80	0.96	0.66
20	0.14	0.52	0.68	0.92	0.45

Effect of H_2O_2 concentration on 2,4-DCP kinetic removal by electro-Fenton's experiment (At current density 0.05 mA cm^{-2})

2,4-DCP concentration remaining in effect of H_2O_2 concentration on kinetic of 2,4-DCP removal by electro-Fenton's experiment

Time (minute)	2,4-DCP Concentration (mM)		
	H_2O_2 1 mM	H_2O_2 3 mM	H_2O_2 5 mM
0	1.02	0.98	0.99
1	0.87	0.87	0.88
2	0.88	0.88	0.8
5	0.82	0.82	0.68
10	0.70	0.70	0.53
20	0.62	0.57	0.46
30	0.54	0.48	0.41
60	0.47	0.42	0.35
90	0.43	0.39	0.31

Fe^{2+} concentration remaining in effect of H_2O_2 concentration on kinetic of 2,4-DCP removal by electro-Fenton's experiment

Time (minute)	Fe^{2+} Remaining (C/C_0)		
	H_2O_2 1 mM	H_2O_2 3 mM	H_2O_2 5 mM
0	1	1	1
1	0.99	1.05	1.01
2	1.01	1.12	1.01
5	1.02	1.30	1.01
10	1.02	1.70	1.02
20	1.05	1.86	1.03

Effect of H_2O_2 concentration on 2,4-DCP kinetic removal by electro-Fenton's experiment (At current density 0.10 mA cm^{-2})

2,4-DCP concentration remaining in effect of H_2O_2 concentration on kinetic of 2,4-DCP removal by electro-Fenton's experiment

Time (minute)	2,4-DCP Concentration (mM)		
	H_2O_2 1 mM	H_2O_2 3 mM	H_2O_2 5 mM
0	0.99	0.99	0.99
1	0.91	0.82	0.87
2	0.83	0.76	0.83
5	0.75	0.73	0.69
10	0.64	0.52	0.61
20	0.59	0.55	0.42
30	0.51	0.45	0.37
60	0.45	0.40	0.31
90	0.40	0.37	0.27

Fe^{2+} concentration remaining in effect of H_2O_2 concentration on kinetic of 2,4-DCP removal by electro-Fenton's experiment

Time (minute)	Fe^{2+} Remaining (C/C_0)		
	H_2O_2 1 mM	H_2O_2 3 mM	H_2O_2 5 mM
0	1	1	1
1	1.01	0.91	0.95
2	1.02	0.83	0.99
5	1.05	0.62	0.98
10	1.10	0.39	0.93
20	1.12	0.25	0.87

Kinetic of triclosan removal by electro-Fenton process

Effect of pH on triclosan kinetic removal by electro-Fenton's experiment

Triclosan concentration remaining in effect of pH on kinetic of triclosan removal by electro-Fenton's experiment

Time (minute)	Triclosan Concentration (mM)		
	pH 2	pH 3	pH 3.5
0	0.99	0.99	0.98
1	0.85	0.83	0.88
2	0.81	0.77	0.88
5	0.65	0.63	0.85
10	0.63	0.60	0.81
20	0.55	0.51	0.75
30	0.48	0.45	0.66
60	0.43	0.39	0.58
90	0.40	0.34	0.49

Fe^{2+} concentration remaining in effect of pH on kinetic of triclosan removal by electro-Fenton's experiment

Time (minute)	Fe^{2+} Remaining (C/C_0)		
	pH 2	pH 3	pH 3.5
0	1	1	1
1	1.02	1.05	1.01
2	1.03	1.07	1.05
5	1.06	1.20	1.09
10	1.09	1.48	1.20
20	1.19	2.25	1.43

Effect of current density on triclosan kinetic removal by electro-Fenton’s experiment

Triclosan concentration remaining in effect of current density on kinetic of triclosan removal by electro-Fenton’s experiment

Time (minute)	Triclosan Concentration (mM)				
	Current Density 0.01 $mAcm^{-2}$	Current Density 0.15 $mAcm^{-2}$	Current Density 0.24 $mAcm^{-2}$	Current Density 0.35 $mAcm^{-2}$	Current Density 0.50 $mAcm^{-2}$
0	0.97	0.99	1.02	1.01	0.98
1	0.95	0.83	0.89	0.86	0.82
2	0.88	0.77	0.84	0.82	0.80
5	0.79	0.63	0.71	0.68	0.69
10	0.73	0.60	0.63	0.57	0.54
20	0.59	0.51	0.52	0.50	0.48
30	0.53	0.45	0.45	0.42	0.40
60	0.45	0.39	0.40	0.36	0.35
90	0.42	0.34	0.36	0.34	0.32

Fe^{2+} concentration remaining in effect of current density on kinetic of triclosan removal by electro-Fenton’s experiment

Time (minute)	Fe^{2+} Remaining (C/C_0)				
	Current Density 0.01 $mAcm^{-2}$	Current Density 0.15 $mAcm^{-2}$	Current Density 0.24 $mAcm^{-2}$	Current Density 0.35 $mAcm^{-2}$	Current Density 0.50 $mAcm^{-2}$
0	1	1	1	1	1
1	1.08	1.04	1.03	1.05	1.03
2	1.21	1.12	1.07	1.09	1.07
5	1.54	1.26	1.22	1.19	1.15
10	2.26	1.63	1.46	1.43	1.32
20	6.05	2.66	2.16	2.25	1.84

Effect of H_2O_2 concentration on triclosan kinetic removal by electro-Fenton’s experiment (At current density 0.15 mA cm^{-2})

Triclosan concentration remaining in effect of H_2O_2 concentration on kinetic of triclosan removal by electro-Fenton’s experiment

Time (minute)	Triclosan Concentration (mM)		
	H_2O_2 1 mM	H_2O_2 3 mM	H_2O_2 5 mM
0	1.01	0.99	1.01
1	0.83	0.80	0.81
2	0.77	0.75	0.75
5	0.63	0.60	0.56
10	0.60	0.50	0.42
20	0.51	0.43	0.35
30	0.45	0.40	0.30
60	0.39	0.34	0.27
90	0.34	0.30	0.25

Fe^{2+} concentration remaining in effect of H_2O_2 concentration on kinetic of triclosan removal by electro-Fenton’s experiment

Time (minute)	Fe^{2+} Remaining (C/C_0)		
	H_2O_2 1 mM	H_2O_2 3 mM	H_2O_2 5 mM
0	1	1	1
1	1.01	1.03	1.01
2	1.05	1.04	1.02
5	1.08	1.12	1.04
10	1.23	1.31	1.09
20	1.45	1.58	1.23

Effect of H_2O_2 concentration on triclosan kinetic removal by electro-Fenton's experiment (At current density 0.24 mA cm^{-2})

Triclosan concentration remaining in effect of H_2O_2 concentration on kinetic of triclosan removal by electro-Fenton's experiment

Time (minute)	Triclosan Concentration (mM)		
	H_2O_2 1 mM	H_2O_2 3 mM	H_2O_2 5 mM
0	0.99	0.99	0.99
1	0.81	0.84	0.80
2	0.80	0.74	0.73
5	0.64	0.61	0.54
10	0.55	0.42	0.33
20	0.50	0.35	0.25
30	0.43	0.30	0.21
60	0.37	0.26	0.18
90	0.32	0.24	0.16

Fe^{2+} concentration remaining in effect of H_2O_2 concentration on kinetic of triclosan removal by electro-Fenton's experiment

Time (minute)	Fe^{2+} Remaining (C/C_0)		
	H_2O_2 1 mM	H_2O_2 3 mM	H_2O_2 5 mM
0	1	1	1
1	1.01	1.02	1.02
2	1.05	1.05	1.03
5	1.12	1.09	1.06
10	1.20	1.22	1.09
20	1.45	1.51	1.19

Removal mechanism of 2,4-dichlorophenol by electro-Fenton process
(For only complete in 2,4-dichlorophenol degradation)

Intermediates evolution of 2,4-dichlorophenol degradation by electro-Fenton's experiment

Time (minute)	Concentration (mg L^{-1})					
	2,4-DCP	TOC	2-CP	Phenol	Hydroquinone	p-benzoquinone
0	112.00	52.02	0.00	0.00	0.00	0.00
1	87.32	48.54	5.30	2.20	0.00	0.00
2	49.56	46.31	7.03	3.17	0.00	0.22
5	23.60	45.72	9.14	5.06	0.00	0.25
10	23.60	45.05	12.45	8.54	0.32	0.57
20	4.72	44.23	22.31	18.49	5.10	1.46
30	2.36	44.02	27.62	21.12	10.01	5.62
60	0.00	43.81	18.03	15.61	16.47	12.74
90	0.00	43.76	9.71	7.85	8.23	15.39

Carboxylic Acids evolution of 2,4-dichlorophenol degradation by electro-Fenton's experiment

Time (minute)	Concentration (mg L^{-1})			
	Maleic Acid	Acetic Acid	Oxalic Acid	Formic Acid
0	0.00	0.00	0.00	0.00
1	0.00	0.00	0.00	0.00
2	0.00	0.00	0.00	0.00
5	0.10	0.10	0.00	0.00
10	0.22	0.12	0.10	0.27
20	2.41	2.14	1.32	1.23
30	7.65	5.51	3.74	4.75
60	10.14	8.67	7.23	7.91
90	12.43	10.45	11.92	9.30

Removal mechanism of 2,4-dichlorophenol by electro-Fenton process
(For complete in 2,4-dichlorophenol mineralization)

Intermediates evolution of 2,4-dichlorophenol degradation by electro-Fenton's experiment

Time (minute)	Concentration (mg L^{-1})					
	2,4-DCP	TOC	2-CP	Phenol	Hydroquinone	p-benzoquinone
0	112.07	51.93	0.00	0.00	0.00	0.00
1	51.14	42.15	0.00	0.00	28.24	0.00
2	3.25	37.21	0.00	0.00	17.19	0.00
5	0.02	32.44	0.00	0.00	3.57	0.00
10	0.00	28.72	0.00	0.00	0.21	0.00
20	0.00	25.54	0.00	0.00	0.00	0.00
30	0.00	24.35	0.00	0.00	0.00	0.00
60	0.00	24.21	0.00	0.00	0.00	0.00
90	0.00	24.03	0.00	0.00	0.00	0.00

Carboxylic Acids evolution of 2,4-dichlorophenol degradation by electro-Fenton's experiment

Time (minute)	Concentration (mg L^{-1})			
	Maleic Acid	Acetic Acid	Oxalic Acid	Formic Acid
0	0.00	0.00	0.00	0.00
1	12.39	9.25	3.21	2.73
2	19.51	14.22	10.34	12.88
5	28.75	25.48	22.86	22.38
10	23.72	24.16	27.31	26.79
20	18.62	19.81	32.27	30.18
30	5.82	14.25	25.19	28.67
60	0.43	3.97	9.87	14.35
90	0.00	0.05	5.83	9.30

Removal mechanism of triclosan by electro-Fenton process
(For only complete in triclosan degradation)

Intermediates evolution of triclosan degradation by electro-Fenton's experiment

Time (minute)	Concentration (mg L^{-1})						
	Triclosan	TOC	2,4-DCP	4-Chlorocatechol	Phenol	Hydroquinone	p-Benzoquinone
0	284.05	138.90	0.00	0.00	0.00	0.00	0.00
1	226.42	137.71	40.17	19.40	0.00	0.00	0.00
2	215.63	136.32	45.42	23.61	2.33	0.00	0.00
5	148.71	135.51	57.83	26.30	8.50	0.10	0.00
10	94.58	135.12	53.51	21.75	15.71	2.12	0.12
20	48.26	134.65	38.22	18.22	19.45	9.30	4.71
30	10.30	134.14	17.67	7.81	28.72	19.21	11.64
60	0.91	132.27	4.53	2.10	9.93	23.63	16.80
90	0.00	131.71	1.12	0.11	2.11	8.25	18.21

Carboxylic Acids evolution of triclosan degradation by electro-Fenton's experiment

Time (minute)	Concentration (mg L^{-1})			
	Maleic Acid	Acetic Acid	Oxalic Acid	Formic Acid
0	0.00	0.00	0.00	0.00
1	0.00	0.00	0.00	0.00
2	0.00	0.00	0.00	0.00
5	0.00	0.00	0.00	0.12
10	0.00	0.00	0.16	0.16
20	5.21	4.70	2.60	2.34
30	9.73	7.05	4.93	5.72
60	17.45	14.83	9.21	10.51
90	22.37	25.31	11.17	16.29

Removal mechanism of triclosan by electro-Fenton process

(For complete in triclosan mineralization)

Intermediates evolution of triclosan degradation by electro-Fenton's experiment

Time (minute)	Concentration (mg L^{-1})						
	Triclosan	TOC	2,4-DCP	4-Chlorocatechol	Phenol	Hydroquinone	p-Benzoquinone
0	285.76	140.45	0.00	0.00	0.00	0.00	0.00
1	104.78	133.36	0.00	0.00	0.00	43.17	0.00
2	25.32	125.74	0.00	0.00	0.00	18.24	0.00
5	2.07	106.83	0.00	0.00	0.00	4.19	0.00
10	0.03	86.47	0.00	0.00	0.00	0.53	0.00
20	0.00	77.11	0.00	0.00	0.00	0.00	0.00
30	0.00	71.34	0.00	0.00	0.00	0.00	0.00
60	0.00	70.19	0.00	0.00	0.00	0.00	0.00
90	0.00	69.27	0.00	0.00	0.00	0.00	0.00

Carboxylic Acids evolution of triclosan degradation by electro-Fenton's experiment

Time (minute)	Concentration (mg L^{-1})			
	Maleic Acid	Acetic Acid	Oxalic Acid	Formic Acid
0	0.00	0.00	0.00	0.00
1	22.21	17.95	7.97	6.76
2	26.72	26.62	18.94	15.54
5	35.68	43.17	39.87	42.11
10	28.37	35.17	51.74	47.42
20	23.53	26.72	47.75	52.67
30	10.01	12.54	35.69	41.45
60	1.12	2.63	12.34	15.93
90	0.03	0.24	3.83	8.77

APPENDIX D

Journal and Conference Publication Lists

Journal publication lists

1. Thanakorn Methatham, Ming-Chun Lu, and Chavalit Ratanatamskul. 2011. Effect of operating parameters on 2,4-dichlorophenol degradation by electro-Fenton ferrous regeneration (EFFR) system. Fresenius Environmental Bulletin: 20, No. 10 2616-2623.
2. Thanakorn Methatham, Ming-Chun Lu, and Chavalit Ratanatamskul. 2011. Removal of 2,4-dichlorophenol as herbicide's by-product by Fenton's reagents combined with an electrochemical. Desalination and Water Treatment 32: 42-48.
3. Thanakorn Methatham, Ming-Chun Lu, and Chavalit Ratanatamskul. 2011. A novel kinetic model of electrochemical regeneration of Fenton's reagents process on chlorinated organic oxidation. Journal of Hazardous Materials (during in the process of submission).
4. Thanakorn Methatham, Ming-Chun Lu, and Chavalit Ratanatamskul. 2011. Oxidation of 2,4,4'-trichloro-2'-hydroxydiphenyl ether (triclosan) by Fenton's reagents combined with electrochemical system. Journal of Hazardous Materials (during preparation process for submission).
5. Thanakorn Methatham and Chavalit Ratanatamskul. 2011. Effect of a longer cleaning-frequency period on nanofiltration membrane fouling for long-term water supply production. Desalination and Water Treatment (in press).

Conference paper publication list

1. Thanakorn Methatham, Chavalit Ratanatamskul and Ming-Chun Lu. 2011. OXIDATION OF 2,4-DICHLOROPHENOL BY ELECTRO-FENTON PROCESS: Asian-Pacific Regional Conference On Practical Environmental Technologies (APRC), International Conference, March 24-27, 2010, Ubonratchathani, Thailand.
2. Thanakorn Methatham, Ming-Chun Lu, and Chavalit Ratanatamskul. 2011. KINETIC OF 2,4-DICHLOROPHENOL OXIDATION BY ELECTRO-FENTON PROCESS: International Advanced Oxidation Processes (AOPs) Conference, International Conference, March 29-30, 2010, Tunghai University, Taichung, Taiwan.
3. Thanakorn Methatham, Ming-Chun Lu, and Chavalit Ratanatamskul. 2011. REMOVAL OF 2,4-DICHLOROPHENOL AS HERBICIDE’S BY-PRODUCT BY FENTON’S REAGENT COMBINED WITH ELECTROCHEMICAL SYSTEM: Challenges in Environmental Science and Engineering, CESE-2010, International Conferences, September 26- October 1, 2010, The SEBEL, Cairns, Queensland, Australia.
4. Thanakorn Methatham and Chavalit Ratanatamskul. 2011. EFFECT OF LONGER CLEANING FREQUENCY PERIOD ON NANOFILTRATION MEMBRANE FOULING FOR LONG TERM WATER SUPPLY PRODUCTION: Challenges in Environmental Science and Engineering, CESE-2010, International Conferences, September 26- October 1, 2010, The SEBEL, Cairns, Queensland, Australia.

BIOGRAPHY

Name:	Mr. Thanakorn Methatham
Date of Birth:	August 30, 1982
Nationality:	Thai

University Education:

1. Bachelor's Degree of Engineering in Environmental Engineering, Faculty of Engineering, Chiang Mai University, Chiang Mai, Thailand.
2. Master's degree of engineering in Environmental Engineering, Faculty of Engineering, Chulalongkorn University, Bangkok, Thailand.

Publications:

1. Thanakorn Methatham, Ming-Chun Lu, and Chavalit Ratanatamskul. 2011. Effect of operating parameters on 2,4-dichlorophenol degradation by electro-Fenton ferrous regeneration (EFFR) system. Fresenius Environmental Bulletin: 20, No. 10 2616-2623.
2. Thanakorn Methatham, Ming-Chun Lu, and Chavalit Ratanatamskul. 2011. Removal of 2,4-dichlorophenol as herbicide's by-product by Fenton's reagents combined with an electrochemical. Desalination and Water Treatment 32: 42-48.
3. Thanakorn Methatham, Ming-Chun Lu, and Chavalit Ratanatamskul. 2011. A novel kinetic model of electrochemical regeneration of Fenton's reagents process on chlorinated organic oxidation. Journal of Hazardous Materials (during in the process of submission).
4. Thanakorn Methatham, Ming-Chun Lu, and Chavalit Ratanatamskul. 2011. Oxidation of 2,4,4'-trichloro-2'-hydroxydiphenyl ether (triclosan) by Fenton's reagents combined with electrochemical system. Journal of Hazardous Materials (during preparation process for submission).

He has carried out this research as a part of studied for a doctoral degree of Doctor of Philosophy Program in Environmental Engineering at Faculty of Engineering, Chulalongkorn University.